Hydrodynamic Study on Fouling Control in Submerged Membrane Microfiltration

Muna Pradhan

A thesis submitted in fulfilment
of the requirements for the degree of
Doctor of Philosophy

Faculty of Engineering and Information technology
University of Technology, Sydney

November 2012

Certificate of Authorship/Originality

I certify that the work in this thesis has not previously been submitted for a degree nor has it been submitted as part of requirements for a degree except as fully acknowledged within the text.

I also certify that the thesis has been written by me. Any help that I have received in my research work and the preparation of the thesis itself has been acknowledged. In addition, I certify that all information sources and literature used are indicated in the thesis.

Muna Pradhan
November 2012

Acknowledgement

Firstly, I would like to express my sincere gratitude to my supervisor Prof. SARAVANAMUTHU VIGNESWARAN for his direction, guidance, wisdom, insight and patience. I am sure that this dissertation would not have been possible without his support, understanding and encouragement. I owe sincere thanks to my research advisor, Prof. Roger Ben Aim, who guided me through the whole process of dissertation writing. I would also like to show my gratitude to A/Prof. Jaya Kandasamy for his help throughout my entire study, as well as Dr. Rupak Aryal, who helped me in my initial period of research, and friends Johir, Chinu, Anil for their help and moral support.

I would like to thank the Australian Federal Government for the Australian Postgraduate Award (APA) to support my study.

My most profound thanks, my most heartfelt appreciation, my deepest gratitude goes to my family, without whom none of this could have been accomplished. To my parents and parents in-law, thanks for your unwavering confidence in me, for your love. Thanks to my brothers and sisters for their love and encouragement. To my son Binam and daughter Manvi, thanks for your gorgeous smiles that helped me to forget all my tiredness, your cheery dispositions and excited cries of 'Maamu' when I get home late from work. I will never be able to thank my husband Binod, who made me believe in myself and encouraged me through the whole process of research. Thank you for your selfless support and belief in me; thank you for loving me the way you do.

Dedication

To my late father Gopal Bhagat Pradhan,

His blessed words of encouragement and silent inspiration

in pursuit of excellence, still dwell on me.

Table of Contents

List of Figures

List of Tables

Abstract

Application of air flow is a promising hydrodynamic technique for membrane fouling control in submerged membrane separation systems. This thesis investigates the effect of operating conditions and hydrodynamic parameters on membrane fouling during submerged membrane microfiltration. The experiments were conducted under different operating conditions such as the application of various air flow rates, permeate flux rates, the addition of external materials (granular activated carbon: GAC, ferric chloride: $FeCl_3$) and with different feed properties (varying viscosity) for model feed suspension (kaolin clay). Membrane fouling was examined with the different geometries of air diffuser plates that generate different sizes of air bubbles. Additionally, this study reports on the effect of adsorbents on the removal of organic matter during the microfiltration of synthetic wastewater.

Membrane fouling was evaluated with a popular hydrodynamic approach: the application of air flow in submerged flat sheet membrane microfiltration. The investigation focused on the measurement of transmembrane pressure (TMP), particle deposition (fouling) and particle size distribution to assess membrane fouling under a variety of filtration conditions. The experimental results show that an increase in air flow rate reduces TMP as well as particle deposition for all the operating conditions studied. Conversely, an increase in permeate flux causes higher TMP development. The linear relationship between the TMP and particle deposition has been established for different air flow and permeate flow rates. Based on experiments, a particle deposition mathematical model was developed for a high concentration of kaolin clay in suspension. In the case of a higher viscosity of feed, elevated TMP indicated higher fouling; however, TMP was reduced by increasing the flow of air bubbles (higher air scour).

The high energy requirement for air flow systems is a challenging issue in submerged membranes, and this study therefore suggests alternative techniques for optimising the air flow rate and limiting fouling. The addition of external material (support medium) in the kaolin suspension caused a further reduction in membrane fouling that was the result of air scour only. Almost the same reduction in TMP was obtained by adding a support medium instead of doubling the air flow rate. Therefore, the addition of a support

medium with low air flow could offer a good alternative for the control of fouling in a submerged membrane microfiltration system. Furthermore, different geometries of air diffuser plates had a significant influence on the performance of the submerged membrane microfiltration. Improved reductions in TMP and particle deposition were observed with the circular aerator (small bubbles) rather than the square aerator (large air bubbles). The results in this study highlight that the effectiveness of the air flow depends on the geometry of the aerator plates and the consequent production of different sizes of air bubbles. The optimisation of the combined effect of the support medium and air flow with the appropriate aerator plate geometry will lead to a less energy-intensive operation in membrane microfiltration systems.

This study also separately examines the effect of flocculation and adsorption coupled with submerged microfiltration on membrane performance. The TMP development at optimal flocculant ($FeCl_3$) concentration was significantly less than it was with unflocculated kaolin feed. The addition of flocculant exhibited better control of colloidal membrane fouling due to the modification of the cake properties (cake structure, porosity, and compactness). In the case of an adsorption-microfiltration system with synthetic wastewater, the adsorbents (powder activated carbon: PAC, GAC and Purolite) introduced into the suspension helped to remove organic matter prior to their contact with the membrane. The submerged membrane adsorption system was very effective in removing dissolved organic matter from the synthetic wastewater. Of these three adsorbents, PAC was observed to be the most effective, with a higher level of removal efficiency for dissolved organic carbon. A higher dose of PAC showed an almost 100% reduction of hydrophobic compounds.

A higher air flow rate was always found to be beneficial to membrane fouling control, whereas high viscosity had a negative impact on fouling. High air flow demands high energy, which leads to high operating costs. This research investigated various options to minimise air flow rate. The addition of a support medium (GAC) could be a good alternative to a high air flow rate. The geometry and design of the aerator plate were also very important parameters that directly influenced membrane fouling. More importantly, the flocculation and adsorption used in this study were found to be very effective in the reduction of membrane fouling.

Chapter 1

Introduction

1.1 Background

The world's population growth coupled with industrialisation and urbanisation has resulted in an increased demand for water and has caused a serious human and environmental problem. By 2025, one third of humanity will face severe water scarcity. This has been described as the single greatest threat to health, the environment and global food security (EUROBRA 2008). Water is essential, and its preservation in quantity and quality is critical to the sustainable development of any society. Wastewater treatment is an important aspect of water management in meeting this challenge. Efficient, cost effective and reliable treatment processes are needed to produce high quality water from wastewater which, following beneficial use, can be returned to human utilities and the hydrological cycle without detrimental effects. Membrane separation technology is the most advanced recent technical development and application in the wastewater industry and offers many advantages over conventional processes. A small footprint and improved effluent quality are the main aspects for selecting a membrane-based separation to replace the conventional activated sludge process. Other advantages include high operational reliability and a high effluent quality.

Worldwide commercialisation of membrane technology has been limited by the problem of membrane fouling during the filtration process. Membrane fouling is the deposition of soluble and particulate materials onto the membrane surface and in the membrane pores due to the physicochemical and biological interactions between the sludge and membrane. Membrane fouling has been considered the most serious problem

affecting system performance (Chang & Fane 2001; Kim, Lee & Chang 2001b; Le-Clech, Chen & Fane 2006) because it leads to a decline in permeate flux and hence demands more frequent membrane cleaning and replacement, ultimately increasing system operation costs. Although it is difficult to develop a general rule about membrane fouling, the nature and extent of fouling are strongly influenced by main three factors, namely sludge characteristics, operating conditions and membrane properties. To maintain the economical viability of a membrane process, membrane fouling has to be kept to a minimum. Therefore, many researchers have devised different strategies to mitigate membrane fouling and improve system performance. These strategies include the development of new membrane materials (Wang et al. 2002), new designs of the membrane module (Bai & Leow 2001, 2002), modification of the feed flow pattern (Yamamoto et al. 1989), the incorporation of in-situ or ex-situ cleaning regimes in the membrane unit (Parameshwaran et al. 2001), and optimising operating conditions.

The application of air flow (aeration) has been a popular strategy to minimise membrane fouling. It maintains the solids in suspension, leading to a well mixed and homogeneous distribution of particulate and scouring deposited layers from the membrane surface, helping to reduce fouling. Cui and Wright (1994) reported a 175% increase in permeate flux in air sparged yeast microfiltration. In another study, Mercier et al. (1997) showed a three-fold increase in filtration flux by the application of air bubbles in ultrafiltration of bentonite and yeast. Although the use of air sparging is unavoidable for controlling membrane fouling, the energy consumption is proportional to the intensity of aeration. This eventually leads to an increase in the operating cost as well as maintenance cost. In many submerged microfiltration systems, aeration consumes 30–50% of the total energy consumption (Yoon, Kim & Yeom 2004).

Despite the progress in membrane fouling control in the past, the energy involved in providing aeration to submerged membranes has become a considerable cost factor. Therefore, efforts must be made to minimise energy consumption. To make membrane technology a more commercially viable alternative to conventional processes, it is necessary to reduce the energy consumption of the aeration system, which is one of the major costs of membrane operation. It is important to optimize the aeration rate in connection with the feed properties and fouling potential; thus the optimisation of aeration is still a subject of practical and research interest in terms of reducing the foulant that accumulates on the membrane and increasing the life of the membrane. The optimisation of aeration leads directly to the minimisation of operating costs, therefore a more detailed investigation of the impact of aeration rates on suspension is needed to gain a better understanding of membrane fouling and to reduce costs.

In this context, the purpose of the current study is to understand the fouling mechanism under the hydrodynamic conditions that exist within the membrane filtration unit so that the aeration requirement can be minimised yet at the same time ensuring that system performance is optimised. The motivation for this research work arose from the importance of optimising operation conditions for fouling control. Therefore, this research investigates the effect of different hydrodynamic approaches on the operating conditions of submerged membrane microfiltration, leading to a reduction in the aeration requirement and enhancing fouling control.

1.2 Objectives

Membrane filtration is an advanced technique that is available for wastewater treatment; however, membrane fouling is a major barrier to its widespread commercialisation and application. Past research has revealed that air flow is one of the best strategies for

mitigating membrane fouling. The main issue related to air flow systems is the high energy consumption which increases both the operating cost and maintenance cost. A fundamental understanding of the processes that lead to and mitigate fouling will enable improvements in the design and operation of membrane processes and will ultimately reduce both the operating and capital costs. The main objective of the study is to investigate the influence of hydrodynamic approaches on fouling mitigation; thus, this study investigates the effects of air flow in different operating conditions. Analysing the hydrodynamic behaviour of particle deposition will be carried out for optimising operating conditions, and these efforts will attempt to minimise the knowledge gap on air flow and its influence on membrane fouling. Following are the objectives of this study;

- to assess the influence of air flow on transmembrane pressure (TMP) and particle deposition in submerged membrane microfiltration;
- to develop a mathematical formula of particle deposition;
- to investigate mechanical scouring by adding a support medium (e.g. Granular Activated Carbon) in an aerated suspension and to assess whether combined air and mechanical scouring is feasible;
- to examine the effect of feed viscosity on aerated submerged membrane microfiltration;
- to study the effect of aerator geometry (bubble size) on particle deposition;
- to assess fouling behaviour during submerged microfiltration coupled with flocculation;
- to investigate the effect of the addition of an ion-exchange resin (Purolite) and activated carbon (granular activated carbon and powdered activated carbon) (used for both adsorption and mechanical scour) on fouling control in a submerged membrane reactor.

This study was carried out with a suspension of kaolin clay with a high solids concentration of 10 g/L, designed to mimic the mixed liquor suspended solids (MLSS) concentration of biological suspension in the membrane bioreactor (MBR). In MBR, however, solids/biomass are in flocculated form with a large particle size distribution of 1-100 μm. It is for this reason that we also studied the effect of air scouring in flocculated suspension. The biological suspension/wastewater has biopolymers, humics, and more which also lead to bio-fouling. This is the reason for considering a synthetic suspension which resembles biologically treated sewage effluent.

1.3 Thesis Structure

This thesis consists ten chapters.

Chapter 1 describes the general background and objectives of this research work.

Chapter 2 provides a literature review of an aerated submerged membrane filtration system, and includes membrane fouling, its causes and possible remedies, and the influence of air flow on membrane fouling. Specific literatures on the aspects investigated in the research are given in Chapters 3 to 9.

Chapter 3 describes the materials and membrane modules in detail, as well as the experimental procedures used in this study. The experimental results on the submerged membrane microfiltration using kaolin clay as the test medium under different operating conditions are presented. The effects of various hydrodynamic conditions on membrane fouling are described here. The effects of different air flow rates and permeate flux rates have been studied, and a comparative analysis of fouling mitigation under different operating conditions is also presented.

In Chapter 4, a simple mathematical formula is derived to describe the particle deposition profile in an aerated submerged membrane microfiltration system by considering the force balance method.

Chapter 5 describes the mechanical scouring of deposited cake layers by adding a support medium (such as GAC) in an aerated suspension. Further improvement in fouling control by the addition of GAC under various operating conditions is presented. The research presented in this chapter is aimed at minimising the air flow rate by adding an external material in the suspension to achieve the optimum condition of a relatively low fouling rate. This chapter proposes an alternative technique for microfiltration operated at a high air flow rate.

In Chapter 6, the effect of changing the viscosity of an aerated suspension is investigated by adding predetermined quantities of glycerol during microfiltration. A comparative study of the detrimental effect of increasing feed viscosity and the need for air flow in fouling control is presented.

Chapter 7 deals with the aerator geometry that produces different sizes of air bubbles. The influence of aerator geometry on membrane fouling is presented through the use of square and circular aerator devices respectively in submerged membrane microfiltration. The characteristics of bubbles generated by different aerator plates at various air flow rates are analysed in relation to microfiltration performance.

Chapter 8 presents the experimental results of microfiltration coupled with flocculation. The fouling behaviour of flocculated kaolin clay during flat sheet membrane microfiltration is investigated through the addition of ferric chloride as a flocculant.

In Chapter 9, the effects of external media/adsorbents (granular activated carbon, powdered activated carbon and Purolite) on the removal of organic matter during the microfiltration of synthetic wastewater are presented. This chapter compares the effectiveness of these adsorbents in removing dissolved organic matters from the synthetic wastewater in an aerated submerged membrane adsorption system. Fouling of membranes is partly attributed to dissolved organic matter.

Chapter 10 provides the conclusions and recommendations for future work. The specific conclusions are presented at the end of each chapter.

Chapter 2

Literature Review

2.1 Membrane Technology

Membrane technology is the latest advancement in wastewater treatment. It has overcome many disadvantages of conventional wastewater treatment and has achieved success in the separation of particular types of materials which have been difficult and expensive to remove in the past, such as: dispersive colloids and fine particles, biological materials in the range of colloidal size, low molecular weight, non-volatile organic, and dissolved salts. The membrane separation technology yields high quality effluent, helping to meet changes in the regulatory requirements of safe drinking water, surface water treatment and wastewater treatment. Moreover, the membrane system in general offers many advantages over the conventional processes currently available, some of which are listed below.

- Small/reduced footprint
- Complete removal of suspended solids
- Effluent disinfection
- Combined COD, solids and nutrients removal in a single unit
- Higher biomass concentration
- Reduced excess sludge production
- High rate of nitrification

The concept of coupling an activated sludge digestion with ultrafiltration and microfiltration was first developed in the mid 1960s by Dorr-Oliver (Smith, Gregorio & Talcott 1969). Japan developed commercial aerobic membrane bioreactor (MBR)

processes in the early 1980s, whereas in North America this system first appeared in the late 1970s. The major step was the development of a submerged membrane system in Japan in 1989, which was rapidly commercialised worldwide. This version of a membrane system entered the European market in the mid 1990s (Stephenson et al. 2000). The commercial value of membrane bioreactor technology was approximately US$217 million in 2005 and its value is rising at an average annual growth rate of 10.9% (Atkinson 2006). One of the major drivers for the rapid growth of the membrane market is the increasingly stringent environmental legislation implemented for drinking water and wastewater disposal over the last decade. As a result, membrane technology has become an important separation technology in the wastewater industry.

Notwithstanding the abovementioned advantages of membrane technology, its widespread commercialisation is principally constrained by membrane fouling. From a practical point of view, membrane fouling denotes a loss of system productivity over time, requiring a higher energy input to maintain desirable system productivity. In general, fouling is the particle deposition on the membrane surfaces of materials present in the feedwater during the filtration process. The occurrence of fouling is almost universal for all filtration systems. Therefore, fouling control or reduction is an unavoidable challenge to both membrane design and system operation. This is evidenced by the rapid evolution of membranes used by industry. The driving force for this evolution is primarily fouling control. Moreover, despite the advance of membrane design, proper operation is still crucial for fouling control of large scale systems. It is often found that membrane fouling can be reduced by pretreatment of the feedwater to partially remove some foulant which reduces the frequency of chemical backwashing and improves operating conditions. With the integration of these design and operation strategies, most large-scale microfiltration plants are now capable of maintaining their

productivity during long term operation, which has boosted the application of microfiltration (MF) and other low pressure membrane filtration techniques in water industries. Advanced research work on fouling control is still required to facilitate the further development and application of this new technology.

2.1.1 Membrane

A number of membrane definitions are described in the literature. In general, a membrane can be defined as a semi-permeable barrier that restricts the transmission of particular substances, while other components may permeate through it. It is a thin film capable of separating materials as a function of their physical and chemical properties when a driving force is applied across its surface. A membrane can be homogeneous or heterogeneous, symmetric or asymmetric in its structure, and its materials can be organic (polymeric, liquid) or inorganic (ceramic, metallic). Membrane thickness ranges from less than 100 nm to more than a centimetre. The properties of the membrane can be hydrophobic or hydrophilic. Driving forces to propel liquid through a membrane may be generated by the diffusion of individual molecules or by convective flow induced by an electrical field, or by a concentration, pressure or temperature gradient (Mulder 1996).

2.1.2 Membrane Module

The membrane module is a single operational unit into which individual membrane elements are assembled. The geometry of the membrane plays a very important role in good separation performance. The membrane modules describe the membrane arrangement, the filtration mode, the packing density and the hydraulic distribution throughout the membrane network. The choice of membrane module (e.g. hollow fibre or flat sheet) is an important aspect for submerged membrane systems, and module

configuration also exerts crucial effects on the performance of the system (Fane, Chang & Chardon 2002). Membranes can be configured in five major types of modules: Pleated cartridge, Plate and frame (flat sheet) (Figure 2.1), Hollow fibre (Figure 2.2), Tubular (Figure 2.3) and Spiral-wound (Figure 2.4).

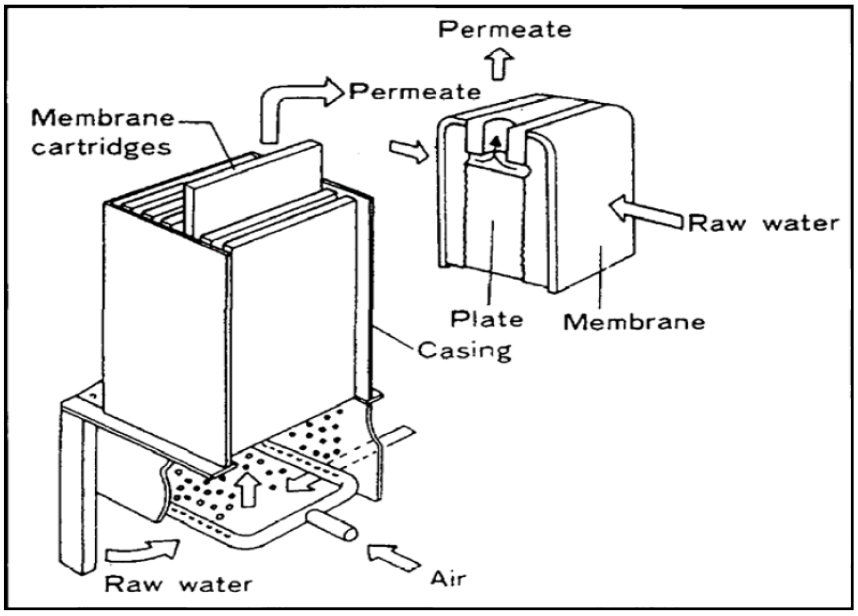

Figure 2.1 Diagram of flat plate submerged MBR (Churchouse 1997)

Figure 2.2 Hollow fibre membrane (ZeeWeed)

Figure 2.3 Tubular membrane

Figure 2.4 Spiral-wound membrane

The application of air flow has been found to be very effective in fouling mitigation in hollow fibre, flat sheet and tubular modules. The selection of the module is influenced by the location of the membrane in the system, and in particular whether the membrane element is placed in the bioreactor or is external to it. The following points highlight the essential characteristics of an optimum membrane module;

- High membrane area to module bulk volume ratio;
- Avoids leakage between the feed and permeate compartments;
- High degree of turbulence on the feed side for mass transfer promotion;
- Low cost per unit membrane area;
- Low energy consumption per product volume of water or wastewater;
- Simple for cleaning and maintenance;
- Simple operation process;
- Ease of membrane replacement.

Hollow fibre and plate and frame (flat sheet) modules are currently exclusively used in the wastewater treatment industry. Hollow fibre membranes are self-supporting membranes that provide the highest packing density at the lowest cost; they are normally operated out-side to in-side with reference to water permeation and are easy to backwash. A general overview of the module configurations is presented in Table 2.1.

Table 2.1 Membrane module configurations (Stephenson et al. 2000)

Configuration Area/Volume Ratio (m^2/m^3)	Cost	Replacement	Advantages	Disadvantages	Applications
Pleated cartridge 800-1000	Low	Cartridge	Robust and compact design	Easily fouled, cannot be cleaned, disposal unit	Dead-end MF
Plate-and-frame 400-600	High	Sheet	Dismantled for cleaning	Complicated design, cannot be backflushed	ED, UF, RO
Spiral-wound 800-1000	Low	Element	Low energy cost, robust and compact	Not easily cleaned, cannot be backflushed	RO, UF
Tubular 20-30	Very high	Tubes	Easy mechanical cleaning and tolerates high TSS levels	High capital and replacement cost	Cross-flow MF
Hollow fibre 5000-40000	Very low	Bundle	Compact, backflushed cleaning and tolerates high colloid levels	Sensitive to pressure shocks	UF, MF, RO

2.1.3 Membrane Process Configurations

There are two basic membrane configurations used in the membrane system. One is submerged configuration, in which the membranes are immersed in the bioreactor, and the other is an external (sidestream) configuration of the bioreactor (Figures 2.5 and 2.6). The submerged configuration was first developed by Yamamoto et al. (1989) who directly immersed the membrane module in the aeration tank containing the mixed liquor. In this system, aeration offers a dual function. The uplifting bubbles generate a scouring effect at the membrane surface which helps to reduce fouling; at the same time, the aeration provides oxygen to micro-organisms. The advantages of submerged configurations are lower energy consumption, simple design and higher hydraulic efficiency compared to external configuration.

In an external configuration, the membrane module is placed outside an activated sludge tank and the membrane and bioreactor are connected with an external recirculation loop. In this system, feed is pumped into the membrane and part of the permeate is extracted, while the other part is returned to the bioreactor. The main advantage of this configuration is better control of membrane fouling resulting in a more constant flux, but the complex design system and high energy consumption are major drawbacks.

In a typical external membrane bioreactor (MBR) process, pumping costs contribute 60 to 80% of the total operating cost, and energy consumption can range from 4 ~ 12 kW h m^{-3} (Cote & Thompson 1999). To minimise the energy consumption in the operation, Yamamoto et al. (1989) immersed the membrane module in the aeration tank and permeate was extracted through the membrane by a suction pump. In this configuration, the need for circulation pumping for the cross-flow was eliminated and the energy demand for the operation was substantially reduced. Cote and Thompson (1999)

reported that the energy requirement for the submerged system is between 0.3 and 0.6 kW h m^{-3} including pumping and aeration, which is far less than the external system. However, this energy demand is still higher than it is for the conventional activated sludge process, which uses gravity and requires very little energy for the solid-liquid separation.

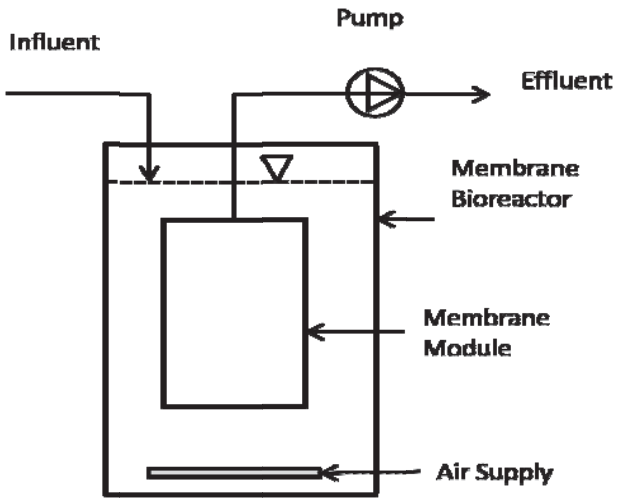

Figure 2.5 Typical set-up of a submerged MBR system

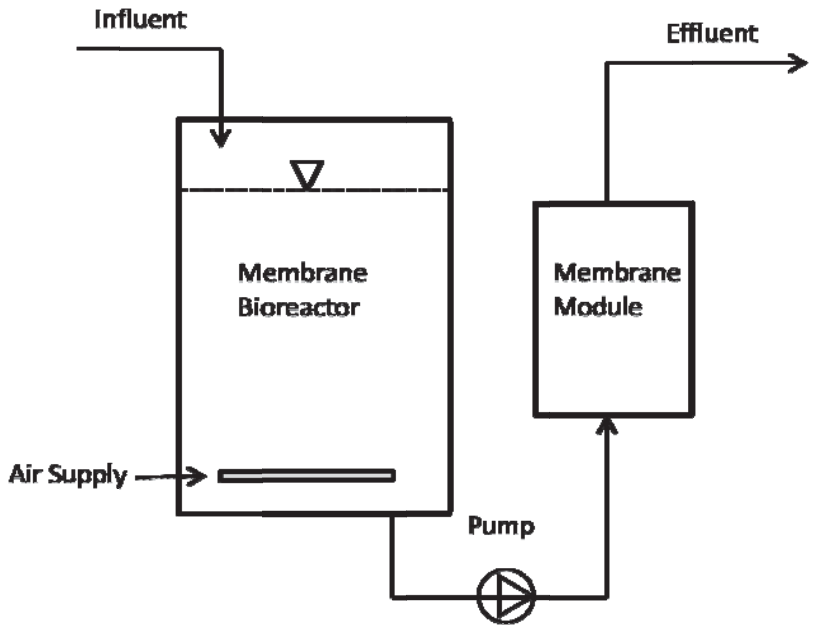

Figure 2.6 Typical set-up of an external MBR system

2.1.4 Membrane Filtration Process

Membrane technology is a generic term for the various filtration processes. Filtration processes are all of the same nature because they all use a membrane in liquid-solid or liquid-liquid separations. The membrane separation process is based on the presence of semi-permeable membranes. Depending on the particle or molecule size and the main driving force generating the filtration system, membrane processes can be divided into a number of categories, namely microfiltration, ultrafiltration, nanofiltration, reverse osmosis, electrodialysis, prevaporation, and membrane distillation. The first four membrane processes (microfiltration, ultrafiltration, nanofiltration, and reverse osmosis) are recognised as pressure driven membrane processes. These processes are distinguished by the membrane pore size associated with the applied pressure and the types of component that may be retained or that may penetrate the membrane. Various driving forces such as pressure gradient, concentration, electric potential and temperature enable water to pass through a membrane.

Microfiltration is the pressure driven membrane process for the filtration of fine particles, micro-organisms and emulsion droplets and typically has membrane pores of 0.02 μm to 20 μm. This filtration is commonly used to separate particles of diameter greater than 0.02 μm from other components in an influent. For this type of separation, it is possible to use a relatively open membrane structure. Low pressure is adequate for obtaining high fluxes due to the small hydrodynamic resistance of these membranes.

Ultrafiltration is used to separate macromolecules (molecular weights ranging from approximately 10^4 to larger than 10^6 Daltons) from an aqueous solution and a more dense membrane structure is needed. Membranes with pores in the range 5 nm to about

50 nm are used in this separation process. The membrane resistance and applied pressure are higher than in microfiltration.

The hydrodynamic resistance increases from microfiltration, ultrafiltration and nanofiltration to reverse osmosis, and consequently a higher driving force is required to perform the separation. The filtration flux through the membrane and the size of the particles being retained decreases. The separation characteristics of pressure driven membrane processes are illustrated in Figure 2.7.

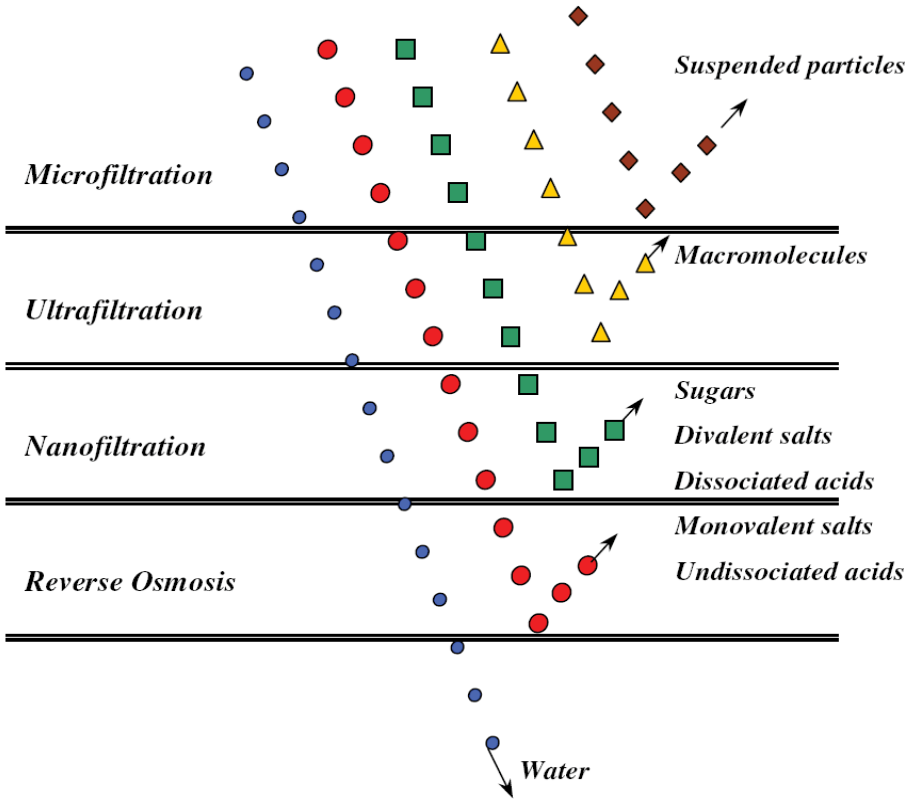

Figure 2.7 Separation characteristics of pressure driven membrane processes (Cheryan 1998)

2.1.5 Membrane Operational Modes

The membrane separation process can be operated in two foundamental modes: (a) Dead-end filtration, and (b) Cross-flow filtration (Figure 2.8). In dead-end filtration, the feed is pumped in a direction that is perpendicular to the filter media and particles are

deposited on the membrane surface, resulting in a cake formation. The cake resistance increases with filtration time, causing permeate flux to decline when a constant transmembrane pressure (TMP) is applied. TMP rises with the increasing cake layer in constant filtration flux mode. Backwash is performed for membrane cleaning. The dead-end operation mode has greater application for water with a low solid content or for a cyclic operation with frequent backwashing.

In the cross-flow filtration mode, the suspension is passed tangentially to the membrane surface. Cross-flow produces turbulence near the membrane surface that detaches the deposited layer; hence, this operation mode has less cake resistance and lower fouling propensity compared to the dead-end mode. Cross-flow is achieved by pumping, stirring or air flow application. The cross-flow mode is more favourable for water with a high solid content, where fouling is unlikely to be due to induced turbulence.

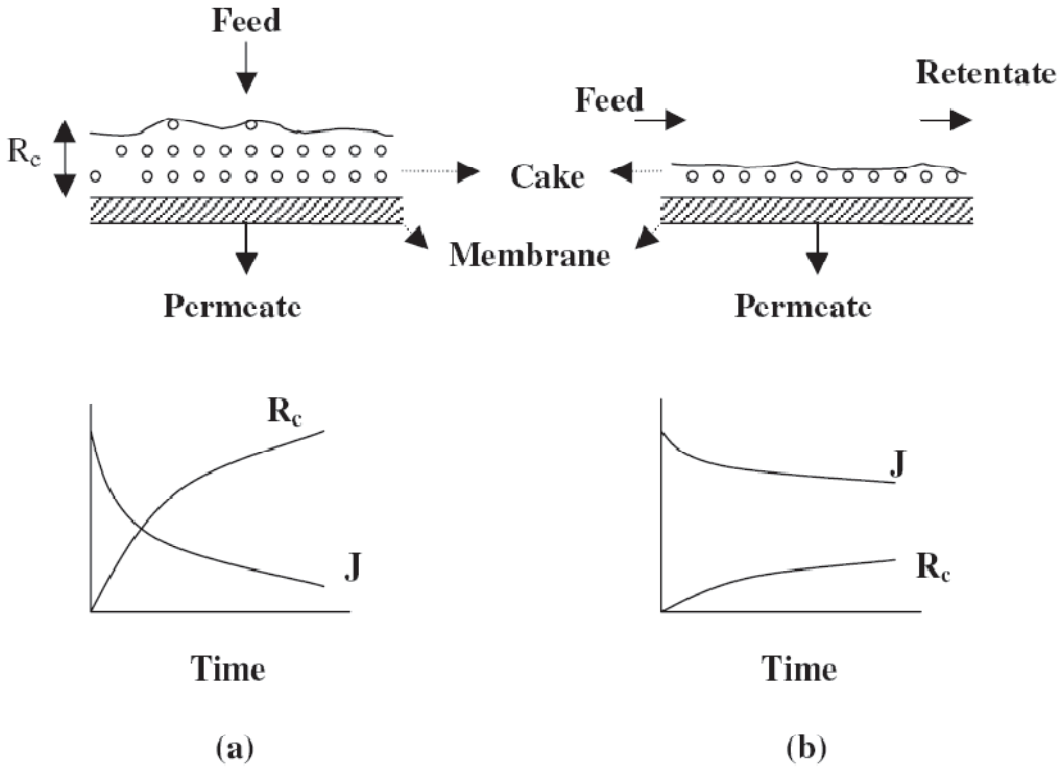

Figure 2.8 Modes of operation for membrane filtration: (a) Dead-end (b) Cross-flow operation modes (Cheryan 1998)

2.2 Membrane Fouling

It is widely accepted that membrane fouling is the most serious problem to affect system performance in membrane separation processes. In recent reviews covering membrane applications in bioreactors, it has been shown that fouling is a major obstacle to the efficient operation of membrane plant used for water and wastewater treatment (Chang & Fane 2001; Kim, Lee & Chang 2001b; Le-Clech, Chen & Fane 2006). Membrane fouling in bioreactors occurs as a result of the interaction between the membrane material and the components of the activated sludge liquor, which include biological flocs formed by a large range of living micro-organisms along with soluble and colloidal particles. During the filtration process, fouling is caused by the attachment, accumulation and adsorption of substances in the sludge onto the membrane surface and/or within the membrane pores. Fouling leads to a significant increase in hydraulic resistance which manifests as permeate flux decline or a rise in transmembrane pressure (TMP) when the process is operated under constant-TMP or constant-flux conditions respectively. Frequent membrane cleaning and replacement is therefore required, resulting in high operating costs.

In filtration systems, it is observed that the flux declines from an initial value and reaches a steady value over time. Therefore, permeate flux can be expressed as a function of resistance:

$$J = \frac{\Delta P}{\mu[R_m + R_c]} \tag{2.1}$$

where J is the permeate flux, ΔP is the TMP, R_m and R_c are resistances due to membrane and cake layer deposited on the membrane surface respectively and μ is the viscosity of the permeate.

2.2.1 Types of Fouling

Fouling can be broadly divided into two types: a) reversible (back-washable) and b) irreversible (Figure 2.9). When the membrane surface comes into contact with activated sludge, various components of biomass are deposited onto it. In the case of reversible fouling, this deposited layer (cake) is readily removable by an appropriate physical washing process (backwashing). On the other hand, irreversible fouling is caused by pore blocking, which is non-washable by normal hydraulic backwashing.

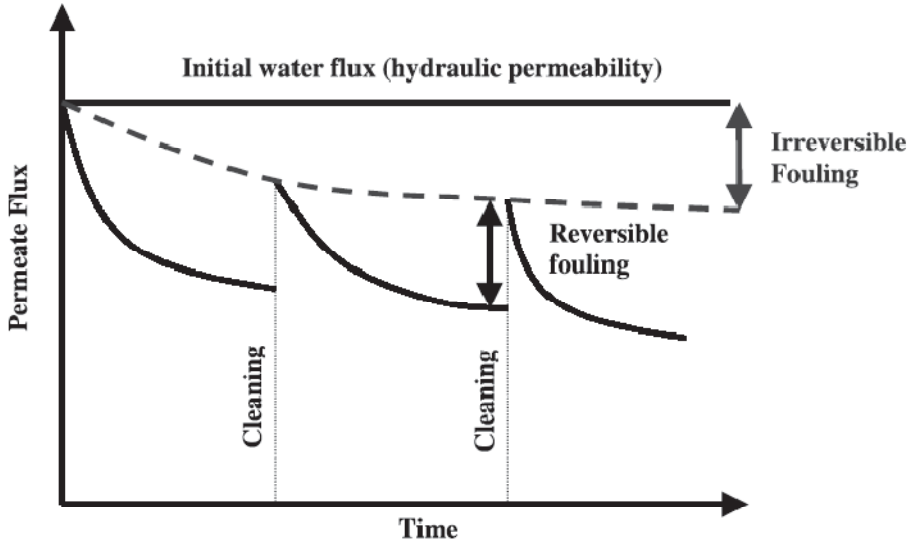

Figure 2.9 Reversible and irreversible fouling in membrane system (Faibish & Cohen 2001)

According to the fouling materials, four types of fouling are recognised.

(a) Inorganic fouling (scaling): Inorganic fouling or scaling is the deposition of inorganic precipitates, such as metal hydroxide, on the membrane surface or within pore structures. Fouling occurs when the concentration of these chemicals exceeds their saturation concentrations. Scaling is a prime concern for reverse osmosis and nanofiltration since these membranes reject inorganic species. In the case of microfiltration and ultrafiltration, inorganic fouling is less profound but can occur as a result of interactions between ions and other fouling materials.

(b) Particle/colloidal fouling: Particles/colloids cover a wide size range, from a few nanometers to a few micrometers. Examples of aquatic colloids are clay minerals, colloidal silica, iron, aluminium and manganese oxides, organic colloids, suspended matter, and calcium carbonate precipitates. During membrane fouling, colloids accumulate on the membrane surface or in membrane pores and cause both reversible and irreversible fouling. The particles/colloids referred to here are biologically inert particles and colloids that are inorganic in nature and originate from weathering rock. Flux decline due to colloidal fouling is easily recoverable by hydraulic cleaning measures such as backwashing and air scouring. Particle deposition on the membrane surface produces a cake layer which eventually becomes compressed and reduces water productivity. In the case of reverse osmosis and nanofiltration, colloidal fouling is mostly caused by the accumulation of particles on the membrane surface in a cake layer. This cake layer provides an additional hydraulic resistance to the permeate flux through the membrane and reduces the product water (Zhu & Elimelech 1995). However in the case of microfiltration, pore blocking by colloidal particles can be an important fouling mechanism, in addition to particle accumulation on the membrane surface (Belfort, Davis & Zydney 1994). The extent of pore blocking and cake layer formation depends on the relative size of the particles compared to the membrane pore size.

In this study, colloidal fouling was investigated to understand the effect of operating parameters on membrane fouling. Kaolin clay was used as the colloidal medium during the submerged membrane microfiltration.

(c) Microbial/biological fouling: Biological fouling is a result of bio-film formation on the membrane surfaces by the adhesion and accumulation of micro-organisms such as bacteria, algae, fungi and bio-polymers. Once the micro-organisms attach to the

membrane surface, they multiply and produce extracellular polymeric substances (EPS) resulting in the formation of viscous, slimy, hydrated gel. This jelly structure protects bacterial cells from hydraulic shearing and chemical attacks by biocides.

(d) Organic fouling: Dissolved naturally occurring matters (NOM) are the major cause of fouling in membrane filtration of natural water. A large percentage of NOM are humic substances which are refractory anionic macromolecules of low to moderate molecular weight and cause irreversible fouling (Jucker & Clark 1994). Aoustin et al. (2001) reported that fulvic acids were the main reason for reversible fouling in ultrafiltration. The majority of natural organic matters penetrate through micro- and ultra-filtration membranes because of their small size. Schafer et al. (2000) observed that there was a high possibility of membrane pore blocking due to organic matters.

2.2.2 Causes of Membrane Fouling

Membrane fouling still presents the most difficult challenge to the design and operation of membrane systems. All the parameters involved in filtration design and operation influence membrane fouling behaviour. Although it is not easy to develop a general rule for membrane fouling, many researchers (Chang & Judd 2002; Le-Clech, Chen & Fane 2006; Zhang et al. 2006) list the following three factors as strongly affecting the nature and extent of fouling: biomass characteristics, operating conditions, and membrane characteristics. The three main factors and the parameters of each factor are illustrated in Figure 2.10.

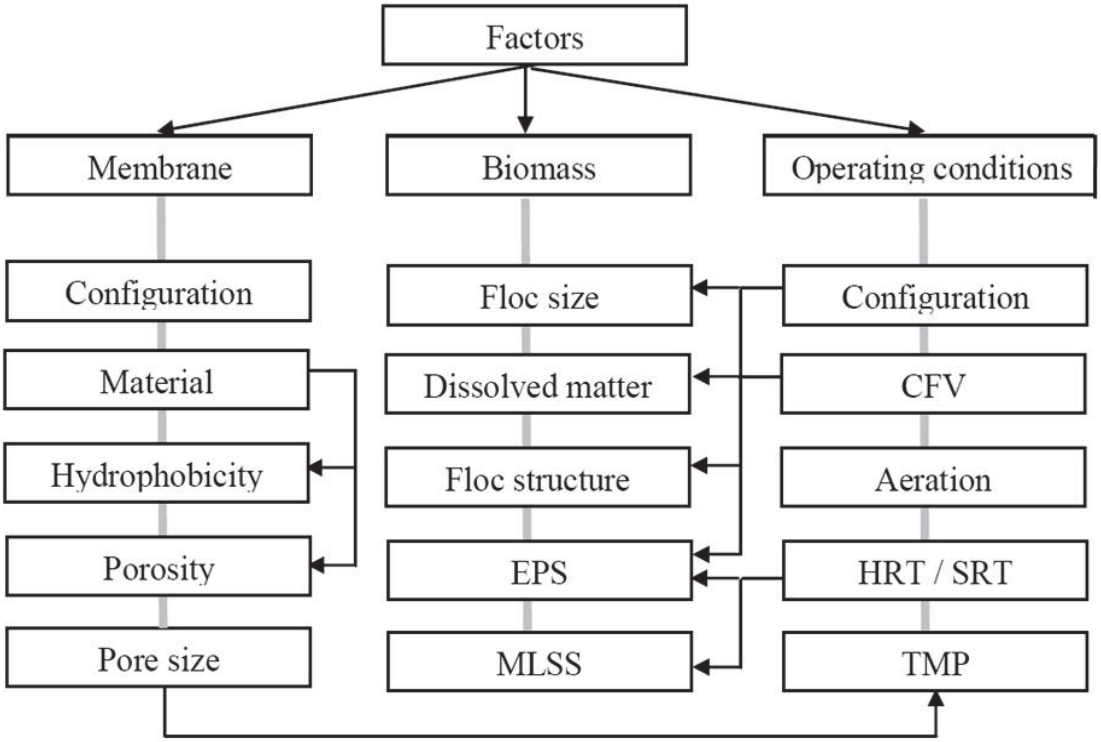

Figure 2.10 Factors influencing membrane fouling in MBR process (Chang & Judd 2002)

Drews (2010a) pointed out the need to divide the operating factors into biological and membrane operation parameters. She also suggested including the geometrical design aspects of both the module and MBR tank. Judd (2006) added two more factors, aeration port and module dimensions, to the original three factors. Filtration performance can be highly influenced by the interactions of the membrane (shape, module, configuration), the biological characteristics of the activated sludge (secondary process: biological growth) and the operating conditions (transmembrane pressure, permeate flux, air flow, backwash, relaxation). Apart from fouling, membrane cleaning approaches and methods also affect system performance. The cleaning chemical might also change the membrane's susceptibility to foulant attachment. Figure 2.11 shows how engineering decision variables affect membrane performance in terms of the loss of permeability of the membrane module via a network of interrelated biomass characteristics and hydrodynamics.

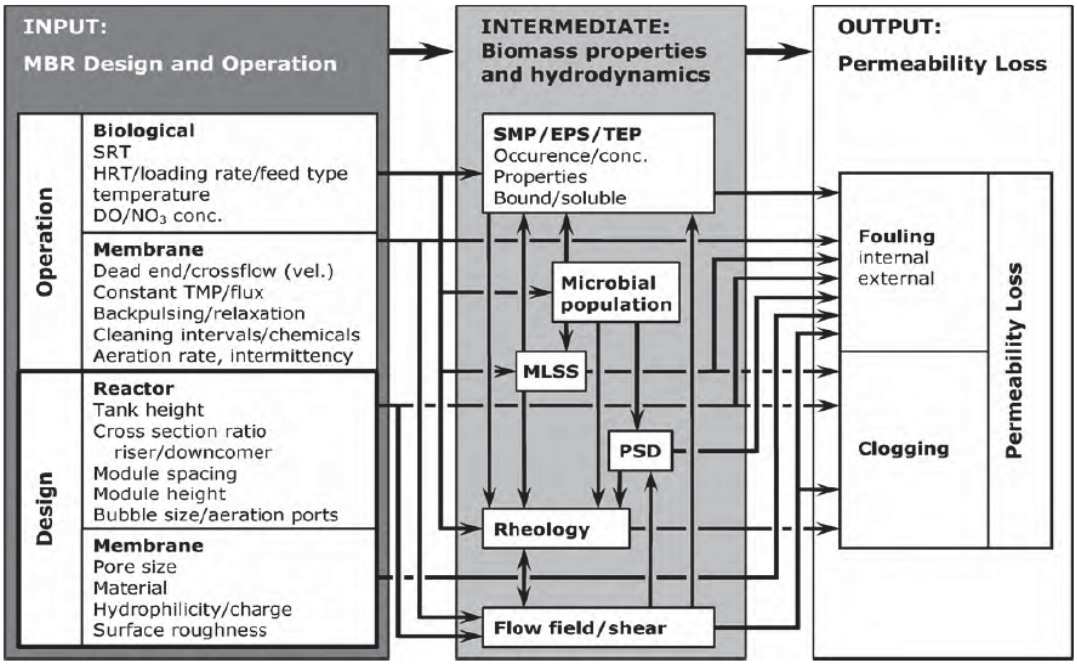

Figure 2.11 Inter-relationship between engineering decisions and permeability loss (Drews 2010a)

2.2.2.1 Membrane Properties

Membrane fouling is highly affected by membrane properties such as porosity, pore size, surface charge, roughness, configuration and hydropholicity/hydrophobicity. The fouling that occurs with porous membranes (microfiltration, ultrafiltration) is generally much more severe than that occurs with dense membranes (reverse osmosis). In the case of microfiltration, membranes hydrophobicity affects wet-ability, applied pressure requirements for liquid flow through the membrane and fouling propensity (Meng et al. 2006). The hydrophilic membranes are less prone to fouling than hydrophobic membranes. More fouling was observed during hydrophobic membrane filtration than filtration with hydrophilic membranes (Belfort, Davis & Zydney 1994; Chang, Lee & AHN 1999; Choi et al. 2002; Judd & Till 2000). Fane et al. (1991) preferred hydrophilic membranes for wastewater treatment.

Practically, filtration membrane selection depends on membrane pore size, the purpose of filtration and the particle size distribution of the feed solution. The effects of pore

size on fouling greatly depend on the characteristics of the activated sludge, particularly particle size distribution. A small pore size distribution can reduce fouling, and it has been observed that UF membrane have a lower tendency to foul because the smaller pores are more impenetrable. Larger pore sizes do not always result in high flux because they are more susceptible to internal fouling (Hong et al. 2002). The influence of membrane pore size modification on membrane fouling was studied by Worrel et al. (Worrel et al. 2007) who reported that flux can be increased and decreased by stretching the membranes. The membrane pore sizes of current commercial submerged MBR processes are approximately 0.04 μm to 0.4 μm.

2.2.2.2 Biomass Characteristics

Depending on its source, the activated sludge may contain various concentrations of suspended solids and dissolved matter. Suspended solids may consist of inorganic particles, colloids and biological debris, such as microorganisms and algae. Dissolved matter may consist of highly soluble salts, such as chlorides, and sparingly soluble salts, such as carbonates, sulfates, and silica. Therefore, activated sludge is a very complex and heterogeneous suspension containing both wastewater components and metabolites produced during biological reactions as well as the biomass itself. Biofouling depends on the structure of the biofilm layer formed on the membrane surface during the filtration process. The new term ‘biocake’ (Lee et al. 2007) was recently introduced to represent the biofouling layer caused by both cake formation and biofilms. Different components of the mixed liquor, ranging from flocculant solids to dissolved polymers such as EPS and soluble microbial product (SMP) can contribute to biocake formation, and mixed liquor suspended solids (MLSS) concentration is directly responsible for

cake layer resistance. Fane et al. (1981) reported a linear relationship between membrane resistance and MLSS concentration.

A number of researchers examined the contributions of different species of activated sludge on membrane fouling. In the literature, activated sludge is divided into three different fractions of suspended solids, colloids and solutes, and their individual influences on fouling are reported separately. Bouhabila et al. (2001) reported that the three fractions of sludge had different levels of influence on membrane fouling. According to their study, MLSS, colloids, and solutes contributed 24%, 50%, and 26% of fouling resistance, respectively. Therefore they concluded that membrane fouling was mainly caused by colloids. Wisniewski and Grasmick (1998) divided the activated sludge into settleable, non-settleable and soluble particles and revealed that solutes, colloids, and MLSS contributed 52%, 25%, and 23% of the total fouling resistance respectively. Defrance et al. (2000) stated that the relative contributions of suspended solids, colloidal and dissolved matters to membrane fouling were 65%, 30% and 5% respectively. Chang and Lee (1998) designated EPS as the main component responsible for fouling by fractionation of the mixed liquor of sludge into floc cell, EPS and dissolved matter.

2.2.2.3 Operating Conditions

It is generally accepted that fouling occurs in the form of adsorption, pore deposition, cake formation, concentration polarization and/or biofouling. Their relative magnitudes depend on the membrane material and configuration, operating conditions and mixed liquor characteristics. Particles are transported to the membrane surface by the drag force of permeate flux. Depending on the particle-particle interactions, the particle-membrane interactions and the hydrodynamic condition on the membrane surfaces,

deposited particles can be transported back into suspension via Brownian diffusion, inertial lift and shear-induced dispersion (Wiesner, Tarabara & Cortalezzi 2005).

Design modifications and operation improvements have significantly improved system efficiency. In early applications, a sidestream configuration was employed to maintain high cross-flow velocities to control fouling. However, this method was considered uneconomical in large scale applications due to the complex operation process, high energy cost associated with pumping and increased fouling from the breakup of large floc (Shimizu et al. 1996). With the introduction of the submerged operation in the mid 1990s, the operation cost was reduced substantially. Vigorous sparging aeration coupled with the lower fluxes resulting from this operating mode greatly reduce fouling. Nevertheless, the energy required to provide sufficient air usually exceeds that required to run a conventional activated sludge plant.

Experimental and empirical studies have identified cross-flow velocity (CFV) has a major influence on membrane fouling (Defrance & Jaffrin 1999; Tardieu et al. 1998). The CFV keeps the particles away from the membrane surface and thus reduces cake layer thickness by increasing the shear and shear-induced diffusion. In submerged membrane systems, CFV is produced by aeration which provides oxygen to the biomass, maintains the solids particles in suspension and scours the deposited layer on the membrane surface (Le-Clech, Chen & Fane 2006).

2.3 Antifouling Remedies

It is universally accepted that fouling is inevitable, but its impact can be limited by a better understanding of the substances and mechanisms responsible. The choice of membrane module, process configuration, pretreatment and operating conditions are all important for membrane fouling control to varying extents. The success of a membrane

operation depends on careful selection of those parameters. Numerous studies have focused on understanding membrane fouling behaviour and many anti-fouling strategies have been proposed for MBR applications. In general, there are three main antifouling practices: improving the antifouling properties of the membrane, pre-treating the biomass suspension, and operating the membrane process under specific non- or low-fouling conditions. The optimisation of these antifouling practices could lead to the best technique for achieving minimum fouling in the system.

2.3.1 Optimising Membrane Characteristics

Membrane characteristics such as pore size, porosity, surface charge, roughness and hydrophilicity/hydrophobicity, have been proven to impact on membrane fouling. The optimisation of these membrane properties has been found to efficiently improve anti-fouling behaviour. A narrow pore size distribution is preferred to control membrane fouling both in the MBR process and in conventional membrane separation processes. Choo and Lee (1996) reported the optimum pore size based on the particle size distribution of anaerobic broth.

The membrane materials always show different fouling behaviours as a result of their varying pore size, morphology and hydrophobicity. Polymeric membranes are more popular than ceramic membranes. Polyvinylidene fluoride (PVDF) membranes were found to be better than polyethylene (PE) membranes in terms of the mitigation of irreversible fouling when used in municipal wastewater treatment MBRs (Yamato et al. 2006). Inorganic membranes, such as aluminium, zirconium and titanium oxide, demonstrate superior hydraulic, thermal and chemical resistance.

Hydrophobic membranes are more susceptible to membrane fouling than hydrophilic membranes because of the hydrophobic interaction between the foulant and the

membrane material. Therefore, special efforts have focused on controlling membrane fouling by modifying hydrophobic membranes to be relatively hydrophilic (Yu et al. 2005a; 2005b).

In addition to membrane modification, the development of economical, high flux, non-fouling membranes (low-fouling membranes) is important before sustainable MBR processes can be achieved (Shannon et al. 2008). The low-fouling (non-fouling) membranes should have much narrower pore size distribution, stronger hydrophilicity and larger porosity than the membranes currently used.

2.3.2 Pretreatment of the Feed

To mitigate membrane fouling and enhance the permeate flux (system performance), a number of different approaches, namely (a) chemical, (b) hydrodynamic and (c) physical (Belfort, Davis & Zydney 1994), have been pursued. Chemical methods involve the modification of the membrane surface chemistry to increase the repulsion between the membrane and the particles available in the feed suspension, as described in 2.3.1. This increased repulsion causes less deposition, resulting in less membrane fouling. Hydrodynamic methods consist of the application of secondary flow to produce turbulence in the membrane module and/or reactor tank in such a way that deposited particles on the membrane are transported back to the tank. While chemical and hydrodynamic approaches focus on changes to the membrane properties and operating conditions respectively of the filtration system, physical methods involve the pretreatment of the feed solution. Pretreatment of biologically treated sewage effluent prior to its subjection to membrane processes will reduce cell deposition and subsequent bio-growth resulting from dissolved organic matter (Redondo & Lomax 2001). Pretreatment also reduces the need for frequent chemical cleaning, which is a major

factor impacting membrane life, and offers considerable potential for improving the efficiency of membrane processes. At present, pretreatment processes used to remove foulants (mainly particles and organic matter) prior to the membrane separation have become an important aspect of any membrane process. Pretreatment prior to membrane filtration can improve the final quality of water and greatly reduce fouling. A range of pretreatment processes is being used in the water industry, among which the most popular methods are coagulation and adsorption.

2.3.2.1 Coagulation/Flocculation

Practical experience and research works indicate that fouling is associated with the presence of dissolved organic materials and small colloidal particles in wastewater. Matsumoto et al. (1988) speculated that significant fouling was due to colloids in cross-flow microfiltration units. Similarly, Haberkamp et al. (2007) observed that the most severe fouling results from colloidal and dissolved organic substances during membrane ultrafiltration in tertiary treatment. In addition, many researchers have focused on identifying the constituents of colloidal matter and dissolved organic matter that most severely contribute to membrane fouling. Lee et al. (2007) observed colloids in the size range of 0.2-1.2 μm as being the most significant cause of fouling during the ultrafiltration of secondary effluent. Previous researchers (Huisman, Tragardh & Tragardh 1999; Tanaka et al. 1994; Wickramasinghe 1999) have reported that the presence of smaller particles results in flux decline for polydispersed feeds during microfiltration. Foley et al. (1992) studied the particle size distribution of yeast cells in the retentate during microfiltration and found that the smaller cells in suspension preferentially deposited on the membrane surface. Therefore, membrane fouling due to colloidal and fine particles is widely recognised as being responsible for the flux decline that impedes the performance of the whole filtration system. A reduction in colloids and

fine particles in the feed solution can greatly mitigate membrane fouling and can be achieved during the coagulation-flocculation process. In coagulation-flocculation processes, external agents (chemical) are added to the feed suspension to facilitate the agglomeration of fine particles and colloids to produce larger particles that can be easily separated from the liquid. Research studies have shown that the flux decline in microfiltration can be substantially improved by flocculation (Guo et al. 2005; Kim, Akeprathumchai & Wickramasinghe 2001a; Peuchot & Ben Aim 1992; Wickramasinghe, Wu & Han 2002). Peuchot and Ben Aim (1992) reported that fine particles are principally responsible for fouling in cross-flow microfiltration and that flocculation causes an increase in the particle size and hence the permeate flux. Lee et al. (2001) reported that small biological colloids (ranging in size from 0.1 to 2 μm) coagulated and formed larger floc when alum was added to the activated sludge. Fan et al. (2007) suggested that this effect is due to the aggregation of colloidal and dissolved matter into particles that are too large to cause pore narrowing and pore plugging.

Kim et al. (2001a) conducted microfiltration of yeast suspension with a number of polymeric flocculants (six catinonic, one nonionic and one anionic). Their results for flocculation prior to microfiltration showed improvement in the filterability of the feed due to the increase in the average particle size and hence the permeate flux. They also found an optimum polymer concentration, which maximized the degree of flocculation. Furthermore, they observed that the mixing conditions during flocculation affected the degree of flocculation.

Wickramasinghe et al. (2002) similarly claimed that the flocculation prior to microfiltration led to an improved permeate flux. They tested different types of commercially available cationic polyacrylamides and determined the optimum

flocculant dose and stirring conditions for each polymer. They also measured the particle size distribution before and after flocculation and concluded that the permeate flux was strongly dependent on the particle size distribution. The permeate flux increased with the larger molecular weight and charge density of the flocculant.

The effect of flocculation conditions on membrane permeability was studied by Cho et al. (2006). They carried out a coagulation–microfiltration process to remove natural organic matter using polyaluminium chloride (PACl) as coagulant. The effect of flocculation conditions on microfiltration performance was investigated using three membrane modules: stirred cell, dead-end, and submerged microfiltration. After analysing their experimental results in terms of filterability, particle size, and floc structure, they concluded that the higher permeate flux with longer flocculation time was due to the formation of loose and porous flocs and the reduction of small colloidal particles.

Citulski et al. (2008) tested the efficacy of alum and ferric chloride in-line coagulation pretreatment of secondary effluent on submerged hollow-fibre ultrafiltration. They found that both coagulants caused a shift in the particle-size distribution of organic matter in the feed towards larger fractions, with a significant reduction in colloidal matter. They observed fouling reduction with both lower and higher membrane packing density modules which was reflected in a reduction of average daily TMP increases, as well as a reduction in TMP.

In-line coagulation refers to the dosing of coagulant into feed water, rapid mixing, allowing flocs to form but not to settle, and finally feeding the resulting water with flocs to microfiltration or ultrafiltration. In-line coagulation, therefore, involves the use of flocculants without the removal of coagulated solids by a prior filtration process. The

coagulation process deals with the destabilization of colloidal particles, which are usually of sub-micron size, that are often encountered in water and wastewater treatment (Johnson & Amirtharajah 1983). During this process, colloids continue to change chemically and overcome the forces that maintain stable suspension, promoting aggregation and the formation of bigger particles called floc. Removal is accomplished through a series of destabilization and precipitation processes, namely (1) compression of diffusion layer, (2) adsorption to produce charge neutralization, (3) enmeshment in precipitate, and (4) adsorption to permit inter-particle bridging (Duan & Gregory 2003; Johnson & Amirtharajah 1983).

Different types of flocculants are used for coagulation-flocculation processes. Ferric chloride and aluminium sulfate (alum) are frequently used as a coagulant for water and wastewater treatments to reduce membrane fouling. Hydroxide precipitates are formed when alum is dissolved in water which adsorb substances such as suspended particles, colloidal particles and soluble organic and produces large floc. Large microbial flocs are expected to have a lower propensity for membrane fouling; therefore, membrane performance enhancement for hybrid coagulant/MBR systems is attributed to the formation of larger flocs during coagulation. Mesdaghinia et al. (2005) evaluated ferric chloride and alum efficiencies in an enhanced coagulation process. They reported that coagulation with ferric chloride proved to be more effective than alum at similar doses with mean values of treatment efficiencies of 51% and 32% for ferric chloride and alum, respectively. Moreover, ferric chloride produced less sludge than alum and is therefore considered to be the better chemical for coagulation. In addition to these coagulants, zeolite (Lee et al. 2001), ferric iron (Park, Lee & Park 2005), and polymeric coagulant (Wu et al. 2006) have also been used in MBRs.

2.3.2.2 Adsorption

Since the MF and UF do not have the capacity to completely remove organic foulant including colour, natural organic matter (especially low molecular humic substances) and synthetic organic chemicals, conventional treatment processes like adsorption are coupled with a membrane process to enhance membrane performance. Membrane hybrid systems are emerging as the most promising solutions for controlling the fouling because they are simple and easy to implement. The incorporation of physico-chemical treatments such as adsorption and ion-exchange in the submerged membrane system depends on the characteristics of the feed water and the quality of the output requirement. Many researchers have studied the short term and long term adsorption effects of PAC with the membrane processes (Guo et al. 2005; Vigneswaran et al. 2007). In these studies, the main aim of adding PAC to the system was to reduce the direct organic loading to the membrane surface. Based on the long term operation of a membrane hybrid system, Vigneswaran et al. (2007) recommended a minimal amount of PAC of 10–15 g/m^3 of water treated. They found that the energy requirement of the submerged membrane system was very low (as low as 0.2 kwh/m^3). Moreover, they also developed a simple mathematical model to predict the effluent quality of the submerged membrane-adsorption hybrid system. Similarly, semi-empirical mathematical models have been used to predict organic removal in adsorption membrane hybrid systems (Campos et al. 2000a; 2000b; Guo et al. 2005). Campos et al. (2000a) reported the effect of organic removal by different methods of PAC application in an adsorption-membrane hybrid system.

Similarly, granular activated carbon (GAC) is also used as an adsorbent in a microfiltration-adsorption system for treating organic-laden wastewater. GAC has a strong affinity for binding organic substances even at low concentrations. Many

researchers found that lower molecular weight fractions of organic matter are more absorbable by GAC in a multi-component system (Lee, Snoeyink & Crittenden 1981; Yuasa et al. 1997). In the competitive adsorption circumstance that usually exists in a multi-component system, hydrophobic substances are more absorbable onto the GAC surface than hydrophilic substances. Chaudhary et al. (2003) investigated a low strength synthetic wastewater for biodegradation and adsorption onto granular activated carbon with and without the presence of background inorganic compounds. They observed slow biodegradation of organic compounds in wastewater and concluded that the state of the adsorption equilibrium depends on the initial adsorbate (organic) concentration.

Adsorption removes large and small molecular weight hydrophobic organic compounds; however, the biologically treated sewage effluent also contains a significant portion of hydrophilic organic compounds. These compounds can successfully be removed by a pretreatment of ion exchange. Ion exchange resins such as Magnetic Ion Exchange resin (MIEX®) resin and Purolite can effectively remove dissolved organic matter from biologically treated sewage effluent (secondary effluent) and produce high quality water. When MIEX® contactor was used as a pretreatment for a submerged membrane hybrid system, a higher effluent quality and longer operation time could be achieved (Zhang et al. 2008). Croue et al. (1999) reported that strong anion exchange resins removed dissolved organic carbon (DOC) better than weak anion exchange resins and the increase in ionic strength enhanced the removal of natural organic matter. The Purolite resins have been used in several water treatment plants to remove toxic ions such as ammonia, nitrate, cyanide, lead, cerium (Abo Farha et al. 2009; Fernando, Tran & Zwolak 2005; Samatya et al. 2006). Very little literature is available on the use of Purolite in the removal of organic matter from wastewater.

2.3.3 Operational/Hydrodynamic Modification

All the parameters involved in the design and operation of membrane processes have an influence on membrane fouling. One major factor concerns the operating conditions of membrane microfiltration. The main objective of improving and modifying operational conditions is to enhance membrane system performance by reducing fouling. Hydrodynamic approaches are very effective and promising in mitigating membrane fouling in a MBR system, and numerous research works have been carried out to investigate the hydrodynamic modification of the membrane system, some of which are described below.

2.3.3.1 Submerged Rotating Disc Membrane

Leiknes et al. (2004) investigated the feasibility and potential of a hybrid process that combines ozonation and biofiltration with a rotating disk membrane for treating drinking water with high NOM concentrations. They introduced a rotating membrane disk bioreactor downstream of an ozonation process to carry out both the biodegradation and biomass separation in the same reactor. The rotation of the membrane discs was targeted to generate shear force adjacent to the liquid membrane interface and facilitate the reduction of mass transfer resistance. The results indicated that the hybrid system can be favourably used in an ozonation/biofiltration process by carrying out both biodegradation and biomass separation in the same reactor.

2.3.3.2 Vibrating Membrane

Culkin and Armando (1992) commercially applied vibrations to mitigate membrane fouling in a process known as vibratory shear enhanced processing (VSEP). This system consists of a stack of membrane discs firmly mounted in a circular casing connected to a torsion spring and a motor. The motor produces a vibrating action on the membrane

elements, and the vibration is aimed at disrupting the concentration's polarisation and deposition layers. In a vibratory module, the shear rate at the membrane is induced by the inertia of the liquid, causing the shear rate to decline with an increase in fluid kinematic viscosity (Al Akoum et al. 2002b). The vibrating membrane unit is promoted by Pall Filtration, USA, and is known as the PallSep Vibrating Membrane Filter. Unlike a conventional cross-flow system, the shear wave induced by the vibrating action of the VSEP unit disturbs the deposited particles on the membrane surface, thereby transporting the particles back to the bulk solution. The shear rate generated by a commercial VSEP module is approximately an order of magnitude higher than that of a cross-flow system (150,000/s at 60 Hz). The shear rate of the PallSep system, which is a similar system to the VSEP unit, is in the range of 100,000 to 150,000/s (PallSep 2004). In addition to the high shear, it was claimed that the permeate rate achieved with PallSep and VSEP modules were respectively 9.5 times and about ten times higher than the cross-flow system (Culkin & Armando 1992; PallSep 2004).

Many studies on the application of the vibrating concept have been reported in the literature (Al Akoum, Ding & Jaffrin 2002a; Al akoum et al. 2002c; Krantz et al. 1997; Low, Han & Jin 2004; Postlethwaite et al. 2004). Al Akoum et al. (2002c) compared the performance of vibratory membranes to other shear-induced diffusion mechanisms, such as dean vortices, and gas-liquid two phase flow. In this study, gas was injected inside the tubular membrane module to produce Taylor bubbles or liquid slugs. The analysis of the mean wall shear stress induced by these mechanisms revealed that gas-liquid two phase flow had the lowest shear stress (0-5 Pa) compared to dean vortices (10-40 Pa) and VSEP (40-70 Pa), causing the correspondingly lowest permeate flux. These findings emphasize the importance of shear rate in controlling membrane fouling.

2.3.3.3 Cross-Flow Velocity (CFV)

The application of cross-flow velocity is another technique to control membrane fouling during filtration. Many studies have investigated the influence of cross-flow velocity on the performance of a filtration system (Bertram, Raymond & Pedley 1991; Riesmeier, Kroner & Kula 1987). Their results demonstrated that higher fluxes were achieved at higher cross-flow velocities. During cross-flow microfiltration, the axial primary flow is supposed to take suspended particles away to prevent their aggregation at the membrane surface. In fact the most significant difference between cross-flow and frontal filtration is the hydrodynamic condition of the main flow. Indeed, in classical frontal filtration, all the suspended particles are accumulated on the filter, resulting in flux decline so that generally, periodic cleaning of the system is required after only a short time. Cross-flow filtration has been developed to avoid this dramatic loss of filtrate flux. In this system, a shear stress is exerted at the membrane surface so that the continuous deposition of particles is prevented.

Both experimental and empirical studies have proved that cross-flow velocity has a major influence on membrane fouling (Defrance & Jaffrin 1999; Tardieu et al. 1998). Choi et al. (2005) studied the influence of cross-flow velocity on the formation of the fouling layer during microfiltration (MF) and ultrafiltration (UF) of biological suspension. Their results showed that permeate flux increased linearly with increasing cross-flow velocity, and that a high cross-flow velocity was more effective in reducing fouling of microfiltration membranes than ultrafiltration membranes. However, high cross-flow velocity is related to high energy requirement.

2.3.3.4 Standing Vortex Waves (SVW)

Bellahouse et al. (1994) introduced a combination of oscillatory flow and altered flow deflectors in a membrane channel to produce standing vortex waves (SVW) to reduce membrane fouling. They used flat plate membrane ultrafilters to filter solutions of bovine serum albumin (BSA) with different geometries of flow deflector. They compared the performance of a Millipore Pellicon ultrafilter and a SVW ultrafilter and found similar filtration flux at low concentrations of BSA. At high concentrations, however, flux was significantly improved in the SVW device. Compared to conventional ultrafiltration, they claimed that the application of a standing vortex wave could enhance the filtration flux by a factor of 4.5 at high concentrations of BSA. Millward et al. (1996) recommended this technique as an effective alternative to conventional bioreactors.

2.3.3.5 Insert/ Baffles and Pulsatile Flow

Another concept to mitigate fouling is the application of insert/baffles and pulsatile flow into the membrane channel. Inserts have been used as static mixing devices and turbulence promoters (Mavrov et al. 1992). Finnigan and Howell (1990) investigated the two distinct modes of filtration with a tubular membrane: (a) using ring-shaped baffles alone, and (b) combining baffles and pulsatile flow. They used baffle inserts together with pulsatile flow to generate a vertex to improve fluid mixing in the region near the membrane surface and to interrupt cake layer development, thereby improving permeate flux. Their findings showed that the installation of baffles improved the flux by a factor of approximately 3 and further enhancement was achieved with a combination of baffles and pulsatile flow (by a factor of about 5 compared to tubular membrane only).

Krstic et al. (2002) reported the effectiveness of turbulence promoters on cross-flow microfiltration with organic membranes. They used a Kenics static mixer as a turbulence promoter and observed a flux enhancement of up to 500%. They found that there was improved energy efficiency with turbulence promoters during cross-flow microfiltration. Many experiments have proved that the application of turbulence promoters improves the filtration flux which is correlated with the increase in wall shear stress generated by the static mixer (Mavrov et al. 1992). The variation in fluid hydrodynamics increases the shear stress that promotes flow vortices, resulting in low membrane fouling.

2.3.3.6 Membrane Cleaning

Membrane cleaning comprises intermittent physical cleaning (backwashing) and periodic chemical cleaning. It is common practice in submerged systems to periodically backflush the membrane, i.e. permeate flux is pumped back through the membrane into the feed channel to remove the deposited particles on the membrane surface (Bouhabila, Ben Aïm & Buisson 2001). The effectiveness of this approach depends on the nature of the fouling mechanism, as backflush may be ineffective for pore blocking and deposition of inorganic materials (Yoon et al. 1999).

The application of air for backflushing is also used in aerated membrane systems (Choo & Stensel 2000; Scott et al. 1998). An important feature of the Memcor® continuous microfiltration operation is the patented air backwash system (Limited 1990). In this system, filtration stops when the pressure difference across the membrane (TMP) approaches a predetermined level, and high pressure air is injected at the permeate sides of the membrane in such a way that air flows through the membrane pores, detaching the deposited particles on the membrane surface.

2.3.3.7 Application of Air Flow

Another promising method for enhancing the performance of membrane systems that has been used and developed over the past decade is to inject air through the membrane module. The degree of enhancement and the mechanisms that lead to improvement in the performance of an aerated membrane system have been the focus of many studies, and are also investigated in this thesis.

2.4 Influence of Air Flow on Membrane Fouling

The application of air flow is a very popular hydrodynamic approach for membrane fouling control. Induced surface shear stress is a major strategy for controlling fouling. When air is injected into a stationary liquid, bubbles form and move upward by buoyancy force. The bubble motion creates a secondary flow which produces shear stress and scours particles deposited on the membrane surface; it also keeps the stationary liquid in motion by mixing. In submerged membrane systems, aeration is considered to be a major parameter in both hydraulic and biological process performance. In addition to the scouring and the mixing phenomena, air provides oxygen to the biomass, leading to better biodegradability (Le-Clech, Chen & Fane 2006). The effect of air bubbles can assist in overcoming issues regarding high packing density in hollow fibre bundles; nevertheless, it is difficult to achieve effective aeration throughout all the fibres in a bundle due to the uneven distribution of air induced shear intensity (Yeo, Law & Fane 2006).

This strategy was first proposed by Imasaka et al. in 1989, the developers of a gas-liquid two phase cross-flow microfiltration process coupled with an anaerobic digester. They verified that the injection of methane gas was an effective fouling control in ceramic membrane modules with low energy consumption. Lee et al. (1993) first carried out

experiments with flat sheet using entrapped bubbles to enhance the filtration of bacterial suspensions. They used a number of membrane plates with varying pore sizes and observed an improvement of 100% in permeate flux with a 300 kDa PS ultrafiltration and 30% using a 0.2 μm microfiltration membrane. Similarly, Cui and Wright (1994) showed up to 175% increase in filtration flux in yeast microfiltration after the application of air bubbles.

A comprehensive investigation on the effect of air flow on cake removal has been reported by Ueda et al. (1997) by using a pilot-scale submerged hollow fibre MBR. They found that the antifouling efficiency of uplifting air flow was affected by the turbulence of the flow. The authors observed that there was improved cake-removing efficiency of the uplifting air flow by augmentation of the air flow rate or by intensification of the aeration intensity (an air flow rate per unit floor area) over a small floor area. An optimum value of the air flow was also identified beyond which further increases had no effect on fouling control (Figure 2.12). Similar results were also reported by Bouhabila et al. (1998; 2001).

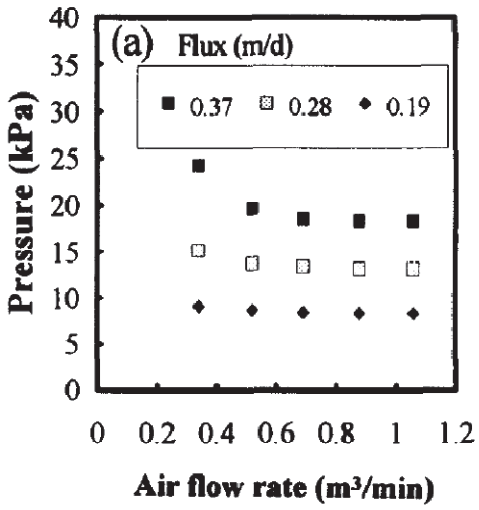

Figure 2.12 Suction pressure vs. air flow rate for different permeate fluxes (Ueda et al. 1997)

Laborie et al. (1997) conducted experiments using hollow fibre ultrafiltration with clay suspension. They reported that the increased air flow increased flux enhancement. In addition, they observed an optimum air velocity beyond which any further increase in air flow had a negative effect on flux. Similarly, Cabassud et al. (1997) demonstrated that the application of air could reduce the decline of permeate flux (Figure 2.13) and concluded that the higher the air flow rate the higher the steady state flux achieved.

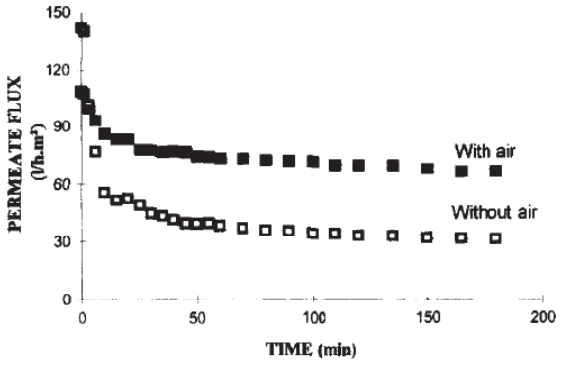

Figure 2.13 Effect of air flow on permeate flux (Cabassud et al. 1997)

Mercier et al. (1997) studied the use of gas-liquid two phase flow to reduce tubular membrane fouling by applying air directly into the feed stream. They conducted the experiments by filtering suspensions (bentonite and yeast) through an ultrafiltration tubular mineral membrane and measured TMP at various liquid and gas flow-rates. They observed a flux increase of 200% in a bubble flow system compared to a non-bubble system.

Tardieu et al. (1998) studied the importance of hydrodynamic control in the formation of a floc particle cake on the membrane surface. They reported that the presence of such a cake leads to the development of hydraulic resistance. In the case of MBR applied to wastewater treatment, the biological floc particles are capable of interacting among themselves, and with the membrane surface, in a differential manner, thus inducing a

change in membrane resistance. The authors therefore suggested that determining the critical flux value as a function of hydrodynamic and biological conditions is important.

Li et al. (1998) investigated the effect of injecting air into the feed side of flat sheet modules using four types of protein solutions: HAS, BSA, human immunoglobulin G (IgG), and lysozyme as test media. They found that gas sparging increased the permeate flux by 7-50%.

Mercier-Bonin et al. (2000) tested the effect of air bubbles for the flux enhancement microfiltration of bakers' yeast suspension using a ceramic flat sheet membrane. The authors reported that the flux increased up to 4 times. These studies used flat sheet membranes as external type applications.

Sur and Cui (2001) carried out a detailed study to investigate the effects of operating parameters such as feed concentration, TMP, cross-flow velocity, gas superficial velocity, and others on flux during an aerated cross-flow microfiltration of bakers' yeast suspension through a 5 mm diameter tubular membrane. They found the most significant flux enhancement occurred during severe cake formation, i.e. at high feed concentration and low liquid velocity. They noticed that as the air velocity increased from 0 to 0.18 m/s, a significant change in flux occurred, but that any further increase in air flow resulted very little change in flux. They revealed that air flow was the most effective at low liquid flow rates.

Ducom et al. (2002) investigated the effect of air flow injection for flat sheet membranes. They carried out nanofiltration with clay suspension (7 g/L) and achieved better flux improvement with higher gas velocity. Similarly, Liu et al., (2002) investigated the influence of hydrodynamic conditions (such as membrane flux, cross-

flow velocity and solid concentration) on membrane filtration resistances. They analysed the correlation between the increasing rate of membrane filtration resistance and the aeration intensity, filtration flux and sludge concentration. The increasing rate of filtration resistance was derived as a power function of the cross-flow velocity, filtration fluxes and suspended solid concentrations. They concluded that membrane filtration resistance sharply increased at a flux over the critical flux or at aeration intensity below the critical aeration intensity.

Cui et al. (2003) carried out a detailed review of the use of gas bubbling to enhance membrane processes that was particularly applicable in biotechnology, bioseparations and water and wastewater treatment. They reported on the applications of aeration in submerged membrane configurations and described the enhancement of performance offered by gas bubbling.

Meng et al. (2007) investigated the effect of aeration intensity (air scour), MLSS concentration, and sludge viscosity on membrane fouling on the basis of rheology and hydrodynamics concepts. The membrane fouling was mitigated more significantly with increased aeration intensity and a very strong effect of MLSS concentration on membrane fouling resistance was observed.

The studies of Mikulasek et al. (2002), Chua et al. (2002), Le-Clech et al. (2003), Cui and Taha (2003), Posposil et al. (2004), Germain et al., (2005b), Sur and Cui (2005), Ji and Zhou (2006), all validated the effectiveness of air flow in a range of membrane systems. They found that membrane fouling mitigation improves with increased air flow.

The hollow fibres (HF) and tubular membrane modules have been extensively studied because most membrane systems apply these types of modules. Few studies have been reported for flat sheet modules. Lee et al. (1993) reported that two phase flow enhanced the flux for ultrafiltration (UF) and microfiltration (MF) for submerged flat sheet organic membranes and for submerged flat sheet membranes. Churchouse and Wildgoose (1998) and Howell et al. (2004) studied gas-liquid two phase flow for fouling reduction and the provision of oxygen required for biological degradation in a membrane bioreactor.

2.5 Air Bubbles-Induced Antifouling Mechanisms

It is clear from the abovementioned studies and experimental observations that gas sparging disrupts the concentration polarisation layer to enhance filtration. Basically, air bubbles passing near the membrane surface induce local shear transients and liquid flow fluctuations, increasing the back transport phenomenon. The tangential shear at the membrane surface prevents particle deposition on the membrane surface. The following mechanisms have been identified as contributing to the observed flux increase, with the dominant mechanism depending on membrane configuration and the individual operation.

(i) *Bubble-induced secondary flow*: Moving bubbles generate secondary flows and wakes which disrupt the mass transfer boundary layer and promote local mixing near the membrane surface. This is similar to the enhancement of heat transfer in liquid convection by injecting gas bubbles. Slug-flow also results in an annular falling film as the displaced liquid flows downwards between the slug and the tube wall. The falling film can be a region of high shear promoting mass transfer.

(ii) *Physical displacement of the concentration polarisation layer*: Gas slugs penetrate the concentration polarisation layer and detach the upper part of it. For example, the liquid film thickness between the membrane wall and the slug in small diameter tubes, including hollow fibres, proves to be less than the calculated mass transfer layer thickness in single-phase liquid flow at the same liquid flow rate (Bellara, Cui & Pepper 1997).

(iii) *Pressure pulsing caused by passing slugs*: A moving slug causes pressure pulsing in the liquid around it, with a higher pressure at its nose and lower pressure at its tail. The mechanism is similar to that in the application of pulsatile flow. The injection of gas bubbles may also increase the mean pressure in the membrane system. Experimental evidence has shown that both factors contribute to flux increase (Sur, Li & Cui 1998).

(iv) *Increase in superficial cross-flow velocity*: High gas flow rate injection can significantly increase cross-flow velocity, which can result in a flux increase, although this is only significant with high gas flow rate sparging.

2.6 Effect of Bubble Characteristics on Mass Transport Process

The benefit of air bubbling for a mass transport process has been known for many years. In the case of membrane systems, the first use of bubbles was proposed by Imasaka et al. in 1989. They showed that an injection of methane gas generated from fermentation recycled to the ceramic membrane filter significantly increased permeate flux with low energy usage. The bubble system soon became popular due to the advantages of considerable flux enhancement and reduced energy cost. Even so, energy consumption by aeration is a major issue in bubble membrane systems. Few researchers have studied the effect of bubble characteristics on antifouling behaviour to minimise the aeration. A number of studies are available that have investigated the effect of air bubbles in

enhancing membrane performance, but few studies have focused on the effect of bubble shape, size and frequency on fouling control.

Li et al. (1997) carried out detailed experiments to study the effect of bubble size and frequency on the performance of gas sparged ultrafiltration with tubular membranes. They injected air in a controlled manner so that bubble size and frequency could be adjusted independently. They found an increased permeate flux with a bubbling frequency range of less than 1 Hz, and by analysing bubble wake dynamics, they concluded that bubble size and frequency have a strong influence on filtration flux during air injected ultrafiltration. Similar results were reported by Zhang et al. (2009). They divided the dependency of mass transfer on bubble size and frequency into two regions: an increasing region and a plateau region. Their findings showed that a higher permeate flux can be obtained by increasing the bubble frequency.

Similarly, Bellara et al. (1997) investigated the effect of bubbling frequency on permeate enhancement through air sparged ultrafiltration of macromolecules. They varied the bubble frequencies from 0.1 to 0.25 Hz under various filtration pressures and feed concentrations. It was found that, for a bubbling frequency range of 0.125 to 0.25 Hz, the flux at two different liquid velocities remained the same despite the fact that there was a difference of a factor of two in the cross-flow velocity. The permeate flux was observed to increase with bubbling frequency up to 0.125 Hz.

The effect of aerator types on the fouling in submerged MBR was investigated by Sofia et al. (2004) for microfiltration of domestic sewage. They applied coarse (2 mm diameter) and fine (0.5 mm diameter) bubble diffusers for air scouring during membrane operations and compared cross-flow velocities induced by these bubbles. They observed higher cross-flow velocity with fine bubbles than coarse bubbles within

an identical range of aeration intensity (Figure 2.14). Fine bubbles were reported to be more effective than coarse bubbles in slowing down fouling, and the authors concluded that uniformly distributed fine air bubbles might cause less uplift resistance and induce higher cross-flow velocities. Contrary to these results, another investigation carried out on single bubbles reported that larger bubbles formed larger wakes which were expected to mitigate the propensity for fouling due to the higher shear rates generated by the larger bubbles (Miyahara, Tsuchiya & Fan 1988). A possible explanation of this phenomenon is that smaller orifices produce higher bubble densities than coarse bubble diffusers at a given aeration rate. Therefore, the total shear generated by numerous fine bubbles could be greater than the total shear induced by a few large bubbles.

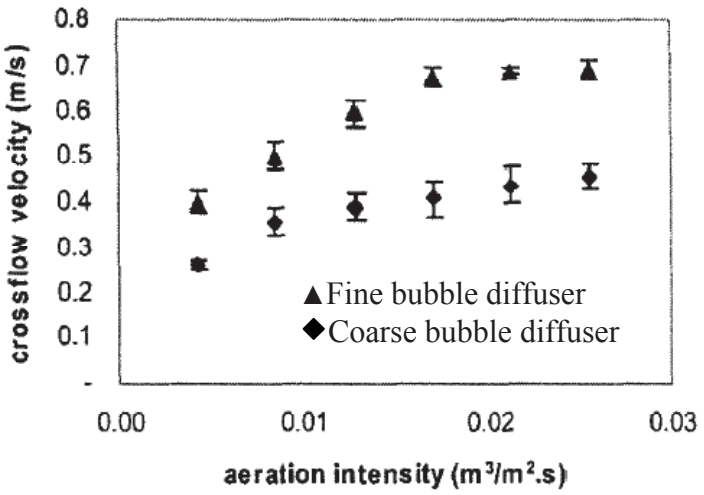

Figure 2.14 Cross-flow velocity vs. aeration intensity for two different types of diffuser (Sofia et al. 2004)

Later, Lu et al. (2008) studied the influence of bubble characteristics on the performance of submerged microfiltration using yeast as a model particle in water. They tested the performance of a hollow fibre membrane system by measuring the TMP under constant flux. They found that nozzle size had an effect on the size and shape of bubbles. They also observed that an increase in nozzle size beyond a threshold value

caused the gas flow pattern to be transformed from bubble flow to a single bullet-shaped slug flow.

Zhang et al. (2011) recently investigated the antifouling properties of two bubbling regimes on a flat sheet membrane microfiltration by treating municipal wastewater at very low aeration rates. The authors found that slug bubbles exhibited better antifouling performance in flat sheet MBR under both short term high flux operation and long term moderate flux operation. They revealed that the slug bubbling at low intensity (2.5 L/min) gave an excellent performance not only in limiting reversible fouling during the bubbling period, but also in releasing fouling that had occurred during the non-bubbling period. They proposed slug bubbling in flat sheet MBRs as an attractive alternative method to free bubbles.

The performance of air bubbles obviously varies for different membrane modules. The abovementioned literature highlights that within a particular membrane module, fouling behaviour is greatly affected by the flow pattern of air bubbles (bubble and slug flow). In the case of tubular and hollow fibre membranes, every slug bubble will sweep over the whole of the membrane surface, but in case of a flat sheet membrane, only some of membrane surface will come into contact with the bubbles. Compared to free bubbles, periodic slug bubbles in flat sheet MBRs are more effective and economic for enhancing fouling control (Zhang et al. 2011). Slug flow generates high wall shear stress while consuming only a very modest amount of air, and it is possible to envisage meeting biological needs through fine bubble aeration coupled with the use of periodic slug bubbling to control fouling in a MBR system. This combined aeration strategy will reduce the air requirement and the energy requirement.

2.6.1 Bubble Characteristics

When air is applied into a stationary liquid in a submerged membrane system, bubbles are generated and uplifted by buoyancy forces. The size and shape of the bubbles depend on the aerator type and air flow rate. The bubble movement produces a secondary flow behind the bubble, i.e. the wake region, and the strength and extent of this region are dependent on the size and shape of the bubble. The bubble motion in a liquid is decided mainly by the bubble's size, by the viscosities of the liquid and of the gas phases, and by the properties of the gas/liquid interface. When gas liquid two phase flow occurs in a wide channel, commonly observed bubble shapes are spherical, ellipsoidal or hemispherical, depending on bubble size. Clift et al. (1978) carried out a detailed investigation and developed a chart that correlates the shape of bubble with the Reynolds number and the Eotvos number (Figure 2.15). The properties of different bubble shapes are described below (Cui, Chang & Fane 2003).

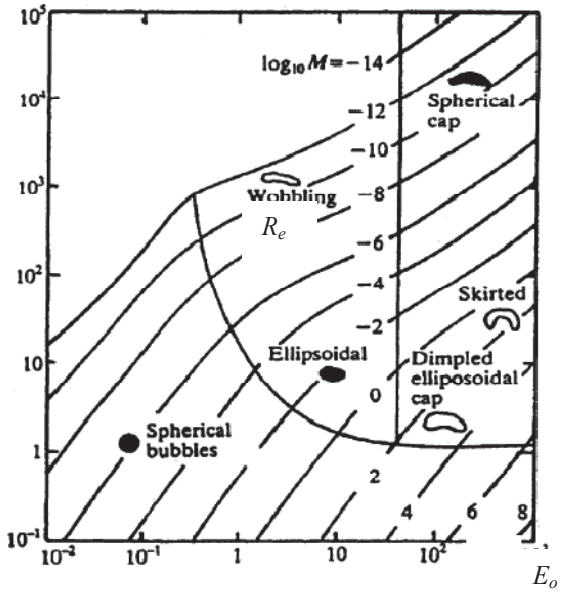

Figure 2.15 Characteristics chart (Clift et al. 1978)

Spherical bubbles: Size is typically less than 1 mm and the bubble can be treated like a solid particle which is lighter than the surrounding liquid. The terminal rise velocity of isolated bubbles is determined by Stokes' law ($Re < 1$),

$$u_{bl} = \frac{d_{bl}^2 g(\rho_l - \rho_g)}{18\mu_l} \tag{2.2}$$

which predicts a rise velocity of about 0.1 m/s for a 0.8 mm bubble. In equation 2.2, u_{bl} is bubble rise velocity, d_{bl} is the equivalent bubble diameter, g is gravitational acceleration, ρ_l and ρ_g are liquid and gas densities respectively and μ_l is the liquid viscosity. Equation 2.2 predicts that the bubble rise velocity is inversely proportional to the liquid viscosity. Therefore, bubble velocity in viscous media such as a biomass suspension can be different than it is in water.

Ellipsoidal bubbles: Sizes typically vary from 1.5 to 15 mm. The boundary layer separation occurs at a point at the bubble rim, and this point moves along the rim. The bubble is observed as a rocking disc and leaves a helical vortex starting at the boundary layer separation point at the rim. In the diameter range of 4–15 mm the bubble rise velocity in water does not change much and is approximately 0.24 m/s. This value would also tend to be lower in a swarm of bubbles and in liquids or suspensions of raised viscosity.

Spherical cap bubbles: Big bubbles (>15 mm) take a spherical cap shape, and the boundary layer separates at the circular rim which shields vortex rings. The primary wake is about 4.5 times the volume of the bubble. These big bubbles can create a strong secondary flow effect and enhance local mixing in the liquid. In water, the rise velocity of these bubbles is calculated by,

$$u_{bl} = 0.71(gd_{bl})^{0.5} \quad (2.3)$$

This equation predicts a rise velocity of about 0.3 m/s for a 20 mm bubble.

2.6.2 Bubble Flow Pattern

In gas-liquid two phase flow systems, different bubble flow patterns may be observed. Depending on the distribution of the two phases in the duct, four basic flow patterns (Figure 2.16) were reported by Taitel et al. (1980). They concluded that flow patterns depend on the gas and liquid flow rate, as well as on the diameter of the duct.

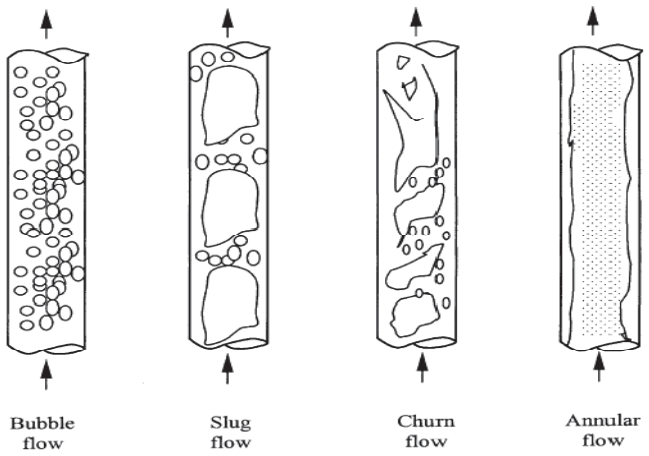

Figure 2.16 Bubble flow patterns for two phase flow in vertical pipe (Taitel et al. 1980)

- Bubble flow: The gas phase is approximately uniformly distributed in the form of discrete bubbles in a continuous liquid phase. The bubbles' behaviour is similar to that of bubbles in a stationary liquid.
- Slug flow: Slug flow occurs when the gas flows as large bullet-shaped bubbles that approach the diameter of the channel size. They move uniformly upward with small bubbles following them. This type of bubble is also known as a Taylor bubble. Around these bubbles, there is a thin falling liquid film which produces turbulence in the wake of the Taylor bubble. There are also small bubbles within the liquid, but many of these coalesce to form large bubbles until they span much of the pipe. In

gas-liquid mixtures, slug flow is similar to plug flow, but the bubbles are generally larger and move faster. As flow rates increase, slug flow becomes churn flow.

- Churn Flow: Churn flow is similar to slug flow but it is more chaotic, unstable, frothy and disordered. Churn flow occurs at relatively high gas velocity. As the gas velocity increases, it changes into annular flow.
- Annular flow: Annular flow is characterised by the continuity of the gas phase along the core of the duct. The liquid phase moves upwards, partly as a wavy liquid film and particularly in the form of drops entrained in the gas flow. Annular flow occurs at high velocities of the lighter fluid, and is observed in both vertical and horizontal wells. As the velocity increases, the film may disappear, leading to mist flow or emulsion flow. When the interface between the fluids is irregular, the term 'wavy annular flow' may be used.

The flow path for the gas-liquid mixture in two phase flow filtration is relatively narrow and the liquid velocity is usually set at a low value, so the bubble flow and slug flow are the most typical flow patterns found in these systems. In terms of flux enhancement, the slug flow pattern has been claimed to be the most efficient regime for controlling membrane fouling (Mercier, Fonade & Lafforgue-Delorme 1997). Numerous studies have demonstrated that the turbulence caused by air injection is effective for the control of particle deposition and cake polarisation on the membrane system (Cabassud, Laborie & Lainé 1997; Cui & Wright 1994; Mercier, Fonade & Lafforgue-Delorme 1995).

2.7 Effect of Air Flow on Energy Consumption

Laborie et al. (1998) compared the energy consumption between single-phase flow and two phase flow with an external HF membrane system in which most of the energy was

consumed by the air compressor and the re-circulation pump. The energy consumed by the system was calculated at two different liquid velocities: 0.5 m/s and 0.9 m/s with and without air bubbling. It was found that, for both liquid velocities, injecting air reduces the energy consumption significantly. Mercier-Bonin et al. (2000) also reported that two phase flow is more energy efficient. During the filtration of yeast suspensions, Mercier et al. (1997) observed that the energy consumption was 10 kW h m^{-3} of permeate with slug flow and 30 kW h m^{-3} under steady-state conditions with no air bubbling.

Gander et al. (2000) found that more than 90% of the energy consumption was for aeration in a submerged membrane system. To reduce this energy consumption, Guibert et al. (2002) formulated an aeration technique called 'air-cycling', which was designed specifically for the Zenon Environmental ZeeWeed 500® series immersed hollow fibre MBR. The air-cycling technique involves creating aerated and non-aerated zones within the HF module which create instability and increase the mixing between the fibres. This technique was found to reduce energy consumption by more than 30%. In an airlift system, in which a dextran solution was ultrafiltered, the energy consumption was found to be lower than that of a pumped system (Cui, Bellara & Homewood 1997). These authors concluded that the gas-liquid two phase system was more energy efficient than the pumped system, although it may result in slightly lower fluxes.

This research aims to study the hydrodynamic behaviour of colloidal particle deposition on the membrane surface under different operating conditions and different characteristics of suspension to contribute to the optimisation of membrane process design.

2.8 Application of External Agent to Reduce Air Flow

Optimisation of aeration is still the subject of practical and research interest, both in terms of reducing the foulant accumulated on the membrane and in relation to increasing the life of the membrane and reducing the energy cost. The optimisation of aeration will significantly reduce the operating cost of membrane filtration. A more detailed investigation on the impact of aeration rates on suspension is needed to gain a better understanding of membrane fouling and to reduce the cost of aeration, which is a major cost in membrane operation) (Chang & Judd 2002).

Another research step has focused on the control of membrane fouling by adding external agents such as powered activated carbon (PAC) and anthracite to the activated sludge in a bubble system. An addition of PAC to the MBR has been reported to increase permeability by improving the hydraulic properties of the cake, principally by increasing its bulk permeability and reducing its compressibility (Kim, Lee & Chun 1998). In addition, PAC addition contributes to a rise in the back-transport velocity of biosolids (Park, Choo & Lee 1999), thereby reducing cake thickness. PAC is also considered to reduce internal fouling by the direct and rapid adsorption of dissolved foulants onto the carbon surface. For the treatment of landfill leachate, Pirbazari et al. (1996) observed a permeate flux reduction almost to zero within the first hours of operation when no PAC was employed. An addition of 1% PAC to the bioreactor improved the permeate flux up to 24 $L/m^2/h$.

Similarly, Guo et al. (2006) found that the addition of PAC can significantly reduce fouling, improve organic removal and increase the critical flux. Ng et al. (2006) used PAC in short term MBR experiments and concluded that the addition of PAC to the activated sludge in an MBR can improve membrane performance. They demonstrated

improved membrane performance as a result of the scouring effect of biologically activated carbon (BAC) at the membrane surface within a bubbled suspension. Basu and Huck (2005) also examined the impact of support material on an integrated bio-filter membrane system. They found that the fouling of the support medium system was at least two times slower than the non-support system. Here, 'support medium' refers to an external agent such as granular activated carbon (GAC) or anthracite placed in a known quantity in suspension in the submerged membrane bioreactor. Aryal et al. (2010) also reported the influence of a support medium (anthracite) in submerged microfiltration. They observed that the presence of the support medium reduced TMP and flux decline by two to three folds. From the abovementioned research, it can be concluded that an external agent, along with the application of air flow, has a significant role in controlling fouling. However, to date, there has been no literature that describes the combined effect of a support medium and air flow for controlling membrane fouling. This study is important for assessing the relative merits of these factors and optimising the parameters. It reports the combined effects of air flow and a support medium on membrane fouling under different operating parameters. It was concluded that an application of air flow incorporating a support medium has additional benefits in membrane fouling control compared to the application of only air flow. Therefore, the addition of a support medium with air could be a good alternative to the application of very high air flows in submerged membrane microfiltration systems. This will, of course, reduce the air flow rate, and the optimisation of the combined effect of support medium and air flow will contribute to the design of less energy-intensive operations.

2.9 Effect of Viscosity on Membrane Fouling

Membrane microfiltration is a very popular pressure driven separation process which has a wide range of applications in water, wastewater, chemical, and dairy industries. In

practice, a major problem associated with its application is membrane fouling, which results in severe flux decline, high energy consumption and frequent membrane cleaning and replacement (Gander, Jefferson & Judd 2000). In submerged membrane filtration used for domestic wastewater treatment applications, membrane modules are immersed in the activated sludge, and membrane fouling phenomena are therefore very complex due to the rheological and physiological characteristics of the mixed liquors. Membrane fouling is caused by various types of physicochemical interactions between the suspension containing biomass and the membrane itself. In the membrane bioreactor, biomass viscosity is closely related to its MLSS concentration and has been referred as a foulant parameter (Yeom et al. 2004), similar to conventional activated sludge processes. In submerged membrane microfiltration, the feed concentration can have a considerable impact on suspension viscosity as this will affect bubble properties and bubble-induced effects. In many industries, the feed viscosity can increase significantly during processing and particularly with concentration during filtration.

Ueda et al. (1996) reported that an increase in MLSS concentration and the corresponding rise in suspension viscosity have a negative impact on membrane permeability. Similarly, Itonaga et al. (2004) investigated the influence of suspension viscosity on membrane permeability in a MBR system. They suggested that a critical MLSS concentration exists under which the viscosity remains low; below this critical level, viscosity increases only slowly with concentration. Suspension viscosity tends to increase exponentially with solids concentration, and this could correspond to a change in rheological behaviour from Newtonian to non-Newtonian. Itonaga et al. (2004) suggested that the upper limit of MLSS concentration for efficient operation was around 10 g/L. Beyond this value, there would be a substantial increase in suspension viscosity. Brookes et al. (2003) suggested this critical value of MLSS ranged from 10 to 17 g

MLSS/L for different operating conditions. The apparent viscosity of the sludge in a submerged membrane bioreactor increased exponentially with an increase in the solid content of sludge and decreased logarithmically with an increase in the velocity of a rotary viscometer (Hasar et al. 2004). The relationship of the MLSS concentration with viscosity at different shear rates observed in a submerged bioreactor is shown in Figure 2.17. Le-Clech et al. (2003) established an exponential relationship between MLSS concentration and viscosity for varying shear rates.

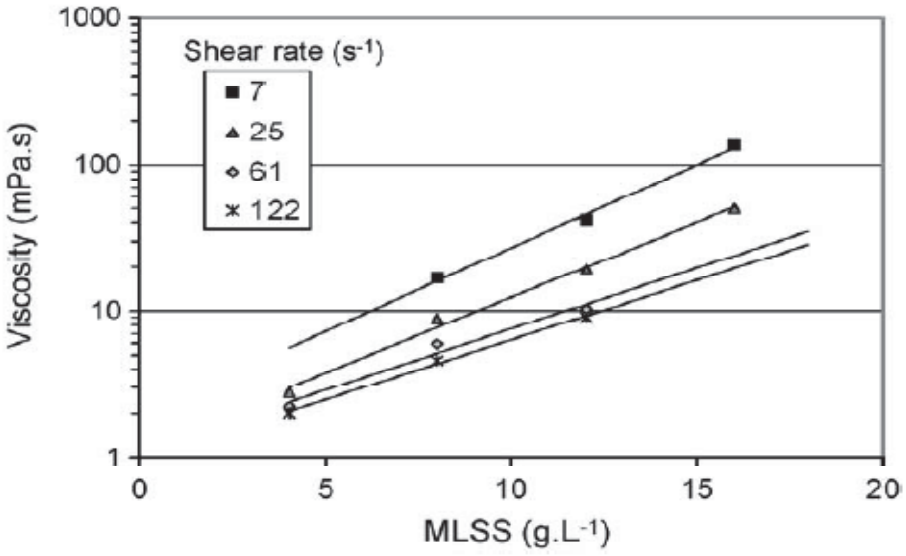

Figure 2.17 Viscosity obtained at different MLSS concentrations and shear rates (Le-Clech et al. 2003)

Rosenberger et al. (2006) observed that mixed liquor suspended solids (MLSS) constituted a major parameter affecting the apparent viscosity of the suspension in membrane bioreactors. MLSS concentration indeed has a complex interaction with membrane fouling, and conflicting findings about the effect of this parameter on membrane filtration have been reported.

The major concern of biomass viscosity in a membrane bioreactor is its detrimental effect on membrane fouling and bubble properties and bubble-induced effects.

Nowadays, the application of air bubbles into a submerged filtration system has proved to be an effective, simple and low-cost technique for fouling control (Cui, Chang & Fane 2003). In air sparged microfiltration systems, turbulence in the bubble wake is responsible for accelerating mass transfer back to the suspension. The strength and size of the bubble wake depends on the bubble size. Tiny bubbles are spherical in shape and do not generate vortices, as the flow around these bubbles does not separate, but larger bubbles produce a symmetric vortex in the wake region (Kumar et al. 1992); secondary flow is therefore much stronger for the larger bubbles. The importance of MLSS or viscosity is that bubble size is modified which can dampen the movement of hollow fibres in submerged bundles (Wicaksana, Fane & Chen 2006b). Wicaksana et al. (2006b) reported that the average value of bubble rise velocity in high viscosity liquid was significantly lower than in less viscous water (Figure 2.18).

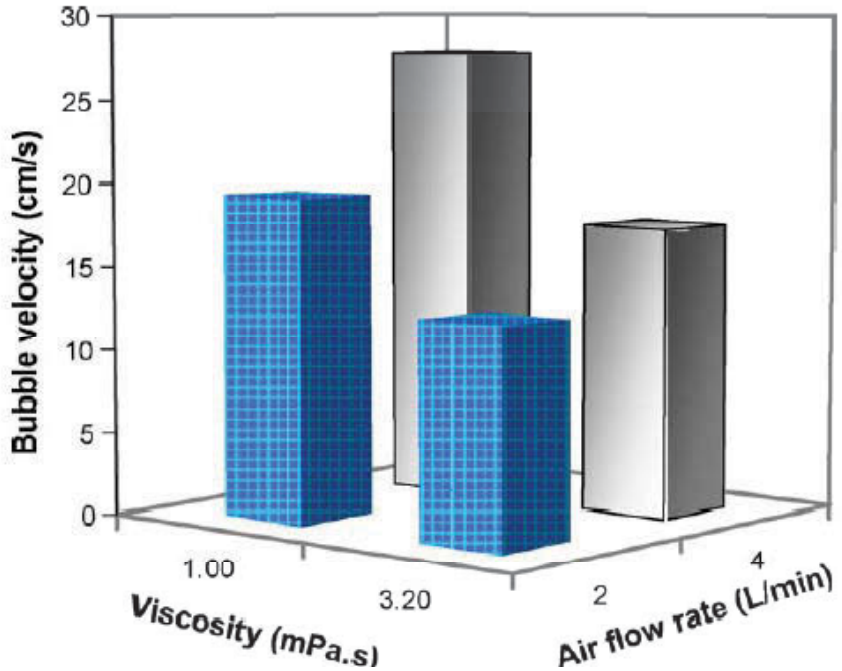

Figure 2.18 Effect of viscosity on average bubble rise velocity at various air flow rates (Wicaksana et al. 2006)

The application of air bubbles reduces the rise in TMP due to its scouring effect on the deposited layer for all operating conditions. More significant reduction in highly viscous

feed could be due to the formation of large bubbles in more viscous liquid. Wicaksana et al. (2006b) found that the bubble sizes in more viscous liquid were larger than those in a less viscous solution (water). Similar results were observed by De Swart et al. (1996) and Schafer et al. (2002). Large bubbles are more beneficial because they have larger wake regions and create stronger secondary flows. They are more effective in promoting local mixing (Cui, Chang & Fane 2003). Li et al. (1997) also reported that increasing bubble size can result in a stronger wake which enhances local mixing and the mass transfer back to suspension. They also observed an apparent rise in permeate flux with bubble size.

In this study, membrane fouling behaviour was studied under varying feed viscosity in the presence of air bubbles. Membrane microfiltration experiments were carried out with a flat sheet membrane module submerged in a kaolin suspension with different concentrations of glycerol. During the experiments, air bubbles were injected at different rates so that the effect of both viscosity and air flow could be identified.

Chapter 3

Application of air flow for mitigation of particle deposition in submerged membrane microfiltration

Abstract

This study investigates the effect of microfiltration operating conditions on membrane fouling of colloidal particles of kaolin clay. Experiments were conducted with a flat sheet membrane submerged in a suspension prepared from kaolin clay powder of size varying from 0.1-4 μm (Sigma) with a mean particle size of 2.10μm. The particle size distribution of the clay was unimodal and the concentration of kaolin clay was similar to the biomass concentration in a membrane bioreactor (10 g/L). The effects of scouring and permeate flux rates were studied in relation to the membrane fouling rate. A linear relationship between the transmembrane pressure (TMP) and particle deposition was established for different air flow rates and permeate flow rates. Air scouring was more effective at a low permeate flux. There was only a minor change in the mean particle size of deposited colloidal particles on the membrane at a given flux under varying air flows and at the outset, all had a similar rise in TMP. As particles accumulated on the membrane surface in the later stages, however, there was a significant rise in TMP. 15 LMH flux was observed as the critical flux beyond which a rise in the permeate flux showed a sharp rise in the TMP, which varied with air flow rates and particle deposition. The sharp TMP rise that occurred during the initial few hours of operation indicated that air flow for fouling mitigation strategies should target this period to optimise the membrane process. The study showed that air flow and flux rates are the two major governing factors for particle deposition on the membrane surface.

3.1 Introduction

The microfiltration process is a high performance separation technique for processing particulate suspensions in wastewater treatment, drinking water production and industrial applications such as biotechnology, food and beverage manufacture and mineral processing. It is a pressure driven separation process typically applied to remove macromolecules, colloidal and suspended particles with linear dimensions ranging from 0.02 to 10 μm, and covers most of the pollutants in water and wastewater.

The major limitation of microfiltration is membrane fouling caused by the deposition and intrusion of macromolecules, colloids and particles onto and into the microporous membrane (Belfort, Davis & Zydney 1994). Fouling leads to a significant increase in hydraulic resistance, causing permeate flux to decline or TMP to rise when the process is operated under constant-TMP or constant-flux conditions respectively. Frequent membrane cleaning and replacement is therefore required, significantly increasing the energy consumption and leading to high operating costs. Numerous studies have therefore focused on understanding the activated sludge behaviour and membrane fouling mechanisms to improve the design and operation of the membrane systems and reduce costs. The effects of the main operating conditions and sludge characteristics on membrane fouling have been a key topic of interest among researchers. The activated sludge is divided into different fractions and their individual influences on fouling are reported in the literature. Bouhabila et al. (2001) established that the three fractions of the sludge, suspended solids, colloid and solutes, had different levels of influence on membrane fouling. They also showed that membrane fouling was mainly caused by colloids, because the MLSS, colloids, and solutes accounted for 24%, 50%, and 26% of fouling resistance, respectively. Wisniewski and Grasmick (1998) concluded that the

solutes, colloids, and mixed liquor suspended solids (MLSS) accounted for 52%, 25%, and 23% of the total fouling resistance, respectively. From these previous studies, it can be concluded that colloidal particulate has a significant effect on membrane fouling.

Several practical approaches have been applied to mitigate membrane fouling, among which, the application of air flow (scouring) is a popular strategy to minimise fouling. Air bubbles keep the solids particles in suspension, leading to a well mixed and homogeneous distribution of particulate, and also act to scour the deposited particle layer that develops on the membrane surface (Aryal, Vigneswaran & Kandasamy 2010; Cui, Chang & Fane 2003). The induced shear stress causes the resuspension of deposited particles from the membrane surface (Liu et al. 2000). Air bubbles pose less risk to a membrane surface than chemical agents and support media. Ueda et al. (1997) also concluded that aeration was a significant factor governing filtration conditions; they found that fouling was reduced by augmenting the air flow rate or aeration intensity.

Despite the progress in membrane system design and operation in recent years, membrane aeration still contributes significantly to the energy demand and operating costs, therefore optimising the air flow directly leads to reduced costs. Understanding the hydrodynamics of particulate fouling could lead to the optimisation of air flow requirements and the enhancement of system performance. This study investigates the effects of air flow and permeate flux rates on membrane fouling.

3.2 Materials and Method

3.2.1 Materials

3.2.1.1 Membrane

A flat sheet membrane with a nominal pore size of 0.14 μm and an effective filtration area of 0.2 m^2 was supplied by A3 Company and used in this study. The membrane consisted of eight flat sheets equally spaced 12 mm apart from each other. Table 3.1 presents the characteristics of the membrane module used in this study.

Table 3.1 Membrane characteristics

Membrane module	Flat sheet
Supplier	A3 Company
Nominal pore size	0.14 μm
Effective filtration area	0.2 m^2
Membrane material	Polyvinylidene fluoride (PVDF), Hydrophilic
Number of flat sheet	8
Gap between flat sheet	12 mm
Dimension of module (mm)	130 x 125 x 225

3.2.1.2 Kaolin Clay

Kaolin clay is used as a model test medium for membrane microfiltration. The main constituent of kaolin is kaolinite which is formed by rock weathering. Its appearance is white, greyish-white, or slightly coloured and it is physically made of very tiny, thin, pseudohexagonal, flexible sheets of triclinic crystal that range in diameter from 0.2 to 12 μm. The cation exchange capacity of kaolin is considerably less than that of

montmorillonite, in the order of 2-10 meq/100 g, depending on the particle size, but the rate of the exchange reaction is rapid and almost instantaneous (Grim 1968). Kaolinite adsorbs small molecular substances such as lecithin, quinoline, paraquat, and diquat, but also proteins, polyacrylonitrile, bacteria, and viruses (Adamis & Timar 1980; Lipson & Stotzky 1983; Schiffenbauer & Stotzky 1982). The adsorbed material can be easily removed from the particles (planes and edges), unlike montmorillonite, where the adsorbed molecules are also bound between the layers (Weber, Perry & Upchurch 1965). The physical characteristics of kaolin clay used in this research are presented in Table 3.2.

Table 3.2 Characteristics of kaolin clay

Size range	0.1-4 μm
Mean particle size of kaolin	2.10 μm
Density of kaolin clay	1667 kg/m^3
Supplier	Sigma, USA

The mean particle sizes based on the volume distribution of D[v,0.9], D[v,0.5] and D[v,0.1] were 3.91 μm, 2.10 μm and 1.61 μm respectively (where D[v,0.9], D[v,0.5] and D[v,0.1] represent 90%, 50% and 10% respectively of volume distribution below the given value). Hence the particle size distribution of kaolin clay was considered to be unimodal. The unimodal particle size distribution is shown in Figure 3.1. The mean particle size is significantly higher than the membrane pore, so the internal pore blocking phenomenon was considered negligible and all particle deposition occurred on the membrane surface.

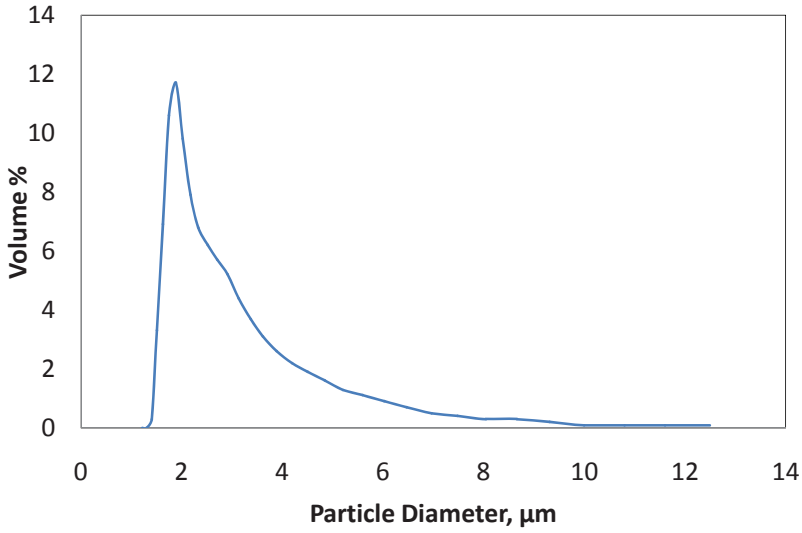

Figure 3.1 Particle size distribution of kaolin clay

3.2.3 Method

Laboratory scale microfiltration tests were carried out with a flat sheet membrane. The membrane reactor, which had a capacity of 12 L, was filled with kaolin clay suspension prepared with kaolin clay powder of mean particle diameter 2.1 µm. The concentration of the kaolin clay suspension was 10 grams per litre (g/L) of tap water. The membrane was submerged in the reactor and air bubbles from different air flow rates were continuously supplied from the bottom of the reactor where the air diffuser plate was attached. The bubbles were considered to be large, having dimensions of 2-4 mm in diameter. According to the result of a dimensional analysis by Fan and Tsuchiya (1990) and air bubble flow observation within the operating conditions in the reactor system, the shape and movement of bubbles were defined as oblate ellipsoidal and zigzag respectively. The schematic diagram and photograph of the experimental setup are presented in Figures 3.2 and 3.3 respectively.

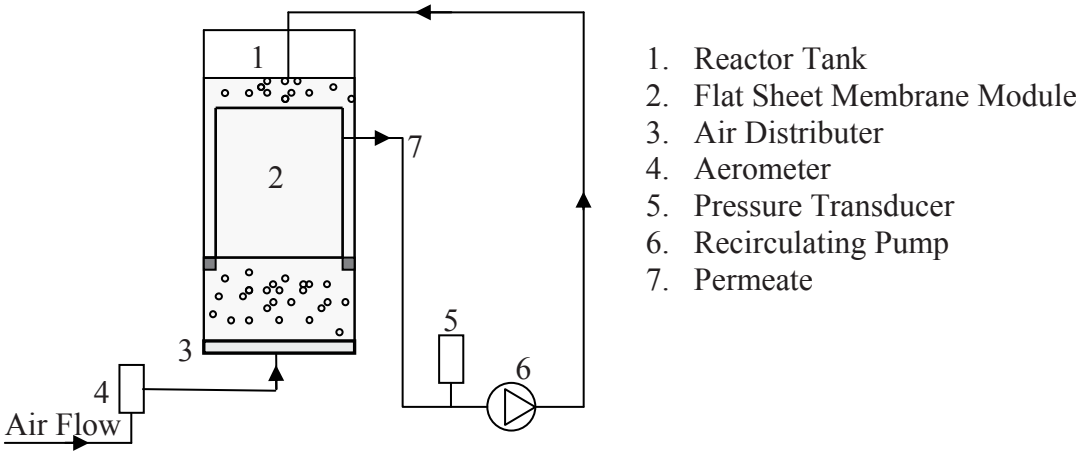

Figure 3.2 Schematic diagram of experimental set-up

Figure 3.3 Photograph of experimental set-up

The pressure driven microfiltration from outside to inside was performed by developing reduced pressure on the permeate side using a peristaltic pump at constant permeate flux. A continuous filtration process and constant concentration of the suspension was maintained by returning permeate back to the feed suspension. No backwash was applied within a set of experiments.

Experiments were carried out at different air flow rates (600, 1200 and 1800 L/h/m²) and different constant permeate flux rates (5, 10, 15 and 20 L/h/m^2 or LMH). The air flow rates were expressed in terms of membrane area (0.2 m^2). The TMP was monitored online by a pressure transducer between the suction pump and the membrane. The use of constant flux mode and monitoring of the resultant TMP rise have proved to be particularly useful in the context of monitoring fouling in complex fluids, and is currently the mode of choice in many membrane bioreactor (MBR) applications (Le-Clech, Jefferson & Judd 2003).

Prior to each experiment, the membrane was tested for its hydraulic resistance after three stages of cleaning (cleaning with tap water, shaking and cleaning with tap water and cleaning with chemical). The membrane was first cleaned with tap water. It was then placed in a specially designed holding unit attached to the shaker for an hour at 120 rpm and cleaned with tap water again. Finally, the membrane was submerged in chemical solution (3% w/w sodium hypochlorite) for three hours. If the hydraulic resistance had not been reduced to its original state (new), the process was repeated.

Particle deposition on the membrane surface was calculated indirectly by measuring the suspended solids concentration. Due to the particle deposition on the membrane, the concentration in the suspension decreased continuously. From the material balance of the particle mass in the whole system, it was possible to calculate the amount of mass deposited on the membrane. A sample from the reactor was collected at 1 h intervals, passed through a 0.45 μm filter and the mass was measured. The particle size distribution was also measured using a particle size analyser (Malvern 2600, United Kingdom).

3.3 Results and Discussion

3.3.1 Effect of Air Flow on TMP Reduction

During membrane filtration, suspended particles are transported to the membrane surface due to the suction pressure. The deposited particles are scoured and back transported to the suspension by the application of air flow, which ultimately causes a reduction in fouling and TMP (Ivanovic & Leiknes 2008a). Ueda et al. (1997) observed a rapid increase in pressure when the air flow rate was reduced, which was possibly due to cake layer development and less membrane scouring from the reduced air flow rate.

Figure 3.4 shows the experimental results of TMP reduction at four different flux rates (5, 10, 15 and 20 LMH) and three different air flow rates (600, 1200 and 1800 L/h/m^2). Four different fluxes produced four distinct patterns. At a lower flux rate (5 LMH), the rise in TMP was negligible and was almost constant throughout the experiment for all air flow rates, indicating negligible deposition of particles (Figure 3.4a). At a higher flux of 10 LMH, the rise in TMP was similar up to a certain time (120 minutes) but the rising trend of the TMP became distinct after this period (Figure 3.4b). This result shows that air flow influences particle deposition only after a certain time; most likely, at an early stage, the deposition was insufficient to be scoured. Once the deposit was sufficiently formed, air bubbles started scouring and transporting the deposited mass back to the suspension. At 15 LMH, the particle deposition became distinct from the outset, indicating a strong air flow influence (Figure 3.4c). This showed equilibrium between the flux and air flow rate. Beyond 15 LMH, a sharp rise in TMP was observed which suggested the existence of a critical flux beyond this permeate flow rate. At 20 LMH, the result was similar to 10 LMH showing a similar trend up to 120 minutes for all three air flow rates but becoming distinct after this for all air flow rates (Figure 3.4d).

It is likely that at the outset (1 h), the drag force (flux rate) was too high for smaller particles to be deposited, during which time the air flow had no effect and scouring was not effective. However, due to the small particle deposition on the membrane during this period, the rise in TMP was high. At a later stage once coarse particles had been deposited, air flow had a significant influence on scouring and mixing.

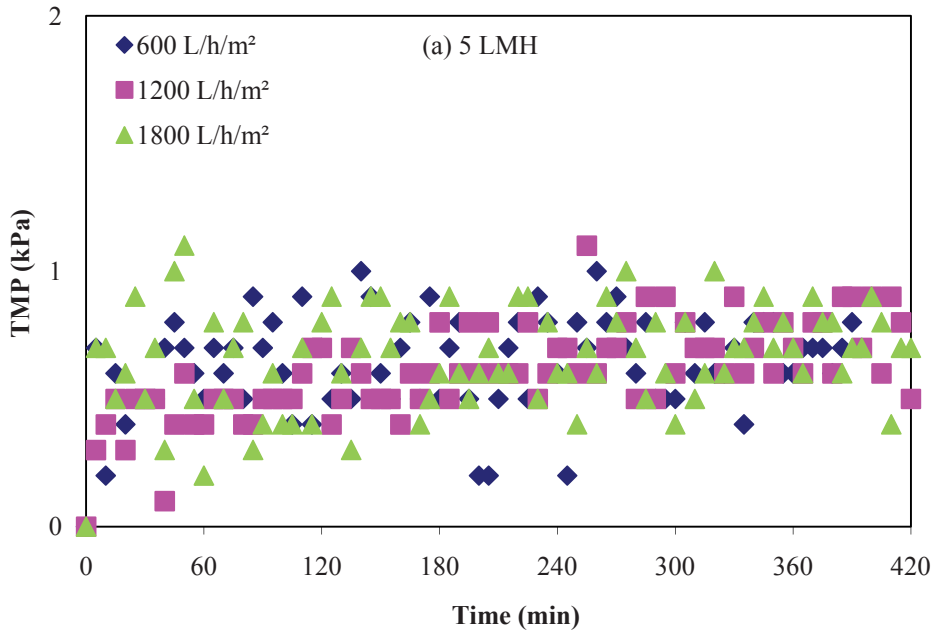

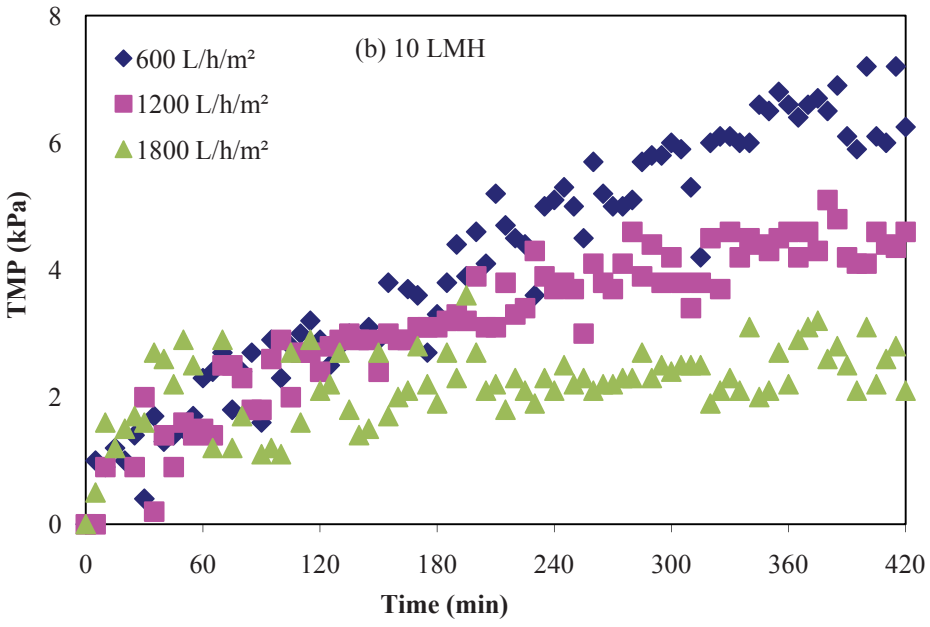

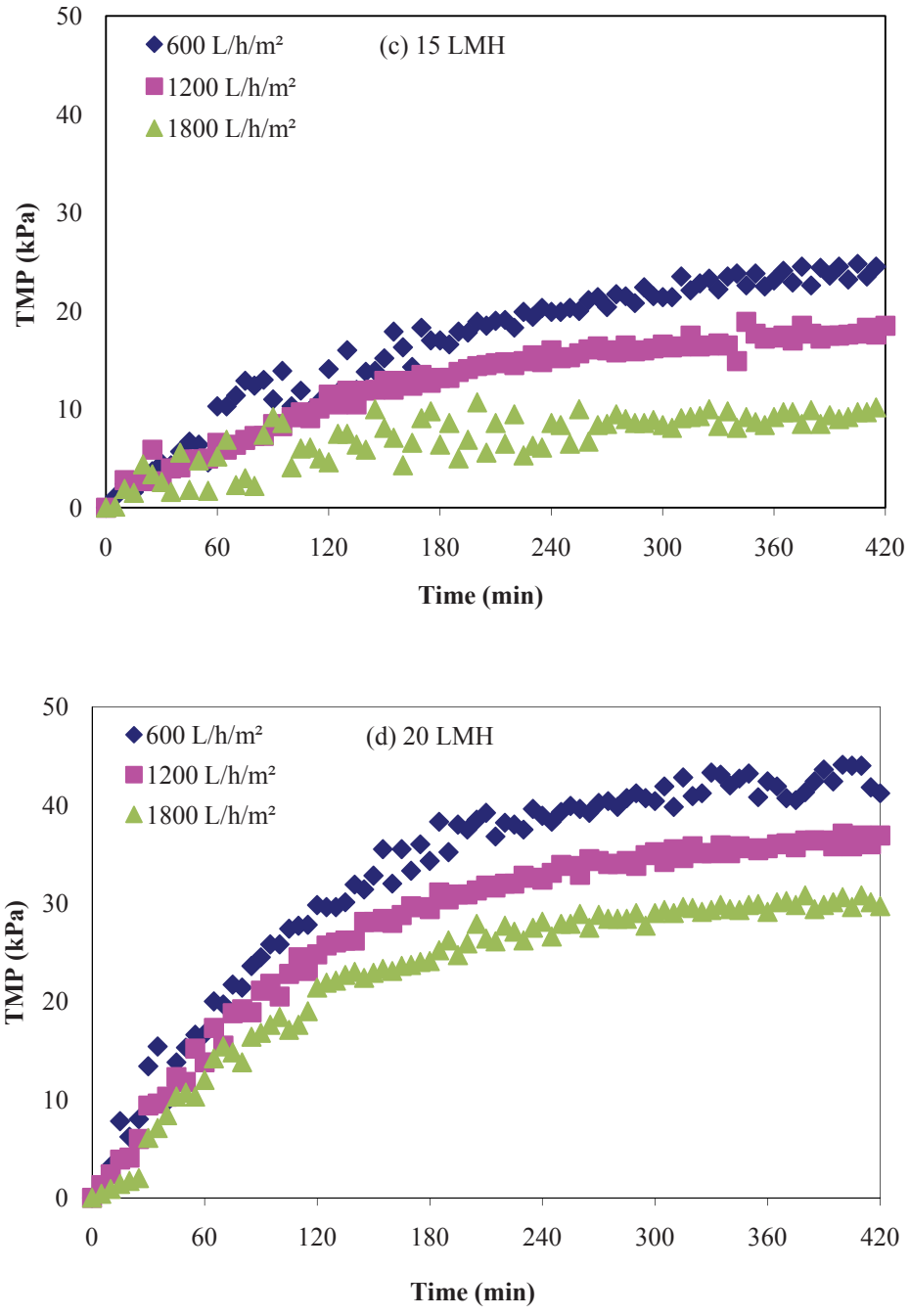

Figure 3.4 Effect of air flow on TMP at different permeate flux and air flow rates

Table 3.3 shows the reduction in TMP when air flow was increased. Doubling and tripling the air flow rate had a negligible effect on the reduction of TMP for a very low permeate flux (5 LMH). Increasing the air flow rate from 600 to 1200 L/h/m^2 caused a 33, 25 and 20% reduction in TMP for 10, 15 and 20 LMH respectively, whereas tripling the air flow (600 to 1800 L/h/m^2) caused a 51%, 60% and 33% reduction in TMP for

10, 15 and 20 LMH respectively. Low permeate fluxes (10 and 15 LMH) were found to be more efficient than higher flux (20 LMH) in terms of the reduction in TMP for the different air flow rates. When tripling the air flow rates, the 15 LMH flux was found to be the most efficient flux rate (for the suspension used) which was verified from the total water produced during the test, Table 3.3.

Table 3.3 TMP Reduction with varying air flow rates

Flux	Air Flow Increment (L/h/m²)			Total Volume of Filtered Water
(LMH)	600 to 1200	600 to 1800	1200 to 1800	(L)
5	Negligible	Negligible	Negligible	7.0
10	33%	51%	31%	14.0
15	25%	**60%**	46%	21.0
20	20%	33%	16%	28.0

3.3.2 Effect of Permeate Flux Rates on TMP at Different Air Flow Rates

To assess the influence of permeate flux on TMP development under different air flow rates, TMP profiles obtained for different permeate flux rates were studied (Figure 3.5). For each flux, the TMP curve was divided into three different parts. First part shows a sharp jump, followed by a slow rise (second part). The third part of the curve clearly shows a plateau state, which demonstrates that a steady state has been reached. Similar trends were observed for all the air flow rates applied. This initial quick jump of TMP was observed to be steep and tended to be more linear for the highest permeate fluxes. Similar results were reported by Fradin et al. (1999). TMP increases with the increasing flow rate, but the influence of permeate on the rise in TMP was significantly higher than the reduction effect of the air flow.

A comparative study on the impact of air flow on different permeate fluxes indicated TMP reduction for all the employed flux rates. In the case of varying permeate flux, almost the same TMP reduction was found when the flux was halved from 20 LMH to 10 LMH for the three different air flow rates. At air flow 600 L/h/m^2, TMP reduction was 88% and slightly higher, i.e. 89% at 1200 L/h/m^2 and 91% at 1800 L/h/m^2 air flow rates. When the permeate flux was reduced to 15 LMH from 20 LMH, however, the TMP reductions were 50%, 52% and 69% for 600, 1200 and 1800 L/h/m^2 air flow rates respectively. Similarly, the TMP reductions were 76%, 77%, and 72% for 600, 1200 and 1800 L/h/m^2 air flow rates when the flux was reduced from 15 to 10 LMH. The different results were obtained for the same air flow rates with permeate flux reduction by 5 LMH. Higher TMP reduction was observed when the flux was reduced from 15 to 10 LMH than when it was reduced from 20 to 15 LMH. This highlights the cumulative behaviour of particle deposition on the membrane surface and the influence of air flow on scouring deposition and particle motion in suspension. The summary of these results is tabulated in Table 3.4. The results highlight that the influence of permeate flux is far higher than the impact of the air flow rate. It is well accepted that the air flow increment helps to reduce TMP for all permeate flux. The results suggest that high air flow is more efficient for low flux.

Table 3.4 TMP reduction with variation of permeate flux rates

Air flow rate	Variation of Permeate flux		
L/h/m^2	20 to 10 LMH	20 to 15 LMH	15 to 10 LMH
600	88%	50%	76%
1200	89%	52%	77%
1800	91%	69%	72%

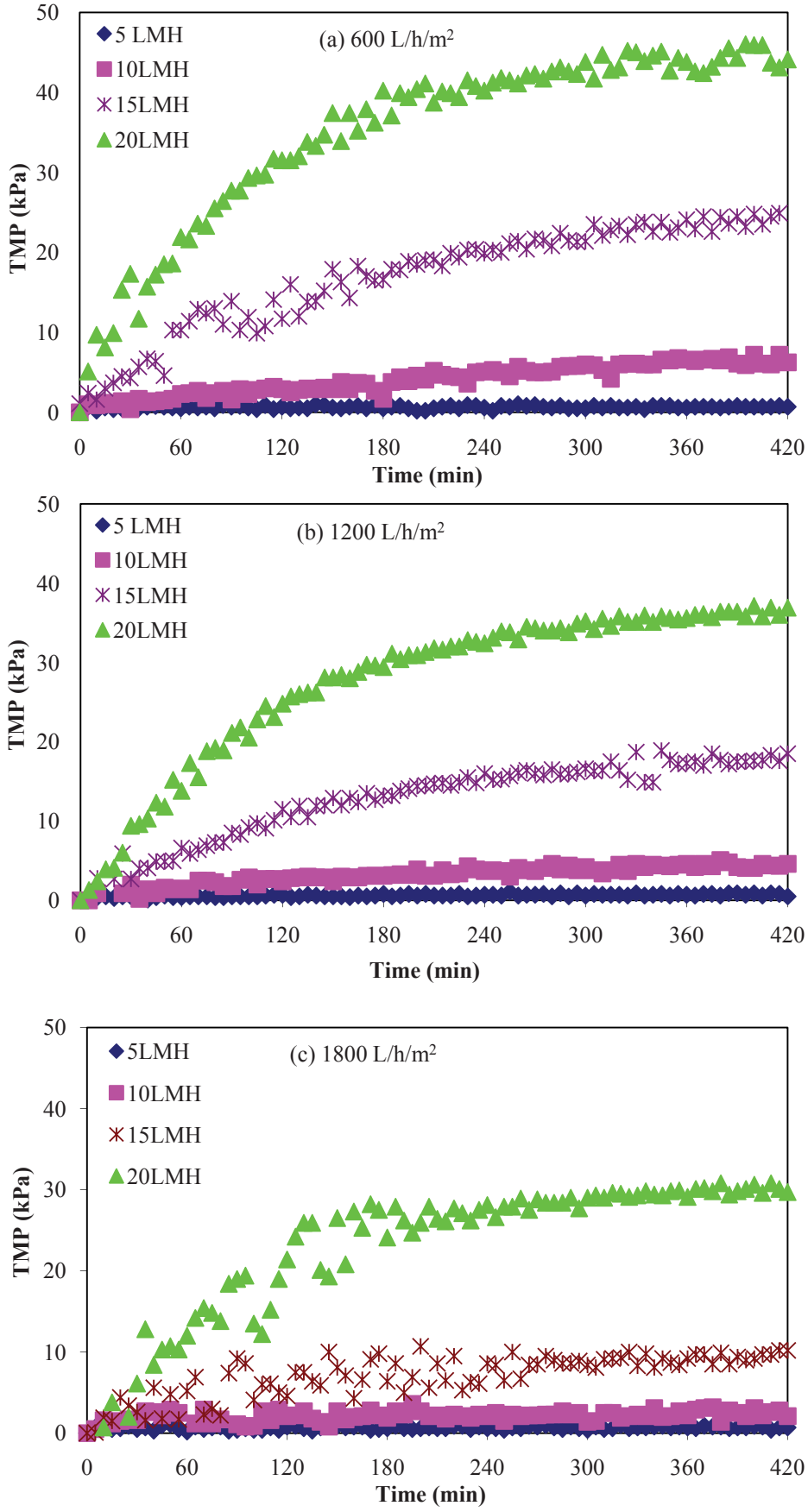

Figure 3.5 Effect of permeate flux on TMP at different air flow rates

3.3.3 Effect of Air Flow on Particle Deposition (Fouling)

The indicators of membrane performance such as the development of TMP with time or particle deposition show an apparent response to the application of air flow. Ivanovic and Leiknes (2008a) observed a higher fouling rate for lower aeration rates, or low particle deposition at higher aeration rates. Their results confirmed the importance of aeration as a means to mitigate fouling in a submerged membrane system.

Figure 3.6 presents the cumulative mass deposition of clay particles at different air flow rates (600, 1200 and 1800 L/h/m²) and flux rates (5, 10, 15 and 20 LMH). At a lower flux rate, the mass deposition was low (compared to higher flux) but the increment in air flow only marginally helped to reduce the deposition (Figure 3.6a). At 10 LMH, deposition was clearly affected by air flow. The mass deposition was significantly reduced from 193.97 to 94.15 g/m^2 when the air flow rate reduced from 600 to 1800 L/h/m^2 (Figure 3.5b). At 15 LMH (Figure 3.6c), there was a clear difference in the mass deposited at the three air flow rates. At 20 LMH (Figure 3.6d), doubling the air flow rate (600 to 1200 L/h/m²) showed minimal difference in deposition, whereas a significant reduction was observed at 1800 L/h/m^2 (261 g/m^2) compared to 600 L/h/m^2 (383 g/m^2). The particle deposition pattern is supported by the TMP graph where 15 LMH was the transition. The increasing deposition patterns were found along the time period for all adopted operating conditions. In conclusion, the increased air flow (scouring) helped to reduce the mass deposition, which was significantly affected by the flux rate. Similar results were reported by Ivanovic and Leiknes (2008a).

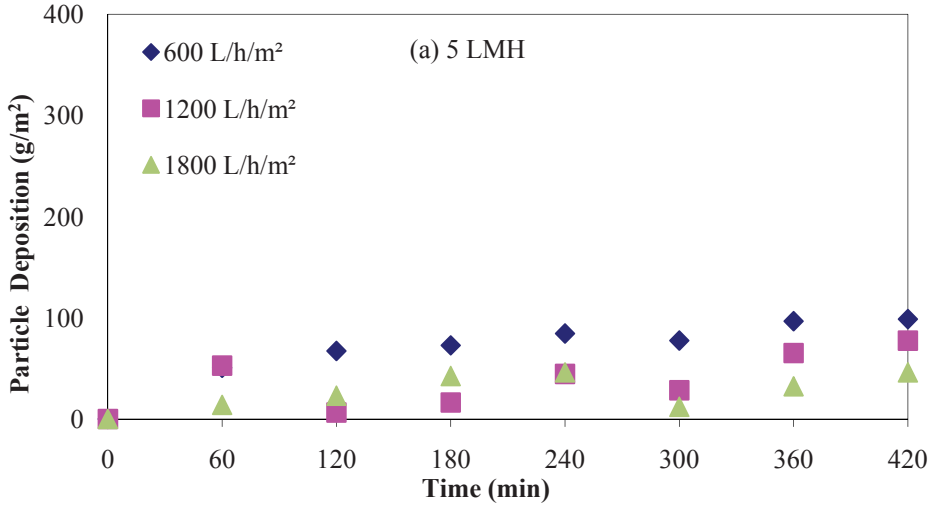
400
300
200
100
0
Particle Deposition (g/m²)
600 L/h/m²
1200 L/h/m²
1800 L/h/m²
(a) 5 LMH
0
60
120
180
240
300
360
420
Time (min)

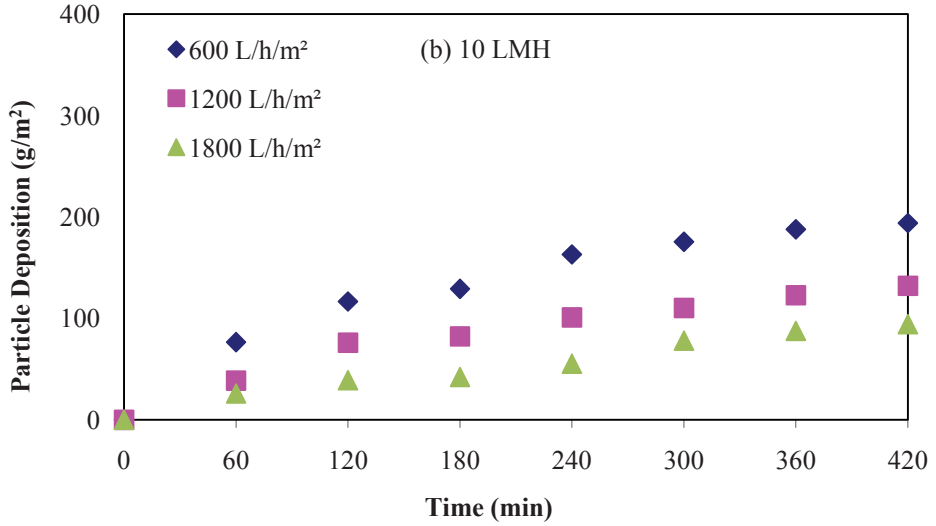
400
300
200
100
0
Particle Deposition (g/m²)
600 L/h/m²
1200 L/h/m²
1800 L/h/m²
(b) 10 LMH
0
60
120
180
240
300
360
420
Time (min)

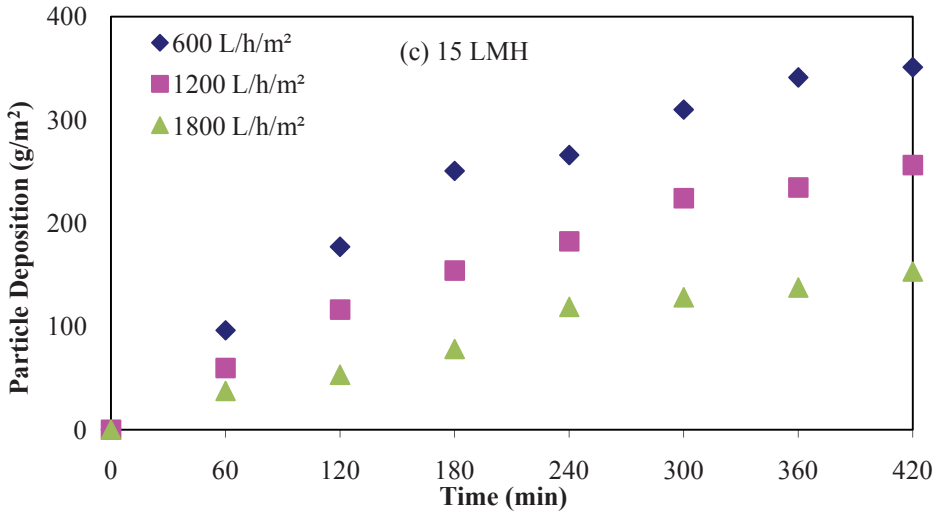
400
300
200
100
0
Particle Deposition (g/m²)
600 L/h/m²
1200 L/h/m²
1800 L/h/m²
(c) 15 LMH
0
60
120
180
240
300
360
420
Time (min)

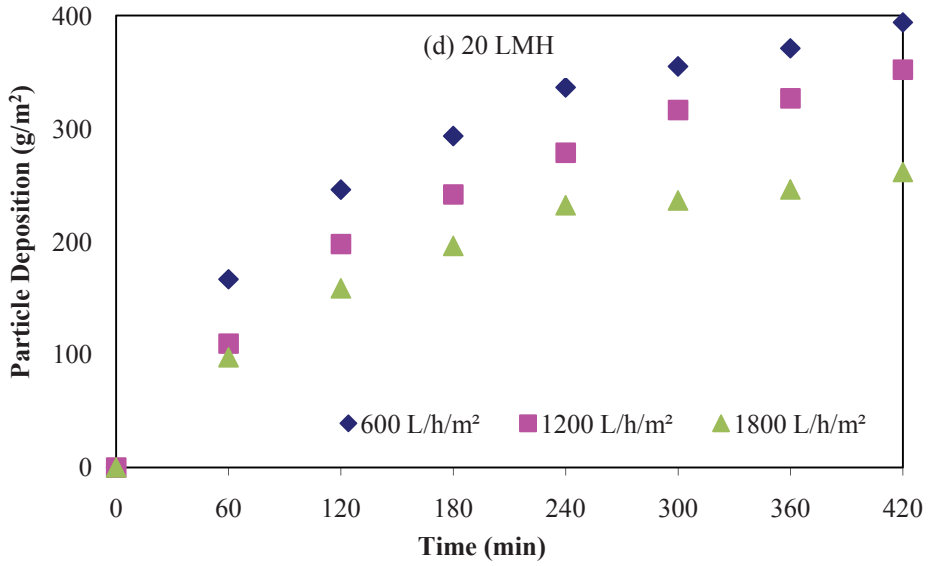

Figure 3.6 Effect of air flow on particle deposition on membrane surface

Table 3.5 summarises the results of the reduction in mass deposition with increasing air flow rates. An increase in the air flow rate from 600 to 1200 L/h/m^2 reduced mass deposition by 36%, 30% and 15% for 10, 15 and 20 LMH respectively, whereas increasing the air flow three times (600 to 1800 L/h/m^2) resulted in a reduction of particle depositions by 64%, 59% and 30% at 10, 15 and 20 LMH respectively.

Table 3.5 Fouling reduction with increasing air flow rates

Flux	Air Flow Increment (L/h/m²)			Total Volume of Filtered Water
(LMH)	600 to 1200	600 to 1800	1200 to 1800	(L)
5	-	-	-	7.0
10	36%	64%	36%	14.0
15	30%	59%	42%	21.0
20	15%	30%	18%	28.0

The data from Table 3.5 suggest that an increased air flow is more efficient for low flux

rates. A three-fold increase in air flow gave the greatest reduction in fouling at 10 LMH, but in terms of the total volume of filtered water, 15 LMH flux was found to be influenced most by the high air flow rate.

3.3.4 Effect of Air Flow on Particle Size Distribution

The hydrodynamic forces in the immediate vicinity of the membrane are the major parameters responsible for particle deposition on the membrane surface. Particle size is one of the most important parameters affecting hydrodynamic forces. TMP and particle deposition behaviour are also affected by the particle size distribution of deposited particles. Small changes in the mean particle size have a significant effect on the TMP rise and fouling. Figure 3.7 describes the effect of operating conditions on the particle size distribution in suspension.

Figures 3.7a and 3.7b present the mean particle size available in suspension for 5 LMH and 10 LMH respectively. The mean particle sizes were observed to be very similar with less fluctuation during the test period for both flow rates. This similarity in particle size during the process may be due to 1) insufficient drag force to hold the deposited particle on the membrane wall, or 2) sufficient air bubbles for scouring and back transport. This is supported by Figures 3.4a and 3.4b (low TMP rise).

At 15 LMH, at lower air flow, a slow increase of particle size in the suspension was observed, indicating deposition of fine particles on the membrane surface. At a higher air flow rate, however, similar particle sizes were observed in lower permeate fluxes of 5 LMH and 10 LMH. At higher air flow rate, a large reduction in TMP and low particle deposition were found compared to other permeate fluxes [Figures 3.4c and 3.6c; Tables 3.5 and 3.6]. This highlights that at critical flux (15 LMH), higher air flow rates were effective in maintaining the equilibrium between the drag force and lift force so that the

air bubbles were sufficient to scour deposited particles, resulting in a lower rise in TMP and smaller particle deposition. It can be concluded from this that the mitigation of particle deposition on the membrane surface is not only a function of air flow rates but also of the combined effects of air flow and permeate flux which determines the best operating condition for the filtration process. Based upon this analysis, 15 LMH was observed as the optimum operating condition.

In the case of 20 LMH, the drag force is sufficient to deposit the particles on the membrane wall. At a lower air flow rate, the deposition of fine particles is observed to occur rapidly. An increase in air flow decreased the deposition of fine particles. This emphasises that small particles attached to the membrane surface from the beginning of the test produced high TMP and deposition.

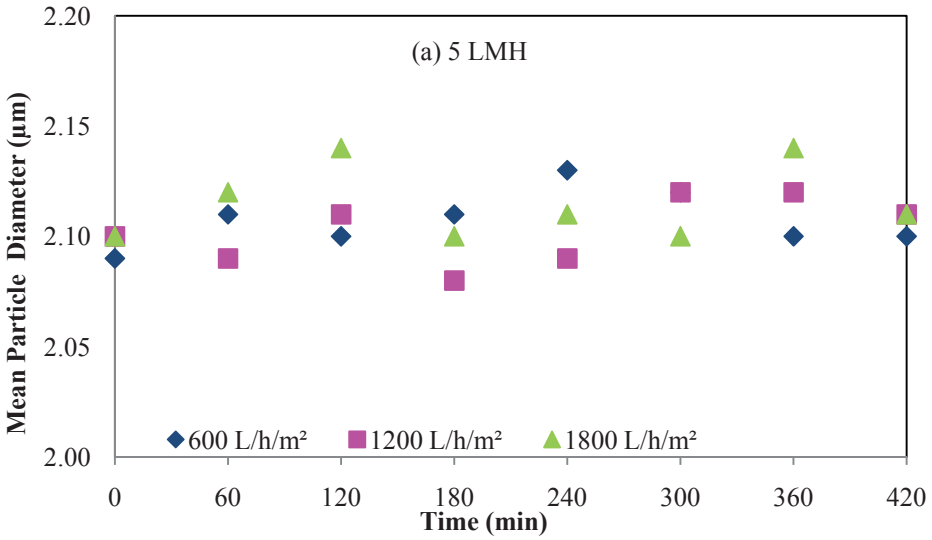

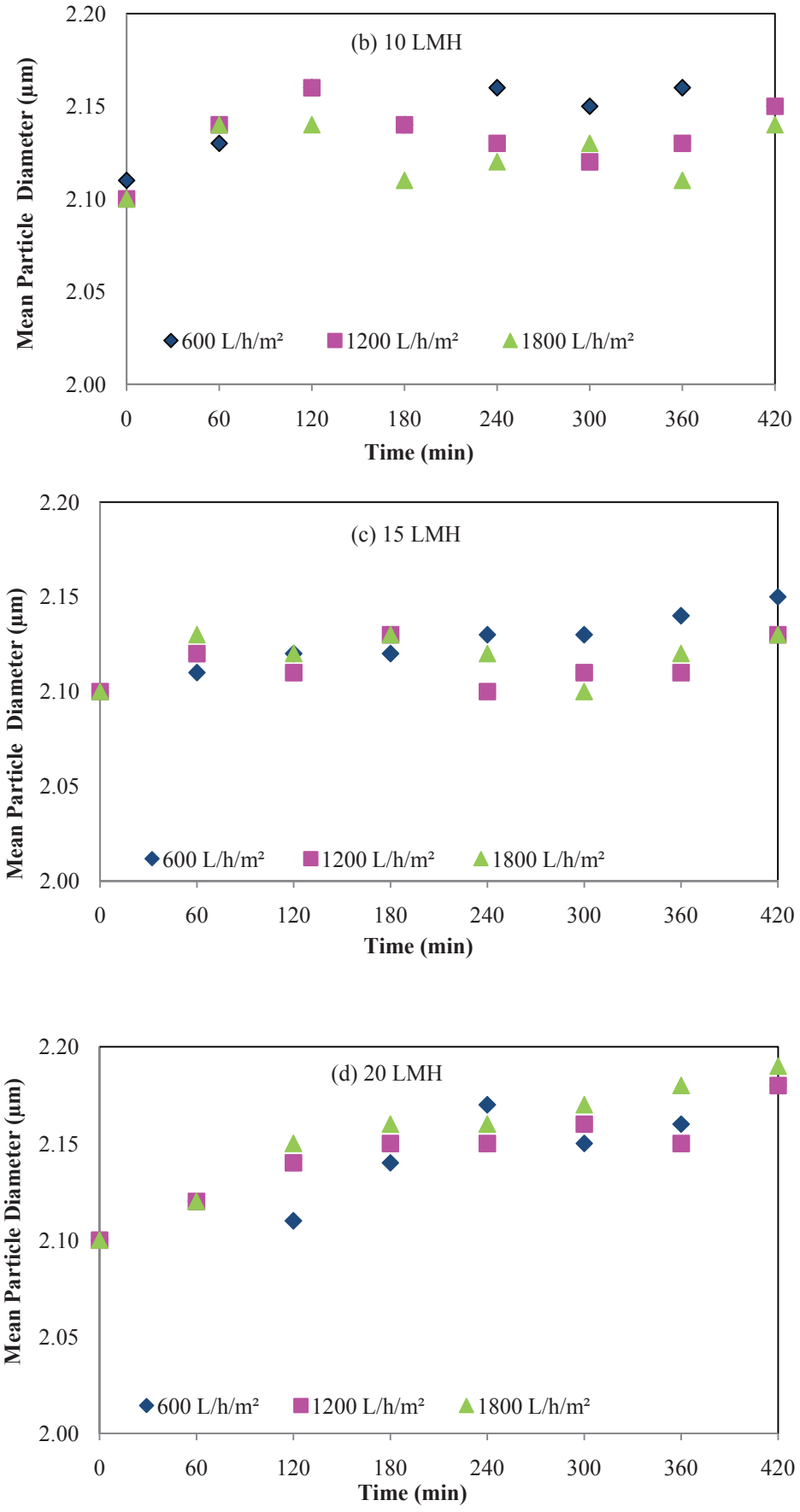

Figure 3.7 Effect of air flow on particle size distribution

3.3.5 The Relationship between TMP and Particle Deposition for Different Air Flow Rates

From the experimental results obtained, a relationship between the TMP and particle deposition was drawn for three air flow rates (600, 1200 and 1800 L/h/m^2) and four permeate flow rates (5, 10, 15 and 20 LMH). The graphical representations are shown in Figure 3.8. A linear regression was applied between the TMP and particle deposition. At lower flux, no relationship between the TMP and particle deposition was observed. At this flux, an increase in particle deposition did not change the TMP. This showed that the deposition was minimal and porous. Between 10-20 LMH, a linear relationship was observed between the TMP and particle deposition in which a significant reduction in TMP and deposition was found to occur with increased air flow rates. The linear equations developed for 5, 10, 15 and 20 LMH at 600, 1200 and 1800 L/h/m^2 are tabulated in Table 3.6 below.

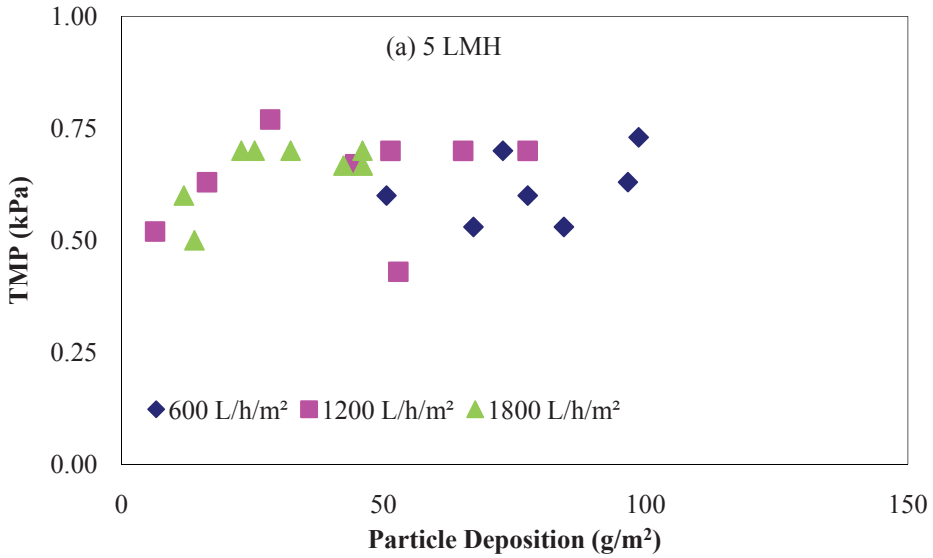

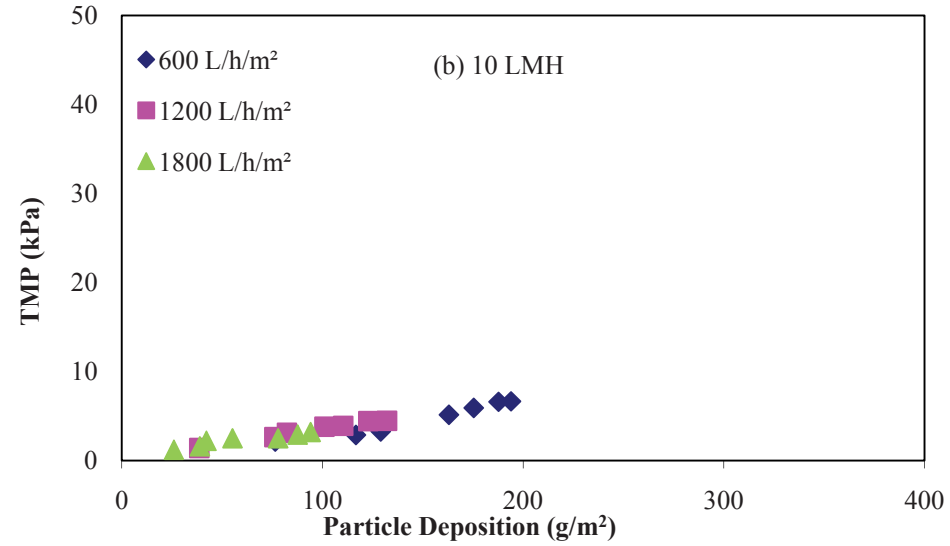

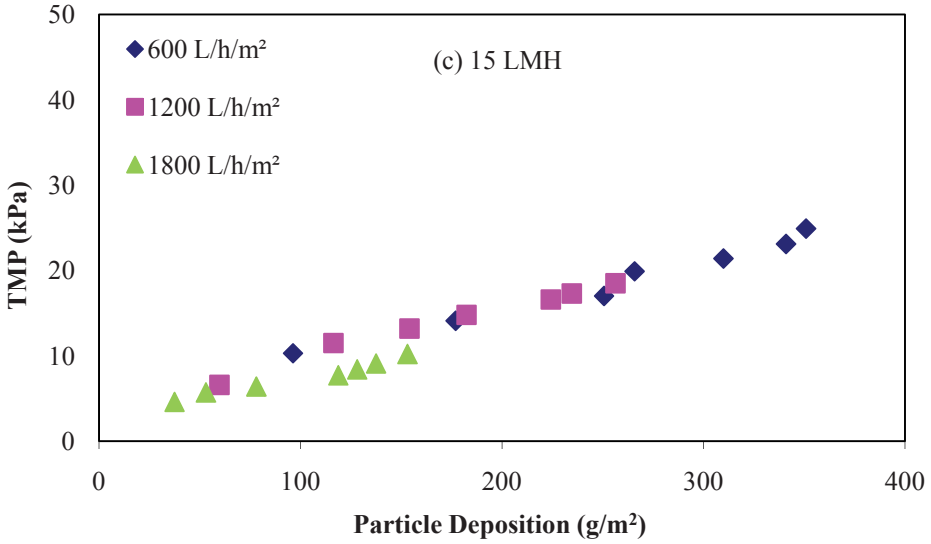

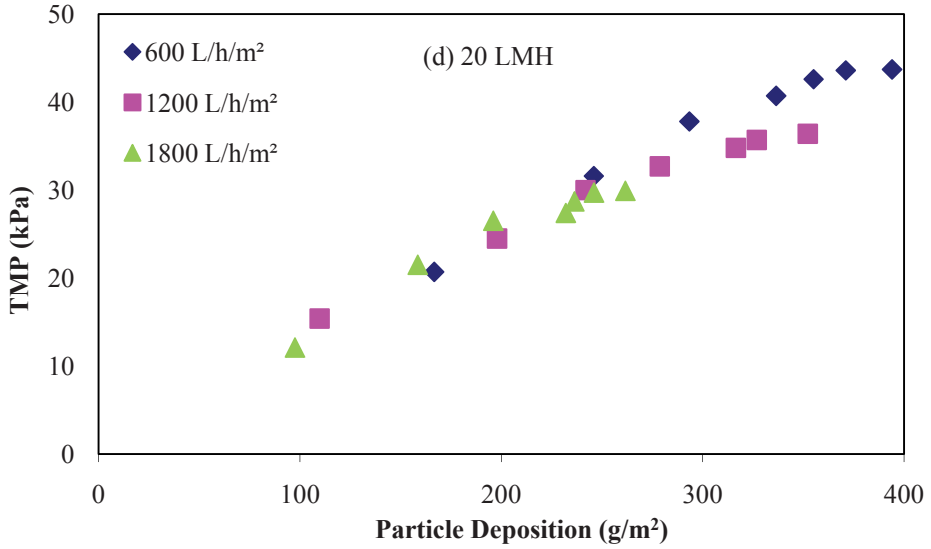

Figure 3.8: Relationship between TMP and particle deposition for different air flow rates

Table 3.6 Relationship between TMP and particle deposition for different permeate flux and air flow rates

Air flow rate	600 L/h/m^2		1200 L/h/m^2		1800 L/h/m^2	
Flux (LMH)	Equation	R^2	Equation	R^2	Equation	R^2
5	-	-	-	-		-
10	$Y = 0.044X - 1.969$	0.877	$Y = 0.048X - 0.545$	0.916	$Y = 0.024X - 0.805$	0.869
15	$Y = 0.055X + 4.492$	0.979	$Y = 0.057X + 3.991$	0.982	$Y = 0.043X + 3.03$	0.971
20	$Y = 0.103X + 5.197$	0.965	$Y = 0.088X + 6.878$	0.975	$Y = 0.107X + 3.214$	0.952

[Y = TMP (kPa), X = Particle Deposition (g/m^2)]

3.4 Conclusions

This study investigated the effects of air flow rates and permeate flux on the deposition of particles on the membrane surface. The main conclusions were:

- A smaller amount of particle deposition was observed on the membrane surface at high air flow rates for all permeate flux rates, whereas at low air flow rate there was a large deposition which caused a high TMP.

- At a lower permeate flux, an increase in air flow rate showed an effective reduction in particle deposition and TMP, whereas at a higher flux rate, the reduction was minimal. A sharp rise in TMP occurred during the first few hours of operation, indicating that air flow for deposition mitigation strategies should focus on this period to optimise membrane operation.

- A flux of 15 LMH was found to be the critical flux beyond which a rise in the permeate flux showed a sharp rise in TMP and particle deposition.

- For a given value of permeate flux, a linear relationship between the TMP and particle deposition has been found regardless of air flow and rates. This relation simply shows interdependency between TMP and particle deposition during the submerged membrane microfiltration of kaolin suspension. Air flow and permeate flux rates are the governing factors for particle deposition, and a single parameter consideration may not be effective for an efficient membrane filtration design process.

Chapter 4

Modelling of particle deposition in submerged membrane microfiltration

Abstract

In this study, a particle deposition mathematical model for submerged membrane microfiltration was developed based on experiments with a high concentration of kaolin clay in suspension. The effects of air flow rate and permeate flux on transmembrane pressure (TMP) and on membrane resistance were studied. The experimental results showed that the filtration resistance due to cake formation played a dominant role in the total filtration resistance. Internal fouling was observed to be negligible during filtration. An increase in permeate flux caused higher TMP development due to an increased amount of particle deposition. Conversely, an increase in air flow rate reduced TMP by detaching deposited layers back into suspension. The particle depositions under different filtration flux and air flow rates were correlated to establish an empirical formula.

4.1 Introduction

Membrane application in wastewater treatment has attracted enormous attention worldwide over the past 10-15 years. A submerged membrane bioreactor (with air bubble scour system for membrane fouling/particle deposition reduction) is increasingly used in many industries for the purification and separation of particles from liquid. In an aerobic submerged microfiltration bioreactor system, the preferred configuration today is a dual tank system in which the membrane tank is separated from the aeration tank. In the membrane tank, the injected large air bubbles not only prevent the deposit of particles due to shear stress and local turbulence but also detach the deposited bio-cake

from the membrane surface and promote a continuous movement of the fibres (Cabassud et al. 2001). Since the performance of the microfiltration is significantly affected by membrane fouling, better understanding of the particle deposition mechanism in an air sparged membrane system could lead to the development of an efficient membrane system that produces minimum membrane fouling.

Cross-flow velocity in a side stream membrane bioreactor and air flow (air scour or air sparging) in submerged membrane system have been considered to be two main hydrodynamic approaches that play an influential role in membrane fouling control. The effect of air flow in the enhancement of membrane system performance has been reported experimentally in several research works (Germain, Stephenson & Pearce 2005a; Le-Clech, Jefferson & Judd 2003; Pradhan et al. 2011; 2012; Ueda et al. 1997). However, little information is available on the hydrodynamic analysis of particles in an aerated submerged membrane system. In 1997, Laborie et al. studied the effect of air injection into the feed stream, generating a gas/liquid two phase on the membrane surface to reduce particulate membrane fouling. They found that the air injection process enhanced the permeate flux for all experiments studied in UF hollow fibres with clay suspension. Their finding reported that the air injection clearly modified the cake structure, and seemed to expand the cake. Cabassud et al. (2001) also used clay suspension for a hollow fibres membrane and investigated the effect of applying gas to the feed during ultrafiltration. They mainly linked the flux enhancement to hydrodynamic control: the mixing and turbulence created by the bubbles in the liquid phase. Significant increases in permeate flux have been reported, even at very low air velocity, for all the concentrations studied. Cabussud et al. (2001) found that the air injection resulted in an increase in flux enhancement up to 155% in specific conditions.

Significant development in understanding the fouling of individual components such as bacteria, yeast, proteins and colloids has been achieved in microfiltration and ultrafiltration (Belfort, Davis & Zydney 1994; Fane & Fell 1987). Suspended solids are very often identified as a main foulant (Bae & Tak 2005; Defrance et al. 2000), where the significance of the submicron colloidal fraction in the suspended solids has been correlated with membrane fouling rates (Rosenberger et al. 2006; Wisniewski, Grasmick & Leon Cruz 2000). Ivanovic et al. (2008) studied the role of submicron particles in membrane fouling with the modification of a submerged hollow fibre membrane reactor by introducing a flocculation zone below the aeration device of the membrane module which caused the reduction of submicron particles from 8.2% to 6.9%. They reported that the reduction of submicron particles (colloids) adjacent to the membrane resulted in a better fouling control in the biofilm membrane reactor. Bouhabila et al. (1998) observed that the supernatant of mixed liquor suspended solids (MLSS) had 20-30 times higher specific resistance than the sludge suspension, which highlights the high fouling propensity of soluble and colloidal fractions.

In recent years, many models have been developed with a view to understanding the membrane fouling mechanism or predicting filtration flux during microfiltration. During the filtration of colloidal particles and macromolecules, the diffusion mass transport phenomenon was dominant, and concentration models were used to predict the concentration profile near the membrane surface as well as the pseudo-steady filtration flux (Cheryan 1998). When cake resistance contributed to most of the total membrane resistance, however, the hydrodynamic models were frequently used to describe the particle fouling and flux decline (Belfort, Davis & Zydney 1994). In a submerged membrane reactor filtration of colloidal particles, cake resistance was found to be a major component. The stability of the particles attaching to the membrane surface could

be analysed by a force balance model (Hwang & Lin 2002) or a moment balance model (Lu & Ju 1989).

This study presents the gas-liquid two phase flow method used for microfiltration of kaolin clay with flat sheet membrane module. The effects of operating conditions such as air flow and permeate flux rates on transmembrane pressure (TMP), particle deposition, and membrane filtration resistance were analysed through experiments. The correlation of air flow rate with particle deposition and TMP was established at different permeate flux rates.

4.2 Force Balance Model for Particle Deposition

The deposition of particles depends on the hydrodynamic forces in the immediate vicinity of the membrane surface during filtration. Figure 4.1 shows a schematic diagram of the forces acting on a deposited particle in submerged flat sheet membrane microfiltration. For a fixed flat sheet membrane, the hydrodynamic effect incurred by the two phase flow is obviously different from the effect incurred by a tubular or hollow fibre membrane. In the case of aerated submerged hollow fibre, movement of the fibre (bubble-induced) plays an important role in reducing the fouling rate (Wicaksana, Fane & Chen 2006b), whereas for submerged flat sheet membrane, the gap between adjacent membrane plates can have a significant effect on hydrodynamic conditions. Ndinisa et al. (2006b) reported a negative effect of widening the gap on the shear stresses on the membrane.

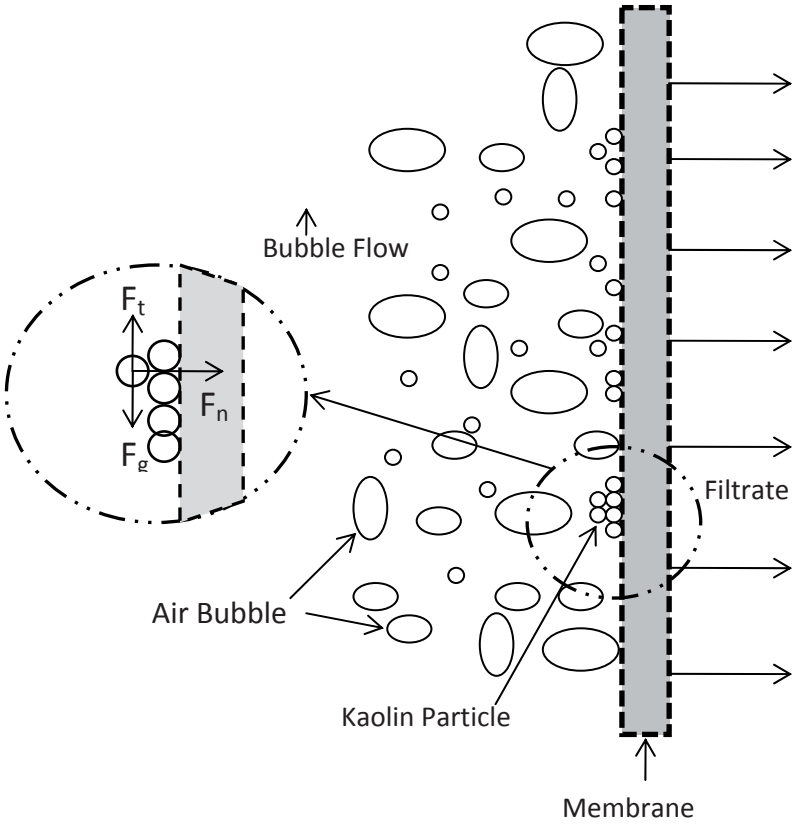

Figure 4.1 Acting forces on a single particle during microfiltration

In this study, a flat sheet membrane is submerged in the suspension tank and air bubbles are injected from the bottom of the tank via an air diffuser. Particles present in the suspension are transported by suspension flow and some are deposited on the membrane surface. The external forces acting on a deposited particle include drag forces in the tangential (F_t) and filtration (F_n) directions and gravitational force (F_g). The drag force in the tangential direction (parallel to the membrane surface) is a shear force due to air bubble flow. The deposited particle would be more stable under larger values of F_n but may be transported back to the tank if the net tangential force exceeds the filtration force. Since the net up-flow velocity of particles is very small and the particle size is greater than 1 μm, the inertial lift force and net inter-particle force are commonly much smaller than the drag forces and so can be neglected. A force balance model in a

pseudo-steady condition, in which the particle can deposit in a stable manner on the membrane surface, can therefore be written as (Lu & Hwang 1995):

$$\left(F_t - F_g\right) = f_c F_n \tag{4.1}$$

where f_c is the frictional coefficient between particles, F_t and F_n are drag forces in the tangential direction and filtration direction respectively and F_g is the gravitational force. No air flow condition allows a convenient way to calculate the friction coefficient between particles. According to equation (4.1), the value of tangential drag force (F_t) becomes zero under no air flow condition, and gravitational force (F_g) and drag force in filtration direction (F_n) can be determined by solving equations (4.9) and (4.10) respectively.

As the Reynolds number in the filtration direction is very small under most conditions, the drag force in the filtration direction (due to permeate flow) can also be estimated by the modified Stokes' law:

$$F_t = C_1 d_p^2 \tau_w \tag{4.2}$$

where d_p is the particle diameter, τ_w is the shear stress acting on the membrane surface, and C_1 is a constant. The shear stress generated by the rising bubbles can be considered to be proportional to the shear stress acting on the bubble surface (τ_b) and bubble generation frequency (f_r) (Hwang & Sz 2010). τ_w can be expressed as:

$$\tau_w = C_2 \tau_b f_r \tag{4.3}$$

where C_2 is constant. According to the definition of drag coefficient (C_D), the shear stress acting on the bubble surface can be determined by:

$$\tau_b = C_D \left(\frac{\rho_b u_b^2}{2}\right) \quad (4.4)$$

where u_b and ρ_b are the rising velocity and density of the bubble respectively. For a single bubble, neglecting its density, the drag coefficient can be estimated as (Fan & Tsuchiya 1990):

$$C_D = \frac{4gd_b}{3u_b^2} \quad (4.5)$$

Substituting C_D in equation (4.4), shear stress can be derived as:

$$\tau_w = C_2 \tau_b f_r = C_2 \frac{2\rho_b g d_b}{3} f_r \quad (4.6)$$

As bubble generation frequency is proportional to the air flow rate, it can be determined as:

$$f_r = \frac{Q}{V_b} = \frac{6Q}{\pi d_b^3} \quad (4.7)$$

where Q is the volumetric air flow rate, V_b is the bubble volume and d_b is the equivalent bubble diameter. Substituting the values of equations (4.6) and (4.7) into equation (4.2), the drag force in the tangential direction can be calculated as:

$$F_t = C_1 C_2 d_p^2 \tau_b f_r = C_3 \frac{\rho_b d_p^2 Q}{d_b^2} \quad (4.8)$$

The coefficient C_3 can be determined by regressing experimental results under the condition in which a particle with a diameter of d_p can deposit in a stable manner.

The net gravitational force on a single particle is calculated from the Stokes' equation:

$$F_g = \frac{\pi d_p^3 (\rho_p - \rho_l) g}{6} \quad (4.9)$$

where ρ_p and ρ_l are densities of particle and liquid respectively.

Since the Reynolds number in the filtration direction is very low in most conditions, the drag force in the filtration direction (i.e. normal drag force) can be calculated by the modified Stokes' law:

$$F_n = 3\pi\mu d_p J C_4 \tag{4.10}$$

where μ is the viscosity of suspension, and J is the pseudo-steady flux. C_4 is a correction factor due to the existence of cake and membrane which can be estimated (Sherwood 1988) as:

$$C_4 = 0.36\left(\frac{R_t d_p^2}{4L_c}\right)^{2/5} \tag{4.11}$$

where R_t is the total membrane resistance and L_c is the cake thickness. Cake thickness is determined by a mass balance method by measuring the cake mass and porosity.

The TMP (ΔP) developed over the filtration period can be used to calculate the total filtration resistance (R_t) according to Darcy's law (Belfort, Davis & Zydney 1994).

$$J = \frac{\Delta P}{\mu R_t} = \frac{\Delta P}{\mu(R_c + R_m)} \tag{4.12}$$

The total membrane resistance is the sum of cake resistance and clean membrane resistance only. Resistance due to pore blocking is neglected because particle diameter is greater than membrane pore size. The cake resistance can be used to calculate the cake mass (w_c) as:

$$R_c = w_c \alpha_{av} \tag{4.13}$$

where α_{av} is an average specific membrane resistance determined experimentally by the modified fouling index (MFI) method. This is an approximate value only as the structure of the cake is not the same in the MFI test (dead-end filtration) and aerated submerged membrane system.

Based on the mass balance, the cake thickness (L_c) can be calculated as:

$$L_c = w_c/(\rho_p(1-\epsilon_{av})) \tag{4.14}$$

where ε_{av} is the average cake porosity, which can be calculated from Kozeny's equation:

$$R_c = \frac{180(1-\varepsilon_c)^2}{(d_p^2\varepsilon_c^3)} \tag{4.15}$$

where ε_c stands for the porosity of the cake and d_p is the average diameter of the particles.

Substituting equation (4.13) into equation (4.14), we will obtain the cake thickness as,

$$L_c = \frac{R_c}{\alpha_{av}\rho_p(1-\varepsilon_{av})} \tag{4.16}$$

The total membrane resistance can be calculated from the TMP, measured in experiments. Hence, the cake resistance can easily be derived by deducting the known value of clean membrane resistance from the total membrane resistance. The average cake porosity (ε_{av}) is calculated from the Kozeny equation. C_3 is determined from the graphical plot between F_t and $\frac{\rho_b d_p^2 Q}{d_b^2}$. Similarly C_4 is calculated from equation (4.1). Once cake thickness is related to cake resistance, the cake thickness can be estimated from equation (4.11).

4.3 Materials and Method

The experimental set-up and procedure used in this chapter are identical to those used in Chapter 3 and hence are not presented here. The experimental set-up is presented in Figure 3.2 and the procedure is described in section 3.2 of Chapter 3.

4.4 Results and Discussion

4.4.1 Effect of Air Flow Rate on Feed Concentration

An aerated submerged membrane microfiltration was performed with kaolin clay as the model suspension. All experiments were started with the kaolin concentration of 10 g/L. The concentration reduced as time elapsed with increasing specific filtrate volume. The permeate was returned to the tank. According to mass balance theory, the change in concentration should be due to the deposition on the membrane at that particular time because no kaolin settled at the bottom of the tank.

Figure 4.2 shows the variation of kaolin concentration with time and specific filtrate volume under various air flow and permeate flux rates. As the filtration time increases, the specific filtrate volume also increases but the feed concentration decreases. During the filtration process, kaolin particles were deposited on the membrane surface, resulting in lower concentration at the reactor tank. A high concentration of feed represents low fouling on the membrane and vice-versa. Higher feed concentration was observed at a higher air flow rate. This was due to the scouring phenomenon of the air bubbles that transported deposited kaolin particles back to the tank. Higher permeate flux experienced rapid change in the feed concentration. At low air flow rate (600 $L/h/m^2$), a flux of 20 $L/m^2/h$ led to less than half of the initial concentration (4.13 g/L) within 180 minutes of the filtration period.

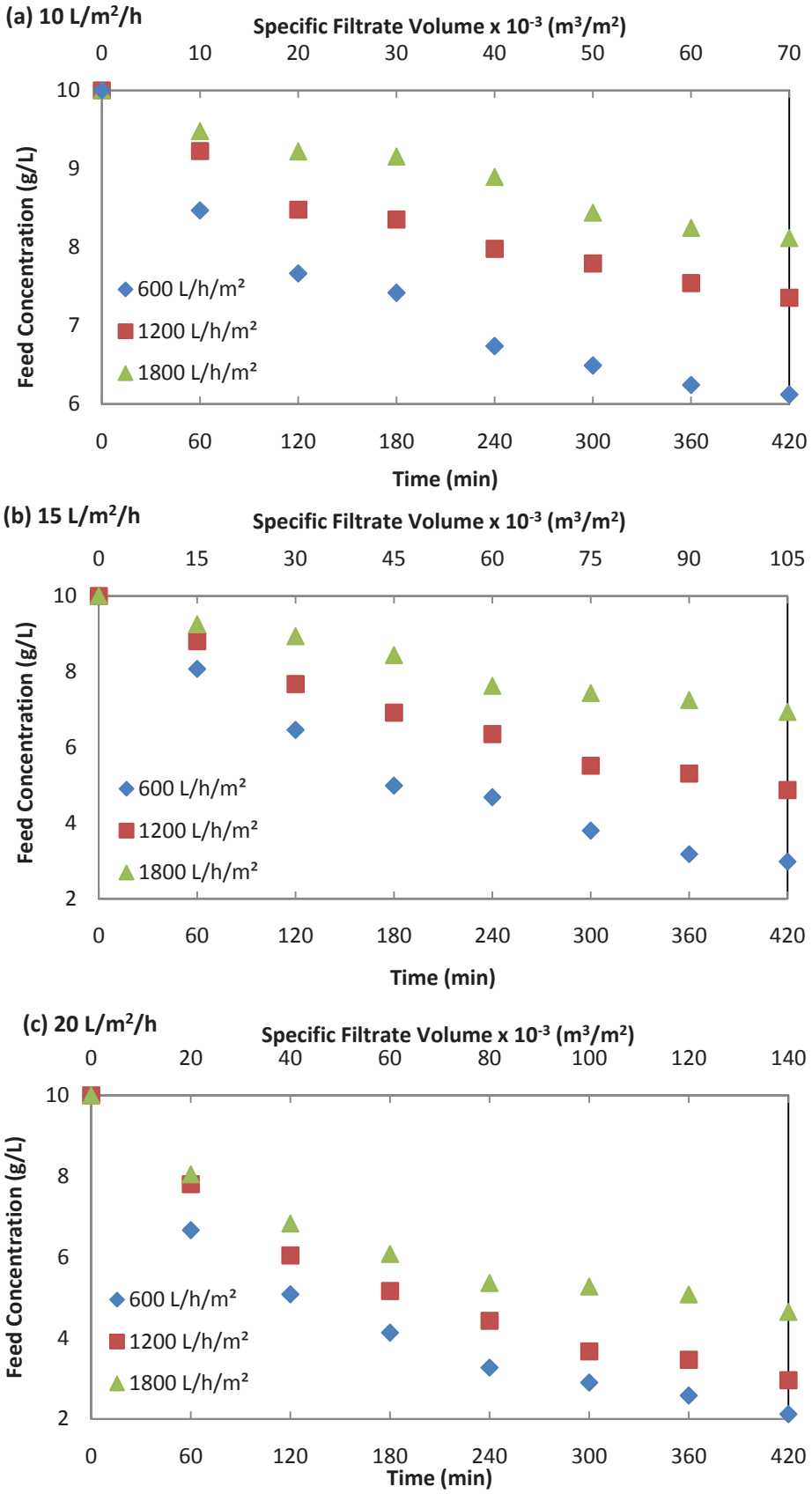

Figure 4.2 Effect of air flow on feed concentration in a submerged reactor tank

4.4.2 Effect of Air Flow Rate on Total Membrane Resistance

To understand the fouling mechanism during the submerged membrane microfiltration, total membrane resistance was calculated. According to the resistance in series model, the total membrane resistance (total hydraulic resistance) is the sum of the filtration resistance due to (i) the filter cake (R_c), (ii) membrane pore blocking (R_p) and (iii) the clean membrane (R_m).

$$R_t = R_c + R_p + R_m \tag{4.17}$$

The total membrane resistance can be calculated by solving equation (4.12), while the resistance of the clean membrane was measured by filtering clean water through the membrane. It was assumed that the fouling resistance due to pore blocking was negligible because the mean particle size of the kaolin was larger than the membrane pore size. When the microfiltration test in an experiment was terminated, however, resistance due to internal fouling was measured by the difference between the pressure developed in clean water before and after removing the deposit on the membrane. The resistance due to pore clogging was found to be very negligible ($5.4x10^{10}$ m^{-1}) compared to cake resistance. Thus, the assumption was also verified by the experiment results.

In this study, permeate viscosity and flux rates are constant, therefore the variation of TMP and total membrane resistance are the same. These parameters are plotted against the specific filtrate volume at Figure 4.3. At the start of filtration, the TMP and total membrane resistance increased very rapidly due to fine particle deposition on the membrane surface. The TMP gradually reached a saturation state, but the saturation time was dependent on both the filtration flux and the air flow rate. The higher filtration flux (20 $L/m^2/H$) reached saturation state quickly compared to the lower flux. The total resistance (and also TMP) decreased significantly as air flow rate increased. Air bubbles

were relatively more effective at lower filtration flux. A faster particle deposition and tendency to reach a TMP plateau was observed at 20 L/m^2/h.

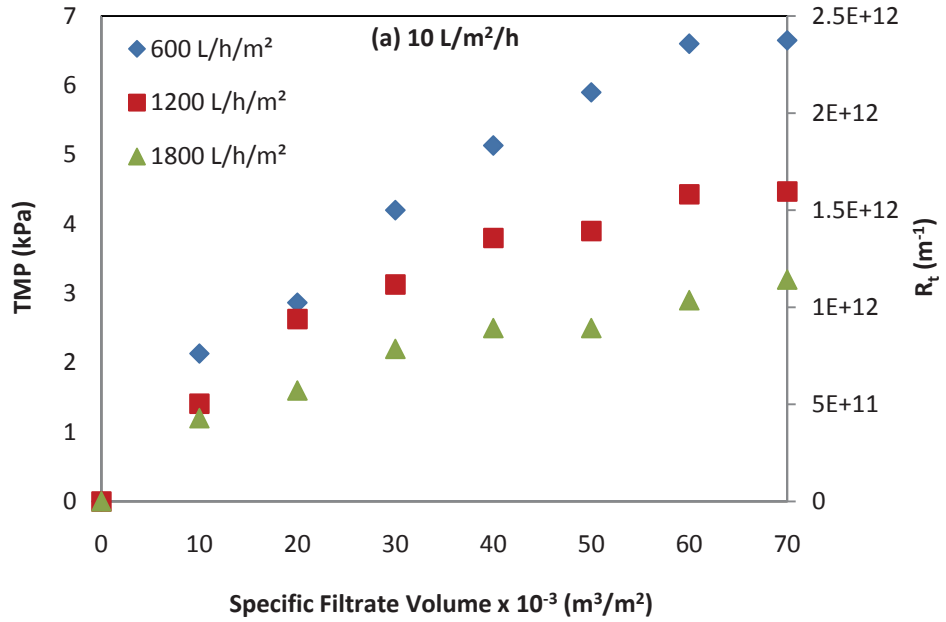

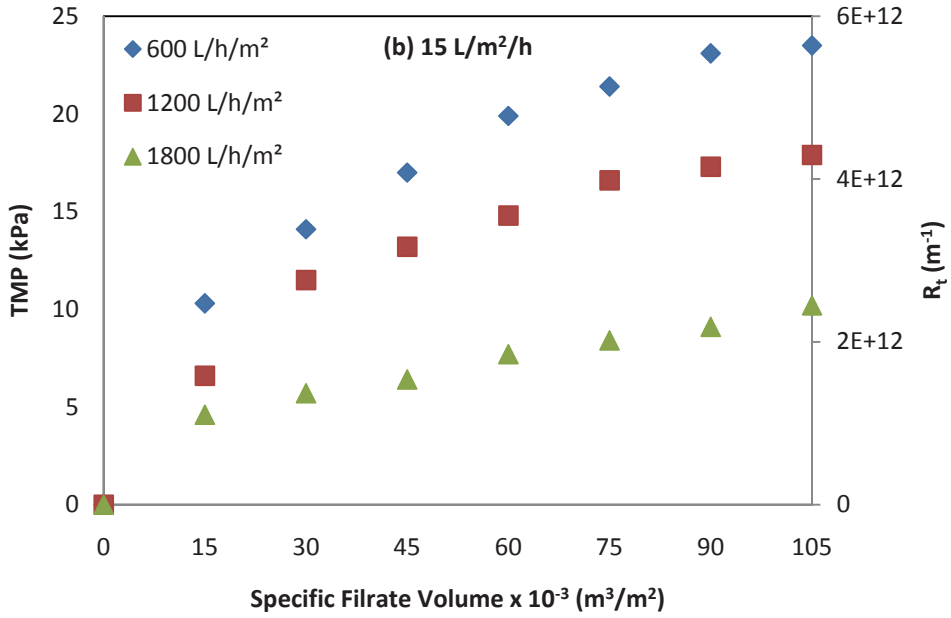

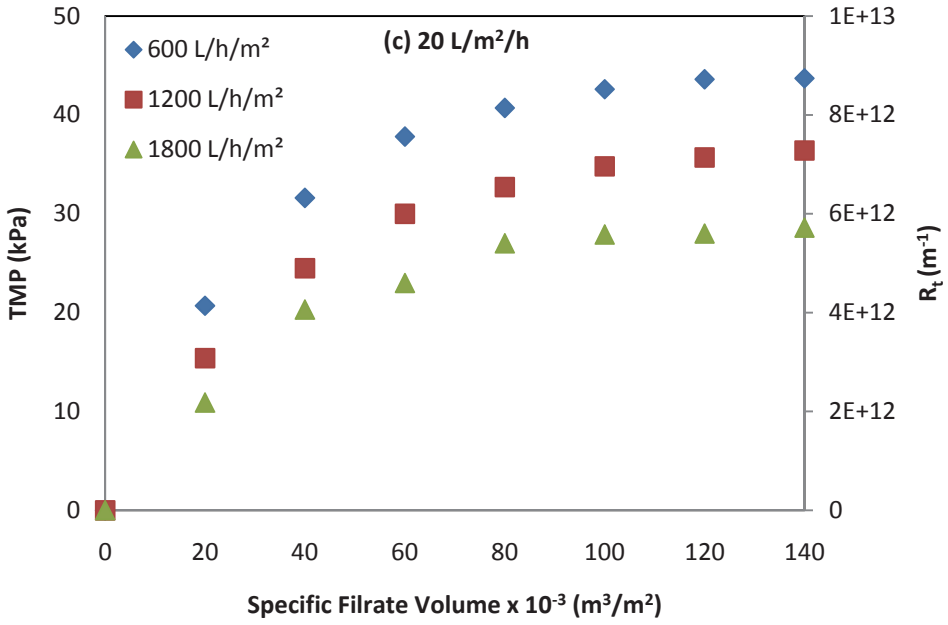

Figure 4.3 TMP and total membrane resistance developments for constant flux rates

Figure 4.3 also presents the TMP variation during the application of air flow to collect a particular amount of filtrate. For example, the filtration process operated at a flux of 10 L/m^2/h developed a TMP of 6.6 kPa at 600 L/h/m^2 air flow rate and took 6 hours to produce a specific filtrate of 0.06 m^3/m^2, whereas at flux rates of 15 and 20 L/m^2/h, the TMP reached 19.9 and 37.8 kPa respectively to produce the same volume of filtrate. The time taken was 4 and 3 hours respectively; however, the increased air flow rate (1800 L/h/m^2) limited the TMP rise to 2.9, 7.7 and 23 kPa for 10, 15 and 20 L/m^2/h respectively.

Figure 4.4 summarises the variation of TMP development due to increased air flow rate for different permeate flux rates. The summary graph shows that the effect of permeate flux on TMP development is far higher than that of air flow rate.

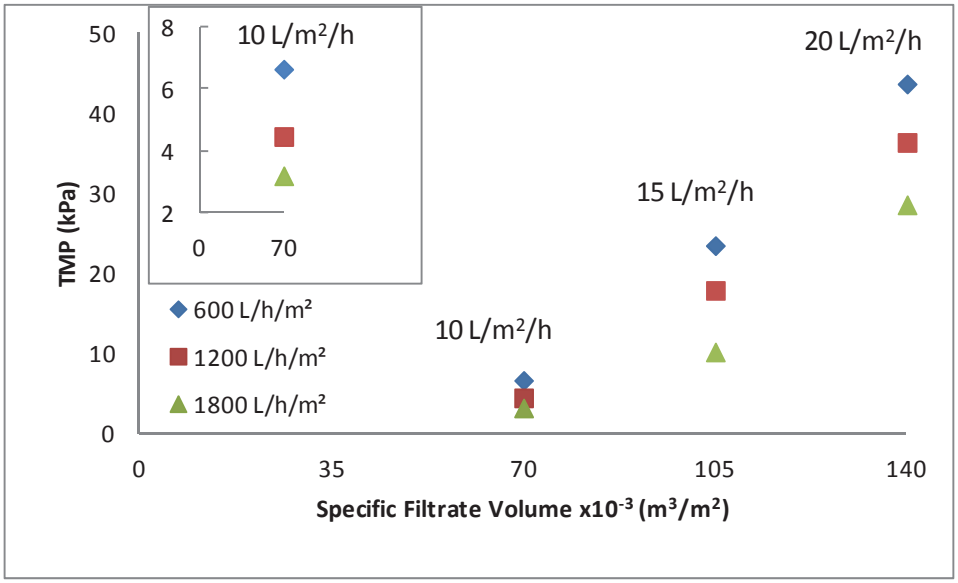

Figure 4.4 TMP developments after 7 hours of microfiltration under different air flow rates

Figure 4.5 presents the particle deposition profiles with the specific volume filtrated. The particle deposition values were obtained from the feed turbidity of particular time. These figures indicate that particle deposition due to colloidal particle increases with the increasing permeate flux and the volume filtered. However, the application of higher air flow has limited the particle deposition. Similar results were obtained in terms of TMP development during the microfiltration process (Figure 4.3).

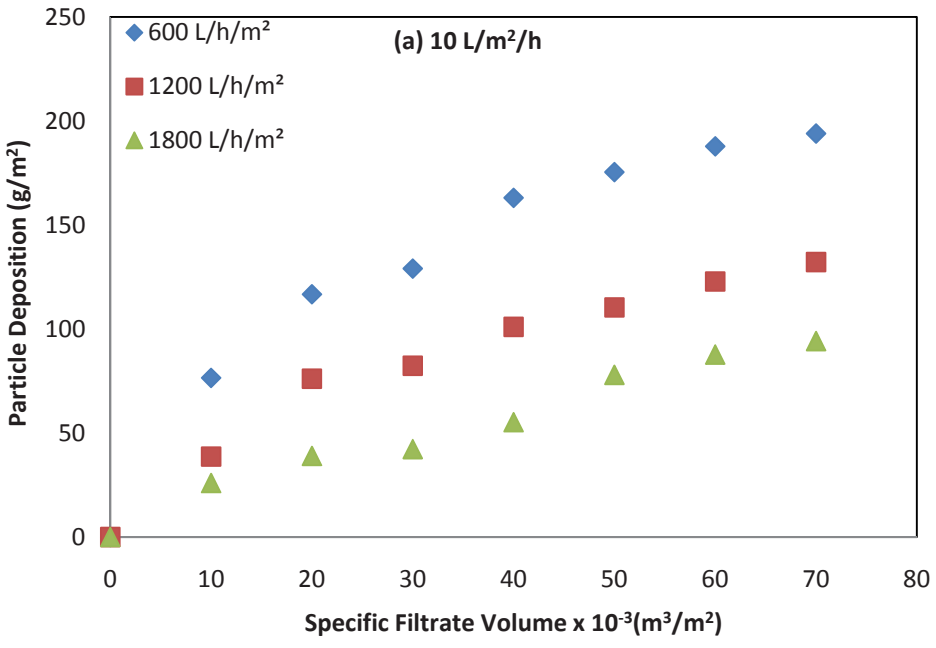

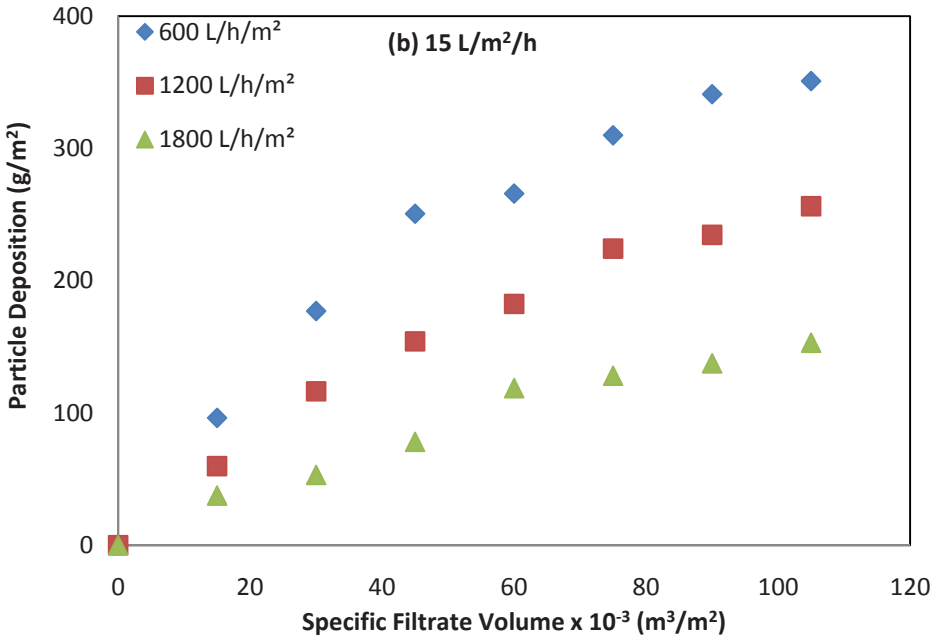

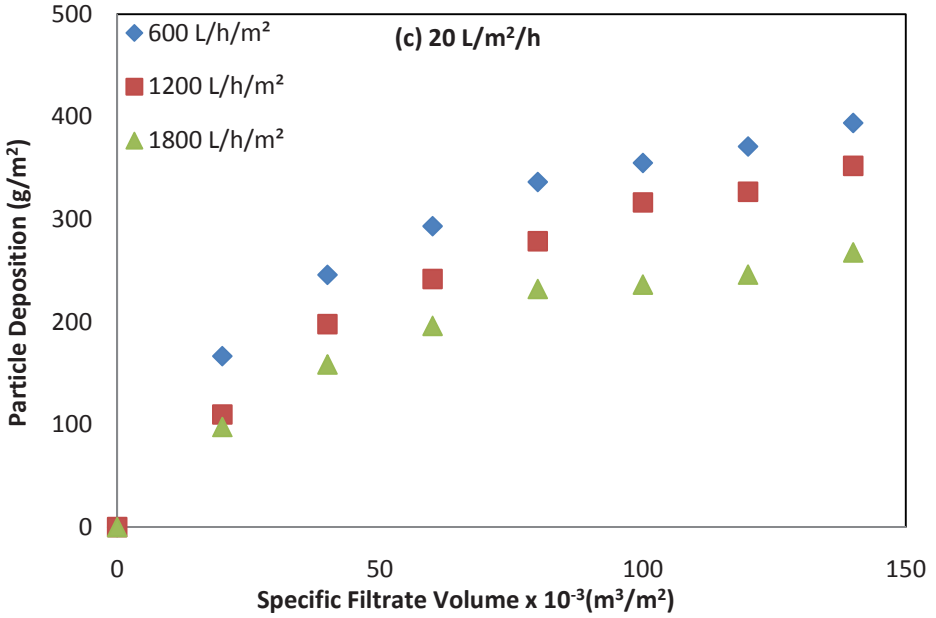

Figure 4.5 Particle deposition vs. specific filtrate volume at different air flow and permeate flux rates

4.4.3 Cake Resistance

The relationship between cake resistance and particle deposition is presented in Figure 4.6. A quasi-linear relationship was observed between these parameters which were significantly affected by both filtration flux and air flow rate. An increased air flow reduced both cake resistance and particle deposition. A high flux is associated with a

steep slope (gradient) which directly leads to higher cake resistance (Figure 4.6 c). This slope is directly related to the specific filtration resistance (α_{av}). Slopes obtained from these graphs are plotted against the permeate flux rate (Figure 4.7). The relationship between the cake resistance and particle deposition can be regressed as;

$$R_c = 9.1x10^{12}\delta;\ R^2 = 0.91 \text{ (for 10 L/m}^2\text{/h)} \quad (4.18)$$

$$R_c = 15.7x10^{12}\delta;\ R^2 = 0.98 \text{ (for 15 L/m}^2\text{/h)} \quad (4.19)$$

$$R_c = 20.3x10^{12}\delta;\ R^2 = 0.98 \text{ (for 20 L/m}^2\text{/h)} \quad (4.20)$$

where R_C and δ are cake resistance (m^{-1}) and particle deposition (kg/m^2). The equations (4.18-4.20) suggest the gradient is proportional to the flux. Thus a general formula could be $R_c = 1.01x10^{12}J\delta$ ($1.01x10^{12}$ can be obtained from Figure 4.7 and J is permeate flux expressed in $L/m^2/h$). Therefore, it can be concluded that the cake resistance is proportional to the multiplication of flux and cake deposition.

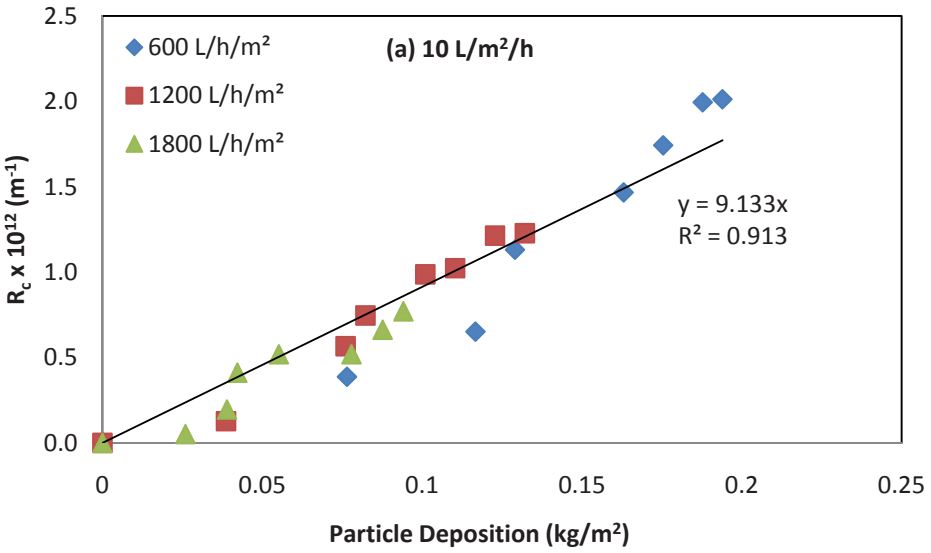

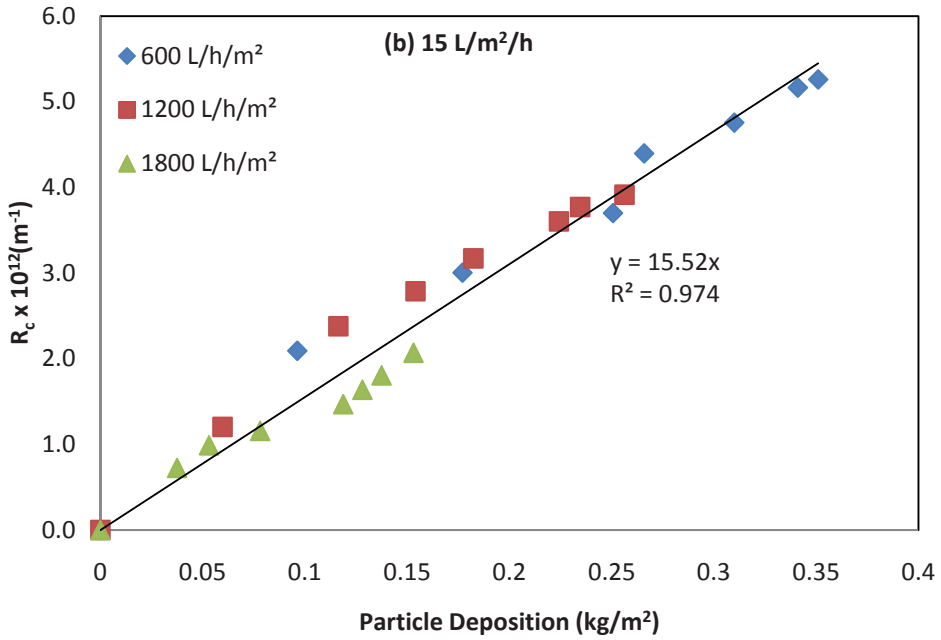

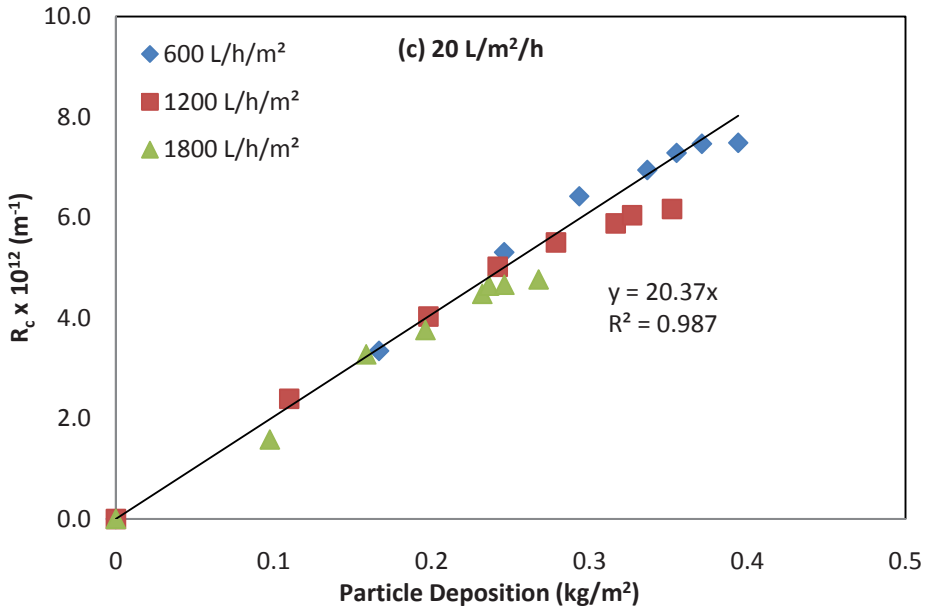

Figure 4.6 Relationship of cake resistance and particle deposition under different air flow rates and permeate fluxes of 10, 15 and 20 L/m^2/h

It can be also noted that at lower flux (Figure 4.6a), the cake resistance is not exactly proportional to particle deposition and the proportionality constant depends to an extent on the rate of air flow rate. But at higher fluxes (figures 4.6b and c), the effect of air flow rate does not influence the proportionality constant much (at all air flow rates, the data fall onto a linear plot). This could be evaluated further in terms of hydrodynamics.

Figure 4.7 correlates the permeate flux with the slopes obtained from Figure 4.6. The values of slopes denoted in abscissa are proportional to the average specific filtration resistance. This figure proves that the formation (structure) of the cake is dependent upon the filtration flux or on the balance of forces acting on particle deposition.

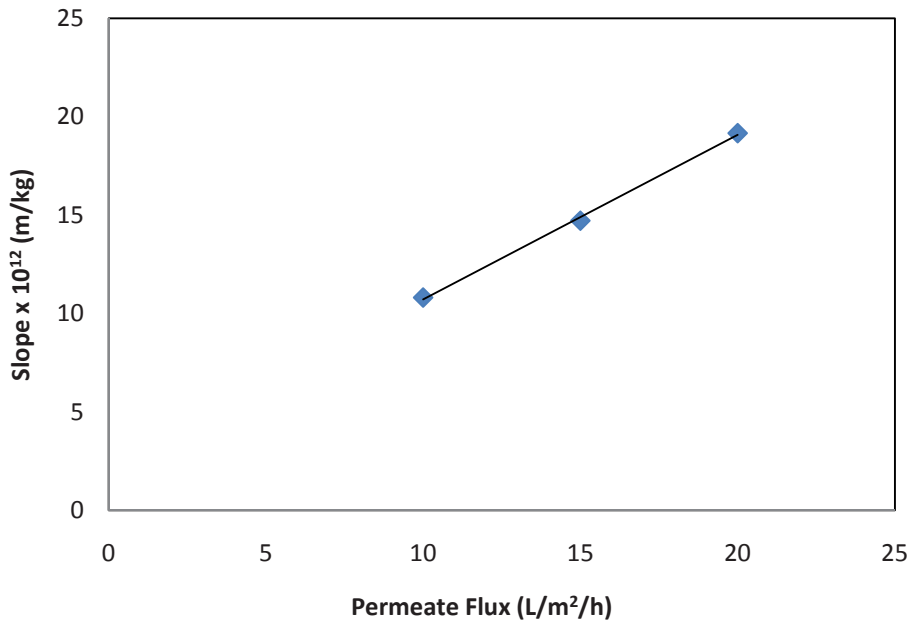

Figure 4.7 Effect of permeate flux on specific filtration resistance of cake

4.4.4 Specific Filtration Resistance of Cake

The specific resistance is an intrinsic characteristic of the cake. It is defined by using equation (4.13) as:

$$\alpha_{av} = \frac{R_c}{W_{c_c}} \tag{4.21}$$

where w_c is the mass of suspended solids deposited from the unit volume of filtrate. The calculated average specific cake resistance, based on experimental data, is plotted with filtration flux in Figure 4.7. Increased permeate flux creating high pressure causes more cake compression, resulting in a higher specific filtration resistance. The compact cake structure causes the average specific cake resistance to be high (x10^{13} m/kg) for kaolin

clay particles of 2 μm in size (used in suspension). To check this cake resistance value, a Modified Fouling Index (MFI) test was carried out for different TMP. In each MFI test, new membranes (of pore size of 0.45 μm and diameter of 47 mm) were used to avoid residual fouling. The details of MFI can be found elsewhere (Chinu et al. 2010). The kaolin feed was pressurised at 80, 40 and 10 kPa using N_2 gas. The MFI value was obtained from the slope of the plot between *t/V* and *V* (where t = time and V = volume of filtrate water). The following equation was used to calculate average specific filtration resistance (α_{av}).

$$\frac{t}{v} = \frac{\mu R_m}{\Delta P A} + \frac{\mu \alpha_{av} C_b}{2 \Delta P A^2} V \tag{4.22}$$

where

V is the total permeate volume (L)

R_m is the membrane resistance (m/kg)

T is the filtration time (s)

ΔP is the TMP, transmembrane pressure (Pa)

μ is the water viscosity at 20˚C

α_{av} is the specific resistance of the cake deposited

C_b is the concentration of particles in feed water (mg/L), and

A is the membrane surface area (m^2)

The comparison of specific resistance (α_{av}) obtained from microfiltration and MFI is shown in Figure 4.8. In the case of microfiltration, average specific resistance was

calculated from equation (4.13) by using the experimental values of cake resistance (R_c in m^{-1}) and cake mass (w_c in kg/m^2). For comparison, steady state TMP (after 7 hours of experiment) was used for microfiltration, and the same test period was employed for the MFI test. This figure shows that the α_{av} calculated by both methods matches well for a low permeate flux.

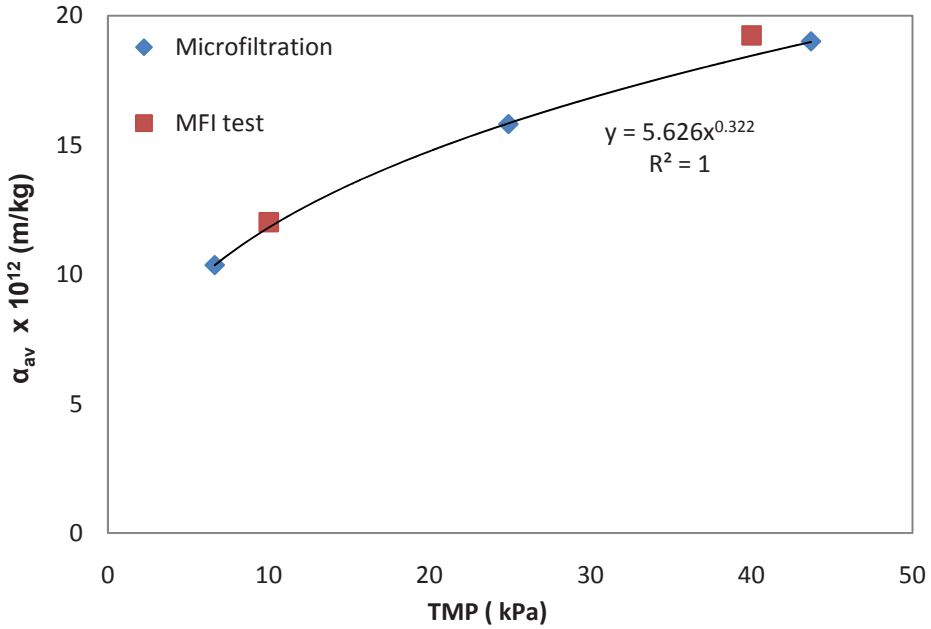

Figure 4.8 Comparison of specific filtration cake resistance

Figure 4.9 presents the effects of air flow and permeate flux rates on average specific filtration resistance. For a given flux, the specific resistance decreases when the air flow increases. This proves that the air flow rate has an effect not only on the total membrane resistance but also on specific resistance. This could be a consequence of variation in the porosity of the cake and its eventual particle size distribution. However, it can clearly be seen from the figure that permeate flux predominates in the range of variation of permeate flux and air flow rate, resulting in α_{av} variation of about 100%, with about 10% for air flow rate.

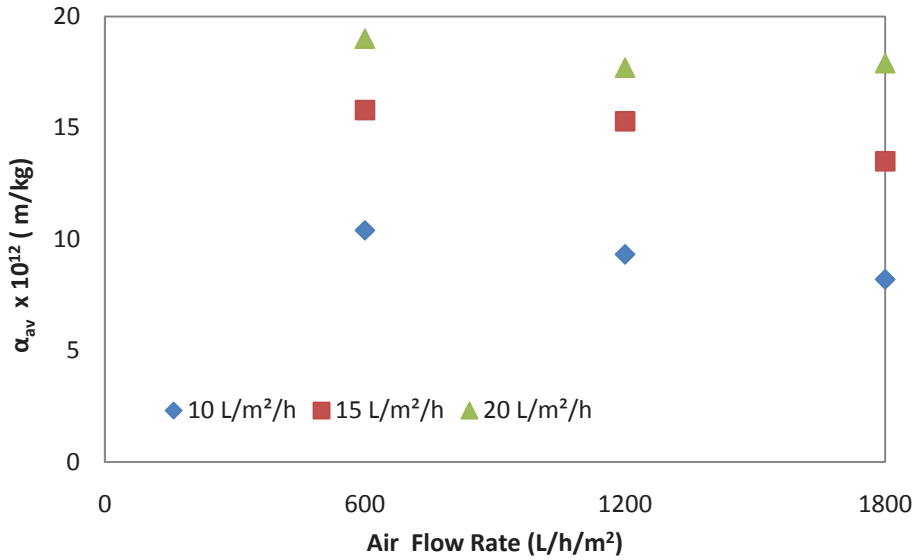

Figure 4.9 Effect of air flow on specific filtration cake resistance

4.4.5 Effects of Air Flow Rate and Permeate Flux on Particle Deposition

Figure 4.10 presents the effect of air flow rate and filtration flux on the mass of particle deposited. As discussed earlier, particle deposition increases with an increase of filtration flux for a given air flow rate. An application of air flow (scour) reduces the cake formation on the membrane surface for a particular permeate flux. This pattern is similar to the results in other filtration studies (Bouhabila, Ben Aim & Buisson 1998).

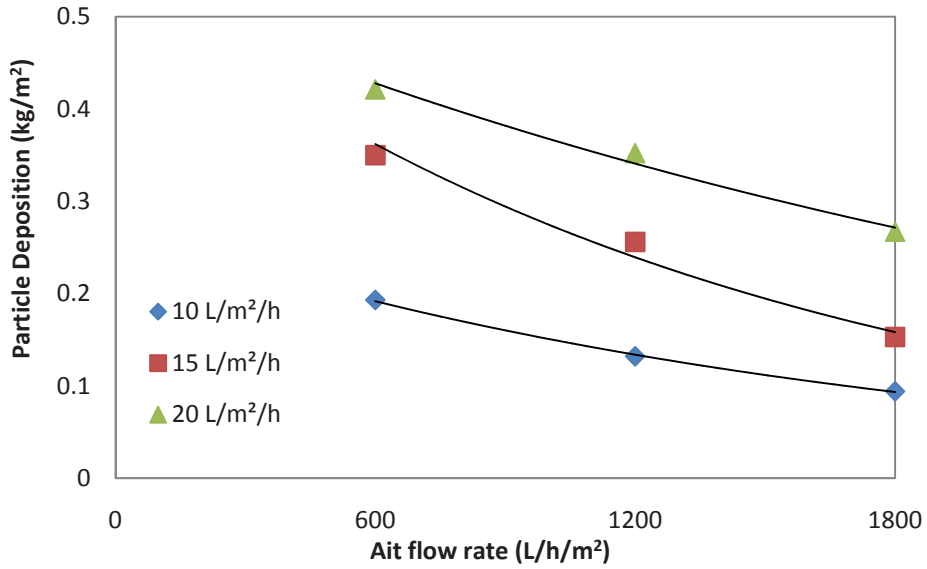

Figure 4.10 Effects of air flow rate and filtration flux on the particle deposition

4.4.6 Correlation of Air Flow with Particle Deposition and TMP

TMP is an indicator of particle deposition on the membrane surface and in the membrane pores, and many researchers have analysed TMP to study membrane fouling. In this study, besides the measurement of TMP, particle deposition on the membrane surface was measured experimentally and these parameters were correlated under various operating conditions. TMP development and particle deposition occurring at different times are presented in Figure 4.11. These parameters were varied with time while air flow was supplied at a fixed rate. This figure shows the variation of TMP and particle deposition with air flow rates at the three specific times of the filtration process (120, 240 and 420 minutes). In this study, a linear relationship of air flow between TMP and particle deposition was observed. These results indicate that TMP is linearly related to particle deposition. Moreover, the effect of air flow on both TMP and particle deposition was observed to be similar (Figure 4.11). The TMP and particle deposition at those three particular time periods followed almost the same pattern at different air flow rates. Therefore, it can be concluded that TMP can well represent particle deposition in this study. The direct relationship between TMP and particle deposition is described in Chapter 3 (Figure 3.8 and Table 3.6). For example, at the air flow rate of 600 L/h/m^2, the following linear relations were developed.

$$Y = 0.044X - 1.969;\ R^2 = 0.87\ (10\ L/m^2/h) \quad (4.23)$$

$$Y = 0.055X + 4.492;\ R^2 = 0.97\ (15\ L/m^2/h) \quad (4.24)$$

$$Y = 0.103X + 5.197;\ R^2 = 0.96\ (20\ L/m^2/h) \quad (4.25)$$

Where X and Y represents particle deposition and TMP respectively.

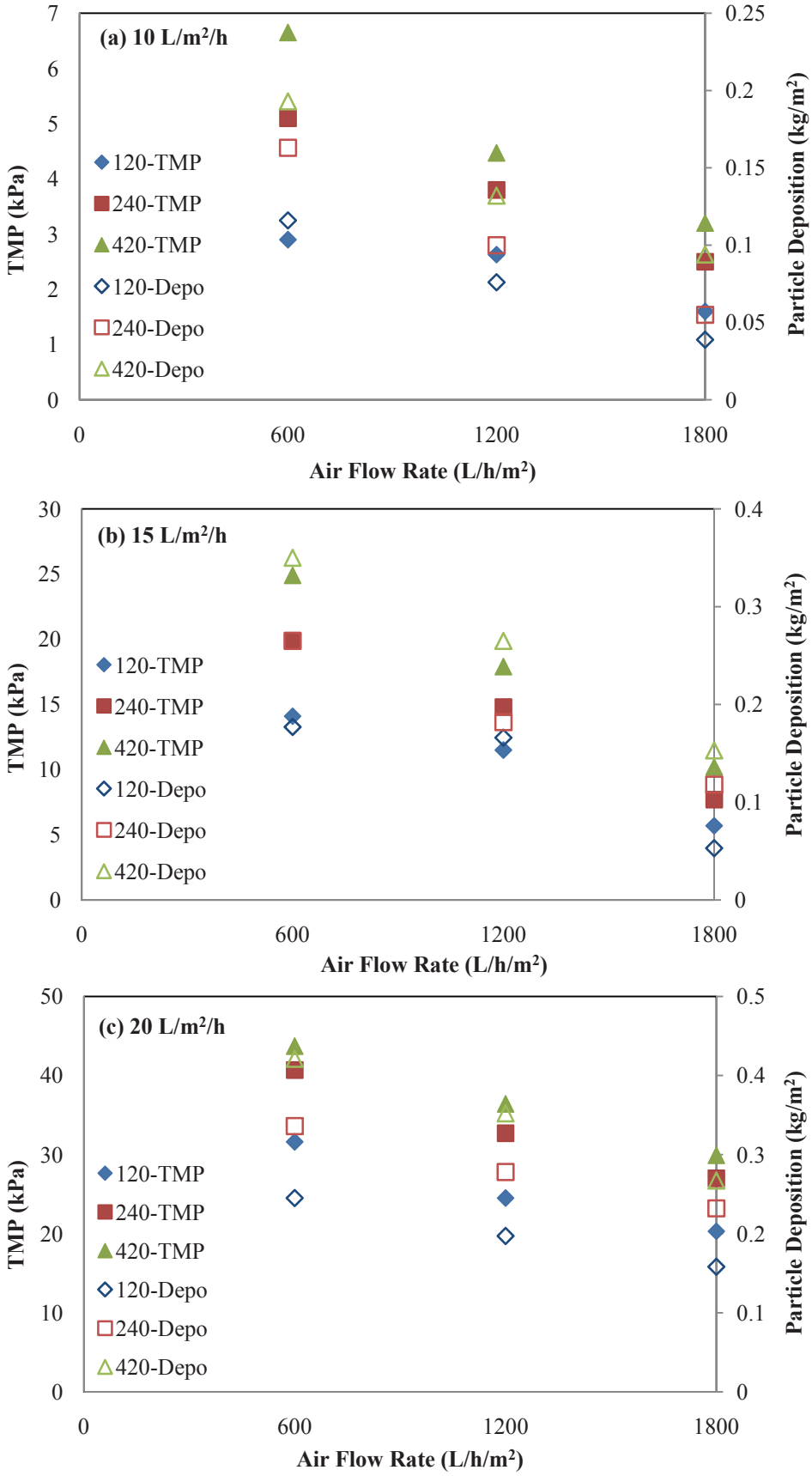

Figure 4.11 TMP and particle deposition at different filtration times with different air flow rates

4.5 Conclusions

The effect of operating conditions, such as filtration flux, air flow rates in terms of TMP, specific filtrate volume (volume of filtered water), membrane resistance, and particle deposition were studied in detail. Membrane internal fouling was observed to be negligible due to the larger feed particle size compared to membrane pore size, and measured resistance due to the cake layer was the major resistance contributing to total membrane resistance. Almost 60% reduction in particle deposition was observed when the air flow rate was tripled from 600 to 1800 L/h/m^2 at a flux rate of 15 L/m^2/h. Higher permeate flux increased particle deposition as well as TMP, but an increase in air flow rate reduced both TMP and particle deposition. A linear relationship between TMP and deposition was obtained from experimental results. Empirical equations were regressed to correlate cake resistance and particle deposition for different operating conditions and a quasi-linear relationship was observed between them, representing the equation (4.13) as $R_c = \alpha_{av} w_c$.

A transitional permeate flux was observed to be at 15 L/m^2/h, beyond which a sharp rise in both TMP and particle deposition were observed. At this permeate flux, experimental results showed a better reduction for both TMP and particle deposition with increased air flow rates (Tables 3.3 and 3.5). Moreover, an air flow rate of 1200 L/h/m^2 was found to be the most effective for this permeate flux. Hence, it can be concluded that 15 L/m^2/h permeate flux operated at 1200 L/h/m^2 air flow rate is the most efficient operating condition compared to other conditions.

Chapter 5

Combined effect of air and mechanical scouring of membranes for fouling reduction in submerged membrane reactor

Abstract

This study investigated the combined effect of air flow and the use of a granular support medium in suspension in a submerged membrane reactor to reduce membrane fouling. Lower membrane fouling and a slower rise in transmembrane pressure (TMP) were noticed when a higher air flow rate was used for membrane scouring. Further fouling reduction was achieved by adding a granular medium in the reactor. The results showed that in the absence of the granular medium, when air flow was tripled (from 600 to 1800 L/h/m^2), TMP development was decreased by 60%. TMP further dropped to 85% with the addition of a granular medium (for the same air flow rate). The doubling of the air flow rate (from 600 to 1200 L/h/m^2) without granular medium led to a 32% reduction in TMP development at 10 L/m^2/h. The same result was obtained at a lower air flow rate of 600 L/h/m^2 with the granular medium. This result shows that the same reduction of TMP can be obtained by adding a granular medium instead of doubling the air flow rate. Therefore, adding a granular medium in the suspension (mechanical scouring) with air flow (air scouring) could be a sustainable alternative to applying high air flow in submerged membrane systems.

5.1 Introduction

Although membrane filtration has several advantages over conventional treatment processes, its wider application has been constrained by membrane fouling due to particle deposition and the intrusion of macromolecules, colloids and particles onto and

into the micro-porous membrane (Belfort, Davis & Zydney 1994). Fouling causes a significant increase in hydraulic resistance which leads to permeate flux decline or a rise in transmembrane pressure (TMP) when the membrane process is operated under constant-TMP or constant-flux conditions, respectively. Frequent membrane cleaning is thus required. This significantly increases energy consumption, resulting in higher operating costs.

Several approaches have been applied to mitigate membrane fouling. The injection of air into the feed stream (air scouring) has been found to be an effective means of mitigating the adverse effect on filtration flux (Cui, Bellara & Homewood 1997). When air is injected through an air distributor into a stationary feed in a submerged membrane system, air bubbles are formed and the buoyancy forces associated with the bubbles keep the suspension in motion (Cui, Chang & Fane 2003). The air bubbles also scour the membrane surface, detaching the deposited cake layer and reducing fouling. Air scouring poses a lesser risk to membrane surfaces than chemical agents. Ueda et al. (1997) stated from their detailed experimental study that air flow was a significant factor governing filtration conditions. They found that reductions in fouling could be achieved by augmenting air flow rates or aeration intensity. Various other methods, such as vortex generation on a corrugated membrane surface (Bellhouse & Sobey 1994), development of new membrane materials (Wang et al. 2002), new design of a membrane module (Bai & Leow 2001, 2002), modification of feed flow pattern (Yamamoto et al. 1989), incorporation of in-situ or ex-situ cleaning regimes for membrane units (Parameshwaran et al. 2001) and the addition of organic or inorganic additives (Lee et al. 2007; Ng, Sun & Fane 2006), have been used to reduce membrane fouling and enhance filtration flux.

One of the most common strategies to reduce and control sludging/fouling in a submerged membrane bio-reactor (MBR) is to provide aeration (air scouring) close to the membrane surface. This induces local shear stress which controls fouling and creates a favourable hydraulic distribution throughout the membrane surface (Bouhabila, Ben Aïm & Buisson 2001). Membrane aeration forms an important part of the operating cost of the MBR (Cui, Chang & Fane 2003; Judd 2006) and it is important to optimise the membrane aeration process. It is commonly accepted that air bubbling close to the membrane is one of the most efficient means of minimizing fouling and ensuring sustainable operation (Meng et al. 2008; Wicaksana, Fane & Chen 2006a).

Aeration is important in MBR for both the biological oxidation of organic matter and membrane defouling. Parameters related to aeration are the bubble size and shape, the density and viscosity of wastewater, internal circulation, and the temperature and presence of surface active compounds (Malysa, Krasowska & Krzan 2005). Recent studies have separated the submerged membrane reactor from the bioreactor tanks to achieve the maximum efficiency of aeration, to remove foulants and to minimise the cost of aeration for biological oxidation (Lebegue 2007; Lebegue, Heran & Grasmick 2009). In theory, small bubbles are better for biological oxidation, while large bubbles facilitate membrane defouling. Sofia et al. (2004) reported that the smallest bubbles produced the best performance, whereas Madec (2000) concluded that the size of the bubbles had no effect on membrane performance.

Optimisation of aeration is still the subject of practical and research interest, both in terms of reducing the foulant accumulating on the membrane and increasing the life of the membrane. By reducing the energy cost, the operating cost of membrane filtration will also be significantly reduced. A more detailed investigation on the impact of

aeration rates on suspension is needed to gain a better understanding of membrane fouling and to reduce the cost of aeration, which is one of the major costs of membrane operation.

Some research has focused on the control of membrane fouling by adding external agents such as powered activated carbon (PAC) and anthracite to the activated sludge. Guo et al. (2006) found that PAC addition can significantly reduce fouling, improve organic removal and increase the critical flux. Ng et al. (2006) used PAC in short term MBR experiments and concluded that the addition of PAC to the activated sludge in an MBR can improve membrane performance. They demonstrated improved membrane performance due to the scouring effect of biologically activated carbon (BAC) at the membrane surface within a bubbled suspension. Basu and Huck (2005) also examined the impact of a support material on an integrated bio-filter membrane system and found that the fouling of the support medium system was at least two times slower than the non-support system. Here, 'support medium' refers to external agents such as granular activated carbon (GAC) or anthracite placed in a known quantity in suspension in the submerged membrane bioreactor. Krause et al. (2008a; 2008b), Siembida et al. (2010) and Johir et al. (2011) used mechanical cleaning of membranes by introducing granular material into the submerged membrane reactor. The granular medium resulted in the enhancement of scouring of the membrane surface. Aryal et al. (2010) also reported the influence of anthracite granules in submerged microfiltration, observing that the presence of anthracite in suspension reduced TMP and flux decline two- or three-fold. These results indicate that introducing a granular medium in suspension plays a significant role in controlling fouling. However, to date there has been no literature that has investigated the relative effect of a granular medium in suspension (for mechanical scouring) and air flow (air scouring) when they are used together. This study highlights

the relative merits of these two factors through detailed experiments conducted under different operating parameters.

5.2 Theory

It is observed that in filtration systems, the flux declines from an initial value to reach a steady value over time. Permeate flux can be expressed as a function of resistance by Darcy's law as already mentioned in equation 4.12 at Chapter 4.

In this study, the cake is assumed to be incompressible, and that the particles are deposited on the successive layers of cake. It is also assumed that each deposited layer has the same permeability as preceding and subsequent layers. As the membrane resistance remains constant, this makes the permeate flux exclusively dependent upon R_c, the cake resistance, if all other filtration conditions remain the same. It highlights that if the membrane fouling can be kept to a minimum, the permeate flux can be increased. Therefore Darcy's law can be re-written as:

$$J = \frac{\Delta P}{\mu[R_m + \alpha_{av} w_c]} \tag{5.1}$$

In the above equation, α_{av} is the flow resistance per unit mass of solid or the specific cake layer resistance, w_c is the quantity of solids deposited on the membrane surface as a function of time.

To calculate ΔP using equation (5.1), it is essential to know the quantity of particles deposited on the membrane surface as a function of time. This can be determined by measuring the concentration of solids as a function of time. The mass deposited on the membrane surface as a function of time can be calculated from the equation below:

$$w_c = V(t)\frac{C_o - C_t}{A} \tag{5.2}$$

where V(t) is the volume in m^3 and A is the membrane area in m^2.The filtrate is recirculated into the suspension tank to maintain a constant volume of suspension, where C_0 and C_t are concentrations of suspension at initial time and time t.

5.3 Materials and Method

Submerged microfiltration experiments were carried out using a flat sheet membrane (Figure 5.1). The flat sheet membrane used in this study was supplied by the A3 Company and had a nominal pore size of 0.14 μm and an effective filtration area of 0.2 m^2. The membrane consisted of eight flat sheets separated from each other by gaps of 12 mm. The reactor tank with a capacity of 12 L was filled with a suspension of kaolin clay (Sigma, USA). Kaolin is naturally occurring white clay which may be generally described as an Aluminum silicate hydroxide.

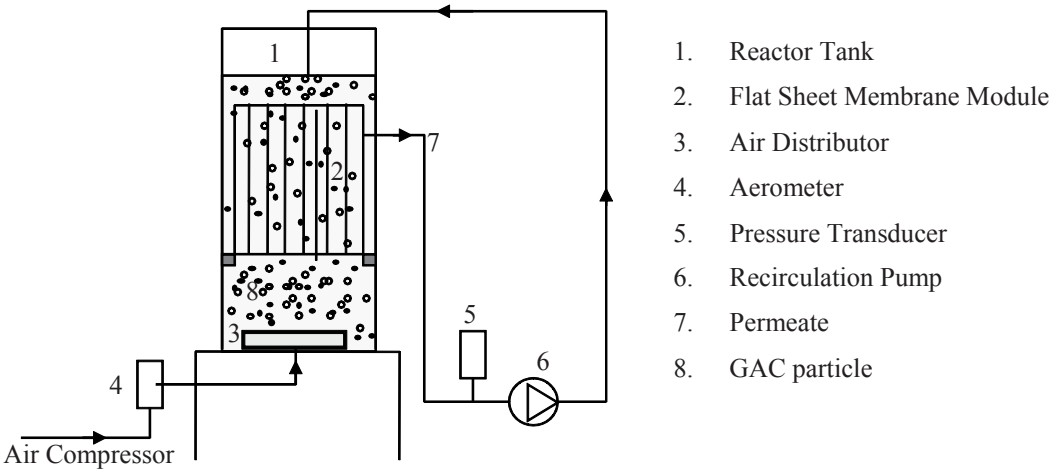

Figure 5.1 Schematic diagram of experimental set-up

Experiments were carried out at various air flow rates (600, 1200 and 1800 L/h/m^2 of membrane area) and permeate flux rates (10, 15 and 20 LMH). The experiments focused on two types of operating conditions: 1) without a support medium and 2) with a support medium. The support medium was granular activated carbon (GAC) and the GAC particle size was 300-600 μm. It was added to the kaolin clay suspension at a dose

of 1 g/L. The experimental procedures for all laboratory tests with operating condition (1) are identical to those described in section 3.2 of Chapter 3 and hence will not be repeated here. For laboratory works with operating condition (2), the only difference was that a predetermined quantity of GAC was added to the kaolin suspension; otherwise, similar procedures to those described in section 3.2 of Chapter 3 were followed. The GAC was thoroughly cleaned so it did not caused any turbidity effect to the suspension.

Particle deposition on the membrane surface was calculated indirectly through the measurement of the kaolin concentration in suspension at different times. Due to the particle deposition on the membrane, the concentration in the suspension decreased continuously with the evolution of time. The mass of particles deposited was calculated based on the mass balance of the particles in the whole system. Turbidity was measured for all samples collected from the reactor at regular time intervals to calculate the particle deposition. At any given time, the difference in concentration is attributed to the particle deposition on the membrane surface.

5.4 Results and Discussion

5.4.1 Transmembrane Pressure (TMP)

The rate of air flow and permeate flux were varied to study their effect on membrane fouling. Figure 5.2 presents the transmembrane pressure (TMP) development at various air flow rates (600, 1200 and 1800 L/h/m^2 of membrane area) and permeate flux rates (10, 15 and 20 L/m^2/h) in the presence and absence of GAC as the support medium. The development of TMP was lower with the support medium of GAC. The TMP development represents the fouling behaviour of kaolin suspension during membrane microfiltration under each operating condition.

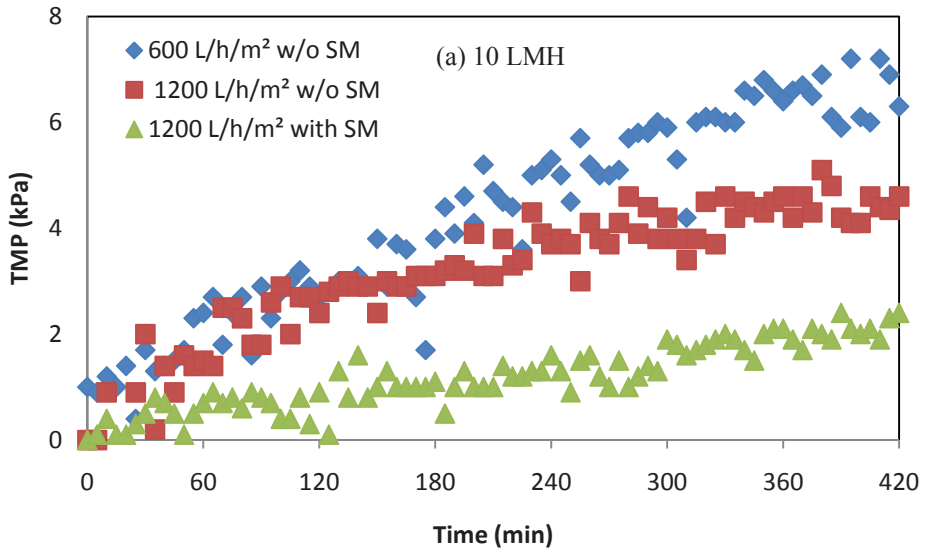
600 L/h/m² w/o SM
1200 L/h/m² w/o SM
1200 L/h/m² with SM
(a) 10 LMH
TMP (kPa)
Time (min)
0
2
4
6
8
0
60
120
180
240
300
360
420

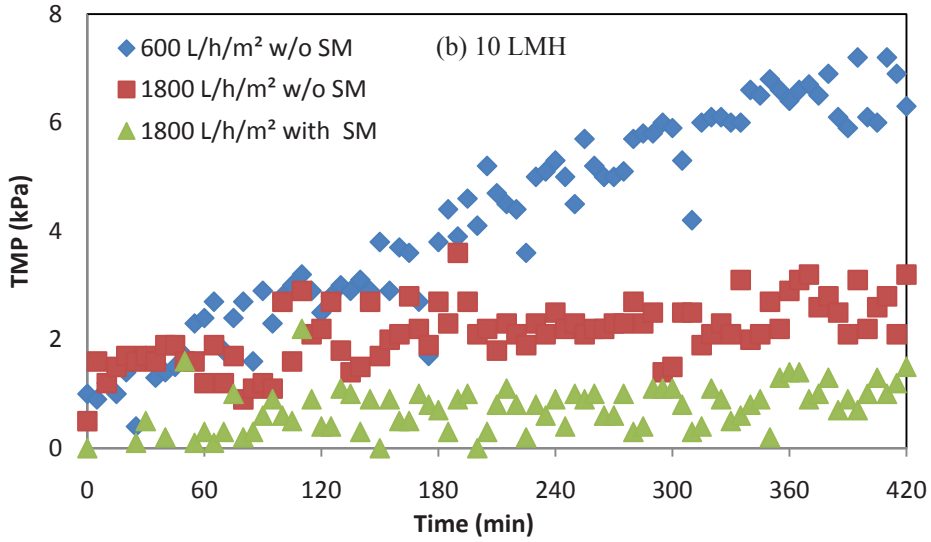
600 L/h/m² w/o SM
1800 L/h/m² w/o SM
1800 L/h/m² with SM
(b) 10 LMH
TMP (kPa)
Time (min)
0
2
4
6
8
0
60
120
180
240
300
360
420

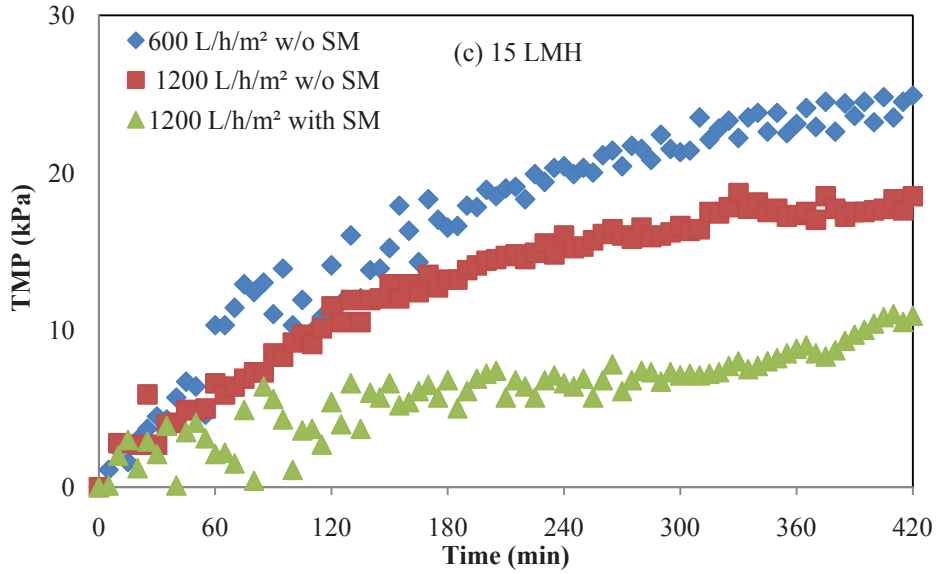
600 L/h/m² w/o SM
1200 L/h/m² w/o SM
1200 L/h/m² with SM
(c) 15 LMH
TMP (kPa)
Time (min)
0
10
20
30
0
60
120
180
240
300
360
420

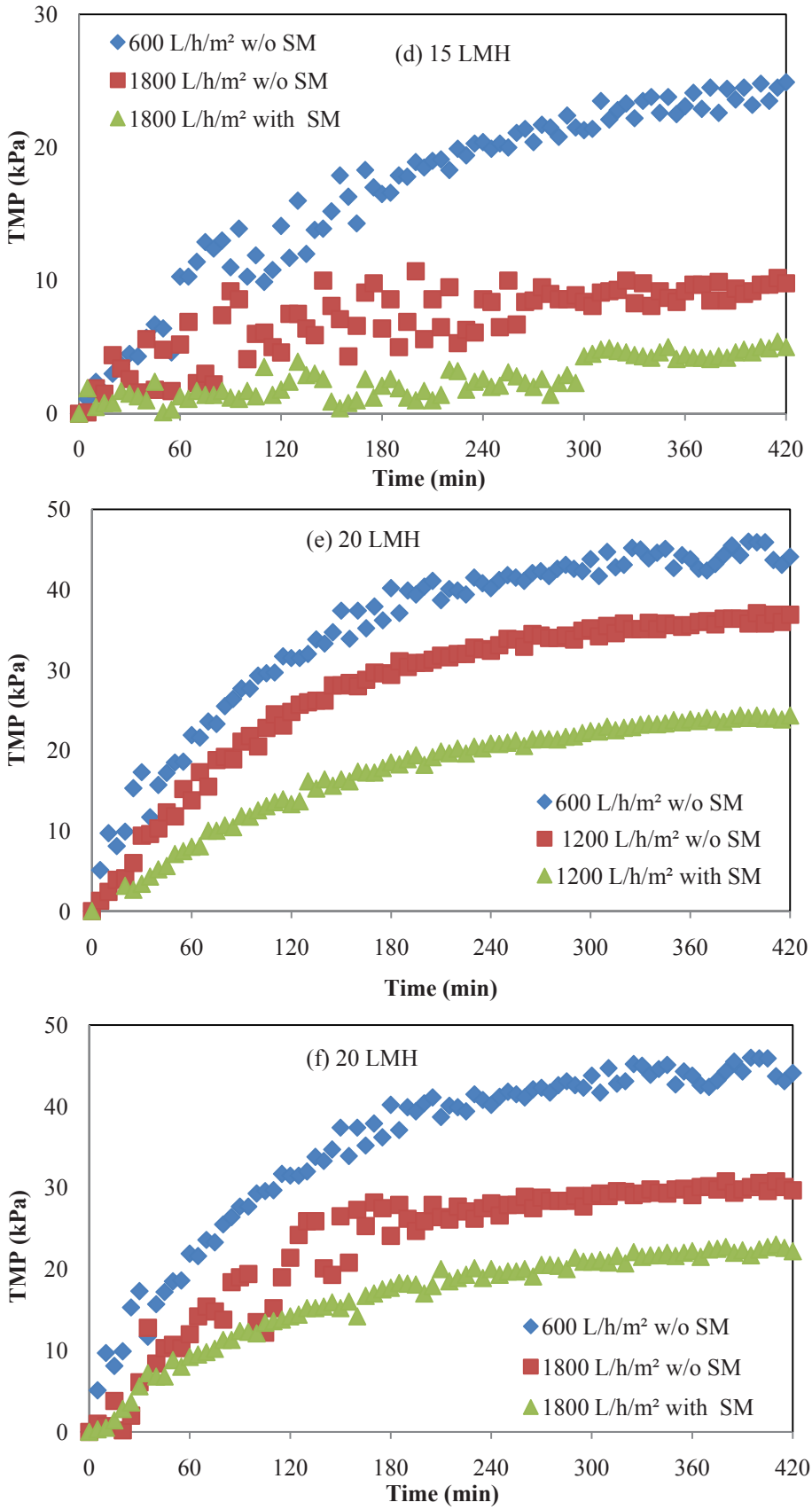

Figure 5.2 Effects of air flow rates and the addition of a support medium on TMP

TMP development reduced with increased air flow rates, and an additional reduction in TMP was noticed in the experiments conducted in the presence of the support medium. For all operating conditions, the trend of TMP development was fast at the outset followed by a slow rise and finally it was almost flat. Therefore, the evolution of TMP with time could be generalised into three categories: a sharp exponential rise during the initial period, followed by a slow rise that was near linear, then virtually no further rise in TMP with time. With increased air flow rates, the TMP curves were less steep and more linear. The addition of a support medium further reduced the TMP rise, resulting in a more linear TMP curve.

A higher filtration flux resulted in a rapid rise in TMP during the initial periods of operation (Figure 5.2c). A similar TMP curve was reported by others (Aryal, Vigneswaran & Kandasamy 2010; Fradin & Field 1999; Ivanovic, Leiknes & Odegaard 2008). This TMP behaviour is due to the higher driving force towards the membrane at higher flux, which could be explained by Darcy's law. Finer particles are easily attracted towards and onto the membrane surface at higher flux, forming more compact cake layers. The deposition of finer particles is responsible for a sharp TMP rise at the beginning of the experiment (Pradhan et al. 2011). Since the TMP rise and the particle deposition are significant during the initial period of an experiment, membrane fouling control strategies should be focused on this period.

In the absence of the GAC support medium when the air flow was tripled (from 600 to 1800 L/h/m^2), the rise in the TMP decreased by 60%. The TMP further dropped to 85% with the addition of the support medium (for the same increased air flow condition) at a flux rate of 15 L/m^2/h. The doubling of the air flow rate (from 600 to 1200 L/h/m^2), without a support medium, caused a 32% reduction in TMP development at 10 L/m^2/h.

The same result (31% reduction) was obtained at a lower air flow rate of 600 L/h/m^2 with the addition of the support medium. This result shows that the same reduction of TMP can be obtained by adding a support medium instead of doubling the air flow rate.

Table 5.1 TMP Reduction percentage in different operating conditions

Operating Conditions	10 L/m²/h	15 L/m²/h	20 L/m²/h
	Percentage of TMP Reduction (%)		
600 L/h/m² w/o SM - 600 L/h/m² with SM	31	31	25
600 L/h/m² w/o SM - 1200 L/h/m² w/o SM	32	23	20
600 L/h /m² w/o SM - 1200 L/h/m² with SM	66	65	51
600 L/h/m² w/o SM - 1800 L/h/m² w/o SM	59	60	33
600 L/h/m² w/o SM - 1800 L/h/m² with SM	81	85	52

(Note: w/o = without, SM = support medium)

Table 5.1 compares the reduction in TMP in different operating conditions. The TMP reduction was averaged with hourly TMP reduction for each seven hours long experiment. Of the three fluxes tested in this study, 15 L/m^2/h was the most suitable flux for the experimental conditions used. The TMP development was high when a low air flow rate of 600 L/h/m^2 was used. TMP reduced by 85% when an air flow rate of 1800 L/h/m^2 was used with the support medium. The main reason for this considerable reduction in TMP is an accelerated scouring action on the layers of particles deposited on the membrane by a combination of support medium and air flow. For the permeate flux of 10 L/m^2/h, the TMP reduction was better in facilitating mechanical scouring with the support medium at the same air flow rate than it was when the air flow rate was doubled without a support medium. Therefore, it can be argued that the addition of a

support medium can achieve similar or better reductions in TMP than an increase in air flow rates.

5.4.2 Particle Deposition

The TMP curves (Figure 5.2) indirectly indicate the behaviour of the particle deposition of kaolin clay in a variety of filtration conditions. The preliminary experiments indicated that there was no adsorption of the kaolin clay on the GAC used as a support medium to scour the membranes. The influence of air flow rates (air scouring) and support medium (mechanical scouring) on the particle deposition on the membrane surface is shown in Figure 5.3. A higher flux produces a high tendency to particle deposition on the membrane surface. Though an increased air flow helped to reduce the deposition, it is highly susceptible to the flux rate. Similar results were reported by Ivanovic and Leiknes (2008a). Furthermore, these particle deposition patterns are supported by the TMP graphs (Figure 5.2). High air flow rates resulted in less particle deposition due to scouring of the deposited layers by air bubbles. This phenomenon was further attenuated in the presence of the support medium. Aryal et al. (2010) also observed a significant reduction in membrane fouling in the presence of a support medium.

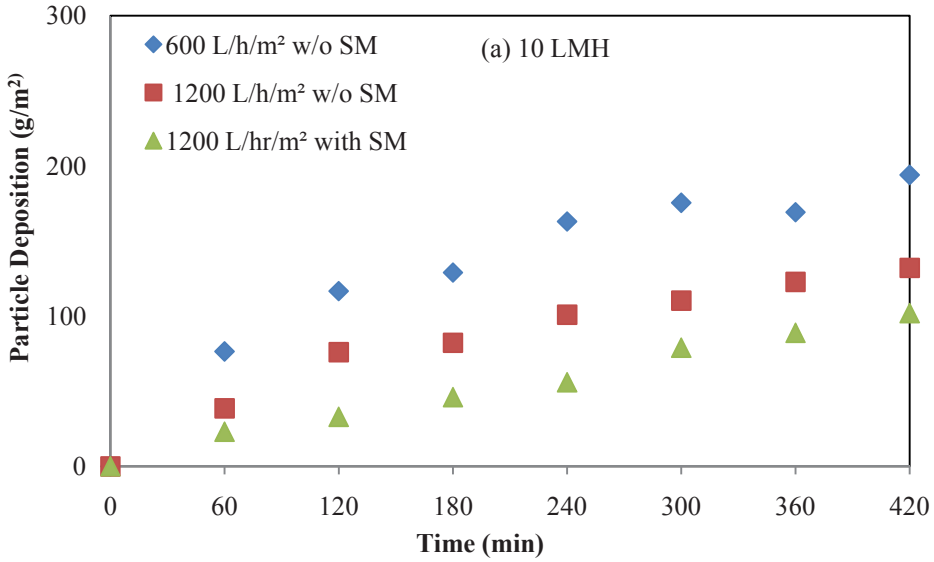
300
200
100
0
Particle Deposition (g/m²)
600 L/h/m² w/o SM
1200 L/h/m² w/o SM
1200 L/hr/m² with SM
(a) 10 LMH
0
60
120
180
240
300
360
420
Time (min)

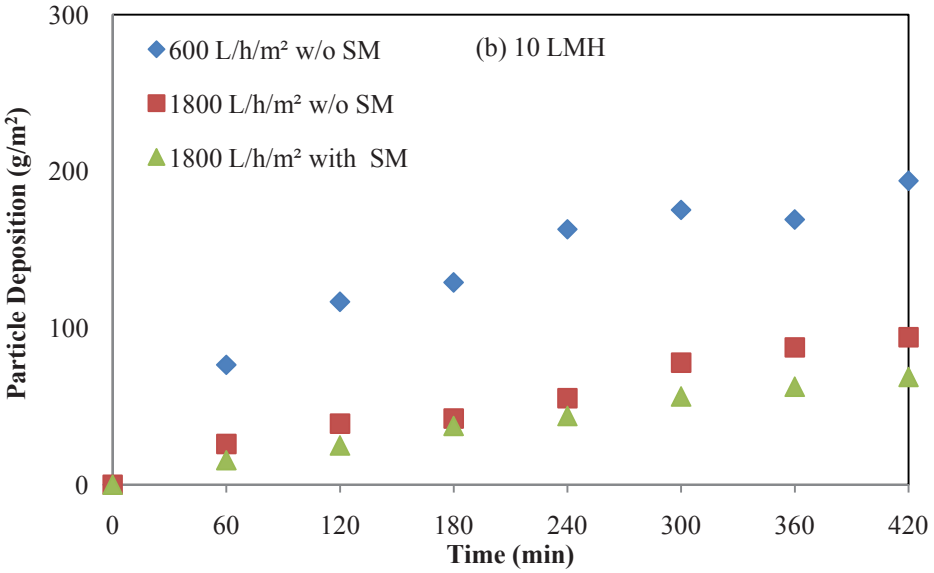
300
200
100
0
Particle Deposition (g/m²)
600 L/h/m² w/o SM
1800 L/h/m² w/o SM
1800 L/h/m² with SM
(b) 10 LMH
0
60
120
180
240
300
360
420
Time (min)

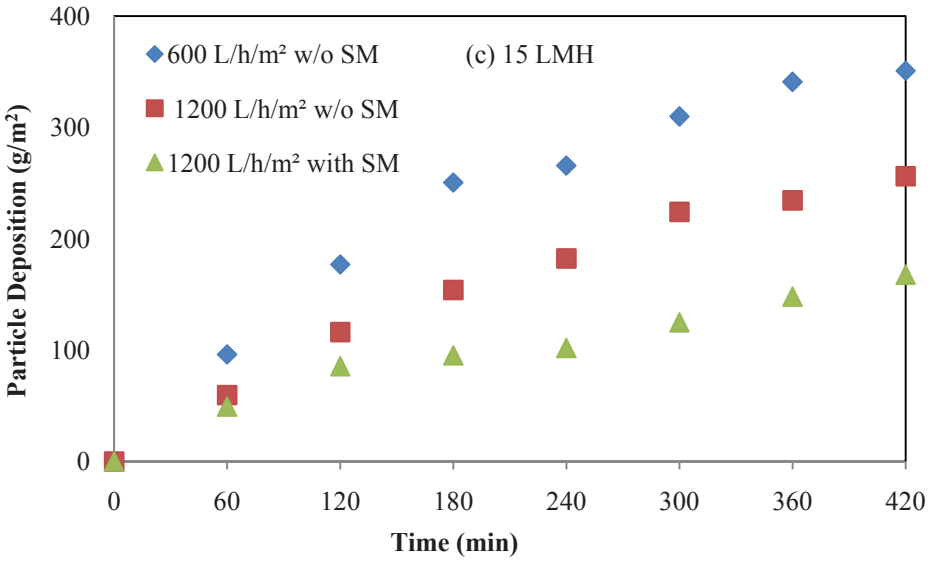
400
300
200
100
0
Particle Deposition (g/m²)
600 L/h/m² w/o SM
1200 L/h/m² w/o SM
1200 L/h/m² with SM
(c) 15 LMH
0
60
120
180
240
300
360
420
Time (min)

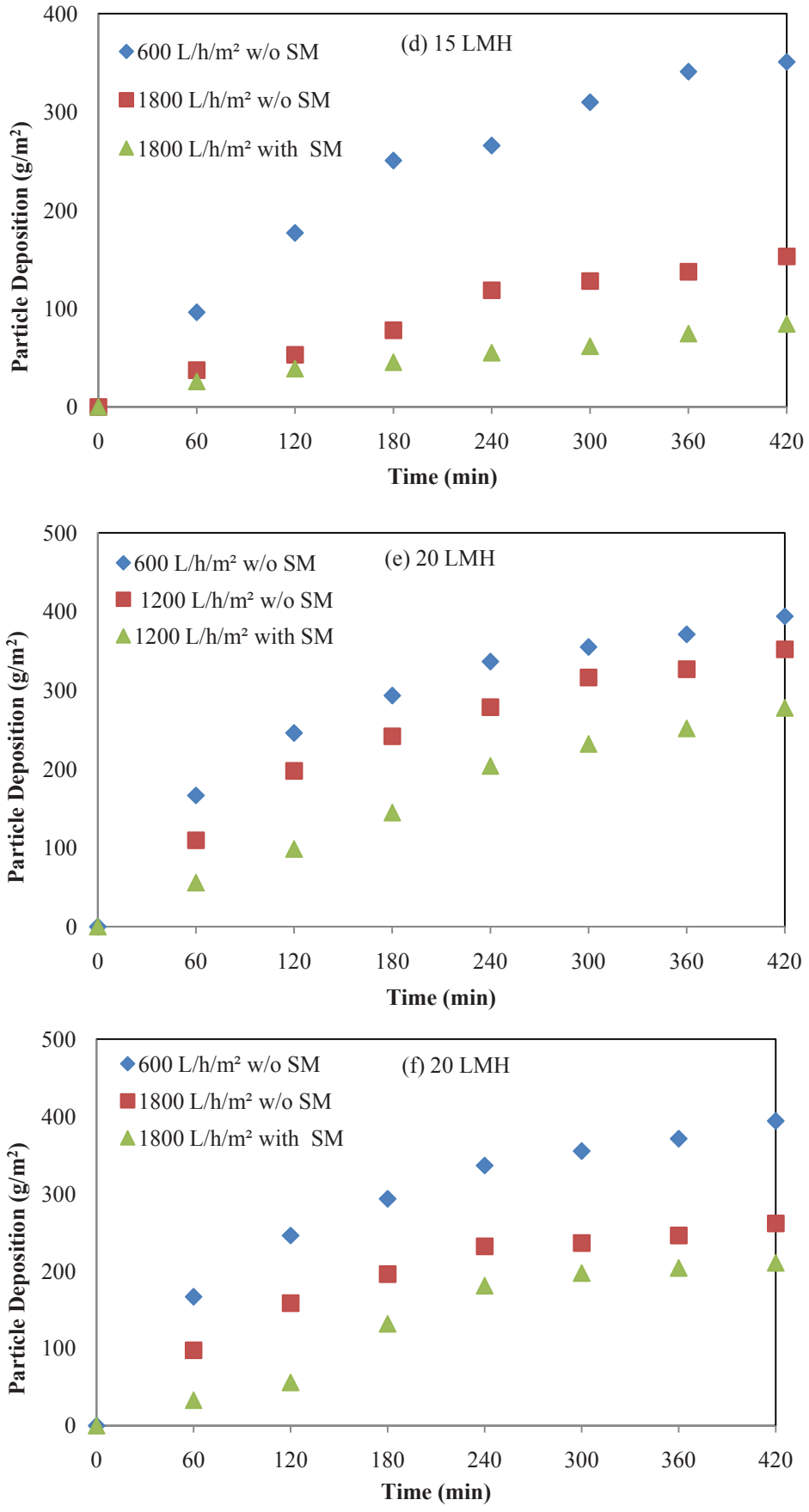

Figure 5.3 Effects of air flow rates and the addition of a support medium to the particle deposition on the membrane surface

The initial steep rise of the TMP curve indicates a high deposition on the membrane, surface especially with finer particles. The subsequent slow TMP rise is a result of less particle deposition. Hence, the particle deposition graphs presented in Figure 5.3 can be divided into three parts. The first part represents a sharp rise in fouling at the outset which tends to be more linear for higher flux rates. A slower increment represents the second part, followed by flat portion (third part). For a given air flow rate, when the filtration flux was increased, both the TMP development and particle deposition increased (Figures 5.2c and 5.3c); however, the deposition was significantly reduced with the increase in air flow rates and the provision of a support medium.

Table 5.2 summarises the percentage of fouling reduction (reduction in particle deposition) in different operating conditions. The fouling reduction was calculated by averaging the hourly fouling reduction for seven hours long membrane microfiltration test. A substantial reduction (78%) was obtained for 15 L/m^2/h when the air flow was tripled from 600 L/h/m^2 air flow with a support medium. The effects of doubling and tripling air flow were more significant for low flux rates (10 and 15 L/m^2/h) than for a high flux rate (20 L/m^2/h). Even at the same air flow rate, the addition of a support medium in suspension resulted in less deposition. Therefore, the addition of a support medium with air could be an alternative to the application of very high air flow rates alone in a submerged membrane microfiltration system. The latter increases the energy costs, so the optimisation of the combined effect of support medium and air flow would help to reduce energy consumption.

Table 5.2 Fouling reduction percentage in different operating conditions

Operating Conditions	10 L/m²/h	15 L/m²/h	20 L/m²/h
	Percentage of TMP Reduction (%)		
600 L/h/m² w/o SM- 600 L/h/m² with SM	34	29	24
600 L/h/m² w/o SM- 1200 L/h/m² w/o SM	36	33	17
600 L/h /m² w/o SM- 1200 L/h/m² with SM	60	56	45
600 L/h/m² w/o SM- 1800 L/h/m² w/o SM	60	61	35
600 L/h/m² w/o SM- 1800 L/h/m² with SM	71	78	56

(Note: w/o = without, SM = support medium)

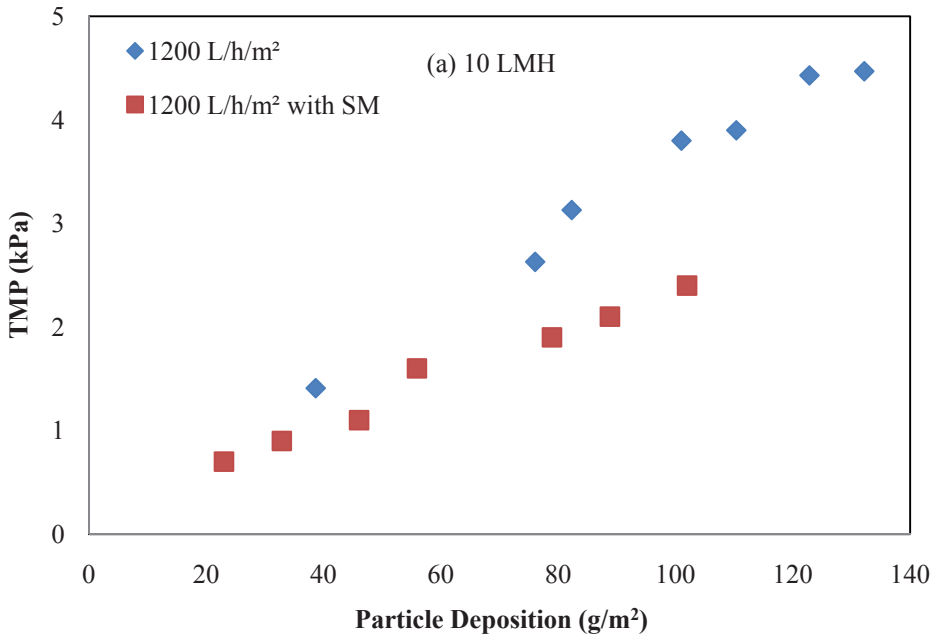

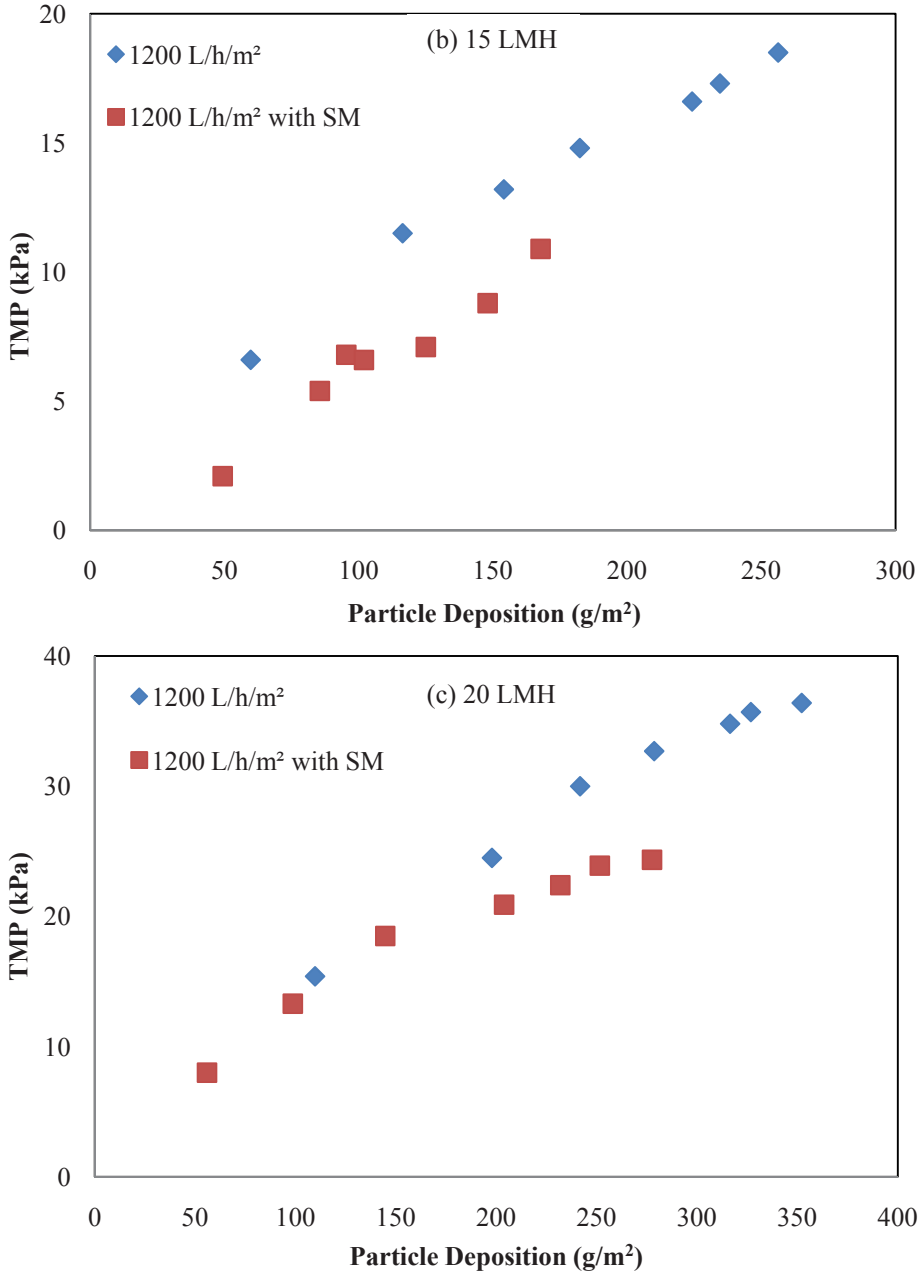

Figure 5.4 Effects of support medium on TMP deposition at 1200 L/h/m^2 air flow rate under various filtration flux rates

Figure 5.4 shows the relationship between TMP and particle deposition at an air flow rate of 1200 L/h/m^2 for different filtration flux in two operating conditions: a) with air only and b) air coupled with support medium. Low TMP and less deposition were obtained with increased air flow rate. The TMP development was lower for all operating conditions with the application of air flow with the support medium compared to runs without a support medium. Empirical curve fits were made between TMP and

deposition. A linear relation between the TMP and deposition was obtained as shown below:

$TMP = aDeposition + b$ (without support medium) (5.4)

$TMP = a_1 Deposition + b_1$ (with support medium) (5.5)

where

(a) For 10 L/m^2/h and at an air flow rate of 1200 L/h/m^2

a = 0.034, b = 0.166, R_1^2 = 0.977, a_1 = 0.021, b_1 = 0.21, R_2^2 = 0.981

(b) For 15 L/m^2/h and at an air flow rate of 1200 L/h/m^2

a = 0.057, b = 3.991, R_1^2 = 0.982, a_1 = 0.066, b_1 = 0.557, R_2^2 = 0.947

(c) For 20 L/m^2/h and at an air flow rate of 1200 L/h/m^2

a = 0.088, b = 6.878, R_1^2 = 0.975, a_1 = 0.071, b_1 = 5.857, R_2^2 = 0.950

(Note: TMP is in kPa, Particle deposition is in g/m^2, R_1 = without support medium,

R_2 = with support medium)

The gradient of the curve gives the rate of change in the TMP corresponding to the particle deposition.

The total membrane resistance increased with time for all experiments, while the increase was lower with an increased air flow rate. Figure 5.5 shows the effect of air flow rate on the total membrane resistance for various filtration flux rates in the presence and absence of the support medium.

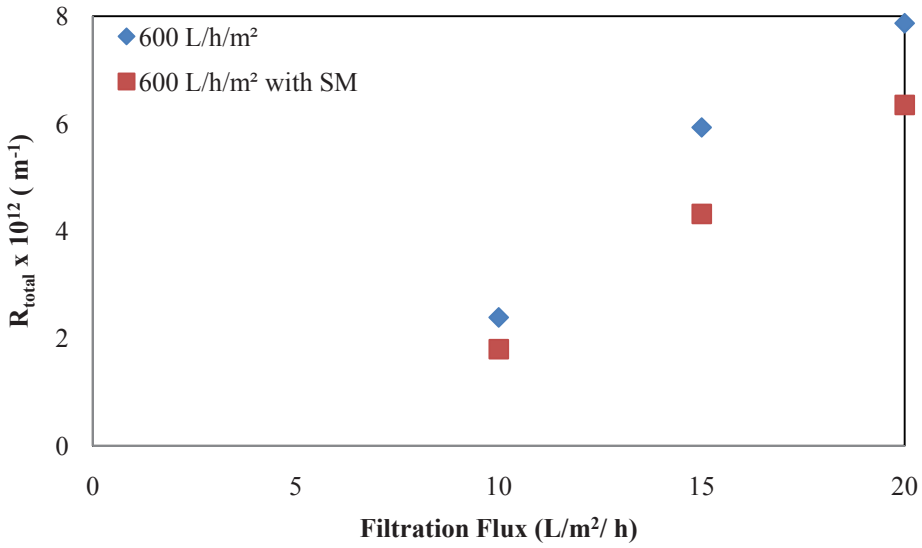

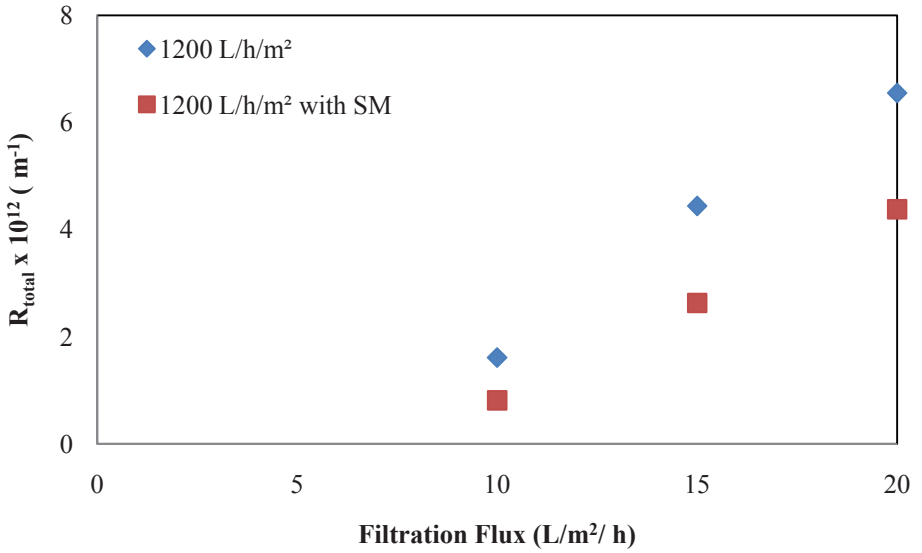

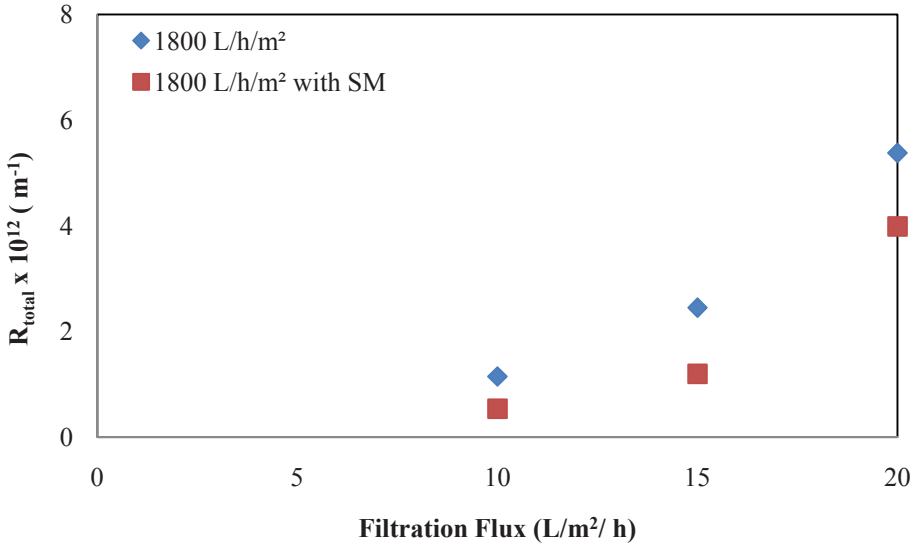

Figure 5.5 Effect of support medium and air flow rates on total filtration resistances for different filtration flux rates

From Figure 5.5, it is clearly observed that the filtration resistance was larger with increased filtration flux, but air flow helped to reduce this, and the addition of a support medium further assisted the decrease in total membrane resistance. The relationship between total membrane resistance and filtration flux for an air flow rate of 1200 L/h/m^2 without a support medium can be expressed as:

$$R_t = 4.39x10^{11}\, e^{(0.14J)} \text{ ; } R^2 = 0.94 \quad (5.6)$$

In the case of the support medium, the same relationship for air flow rate of 1200 L/h/m^2 can be expressed as:

$$R_t = 1.68x10^{11}\, e^{(0.168J)} \text{; } R^2 = 0.95 \quad (5.7)$$

where R_t is total membrane resistance (m^{-1}) and J is filtration flux (L/m^2/h).

These empirical equations suggest a significant reduction in the total membrane resistance in the presence of air flow and the support medium. Consequently, the total membrane resistance under a specified filtration flux can be estimated by using the above exponential-type empirical equation for a specified air flow rate with and without a support medium.

Increased air flow reduces TMP and mass deposition in submerged microfiltration. Reduced deposition causes less cake resistance in the system. Figure 5.6 shows the effects of air flow and the support medium on cake resistance. Increased air flow caused less particle deposition resistance; similar results were obtained without increasing air flow but by introducing a support medium in the suspension. The results suggest that incorporating a granular medium in suspension in the reactor could be a sustainable alternative to increasing air flow rate.

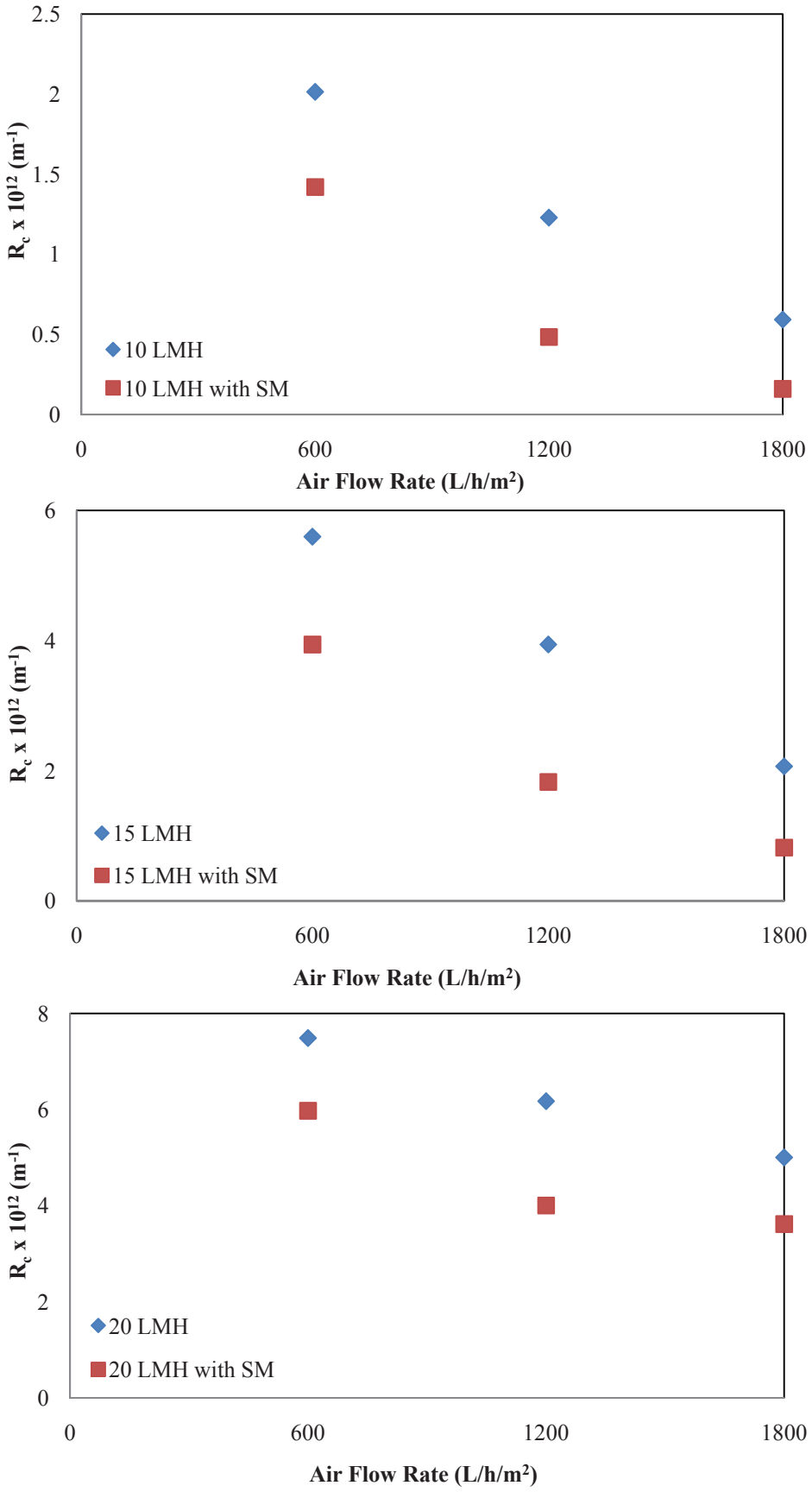

Figure 5.6 Effects of air flow rate, support medium and filtration flux on cake filtration resistance

5.5 Conclusions

This study investigated the effects of air flow (air scouring) and the addition of a granular medium in suspension (mechanical scouring) on membrane fouling. Low membrane fouling was observed for high air flow rates for all permeate flux rates. Further reductions in particle deposition were observed in the presence of a support medium. A substantial reduction in particle deposition (78%) was obtained for 15 $L/m^2/h$ when the air flow rate was tripled in the presence of the support medium from a base case of 600 $L/h/m^2$ air flow without a support medium. The doubling of the air flow rate (from 600 to 1200 $L/h/m^2$) without the granular medium led to a 32% reduction in TMP development at 10 $L/m^2/h$. The same result (31% reduction) was obtained at a lower air flow rate of 600 $L/h/m^2$ with the addition of the granular medium. The addition of a support medium with air could therefore be a good alternative to the application of very high air flow in submerged membrane microfiltration systems. The optimisation of the combined effect of support medium and air flow will help in the design of less energy-intensive operations.

Chapter 6

Experimental investigations on the effects of viscosity and air bubbles on membrane fouling in submerged membrane microfiltration

Abstract

In this study, the effect of changing viscosity was investigated by adding predetermined quantities of glycerol in the kaolin clay suspension. This solution was filtered through a flat sheet membrane module submerged in the kaolin suspension with different concentrations of glycerol. Air scouring was provided with known quantities of air flow. The glycerol altered the viscosity values, and the increase in viscosity caused higher fouling resulting in a large rise in the trans-membrane pressure (TMP). The TMP was reduced by increasing the flow of air bubbles (higher air scour).

6.1 Introduction

Membrane microfiltration is a very popular pressure driven separation process which has a wide range of applications in water, wastewater treatment, chemical, and dairy industries. In practice, a major problem associated with its application arises from membrane fouling which results in a severe decline in flux, high energy consumption and frequent membrane cleaning and replacement (Gander, Jefferson & Judd 2000). In submerged membrane filtration used for domestic wastewater treatment application, membrane modules are immersed in the aeration basin which consists of mixed liquor (wastewater with biomass). Therefore, membrane fouling phenomena are very complex due to the rheological and physiological characteristics of mixed liquor. Membrane fouling is caused by various types of physicochemical interactions between suspension containing biomass and the membrane itself. Similar to conventional activated sludge

processes, biomass viscosity in the membrane bioreactor is closely related to its mixed liquor suspended solids (MLSS) concentration and has been referred to as a foulant parameter (Yeom et al. 2004). The viscosity of the solution will affect the bubble properties and bubble-induced effects. In many industries, the feed viscosity can increase significantly during processing and particularly during concentration by filtration, which directly affects membrane fouling.

Ueda et al. (1996) reported that an increase in MLSS concentration and the corresponding rise in suspension viscosity have a negative impact on membrane permeability. Similarly, Itonaga et al. (2004) investigated the influence of suspension viscosity on membrane permeability in the MBR system. They suggested that a critical MLSS concentration exists under which the viscosity remains low up to this concentration and that viscosity increases only slowly with the concentration value. The suspension viscosity tends to increase exponentially with the solids concentration. This could correspond to a change in rheological behaviour from Newtonian to non-Newtonian. They suggested that the upper limit of MLSS concentration for efficient operation should be around 10 g/L. Beyond this value, there will be a substantial increase in suspension viscosity. Brookes et al. (2003) suggested that this critical value of MLSS ranged from 10 to 17 g MLSS/L for different operating conditions. The apparent viscosity of the sludge in a submerged membrane bioreactor increases exponentially with an increase in the solid content of sludge and decreases logarithmically with an increase in the velocity of the rotary viscometer (Hasar et al. 2004). The relationship of the MLSS concentration with viscosity at different shear rates observed at a submerged bioreactor is shown in Figure 6.1. Le-Clech et al. (2003) established an exponential relationship between MLSS concentration and viscosity for varying shear rates.

Rosenberger et al. (2002) observed that MLSS was a major parameter affecting the apparent viscosity of the suspension in membrane bioreactors. MLSS concentration certainly has a complex interaction with membrane fouling, and conflicting findings about the effect of this parameter on membrane filtration have been reported.

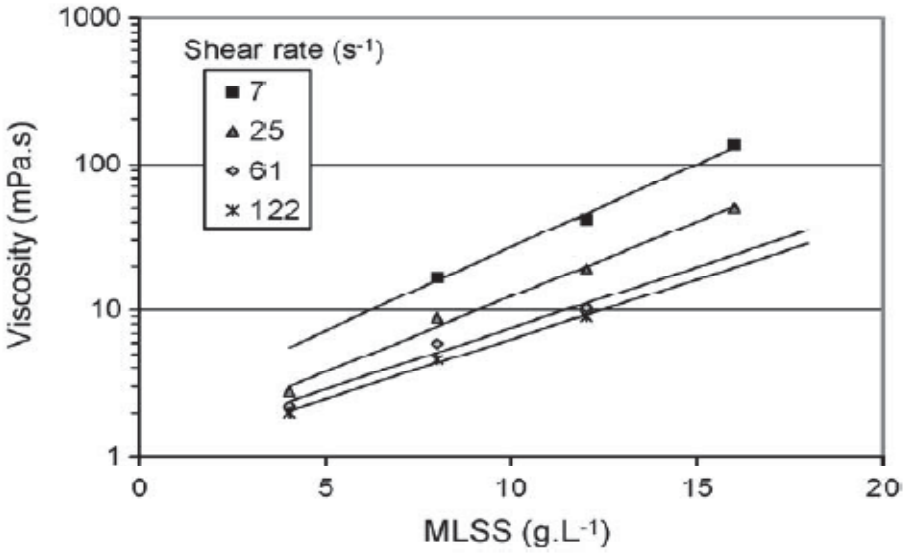

Figure 6.1 Viscosity obtained at different MLSS concentrations and shear rates (Le-Clech et al. 2003)

The major concern regarding biomass viscosity in a membrane bioreactor is its detrimental effect on membrane fouling, bubble properties and bubble-induced effects. To date, the application of air bubbles into the submerged filtration system has proved to be an effective, simple and low-cost technique for fouling control (Cui et al. 2003). In an air sparged microfiltration system, turbulence in the bubble wake is responsible for accelerating mass transfer back to the suspension. The strength and size of the bubble wake depends on bubble size; tiny bubbles are spherical in shape and do not generate vortices because the flow around these bubbles does not separate, but larger bubbles produce a symmetric vortex in the wake region (Kumar et al. 1992). Therefore, the secondary flow is much stronger for the larger bubbles. The importance of MLSS or viscosity is that it modifies bubble size and can dampen the movement of hollow fibres

in submerged bundles (Wicaksana, Fane & Chen 2006b). Wicaksana et al. (2006b) reported that average values of bubble rise velocity in higher viscosity liquid was significantly lower than in the less viscous solution (water).

The application of air bubbles reduces the rise in TMP due to its scouring effect on the deposited layer in all operating conditions. A more significant reduction in highly viscous feed could be due to the formation of large bubbles in a raised viscous liquid. Wicaksana et al. (2006b) found that bubble sizes in a more viscous liquid were larger than in a less viscous solution (water). Similar results were observed by De Swart et al. (1996) and Schafer et al. (2002). Large bubbles are more beneficial because they have larger wake regions and create stronger secondary flows. They are more effective in promoting local mixing (Cui et al. 2003). Li et al. (1997) also reported that increasing bubble size can result in a stronger wake, which enhances local mixing and the mass transfer back to suspension. They also observed an apparent rise in permeate flux with bubble size.

A detailed study with a synthetic suspension of known characteristics and viscosity will be useful in investigating the effect of viscosity on fouling control. Thus, membrane fouling behaviour was studied under varying feed viscosity in the presence of air bubbles. Membrane microfiltration experiments were carried out with a flat sheet membrane module submerged into a kaolin suspension with different concentrations of glycerol. During the experiments, air bubbles are injected at different rates so that the effect of both viscosity and air flow can be evaluated.

6.2 Materials and Method

6.2.1 Materials

Laboratory experiments were performed using a flat sheet membrane module with a nominal pore size of 0.14 µm and effective filtration area of 0.2 m^2. The membrane reactor with a capacity of 12 L was filled with 10 L suspension prepared with kaolin clay powder (Sigma, USA) varying in size from 0.1-4 µm. The particle size distribution was measured by a Malvern particle size analyser and the average particle size was 2.1 µm. The concentration of clay was kept at 10 g/L (similar to the range of MLSS concentration in MBR). The feed viscosity was varied by adding a predetermined quantity of glycerol to the feed suspension.

Feeds with viscosities of 0.001, 0.002 and 0.003 Pa.s were prepared. Based on data in the literature, a correlation between the viscosity and quantity of glycerol was established to determine the amount of glycerol required for a particular viscous feed. Figure 6.2 shows the glycerol fraction to be added to the suspension to achieve different viscosities. This figure was derived from the interpolated values for each glycerol fraction at a temperature of 20˚C (Sheely 1932).

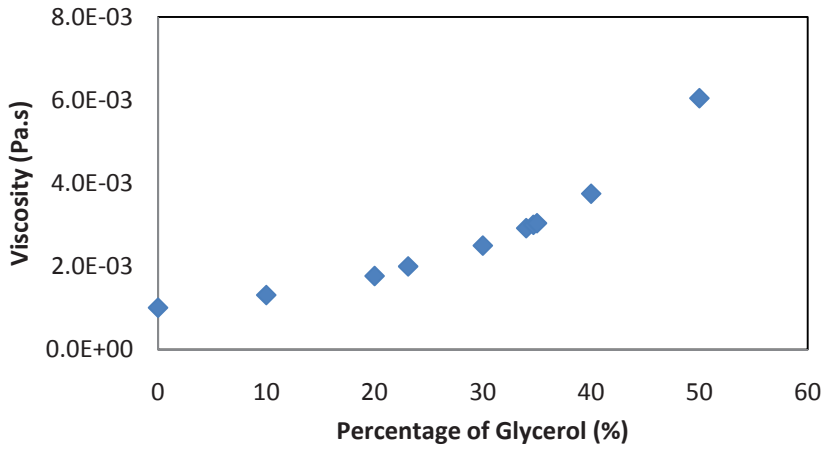

Figure 6.2 Glycerol fractions for varying concentrations of viscosities

Glycerol of an analytical grade was used to vary the viscosity of the kaolin suspension. It is completely soluble in water and alcohol but not soluble in ether. At normal temperatures, glycerine remains a viscous liquid up to 100% concentration. Thus, it is available for use over a wide range of viscosities without crystallisation difficulties. Glycerol refers to the chemical compound 1, 2.3-propanetriol and has a chemical formula CH2OHCHOHCH2OH with molecular weight of 92.10.

6.2.2 Method

A predetermined quantity of glycerol was added to the kaolin suspension to vary the viscosity of the suspension. The different values of viscosity applied in these experiments were 0.001, 0.002 and 0.003 Pa.s. Firstly, a submerged membrane experiment was conducted with tap water at 15 L/m^2/h (for viscosity 0.001 Pa.s). Then known amounts of glycerol were added to tap water to obtain solutions with viscosities of 0.002 and 0.003 Pa.s. To observe TMP at varying viscosity, the submerged membranes were used to filter water with glycerol without any addition of kaolin particles. Similar experiments were carried out with a kaolin concentration of 10 g/L at different air flow rates (0.6, 1.2 and 1.8 $m^3/m^2_{membrane\ area}$/h) and permeate flux rates (5, 10, 15 and 20 L/m^2/h). It should be noted that air flow rate is expressed in terms of membrane area and its unit is denoted as m^3/m^2/h. The experiments with each flux were conducted with all three air flow rates and three viscosity conditions, as explained in Chapter 3. All experiments were carried out at room temperature (20-22˚C).

6.3 Results and Discussion

Firstly, submerged membrane experiments were performed with different concentrations (predetermined) of glycerol added to tap water i.e. without the addition of kaolin clay, in order to study the effect of viscosity on TMP. Figure 6.3 presents

TMP development for clean tap water only (0.001 Pa.s) and water-glycerol mixtures (0.002 Pa.s and 0.003 Pa.s). At 15 L/m^2/h, clean water TMP was in the range of 2 kPa, but after the addition of glycerol (to make 0.002 Pa.s and 0.003 Pa.s viscosities), TMP was approximately 4 kPa and 6 kPa respectively. Besides the TMP rise due to increased viscosity, there was no TMP development throughout the experiment period. The directly proportional relationship between the TMP and the viscosity is already mentioned in equation 4.12 (Darcy's law).

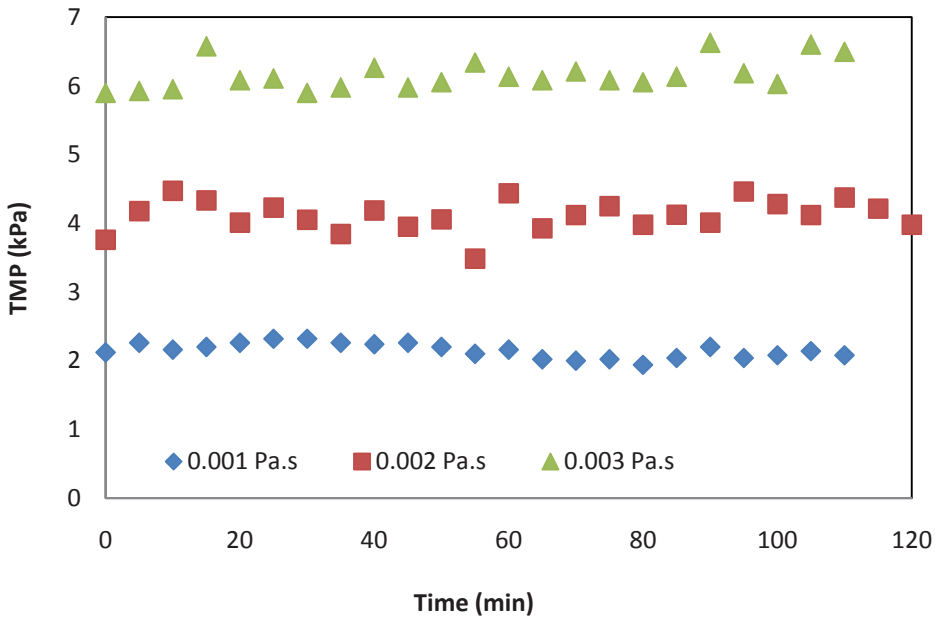

Figure 6.3 TMP development for water only and water-glycerol mixture of different viscosity

Figure 6.4 shows the relationship of TMP and viscosity. As expected, TMP is linearly proportional to the liquid viscosity. This also shows the correct operation of the pressure probes used in the experimental study.

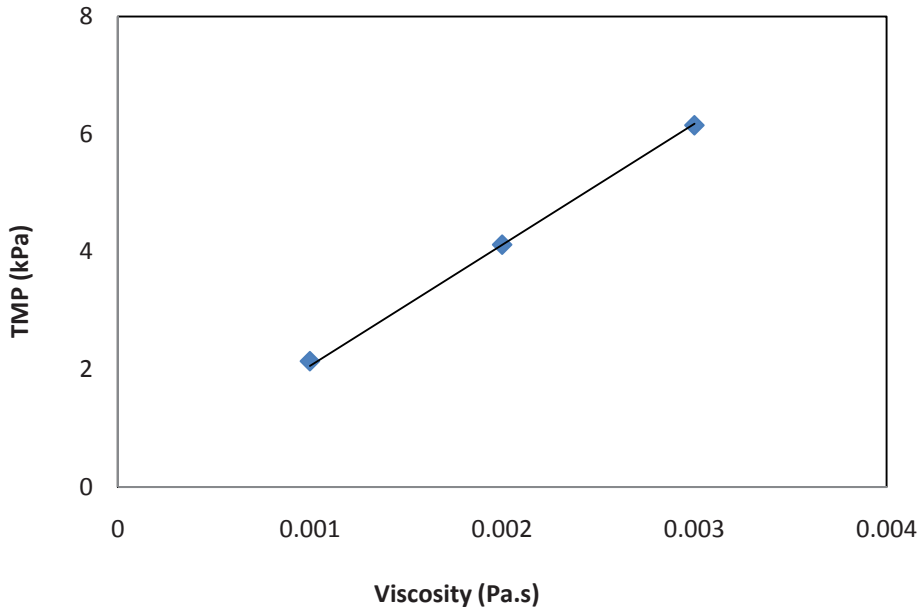

Figure 6.4 Variation of TMP and viscosity

Chapter 3 describes the effect of air flow on TMP development and deposition for non-viscous kaolin suspension. As the kaolin concentration was kept constant, the parameter considered is the variation of suspension viscosity. Here, the influence of changing liquid viscosity on fouling for the submerged membrane microfiltration of kaolin suspension in the presence of air bubbles was studied. Fouling was directly correlated with the variation in the TMP measured during the experiments. Particle deposition was also measured at regular intervals during the filtration. An increase of the TMP corresponded to fouling on the membrane surface; hence cake resistance was determined by Darcy's law using the experimental TMP data. The relationship between cake resistance and particle deposition was analysed and specific cake resistance was evaluated for different operating conditions.

6.3.1 Effect of Viscosity on Cake Resistance (R_c) under Different Air Flow Rates

A study was performed to investigate the effect of viscosity on cake resistance under different operating conditions. Figures 6.5 and 6.6 present the behaviour of cake resistance for viscous suspension at three different air flow rates (0.6, 1.2 and 1.8 $m^3/m^2/h$) and at three permeate fluxes of 10, 15 and 20 $L/m^2/h$. Figure 6.7 presents the cake resistance at a higher flux of 20 $L/m^2/h$ at 1.8 $m^3/m^2/h$ air flow rate for different viscosities. These figures show a similar pattern of cake resistance development with the volume of filtered water and time for all operating conditions. The rise of cake resistance was sharp at the beginning, followed by a slow rise; finally, a plateau (steady state) was observed for most of the conditions used. Moreover, the steady state for cake resistance was dependent on the air flow rate. An application of increased air flow resulted in less cake resistance compared to a low air flow rate. Of all the permeate flux studied, a higher cake resistance was observed with increased viscosity. Changes in viscosity of the suspension played a significant role in the cake layer formation, resulting in a higher cake resistance for high viscous feed. The pattern of cake resistance curves for all three viscosities were almost the same for these fluxes under the air flow rates used. This can be justified by Darcy's law, according to which, total resistance (R_t) can be written as: $R_t = TMP/(\mu J)$ where TMP is a transmembrane pressure (kPa), μ is a permeate viscosity (Pa.s) and J is permeate flux ($m^3/m^2/h$). In this study, internal fouling (pore blocking) was considered negligible because the kaolin particles were larger in size than the membrane pore size. Thus the cake resistance (R_c) was calculated by deducting the membrane resistance from the total resistance (R_t). Membrane resistance was constant for all tests (R_m = 3.8 x 10^{11} m^{-1}), therefore changes in cake resistance are similar to those of TMP development during the filtering of different

viscous feed. At a permeate flux of 10 L/m^2/h, in particular, a higher increment in R_c was observed than for other fluxes when viscosity was varied. This is due to the higher TMP rise resulting from increased viscosity. According to Darcy's equation, an increment in TMP due to change in viscosity at a constant filtration flow system causes the same increment in total resistance.

When suspension viscosity was increased, the change in cake resistance was analysed based on the volume of filtrate water at the end of the run period (7 hours). At a permeate flux of 10 L/m^2/h, when viscosity was doubled (from 0.001 Pa.s to 0.002 Pa.s), cake resistance increased by 2.34 and 2.11 times at 0.6 and 1.8 m^3/m^2/h air flow rates respectively (Figures 6.5a and 6.5c) compared to the result with the base viscosity of 0.001 Pa.s. Similarly, in the case of tripling viscosity (at 0.003 Pa.s), cake resistance was increased by 4.36, 3.38 and 3.16 times at 0.6, 1.2 and 1.8 m^3/m^2/h air flow rates respectively compared to the cake resistance of non-viscous feed. A summary of results is presented in Table 6.1. These results show that to collect the same volume of filtrate water, the filtration system had a higher cake resistance with higher viscous kaolin suspension. However, an increased air flow helped to reduce this cake resistance even in the viscous medium. It is noted that at a particular permeate flux of 10 L/m^2/h, the effect of viscosity was larger than expected by Darcy's law. This is due to the fact that an increase in viscosity increases the fouling rate. The influence of viscosity was found to be more important at a low air flow rate.

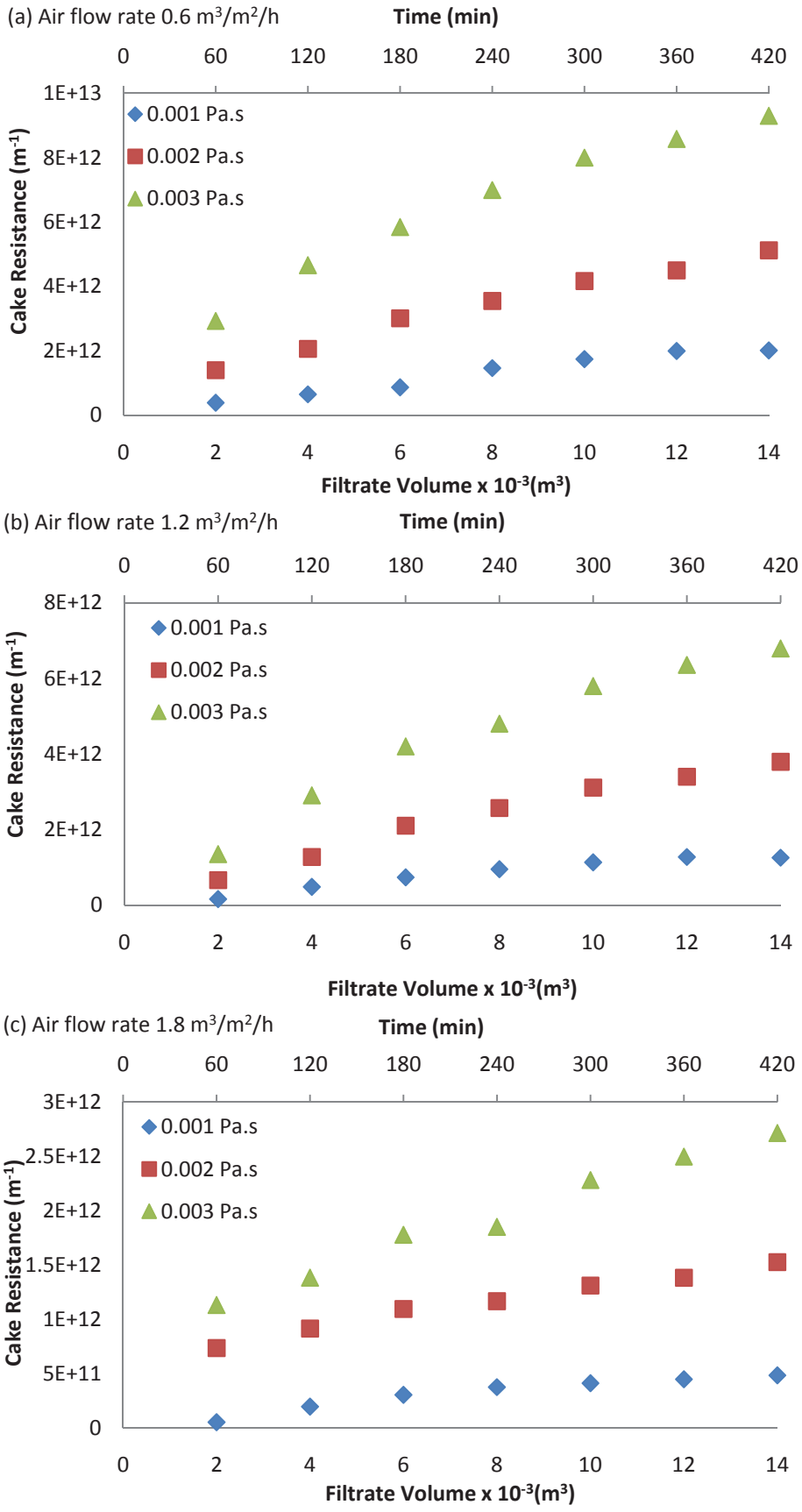

Figure 6.5 Effect of viscosity on cake resistance under various air flow rates at 10 L/m^2/h (Kaolin clay concentration = 10 g/L)

Before adding glycerol, tripling the air flow (to 1.8 $m^3/m^2/h$) at a permeate flux of 10 $L/m^2/h$ reduced cake resistance by 51%, whereas doubling the air flow (to 1.2 $m^3/m^2/h$) reduced it by 33% compared to a base air flow of 0.6 $m^3/m^2/h$. When feed viscosity was 0.002 Pa.s, cake resistance reductions were 28 and 59% with doubled and tripled air flow respectively compared to a base flow rate of 0.6 $m^3/m^2/h$. In the case of 0.003 Pa.s, doubling air flow reduced cake resistance by 42%, whereas a three-fold increment in air flow caused 66% reduction. These results, presented in Table 6.2, show that that higher air flows were more effective for a high viscosity solution. These data highlight that increased air flow reduces cake resistance even at high viscous feed suspension. Higher air flow rates were observed to be more effective in high viscous suspension. A more significant reduction in highly viscous feed could be due to the formation of large bubbles in more viscous liquid. Wicaksana et al. (2006b) found that the bubble sizes in more viscous liquid were larger than those in less viscous solution (water). Similar results were observed by Swart et al. (1996) and Schafer et al. (2002). Large bubbles are more beneficial as they have larger wake regions and create stronger secondary flows. They are more effective not only in promoting local mixing but also in scouring the deposited cake layer on the membrane surface. These air bubbles help to reduce TMP and particle deposition which consequently reduces cake resistance.

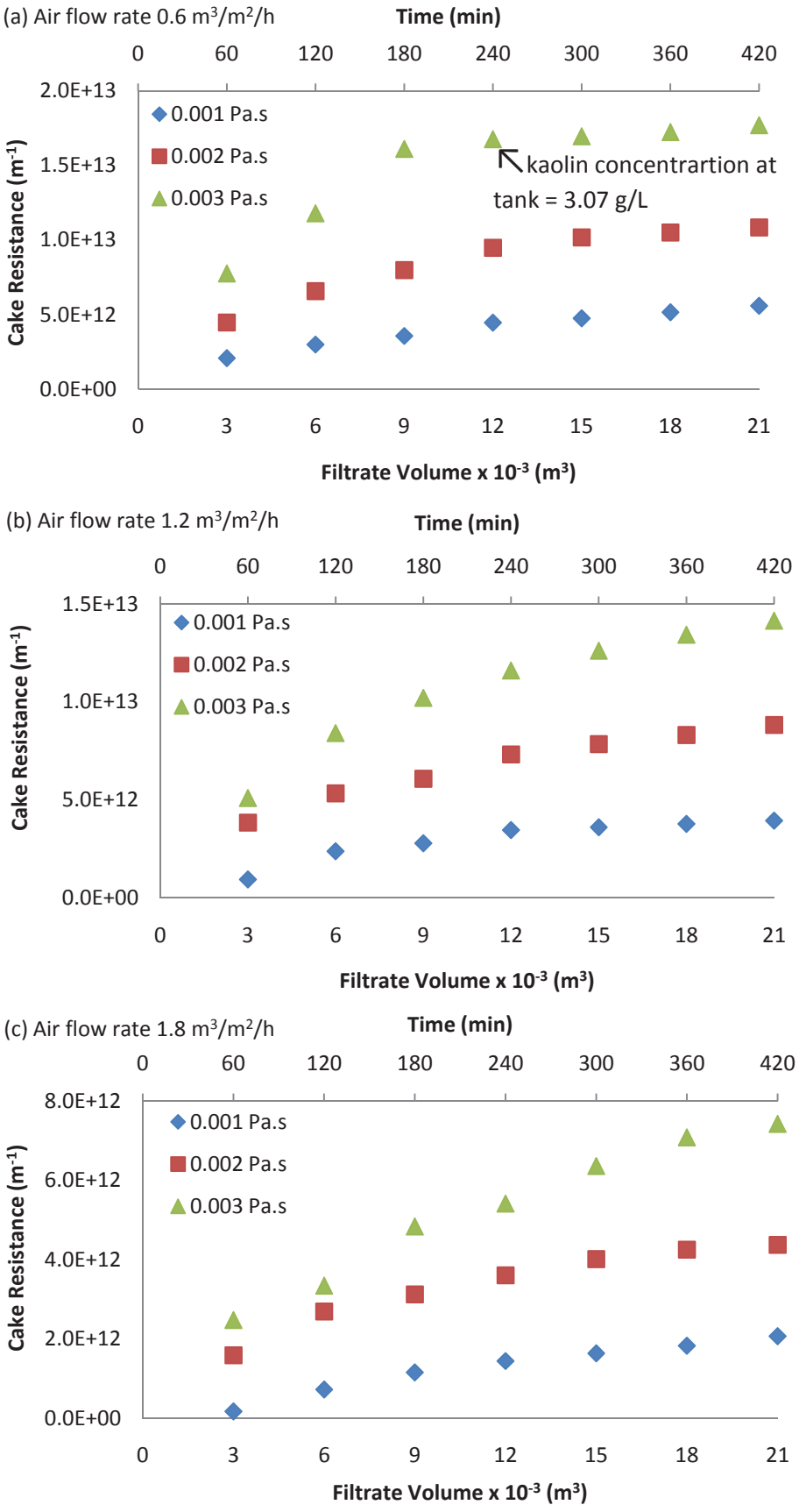

Figure 6.6 Effect of viscosity on cake resistance under various air flow rates at 15 L/m²/h, (Kaolin clay concentration = 10 g/L)

In the case of 15 L/m^2/h with low air flow (0.6 m^3/m^2/h) and high viscosity (0.003 Pa.s), the cake resistance profile showed only two stages of development; a sharp rise and saturation, whereas in other operating conditions, cake resistance profiles were divided into three steps (sharp rise, slow rise and saturation stages). After 180 minutes of filtration, cake resistance reached the saturation stage. An analysis of suspended particle (kaolin) available at this time showed that the kaolin concentration at the tank was reduced to 3.07 g/L, which highlights that almost 70% of the suspended solids available in the suspension were attached on the membrane surface. This is the most probable reason for a very rapid rise in cake resistance which caused a plateau stage beyond this period.

Figure 6.7 presents the cake resistance profiles for different viscosities at 20 L/m^2/h at an air flow rate of 1.8 m^3/m^2/h. At this air flow, doubling the viscosity caused an increment in cake resistance of 2.22 times compared to non-viscous kaolin suspension, while tripling viscosity increased cake resistance by 3.31 times.

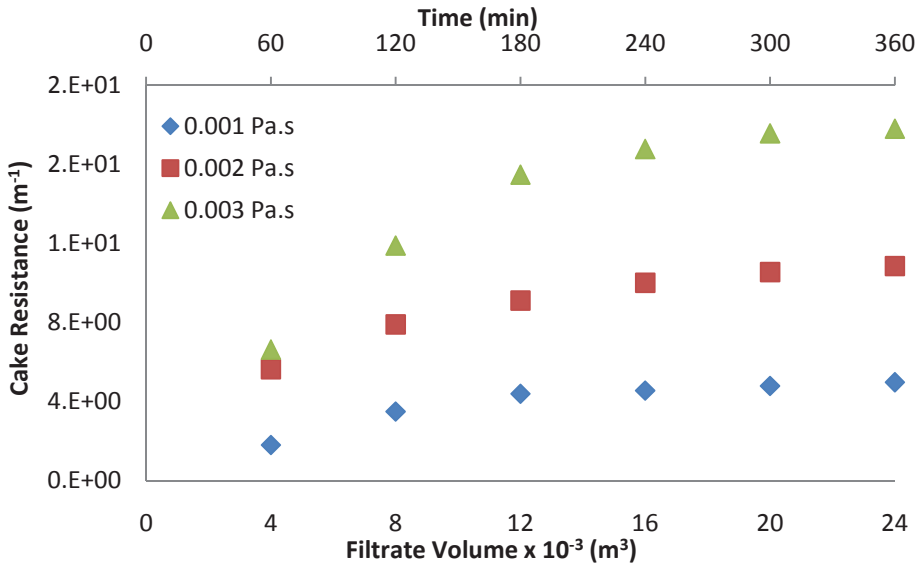

Figure 6.7 Effect of viscosity on cake resistance (J = 20 L/m^2/h)

Viscosity (μ) is explicitly incorporated in Darcy's equation ($TMP = \mu JR_t$). It increases with solute concentration and decreases with higher temperature. For a constant permeate flux, TMP is solely dependent on viscosity and total membrane resistance. The experimental results of changing viscosity and air flow rates indicated that cake resistance was directly proportional to the suspension viscosity and inversely related to the system air flow rates. Table 6.1 summarises the effect of viscosity on cake resistance rise at different permeate flux and air flow rates. Doubling the viscosity produced more than double the cake resistance for all the air flow rates and permeate flux rates employed. In the case of tripling viscosity, low air flow (0.6 $m^3/m^2/h$) resulted in a greater than four times rise in cake resistance, whereas high air flow rates (1.8 $m^3/m^2/h$) limited the increment to between of 3.16 and 3.31 times that of the non-viscous TMP.

Table 6.1 Increment in cake resistance with changing feed viscosity at different air flow rates (after 7 hours of filtration)

Flux ($L/m^2/h$)	AFR-0.6 $m^3/m^2/h$		AFR-1.2 $m^3/m^2/h$		AFR-1.8 $m^3/m^2/h$	
	Viscosity Increment (Pa.s)		Viscosity Increment (Pa.s)		Viscosity Increment (Pa.s)	
	0.001- 0.002	0.001-0.003	0.001-0.002	0.001- 0.003	0.001-0.002	0.001- 0.003
10	2.34	4.36	2.25	3.38	2.11	3.16
15	2.31	4.0	2.24	3.4	2.22	3.22
20			2.15	-	2.22	3.31

From Table 6.2, it is clear that the effect of high air flow is more effective at high viscosity. At 10 $L/m^2/h$, in the absence of glycerol (0.001 Pa.s), tripling the aeration rate (from 0.6 to 1.8 $m^3/m^2/h$) caused a 51% reduction in cake resistance, while at solution viscosities of 0.002 Pa.s and 0.003 Pa.s, the reductions were 59% and 66% respectively. At a higher flux of 15 $L/m^2/h$, cake resistance reduced by 60%, 62% and 65% for corresponding viscosities of 0.001, 0.002 and 0.003 Pa.s in the same operating

conditions mentioned above (tripling air flow). These results allow us to conclude that cake resistance reduction is more significant at high air flow and high viscous feed than at low air flow and less viscous feed.

Table 6.2 Effect of air on cake resistance reduction (%) with varying feed viscosity

Flux ($L/m^2/h$)	Feed viscosity: 0.001 Pa.s			Feed viscosity: 0.002 Pa.s			Feed viscosity: 0.003 Pa.s		
	Air flow increment ($m^3/m^2/h$)			Air flow increment ($m^3/m^2/h$)			Air flow increment ($m^3/m^2/h$)		
	0.6-1.2	0.6-1.8	1.2-1.8	0.6-1.2	0.6-1.8	1.2-1.8	0.6-1.2	0.6-1.8	1.2-1.8
10	33	51	31	28	59	45	42	66	45
15	25	60	46	20	62	51	29	65	50
20	20	33	16	-	-	15	-	-	-

6.3.2 Effect of Viscosity on Particle Deposition (Fouling)

Particle deposition on the membranes during the submerged microfiltration of kaolin suspension with different viscosities was determined by the turbidity method and verified by the gravimetric method. In this method, a fixed quantity of sample (30 ml) was dried in a 103° C to 110° C oven for about one hour and allowed to cool to room temperature. It was then weighed, and heated again for about 30 minutes. The sample was cooled and weighed a second time. The weight of kaolin clay was calculated after deducting the container weight. The particle deposition was assessed for different air flow (0.6, 1.2 and 1.8 $m^3/m^2/h$) and permeate flux rates (10, 15 and 20 $L/m^2/h$) at different viscosities. In all operating conditions, an increased air flow helped to reduce the particle deposition, whereas higher viscosity caused higher deposition during submerged microfiltration. Figures 6.9 and 6.10 present the particle deposition profiles

for permeate flux rates of 10 and 15 L/m^2/h respectively in various operating conditions. In the case of a viscous solution, deposition was rapid during the first hour of the experiment.

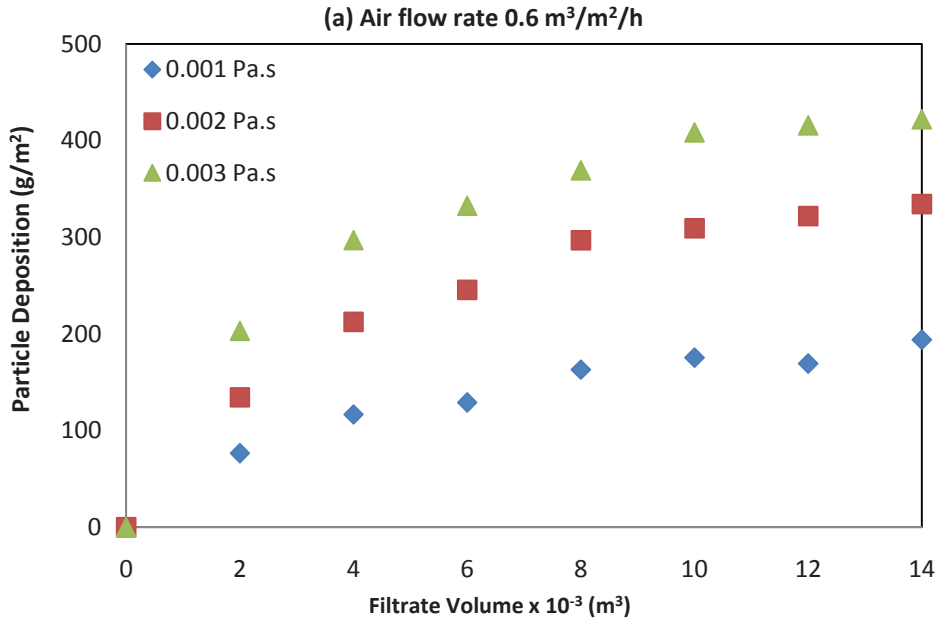

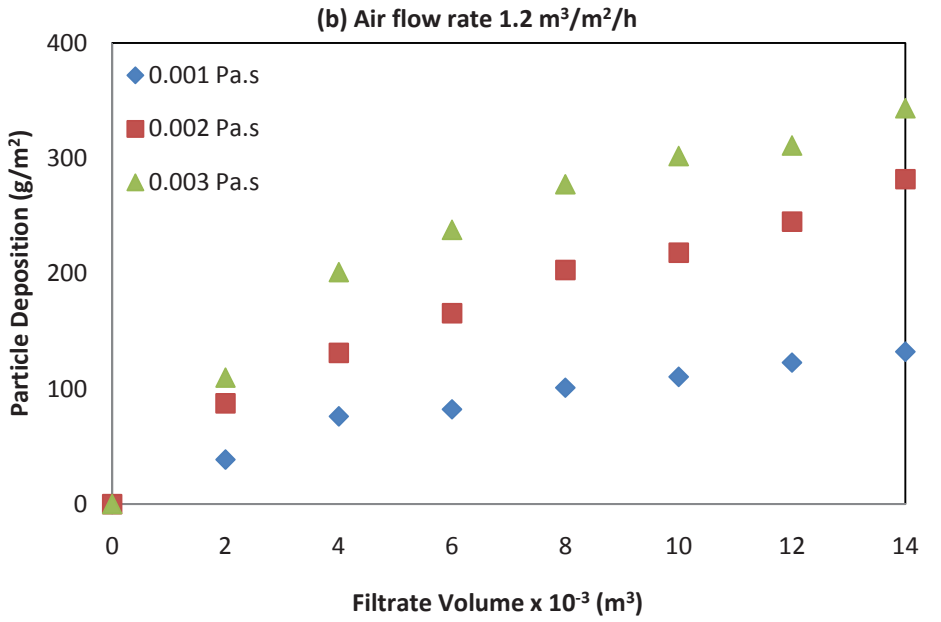

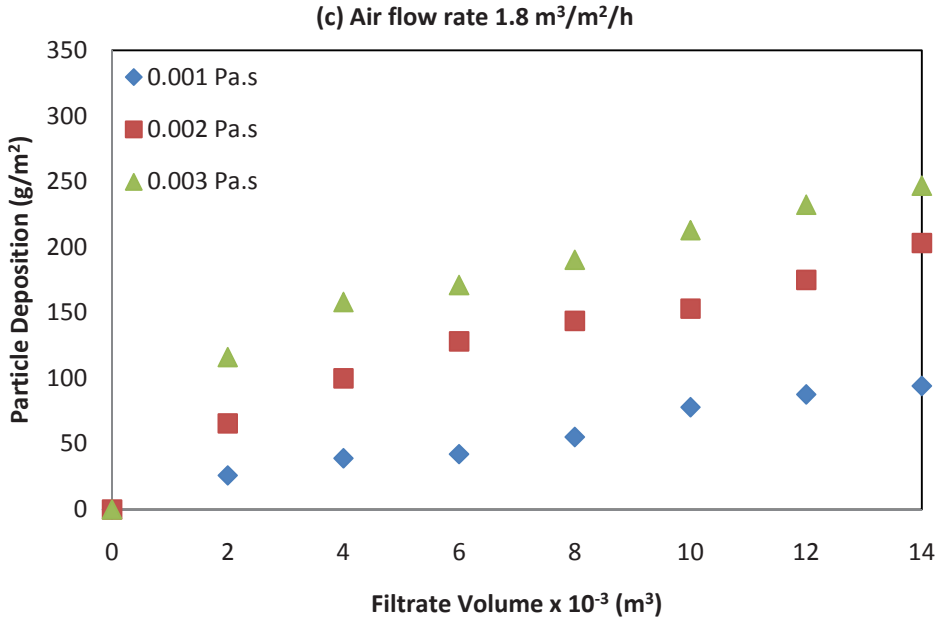

Figure 6.8 Effect of viscosity on particle deposition under various air flow rates at 10 L/m²/h

It is clear from Figure 6.8 that the particle deposition was rapid within the first hour of operating time, especially for the viscous solution (particularly with 0.003 Pa.s). In the case of a permeate flux of 10 L/m^2/h at an air flow 0.6 m^3/m^2/h and viscosity of 0.003 Pa.s, the total particle deposition observed after the 7th hour of the run period was 421 g/m^2 whereas 203 g/m^2 kaolin was deposited during the first hour. This result suggests that about half (48%) of the total deposition occurred within the first hour of test. Even at a higher air flow rate (1.8 m^3/m^2/h), 47% of the total deposition occurred early during the first hour. These data show how critical the early hours of a test are for mitigation of particle deposition.

Figure 6.9 shows the effect of viscosity on particle deposition at different air flow rates for 15 L/m^2/h. At this permeate flux, an increased viscosity resulted in a higher deposition for all adopted air flow rates, however an apparent difference was observed at a higher air flow rate of 1.8 m^3/m^2/h. As observed for a permeate flux of 10 L/m^2/h, deposition jumped very sharply in the first hour of the experiment for all operating

conditions. For example, at a flow rate of 0.6 $m^3/m^2/h$, deposition after an hour was 232 g/m^2, whereas with a 0.003 Pa.s viscosity feed, it was 475 g/m^2 at the 7th hour of experiment. This data highlights that about half (48%) of the deposition took place within the first hour of experiment, which again indicates the criticality of the initial stage for membrane fouling. These facts demand special attention during the early hours of filtration for fouling control.

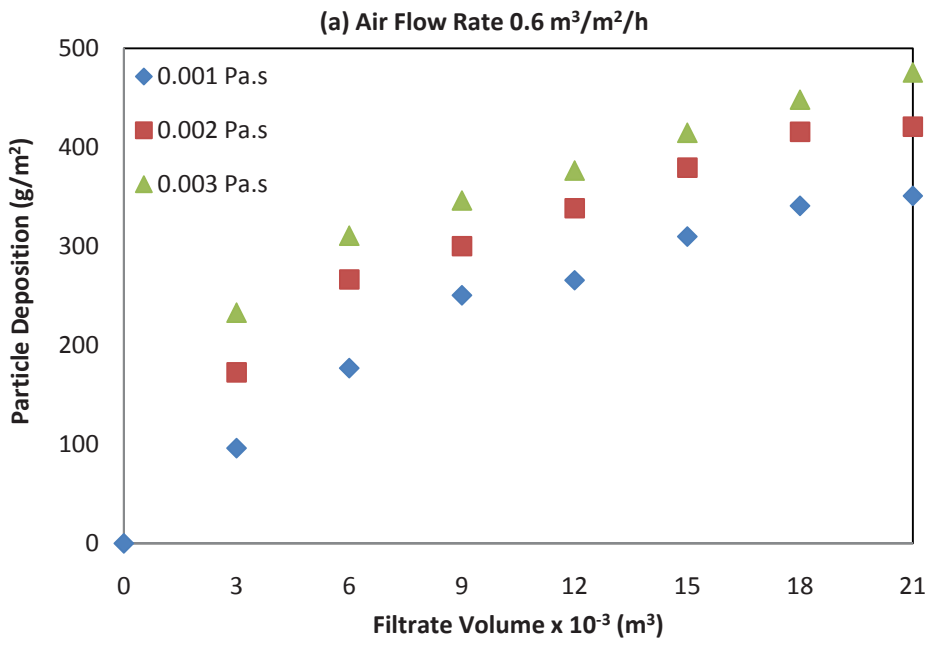

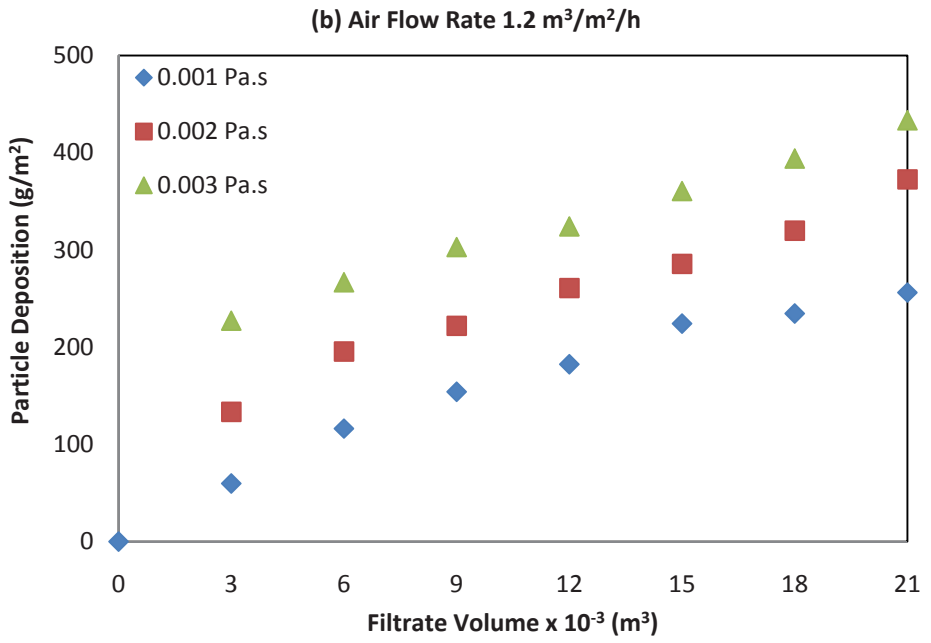

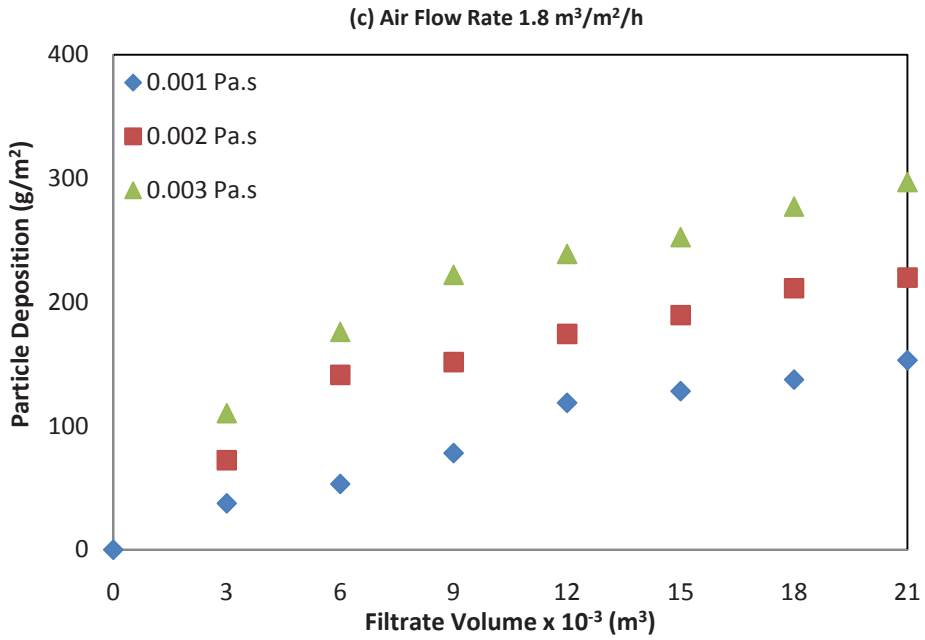

Figure 6.9 Effect of viscosity on particle deposition at a permeate flux of 15 L/m^2/h (air flow rate = 1.8 m^3/m^2/h)

For viscous suspensions (0.002 and 0.003 Pa.s), an increased air flow reduced particle deposition. At a permeate flux of 15 L/m^2/h, the solution with viscosity of 0.002 Pa.s was observed to be more effective with higher air flow, i.e. at this viscosity, deposition reduction was more significant with the increased air flow than the solution with a viscosity of 0.003 Pa.s. This result is similar to the findings obtained at 10 L/m^2/h.

6.3.3 Relationship of Cake Resistance and Particle Deposition

In general, the increment in TMP corresponds to an increase in cake resistance which is directly related to the increase in particle deposition, and therefore many researchers have analysed the membrane fouling in terms of TMP. In this study, both these parameters (TMP and particle deposition) were measured experimentally and cake resistance was calculated using Darcy's law so that a relationship between cake resistance and particle deposition could be established. The relationship was regressed and compared to equation $R_c = \alpha_{av} w_c$ (w_c is particle deposition) to identify the average specific cake resistance (α_{av}) at different operating conditions.

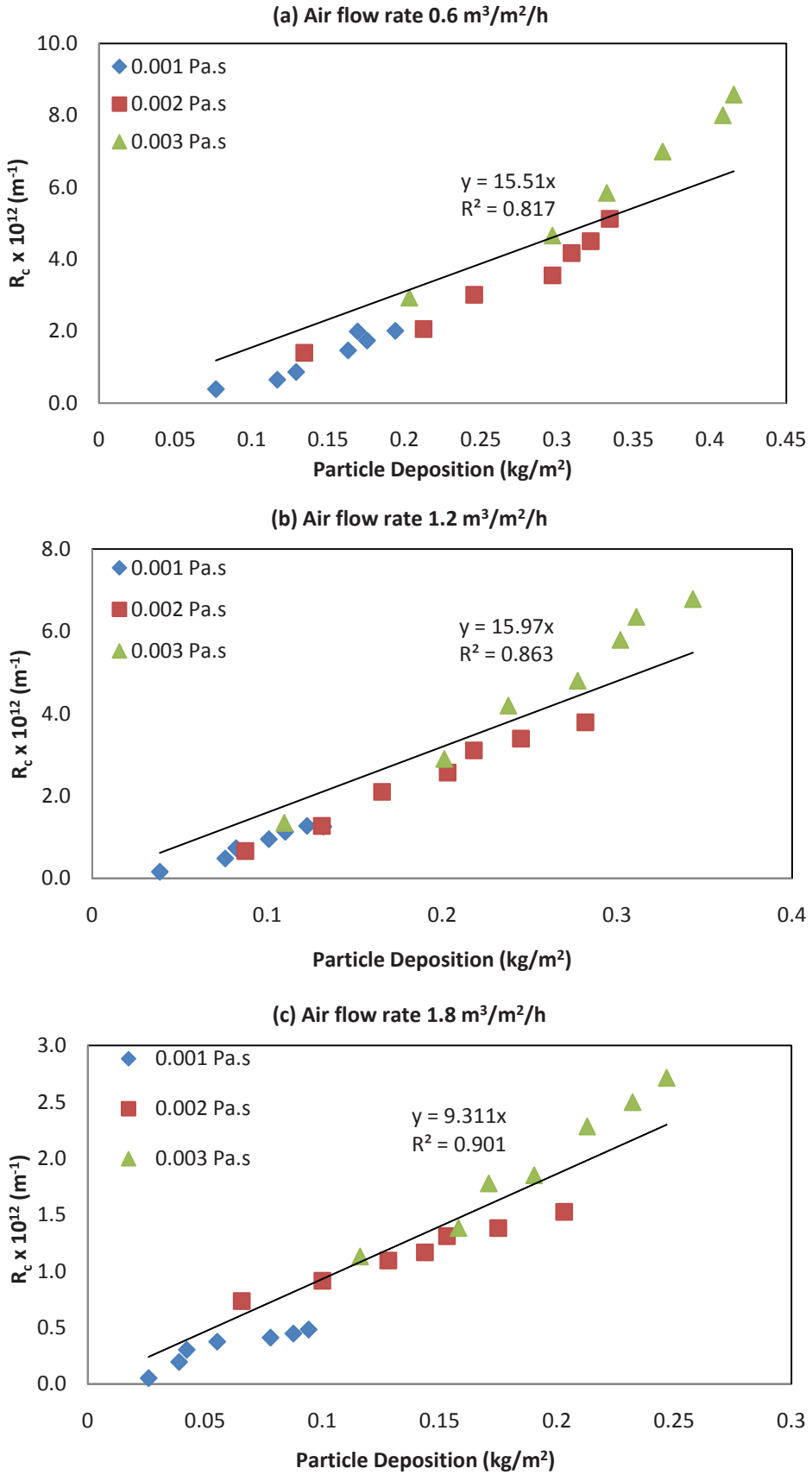

Figure 6.10 Relationship between cake resistance and particle deposition at 10 L/m^2/h

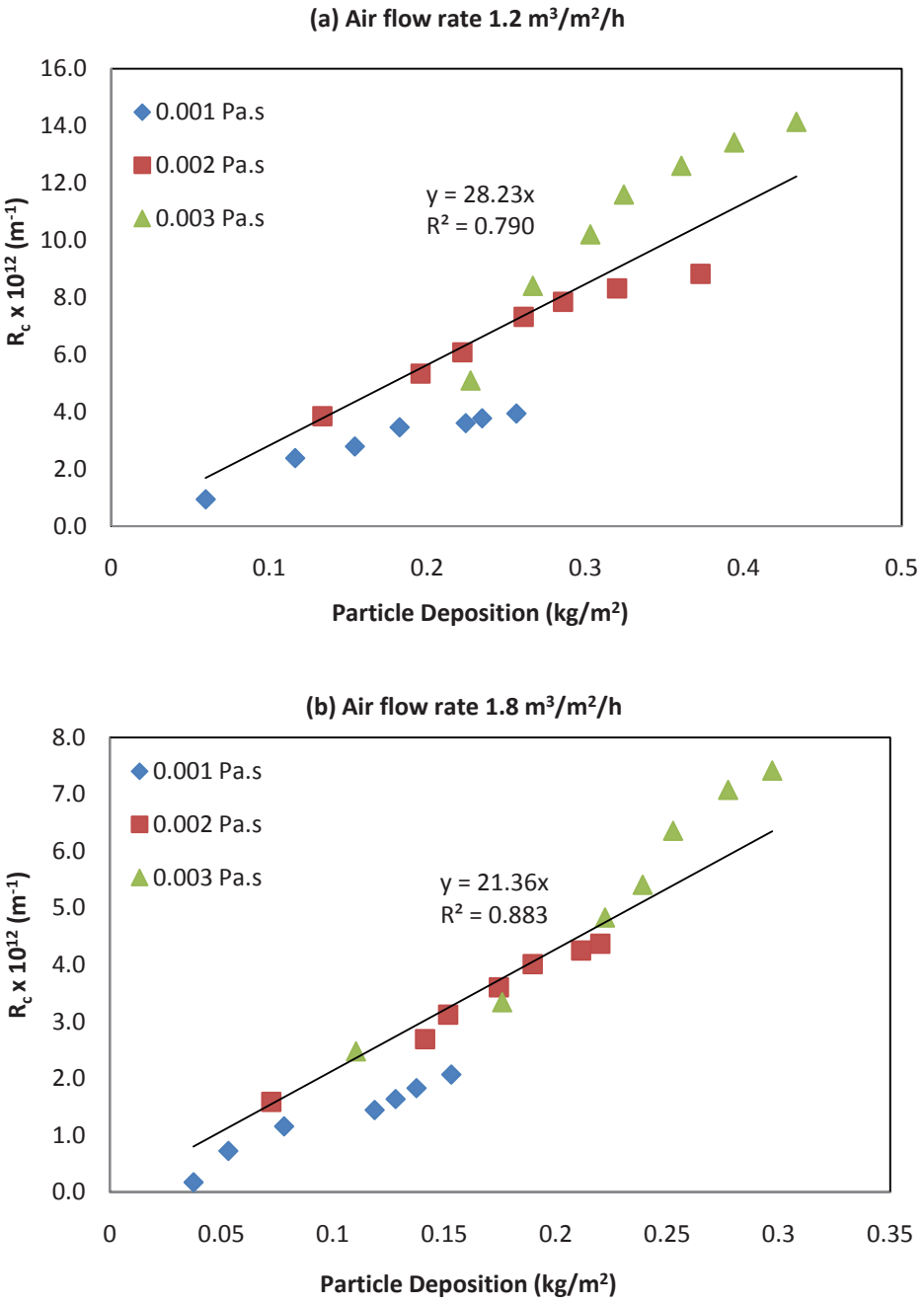

Figure 6.11 Relationship between cake resistance and particle deposition at 15 L/m^2/h

Figures 6.10 and 6.11 show the relationship between the cake resistance and particle deposition at different viscosities and air flow rates for two permeate fluxes of 10 and 15 L/m^2/h respectively. The relationship followed an almost linear pattern for kaolin clay suspension with all the viscosities tested. All operating conditions experienced higher particle deposition with high cake resistance and viscosity; however, an increased air flow caused a reduction in both cake resistance and particle deposition.

The regressed equations showed that an average specific cake resistance at permeate flux of 10 L/m^2/h was almost the same for the air flow rates of 0.6 and 1.2 m^3/m^2/h, but a significant reduction was observed at 1.8 m^3/m^2/h air flow rate. At 15 L/m^2/h, increased air flow also reduced specific resistance (Figure 6.11).

A higher permeate flux led to a higher TMP causing higher particle deposition. The relationship between cake resistance and particle deposition for solutions with two different viscosities is presented in Figure 6.12. In both viscous suspensions, the permeate flux displayed a dominant role, highlighting that an increased permeate flux has a far higher impact than the increased value of suspension viscosity. The gradient (specific resistance) was found to be very high at 20 L/m^2/h.

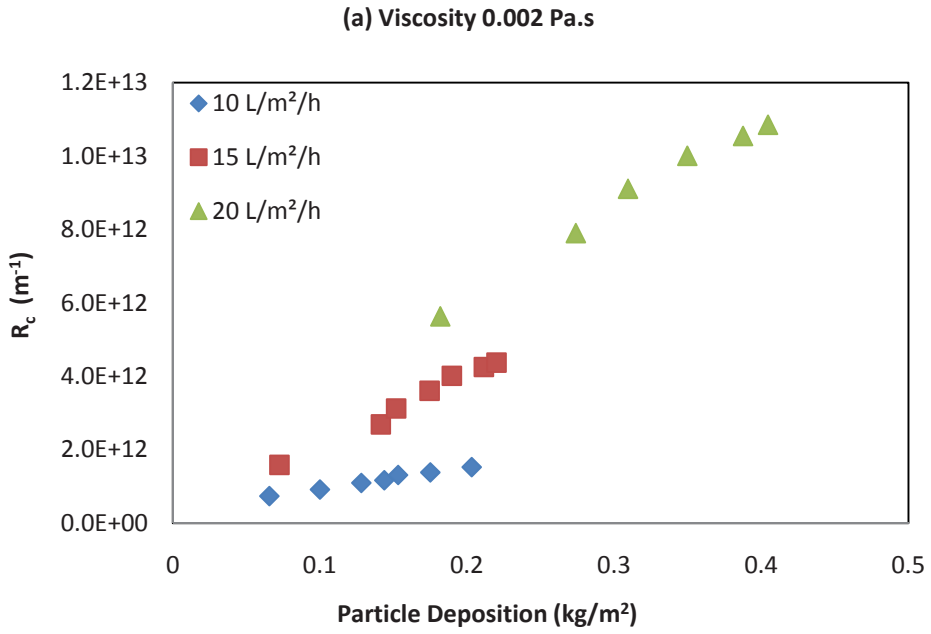

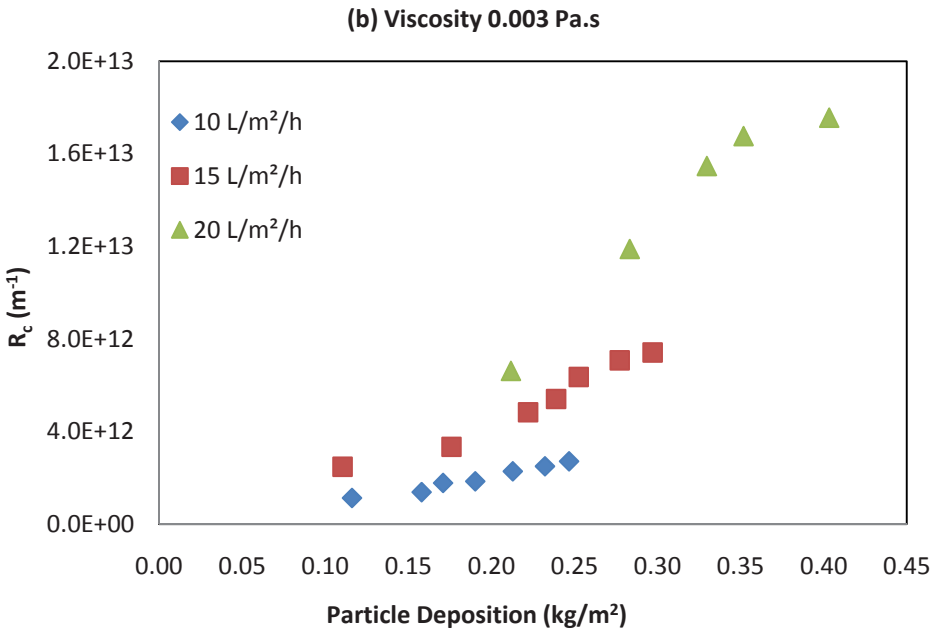

Figure 6.12 Relationship between cake resistance and particle deposition at different flux rates (air flow rate = 1.8 $m^3/m^2/h$)

Figure 6.13 shows the effect of viscosity on the average specific filtration resistance. Compared to the effect of air flow, an increase in viscosity significantly increased the specific filtration resistance.

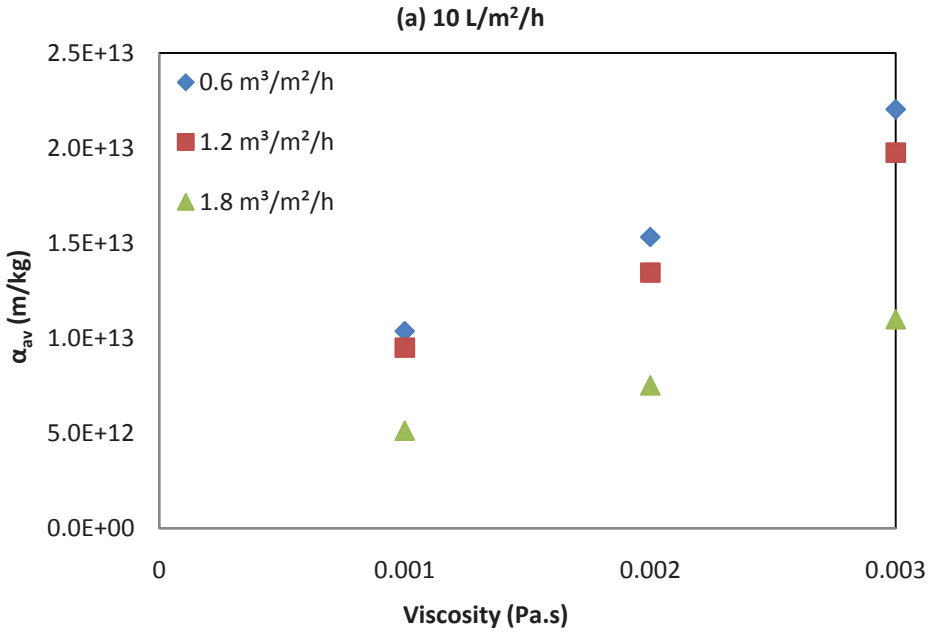

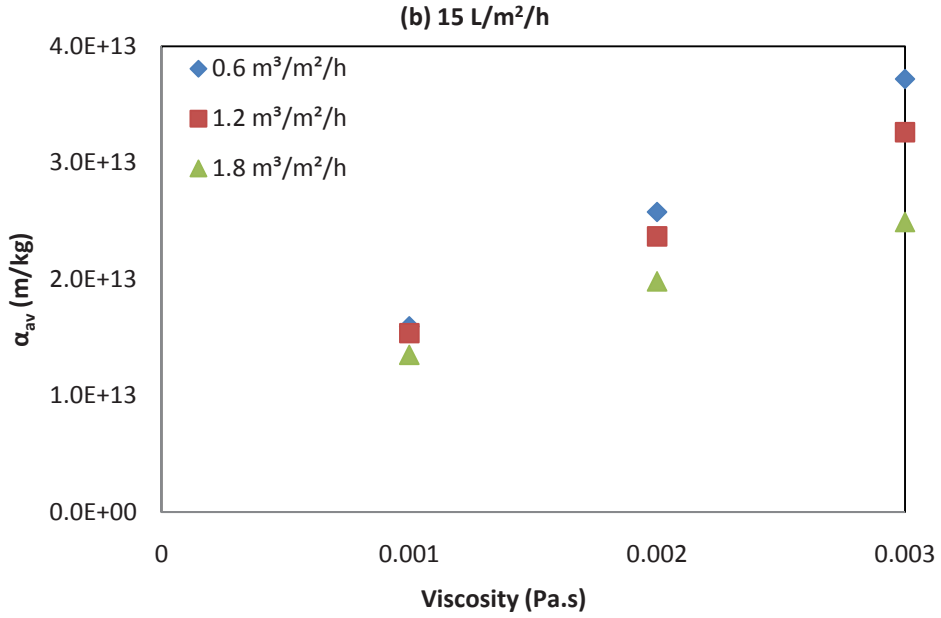

Figure 6.13 Effect of viscosity on specific filtration resistance

6.3.4 Effect of Permeate Flux on TMP

In this study, both parameters, TMP and particle deposition, were measured during microfiltration. Figures 6.14 and 6.16a show the development of TMP at different permeate fluxes (10, 15 and 20 L/m^2/h) and air flow rates. The viscosity was kept at 0.002 and 0.003 Pa.s respectively. At an early stage, a sharp rise in TMP was observed, but the rate of rise slowly decreased with the passage of time. Toward the end of the experiments, a steady state was observed in which a plateau was reached for all three permeate flux rates studied. The trend was more linear for lower permeate flux and nonlinear for higher permeate flux (Figure 6.14). Moreover, TMP at a viscosity of 0.003 Pa.s was higher than 0.002 Pa.s for all flux rates. The TMP clearly rose at a higher rate for higher permeate flux rates. This result highlighted that the fouling propensity increased with increasing permeate flux due to high TMP development. A higher permeate flux develops a higher drag force that causes more particles to be deposited on the membrane surface or to penetrate the membrane pores. An increase in viscosity aggravates this situation of membrane fouling.

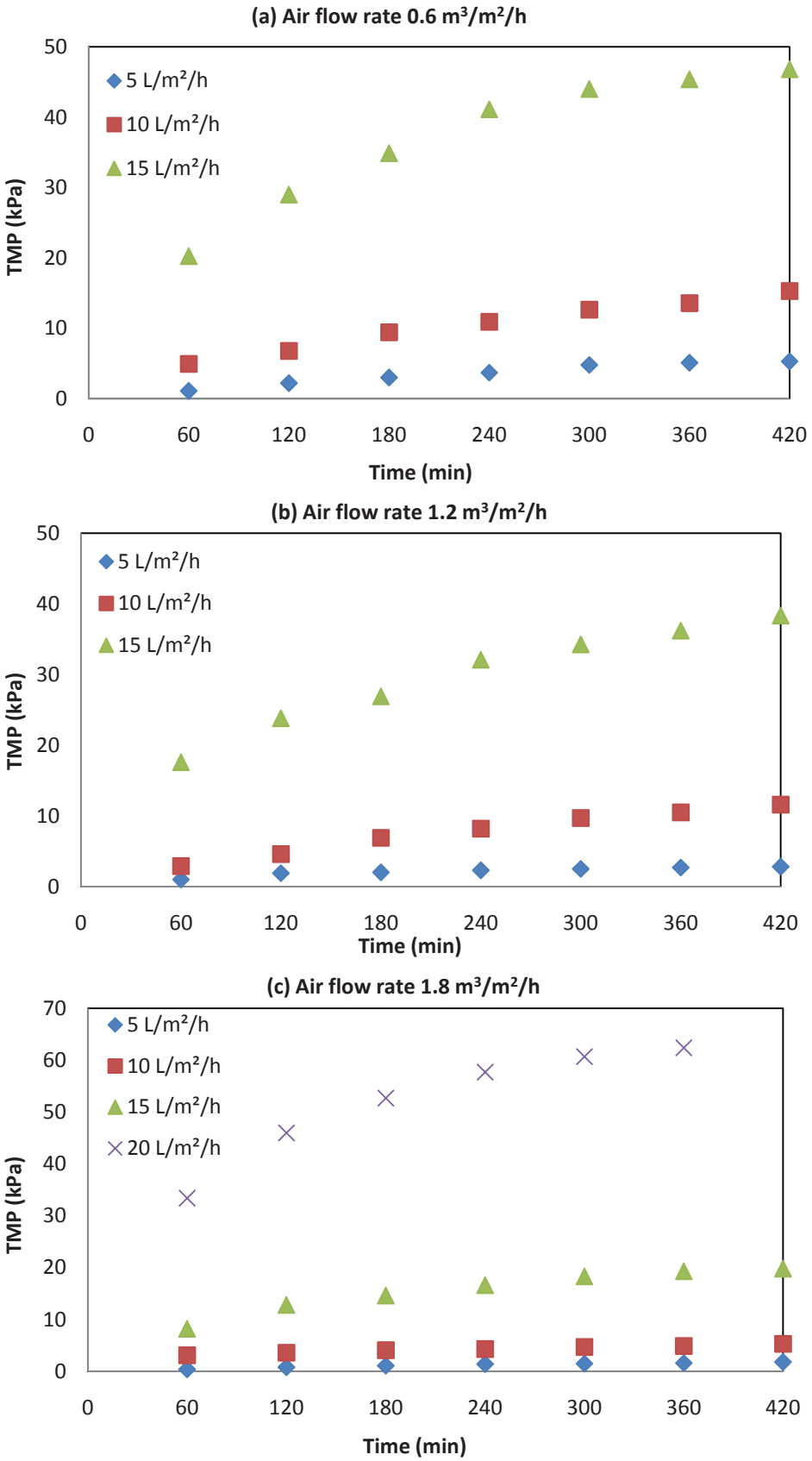

Figure 6.14 Effect of permeate flux on transmembrane pressure under various air flow rates (viscosity = 0.002 Pa.s)

It is evident that an increased permeate flux experiences higher TMP, but the change of TMP due to the increment in permeate flux was surprisingly varied for low and high permeate flux. For example, when permeate flux was doubled (from 5 $L/m^2/h$ to 10 $L/m^2/h$) for a kaolin clay solution with a viscosity of 0.002 Pa.s and an air flow rate of 0.6 $m^3/m^2/h$, the TMP at 10 $L/m^2/h$ was 3 times higher that of 5 $L/m^2/h$ after 7 hours of filtration. However under the same operating conditions but increasing the permeate flux by 3 times (at 15 $L/m^2/h$), a very high TMP increment (8.8 times) was observed compared to 5 $L/m^2/h$. Similarly, at 1.8 $m^3/m^2/h$ air flow rate and 0.002 Pa.s viscosity, a huge increment in TMP was observed when the permeate was increased to 20 from 10 $L/m^2/h$, i. e. TMP at 20 $L/m^2/h$ was 12.73 times higher than that of 10 $L/m^2/h$ (Figure 6.14c). In the case of a higher viscous suspension of 0.003 Pa.s, 20 $L/m^2/h$ achieved 13.47 times the TMP of 10 $L/m^2/h$ at 1.8 $m^3/m^2/h$ air flow rate (Figure 6.16a). These results suggest that the effect of permeate flux is far higher than the effect of viscosity on the development of TMP. It can be concluded that 15 $L/m^2/h$ is the best permeate flux for membrane operation because TMP development and particle deposition fall far below 20 $L/m^2/h$ but are just above 10 $L/m^2/h$. Quantitatively, under the same operating conditions (1.8 $m^3/m^2/h$ air flow rate and viscosity of 0.002 Pa.s), the difference in TMP development between 15 and 10 $L/m^2/h$ was 14.5 kPa whereas it was 43.1 kPa between 20 and 15 $L/m^2/h$ (Figure 6.14c).

Similarly, Figures 6.15 and 6.16b present graphs plotted between the total resistance and time. These plots clearly demonstrate the influence of permeate flux on the total membrane resistance. The total resistance increased with the evolution of time but, more importantly, the increase in resistance at higher permeate flux was very high compared to the increase at a low permeate flux. Due to the higher deposition of kaolin on the membrane surface, an increase in permeate flux augmented the total resistance very

rapidly. Although increased air flow rate reduced the total resistance for all employed permeate flux, the influence of the permeate flux was far higher than the effect of the air flow increment. Therefore, the selection of the permeate flux for membrane microfiltration is the most crucial task in minimising membrane fouling.

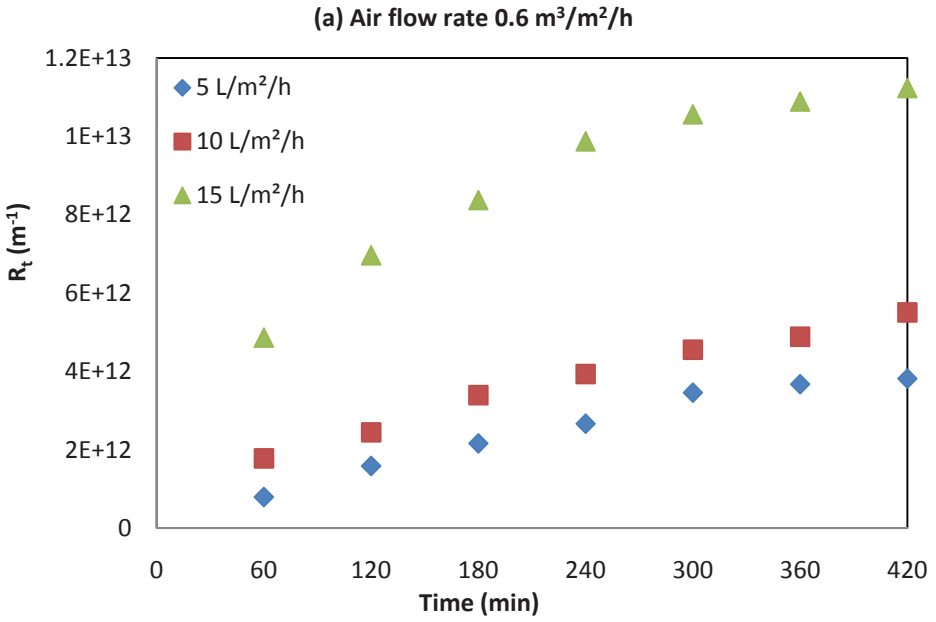

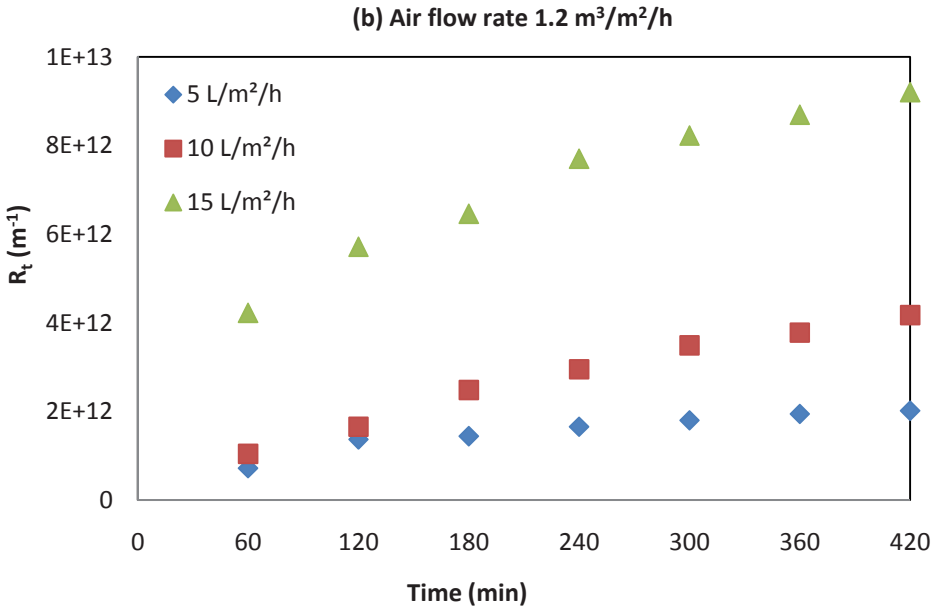

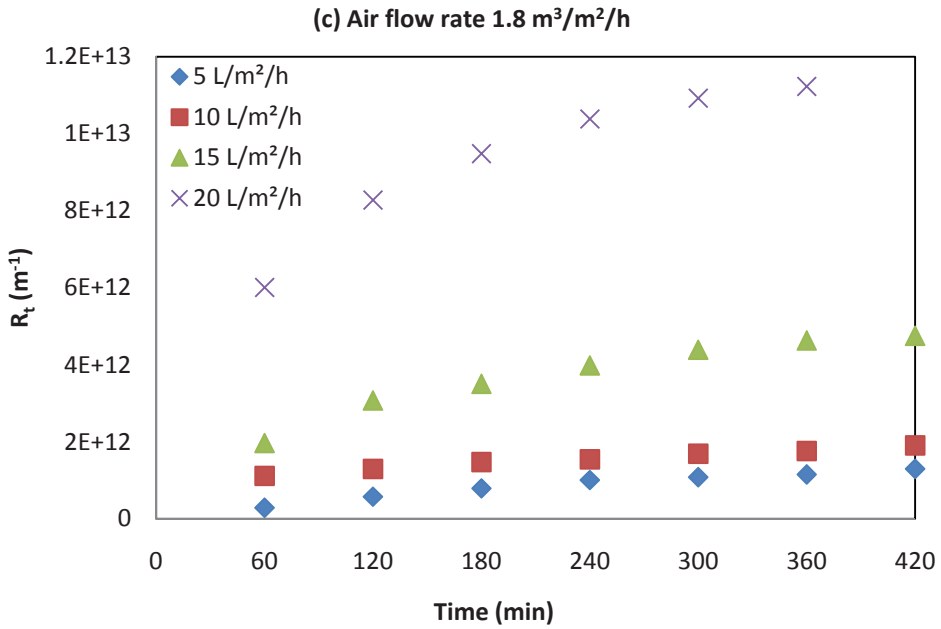

Figure 6.15 Effect of permeate flux on the total membrane resistance under various air flow rates (viscosity = 0.002 Pa.s)

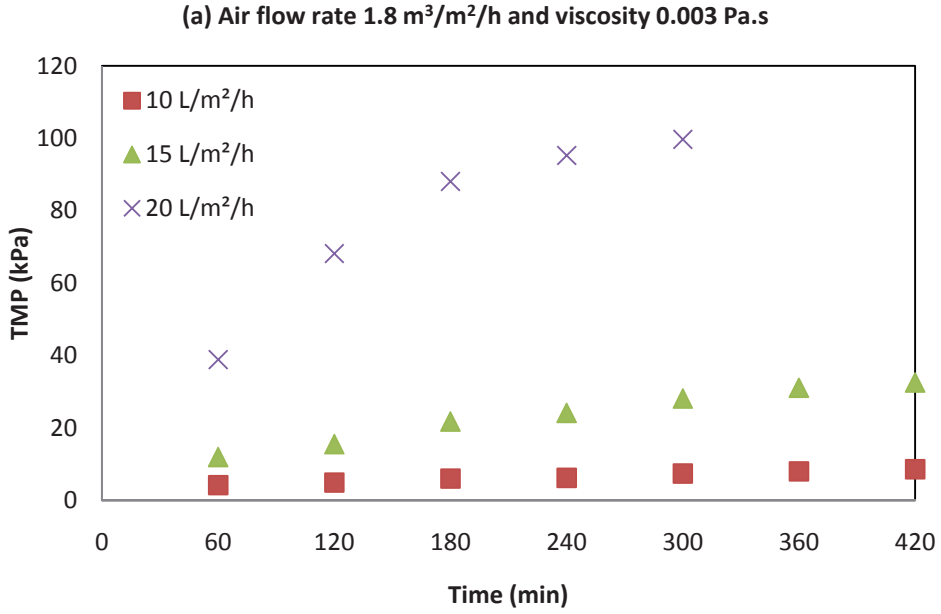

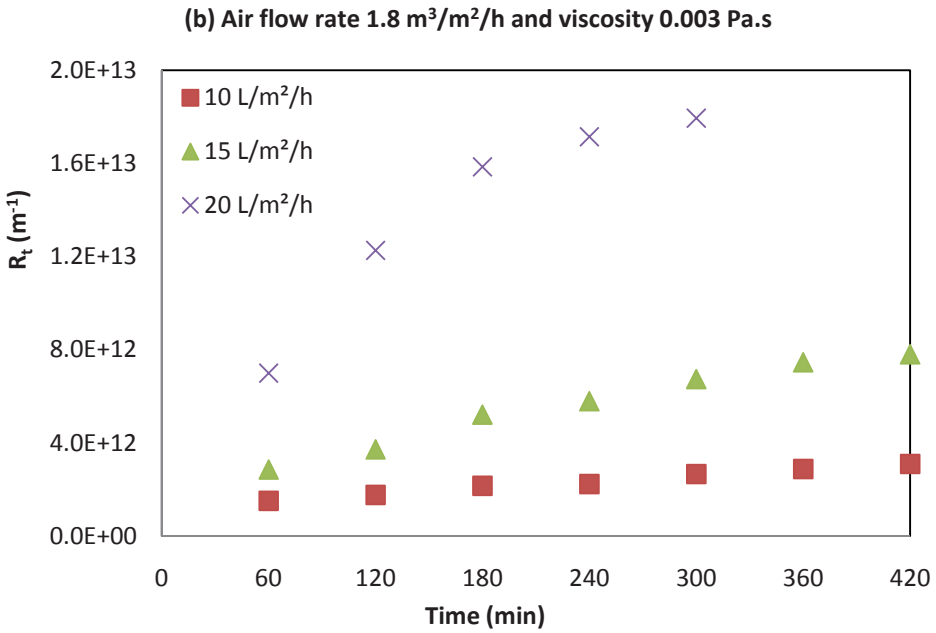

Figure 6.16 Effect of permeate flux on (a) TMP (b) total membrane resistance (viscosity 0.003 Pa.s)

6.4 Conclusions

The influence of changing viscosity was investigated by adding predetermined quantities of glycerol during the submerged membrane microfiltration of kaolin clay suspension in the presence of air flow bubbles. It has been demonstrated that suspension viscosity plays a significant role in membrane fouling control. An increase in viscosity caused a high TMP rise and particle deposition, leading to the formation of higher cake resistance. The application of air flow (air scour) helped to reduce the TMP and particle deposition on the membrane surface, but the increase in feed viscosity aggravated the fouling situation. Due to the increased viscosity, the increment in cake resistance was far higher than the reduction caused by the increased air flow. Moreover, the strong dependency of the cake resistance on the permeate flux was observed, even at viscous suspension.

The relationship between cake resistance and particle deposition was approximately a linear correlation for different viscous suspensions at various air flow rates. The specific

cake resistance reduced with the application of higher air flow but increased with higher viscosity. The results indicate that the permeate flux, air flow rate and feed viscosity are the most important parameters to influence membrane fouling control.

Chapter 7

Influence of air bubble size (aerator device) on particle deposition control on membrane microfiltration

Abstract

The application of air flow in a submerged membrane system has been proven to be very effective for fouling control. The efficacy of air flow is highly affected by the geometry of the air diffuser device that generates different sizes of air bubbles. This study compares the performance of the air diffuser devices with different geometries (square and circular) during the submerged membrane microfiltration of kaolin suspension under various permeate flux and air flow rates. The air sparging devices were assessed with regard to the size of the air bubbles and their effect on TMP development and particle deposition. Enhanced reductions in TMP and particle deposition were observed with a circular air diffuser plate that produces small bubbles, compared to the square air diffuser plate that produces larger air bubbles for all the permeate flux and air flow rates employed. Fouling was reduced by 19% at a permeate flux of 20 $L/m^2/h$ when air flow was doubled (from 0.6 to 1.2 $m^3/m^2/h$) with large bubbles, i.e. the square aerator plate, while with small bubbles (circular aerator), a 35% fouling reduction was achieved for the same operating condition. After changing the aerator plate from square to circular, the particle deposition was observed to be less by 39% and 49% for 0.6 and 1.2 $m^3/m^2/h$ air flow rates respectively. Based on the analysis of the reductions in TMP and particle deposition, a permeate flux rate of 20 $L/m^2/h$ and an air flow rate of 1.2 $m^3/m^2/h$ with a circular aerator plate were recommended as the most effective operating condition for the kaolin suspension. The experimental results suggest that the efficiency of membrane fouling control by injecting air flow depends

not only on the permeate flux and air flow rate, but also on the geometry of the air diffuser device (size of the air bubbles).

7.1 Introduction

It is commonly accepted that a fundamental understanding of the fouling mechanism and its control constrains the worldwide commercialisation of submerged membrane systems in the wastewater industry. The most popular antifouling approach for particle (or sludge) deposition control is the application of air flow (air scour) through the membrane module that promotes turbulence and scours deposited layers on the membrane surface. Air injection into the feed has been found to be very effective in enhancing membrane microfiltration performance. Cui and Wright (1994) reported a 175% increase in permeate flux in air sparged yeast microfiltration. In another study, Mercier et al. (1998) showed a three-fold increase in filtration flux by the application of air bubbles in the ultrafiltration of bentonite and yeast. While aeration is very successful in controlling membrane fouling, it also increases energy consumption, leading to high operating costs (Yoon, Kim & Yeom 2004). Ueta et al. (1996) studied the power consumption of a pilot scale submerged hollow fibre membrane bioreactor (MBR), and reported that the average power consumption for all units was around 2 $kWh.m^{-3}$ of treated water. However, they did not clearly specify the power consumed by aeration. Tao et al. (2005) reported that in a submerged filtration system, energy consumption rates were found to be less than 1 $kWh.m^{-3}$ and more than half of this energy was used by aeration. Gander et al. (2000) investigated the energy consumption for different bioreactor systems. It was suggested that the cost for aeration in a submerged system could be over 90% of the total operating cost. However, they estimated the total cost based on the power requirement for permeate suction and aeration only. From these

studies, it is clear that in submerged MBRs, the operating cost is mainly due to the power requirement for aeration.

The optimisation of aeration is still the subject of practical and research interest, both in terms of reducing the foulant accumulated on the membrane and increasing the life of the membrane and reducing the energy cost. The optimisation of aeration will significantly reduce the operating cost of membrane filtration. A more detailed investigation on the impact of aeration rates on suspension is needed to gain a better understanding of membrane fouling and to reduce the cost of aeration, which is one of the major operational costs of membrane operation.

Although only a few papers have been published on the optimisation of aeration systems during the membrane separation process, researchers have reported several different approaches to minimising air flow that result in maximum antifouling. These methods include the optimisation of membrane properties (Cote, 2000), the modification of membrane module design, and the optimisation of system operating conditions such as intermittent suction (Hong et al. 2002) and air back flushing (Visvanathan et al. 1997). Wicaksana et al. (2006b) reported on their experimental study of interaction between air bubble and fibre movement in a submerged hollow fibre system. They observed that fouling rates were low with more fibre movement, which was obtained by fibre looseness or higher air flow rate, lower feed viscosity and solids concentration. By changing fibre properties (choosing thinner and longer fibre), movement of the fibre can easily be increased. In another study, Ghosh (2006) investigated permeability enhancement in a submerged hollow fibre system with two different types of membrane module design. He performed ultrafiltration of polysaccharide solutions using two types of module designs (Type 1 and Type 2). The

shell of the Type 1 membrane module was designed with two rows of circular holes (six holes in each row, each of 5 mm diameters) 25 mm from each end. The shell of the Type 2 module had 36 uniformly distributed holes, each of 10mm diameters, arranged in nine rows along the length of the shell. In the Type 1 membrane module, the gas bubbles were confined close to the hollow fibre membranes while within the shell, whereas in the Type 2 module, some bubbles escaped through the holes at various locations on the shell. The Type 1 membrane module was therefore able to maximise the bubble-induced hydrodynamic effects. Ghosh (2006) reported an improvement in the hydraulic permeability by 115% with aeration, depending on the operating conditions and module design. His findings highlighted the importance of module design on process efficiency.

Guibert et al. (2002) compared several new aeration configurations with a continuous aeration system in an industrial scale submerged ultrafiltration system. They observed that changing the local aeration intensity resulted in lower fouling and found that alternating the injection of air in different zones around the hollow fibre bundles significantly improved the overall system performance. The filtration system can therefore be optimised by using intermittent aeration instead of using a continuous system.

Similarly, Ndinisa et al. (2006) investigated the effects of various hydraulic factors such as air flow rate, nozzle size, and intermittent filtration in a submerged flat sheet membrane system. In their experiments, they observed the optimum air flow rate beyond which no further fouling reduction was achieved. They also reported that the bubble-induced effects increased with the nozzle size of the air diffuser. It was suggested that the intermittent filtration was more effective than continuous filtration.

Moreover, their research evaluated the effect of baffles (introduced in the tank) in improving air distribution across a flat sheet submerged membrane system; the application of baffles reduced fouling rates by a factor of at least two.

Pradhan et al. (2011) investigated the combined effect of air flow and the use of a granular support medium in suspension in a submerged membrane reactor. Lower membrane fouling and a slower rise in transmembrane pressure (TMP) were noticed with a higher air flow rate. They achieved further fouling reduction by adding a granular medium in the suspension reactor. Their results showed that the same reduction of TMP could be obtained by adding a granular medium instead of increasing the air flow rate, hence they proposed adding a granular medium in the suspension (mechanical scouring) with air flow (air scouring) as a sustainable alternative to applying high air flow in a submerged membrane system.

Sofia et al. (2004) studied the effect of diffuser types on fouling rate by investigating the cross-flow velocity generated by coarse and fine bubble diffusers during air sparged membrane operations. Their results indicated that the fouling rate could be limited by proper selection of the aeration device and aeration intensity. They observed that with higher cross-flow velocity with fine bubbles under the same aeration intensity, uniformly distributed fine bubbles provided better fouling control and prolonged membrane operation. Yamamoto et al. (1989) also concluded that finer bubbles provided higher oxygen transfer efficiency. However, membrane manufacturers prefer coarse bubbles, to produce high shear for cake removal. Li et al. (1997) stated that the system performance was affected by the bubble size and frequency within the tubular membrane configuration. It may therefore be beneficial to find an optimum bubble size to achieve adequate oxygen transfer and maximum cake scouring; however, the

optimum size of bubble may also depend on the type of membrane module (hollow fibre, flat sheet), the type of air diffuser, and the properties of the feed suspension.

Limited data of a fundamental nature have been published for air bubble interactions in submerged flat sheet membrane systems. There is therefore a need to evaluate the use of air bubble application for submerged flat sheet membranes to understand the mechanisms involved in fouling control, so that the process can be optimised. In a flat sheet membrane, the bubble size, bubbling frequency, bubble motion and bubble distribution will influence the hydrodynamics and hence the detachment of cake layers. The scouring efficacy of air bubbles for tubular or hollow fibre modules is obviously different than the efficacy for the flat sheet module. In the former modules, all bubbles sweep over the whole membrane surface, whereas in the case of the submerged flat sheet membrane, only a portion of the membrane surface will come into contact with bubbles. The bubble distribution within the reactor tank affects feed mixing, biological oxidation and the scouring phenomenon. Bubble size and distribution also depend on the type of air sparger device. Therefore, this study made a preliminary investigation on the effects of air bubble size (large and small) on membrane fouling during the microfiltration of kaolin suspension in a submerged flat sheet membrane system. Experiments were conducted in two different reactor tanks with different air diffusers.

7.2 Materials and Method

The experimental methods and materials applied in this chapter were similar to those explained in Chapter 3. The main difference was that in this experiment, a new reactor with a circular air diffuser plate (Figure 7.1b) that generated small air bubbles (size < 2 mm) was also used. The reactor used in Chapter 3 had a square air diffuser plate (Figure

7.1a) that produced larger air bubbles (size of 2-4 mm). The experimental setup was identical to that used in Chapter 3 (Figure 3.2).

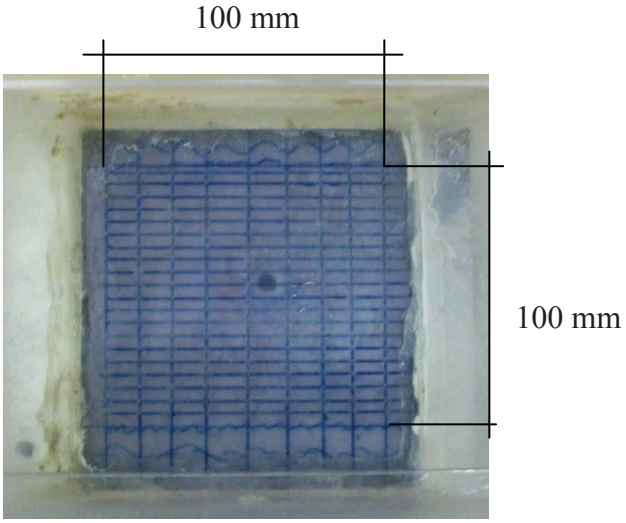

(a) Square air diffuser plate

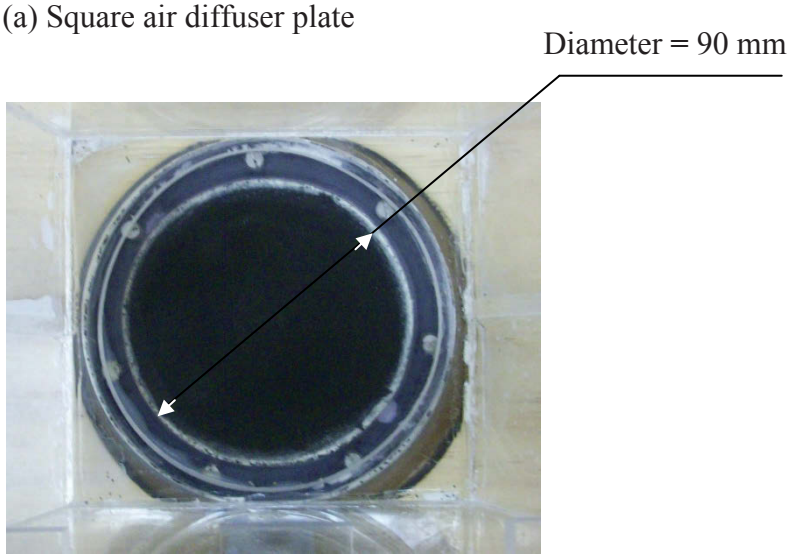

(b) Circular air diffuser plate

Figure 7.1 Photographic images of air diffuser plates

The kaolin clay concentration was maintained at 10 g/L and the filtration system was operated at a constant flux mode for 6-7 hours. The effects of the different designs of air diffuser plate that generates different air bubble sizes were evaluated for various permeate flux rates (15, 20, 30, 40 and 50 L/m^2/h) and air flow rates (0.6, 1.2, 0.96, 1.2

$m^3/m^2/h$). Mechanical scouring by adding granular activated carbon (GAC) into the feed tank was also studied for higher flux rates with small air bubbles.

7.3 Results and Discussion

The influence of bubble size on TMP and particle deposition was investigated by using two different air diffuser plates. Experiments with different filtration flux and air flow rates were conducted in two stages: first with a square aerator plate for large bubbles and second with a circular aerator plate for small bubbles. The TMP and particle deposition were measured for all experiments and the parameters were analysed separately to evaluate the effect of air bubble size (or aeration device). The extent to which each bubble size was effective in reducing fouling was judged in terms of the reduction of TMP development and particle deposition.

7.3.1 A Permeate Flux of 15 $L/m^2/h$

Experiments were run with two types of air diffuser plate that produced large and small bubbles respectively. The TMP and particle deposition were measured experimentally and the total membrane resistance (R_t) was calculated from Darcy's equation [$R_t = R_c + R_m = TMP/(\mu J)$]. Here, R_c and R_m are the membrane resistance due to cake deposition and clean water respectively and μ and J are the viscosity of permeate and flux rate respectively. The clean membrane resistance (R_m) was experimentally measured. The cake resistance (R_c) was calculated by subtracting R_m from R_t. The pore blocking was ignored because the kaolin clay particle size was larger than the membrane pore size.

Figure 7.2 shows the variation of TMP development during the period when two types of air bubbles were applied, and this was compared with the TMP developed when

filtering clean tap water. The same air flow rate of 1.2 $m^3/m^2/h$ was used in both experiments but air scour was not applied during clean water filtration. It can clearly be seen that air flow with small bubbles developed significantly less TMP compared to the same air flow with large bubbles. There was only a marginal rise in TMP when small bubbles were used. A 62% reduction in TMP development was achieved by the introduction of small bubbles compared to the introduction of large bubbles in a kaolin suspension (with kaolin concentration 10g/L).

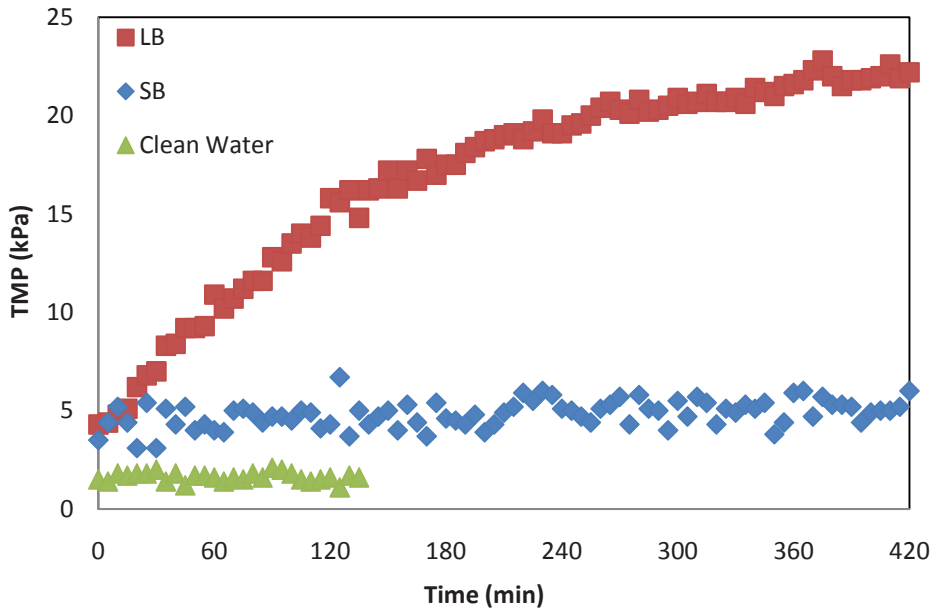

Figure 7.2 Variation of TMP profiles with different bubble sizes at air flow of 1.2 $m^3/m^2/h$

[Note: LB= Large bubble (2-4 mm) and SB = small bubble (< 2 mm)]

In most lab-scale and pilot-scale studies, TMP and flux are typically measured continuously and this information is used to assess fouling status. In general, TMP is considered to be an indirect indicator of membrane fouling (deposition); hence, the fouling rate is derived from the measured value of TMP. In this study, particle deposition was also measured so that fouling could be quantified directly and correlated with the rise in TMP. Figure 7.3 presents the particle deposition profile on the

membrane surface when air scouring with different air bubbles sizes is applied. The deposition trends were similar to TMP development with time, i.e. particle deposition increased with time. Particle deposition was higher with large bubbles than it was with small bubbles. It is noted that very low TMP development was observed with small bubbles throughout the experimental period, but particle deposition was found to slowly increase at the initial stage and reached a plateau after some time. The most likely reason for this is the formation of a loose cake layer with small bubbles. Due to the high porosity, there was no measurable rise in TMP.

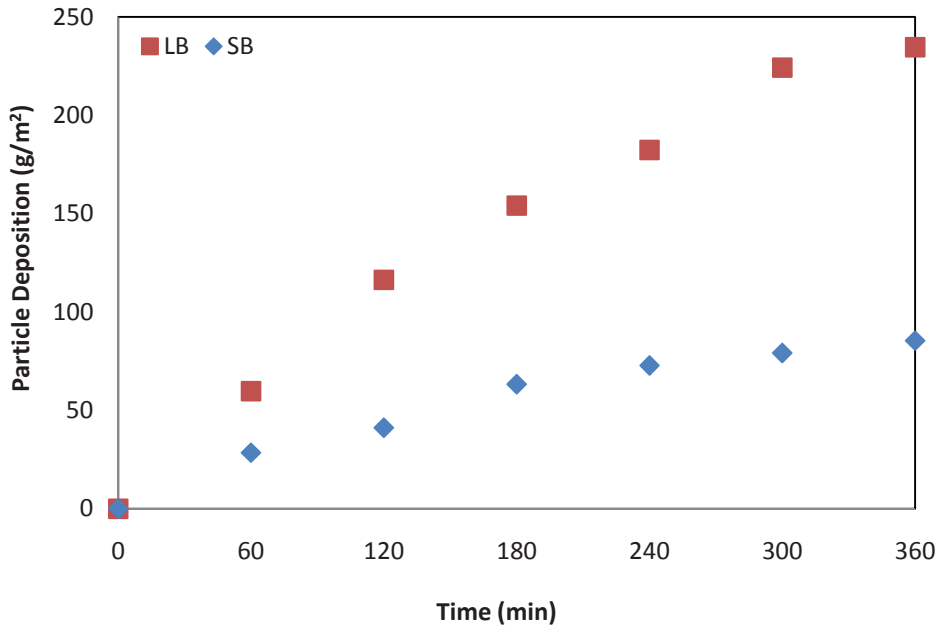

Figure 7.3 Effect of bubble sizes on particle deposition at air flow rate of 1.2 $m^3/m^2/h$

Figure 7.4 presents the relative resistance [(R_t/R_m) or (R_c/R_m +1)] which is the ratio of total membrane resistance to clean membrane resistance. The relative resistance data with large bubbles clearly rises during the initial period of filtration, while the same data with small bubbles is almost flat. Fouling can be evaluated by the relationship between relative TMP ($\Delta P/\Delta P_o$), which is the ratio of the TMP at any time during the fouling test to the initial TMP, and relative resistance (R_c/R_m), which is the ratio of cake resistance

to clean membrane resistance. The development of cake resistance with a square air diffuser plate (large bubbles) was significantly higher than the cake resistance with a circular air diffuser plate (small bubbles).

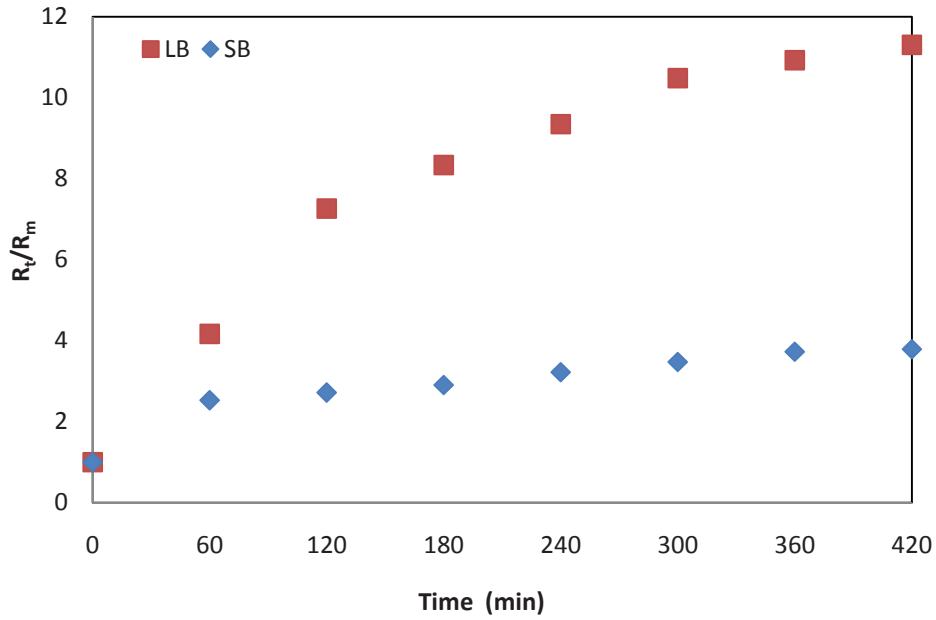

Figure 7.4 Total membrane resistance at different air bubble sizes

Figure 7.5 presents the relationship between cake resistance (R_c) and particle deposition with different sizes of air bubbles. Although cake resistance and particle deposition were remarkably low for small bubbles, a linear relation was observed between them for both operating conditions. An empirical relationship between cake resistance and particle deposition can be regressed as follows:

<u>At air flow rate of 1.2 $m^3/m^2/h$</u>

$$R_c = 16.54x10^{12}w_c \text{ ; (for large bubbles)} \quad (7.1)$$

$$R_c = 12.35x10^{12}w_c \text{ ; (for small bubbles)} \quad (7.2)$$

where w_c is particle deposition (kg/m^2). These empirical equations can be generalised to a linear relationship of $R_c = \alpha_{av}w_c$, where α_{av} stands for average specific filtration

resistance. Significant change was observed in the specific resistance by changing the aerator device. The application of small bubbles affected the structure of the cake layer which resulted in lower fouling.

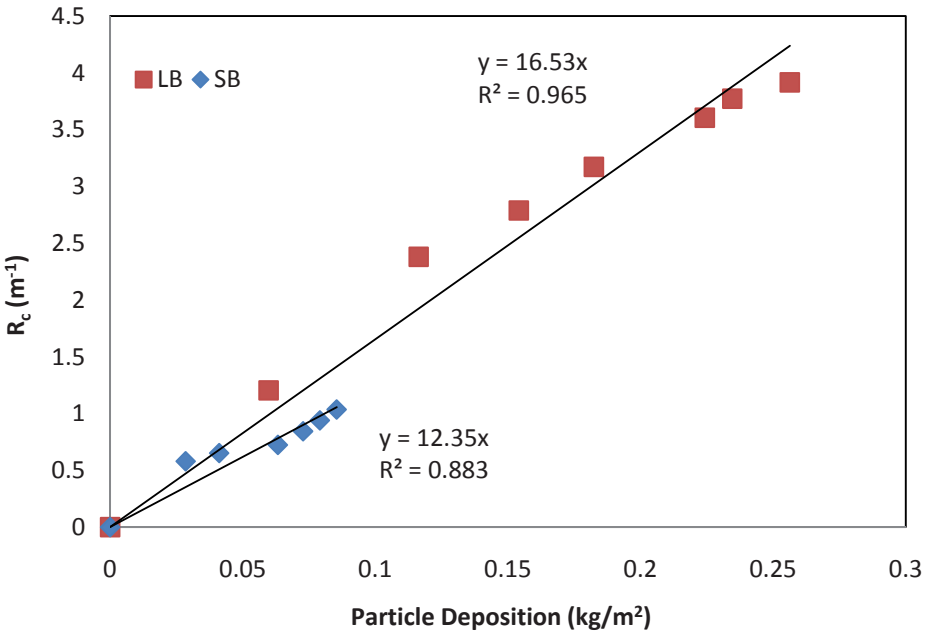

Figure 7.5 Relationship of cake resistance (R_c) and particle deposition for different air bubble sizes (J = 15 L/m^2/h)

7.3.2 A Permeate Flux of 20 L/m^2/h

The effect of bubble size was studied under two different air flows, i.e. 0.6 and 1.2 m^3/m^2/h at a permeate flux of 20 L/m^2/h. Figure 7.6 shows the TMP profiles for two different air flow rates and two bubble sizes. TMP development reduced with the increase in air flow rates, and a further reduction in TMP was clearly evident when small air bubbles were introduced. The TMP development was much lower with small bubbles. The application of a higher air flow rate with small bubbles further limited the TMP rise, resulting in no TMP rise. Thus, the TMP development is dependent on both air flow rates and bubble size. In the case of large bubbles, when air flow was doubled (from 0.6 to 1.2 m^3/m^2/h), TMP was reduced by 21%, whereas in the case of small bubbles, the reduction was more than twice (almost 48%) when air flow rate was

doubled (Figure 7.6). A similar effect of increased air flow and change in bubble size were also observed for particle deposition (Figure 7.7). A 19% reduction in particle deposition was achieved with large bubbles when the air flow rate was doubled (from 0.6 to 1.2 $m^3/m^2/h$). With small bubbles, this reduction was 35%.

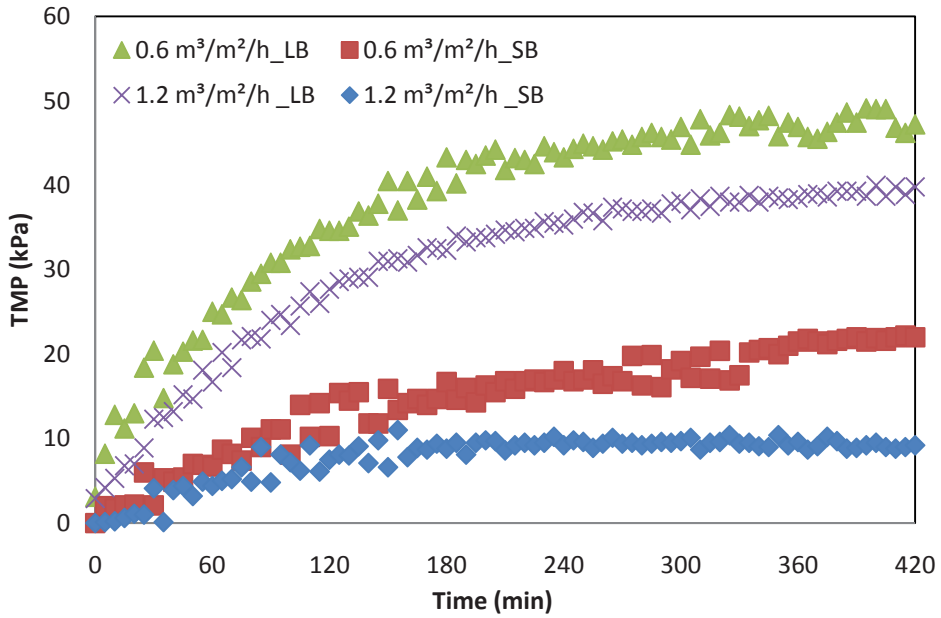

Figure 7.6 Variation of TMP at different air flow and bubble sizes

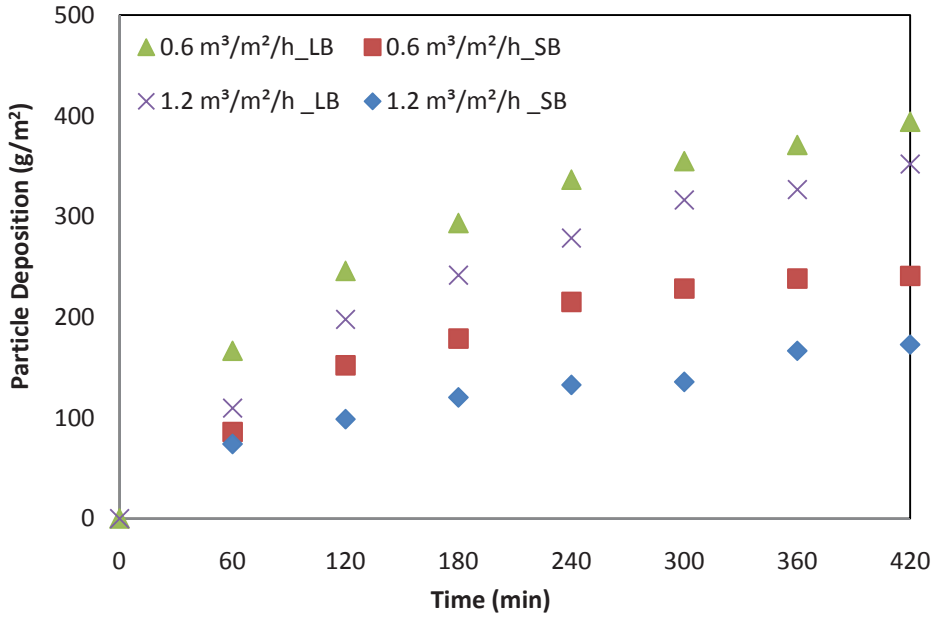

Figure 7.7 Variation of particle deposition at different air flow and bubble sizes

Figure 7.8 presents the relative resistance (R_t/R_m) of total membrane and clean membrane resistance at different air flow and bubble size conditions. In all operating conditions, total resistance increased with time. An increase in air flow and reduction in bubble size gave smaller total membrane resistance.

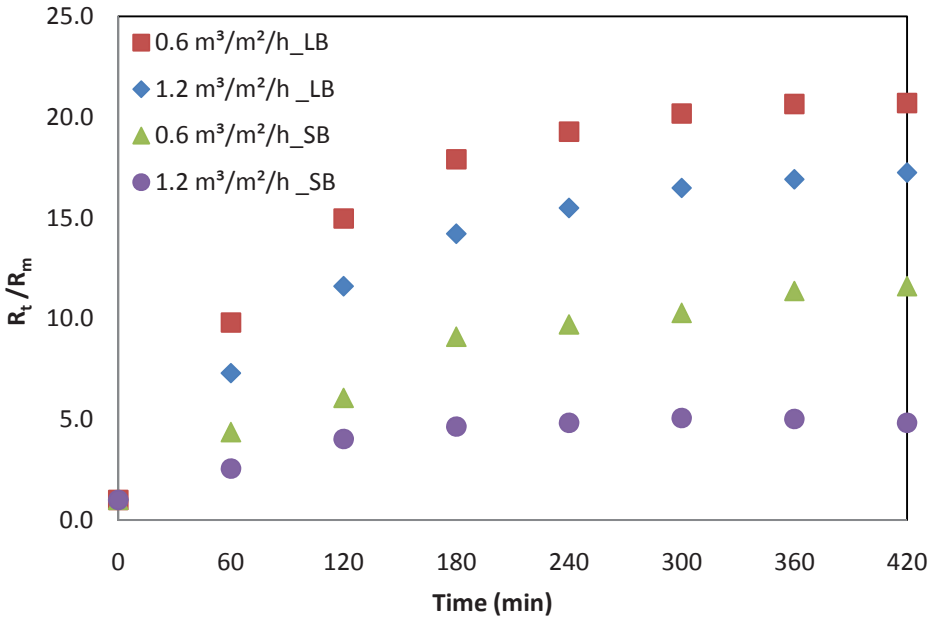

Figure 7.8 Total membrane resistance at different air flow and bubble sizes

Figure 7.9 shows the relationship between cake resistance and particle deposition under different air flow conditions. Linear relationships were observed for all the conditions studied, which were regressed to obtain empirical equations as follows:

<u>At air flow rate of 0.6 $m^3/m^2/h$</u>

$R_c = 20.75x10^{12}w_c$; (for large bubbles) (7.3)

$R_c = 15.65x10^{12}w_c$; (for small bubbles) (7.4)

<u>At air flow rate of 1.2 $m^3/m^2/h$</u>

$R_c = 19.39x10^{12}w_c$; (for large bubbles) (7.5)

$R_c = 10.5x10^{12}w_c$; (for small bubbles) (7.6)

where w_c is particle deposition (kg/m^2). These empirical equations can be generalised to a linear relationship of $R_c = \alpha_{av}\, w_c$, where α_{av} stands for average specific filtration resistance. In the case of large bubbles, aeration has an effect upon the mass of particles returned to the tank but not upon the deposit on the membrane surface, because specific resistance (α_{av}) was found to change only slightly when the air flow was doubled. However the application of small bubbles substantially reduced specific resistance and higher air flow accelerated this reduction. This means that the cake structure is highly influenced by small bubbles.

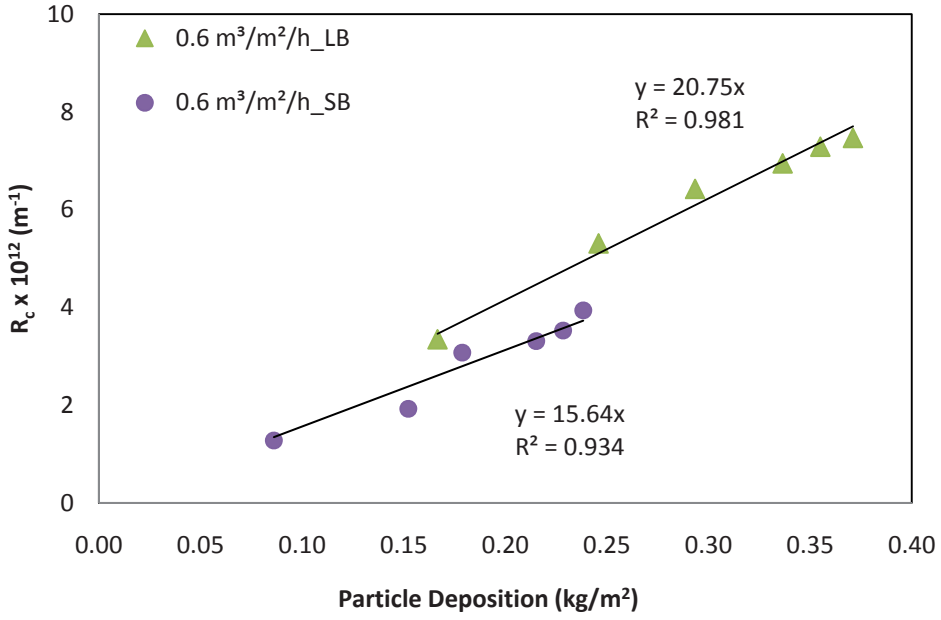

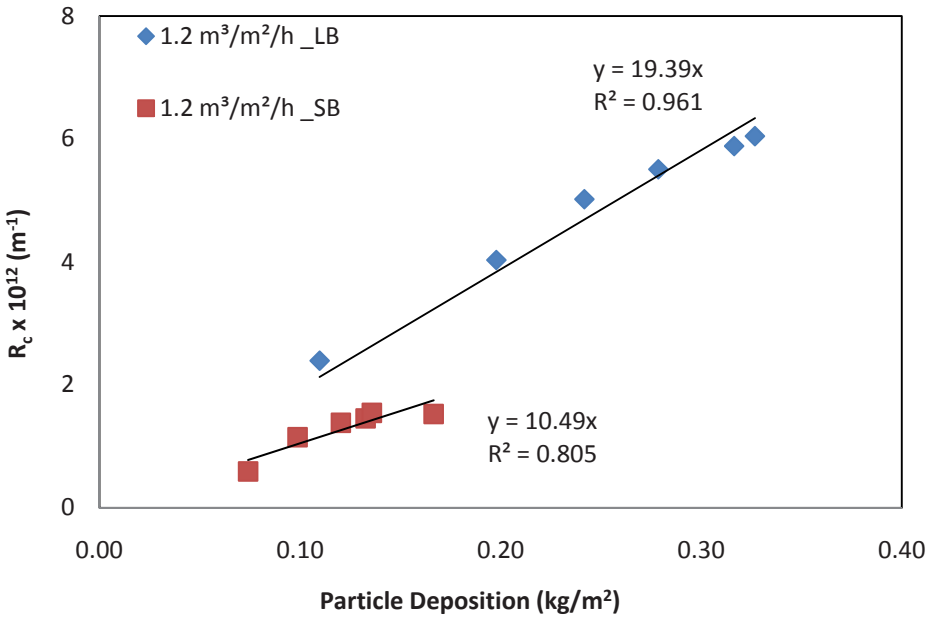

Figure 7.9 Relationship of cake resistance (R_c) and particle deposition at different air flow and bubble sizes (J = 20 L/m^2/h)

7.3.3 A Permeate Flux of 30 L/m^2/h

Similar experiments were conducted at air flow rates of 0.6 and 1.2 m^3/m^2/h using two different aerator devices at a permeate flux of 30 L/m^2/h. The effect of bubble sizes at increased air flows (from 0.6 to 1.2 m^3/m^2/h) is presented in terms of TMP development (Figure 7.10) and particle deposition (Figure 7.11). The TMP rise was lowered by 10% when air flow was increased to 1.2 m^3/m^2/h from a base flow of 0.6 m^3/m^2/h with air scour by large bubbles. This TMP reduction substantially increased to 40% with a small bubble aerator for the same increment in air flow.

Figure 7.11 presents the particle deposition profiles on the membrane surface under different operating conditions. With large air bubbles, deposition was observed to be almost the same (5% reduction) for the two different air flow rates, i.e. 0.6 and 1.2 m^3/m^2/h. On the other hand, with small bubbles, a 31% reduction in deposition was achieved when air flow was doubled from a base flow of 0.6 m^3/m^2/h.

The experimental results shown in Figures 7.10 and 7.11 highlight that at this higher permeate flux (30 L/m^2/h), TMP and particle deposition reduction due to increased air flow was not significant in the case of large bubbles. However with small bubbles, substantial reduction was observed for both TMP and particle deposition when air flow was doubled (from 0.6 to 1.2 m^3/m^2/h). For example, in the case of small bubbles, TMP and deposition reductions were 40% and 31% respectively when the air flow was doubled.

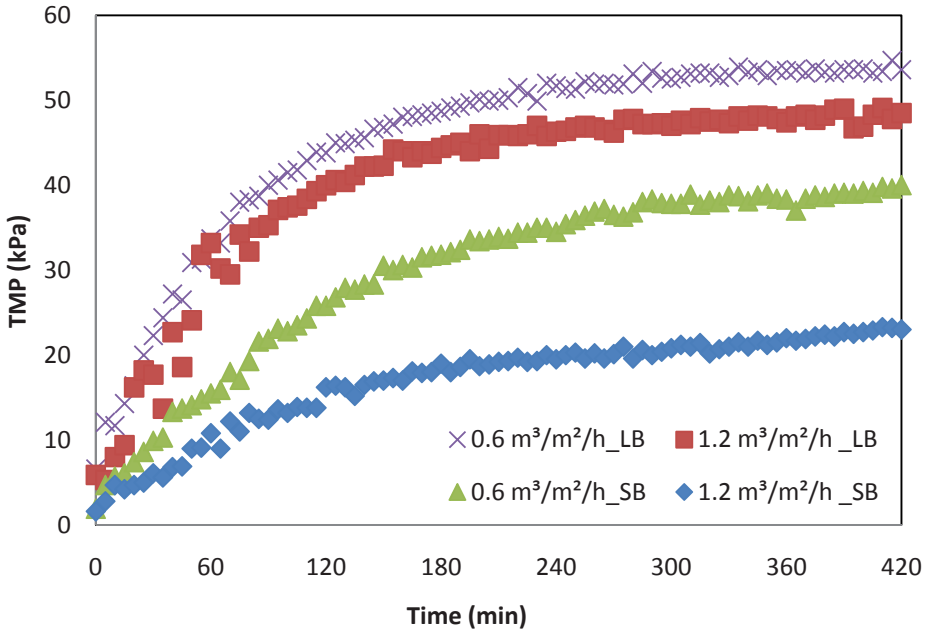

Figure 7.10 TMP profiles at different air flow rates (J = 30 L/m^2/h)

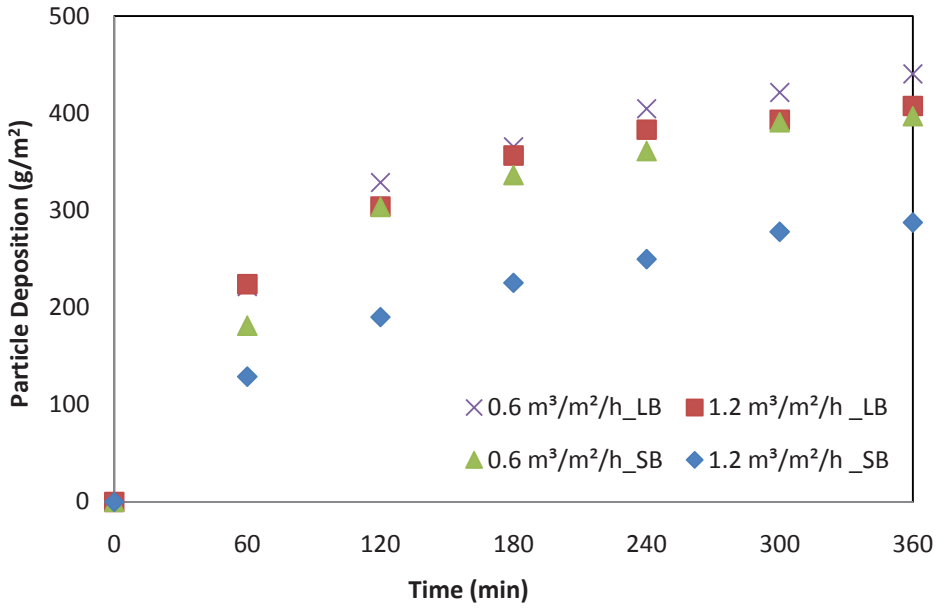

Figure 7.11 Particle deposition at different air flow rates (J = 30 L/m^2/h)

Figure 7.12 shows the ratio of total membrane resistance to clean membrane resistance at different air flow rates for 30 L/m^2/h. Clean membrane resistance (R_m) was the same for all operating conditions. Changes in operating conditions (increased air flow, changing bubble size) helped to reduce total membrane resistance, indicating lower membrane fouling.

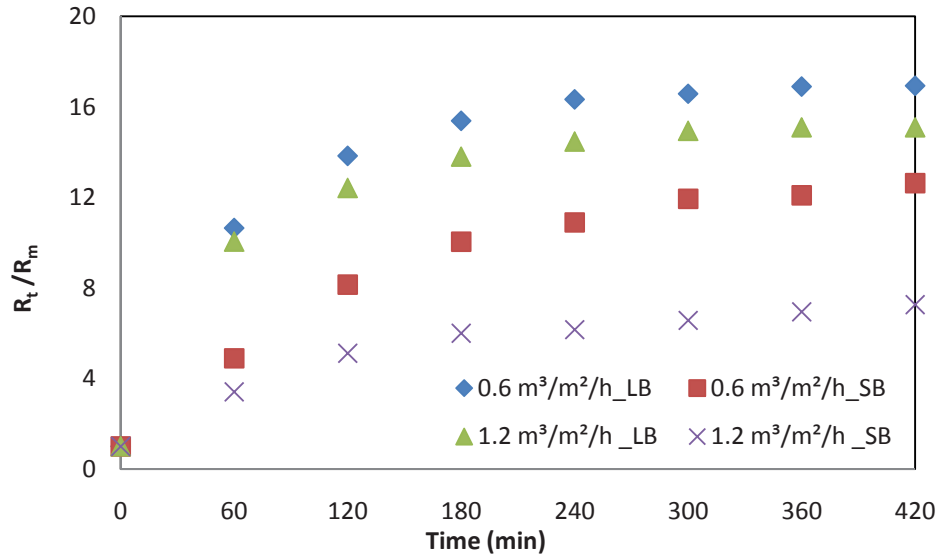

Figure 7.12 Total membrane resistance at different operating conditions (J = 30 L/m^2/h)

7.3.4 A Permeate Flux of 40 L/m²/h

In the case of 40 L/m^2/h, the effect of bubble size was investigated at the low air flow rate only (0.6 m^3/m^2/h). At higher flux (>20 L/m^2/h), increased air flow was found to be less effective than low flux with large bubbles. Thus, a comparison between large and small bubble sizes was made only at an air flow rate of 0.6 m^3/m^2/h.

Figure 7.13 presents the TMP profiles for large and small air bubbles at an air flow of 0.6 m^3/m^2/h. Similar to previous results (15, 20 and 30 L/m^2/h), TMP development was less with small bubbles than it was with large bubbles. With this high permeate flux, the TMP curve trend with large bubble showed two stages only: steep and linear rise and plateau state, whereas with small bubbles there were still three stages: sharp rise, slow rise and plateau. Small bubbles caused 26% less TMP rise compared to large bubbles (on average), but the TMP reduction was 43% during the first hour. This result suggests that small bubbles were more effective at an early stage of filtration when higher filtration flux was employed.

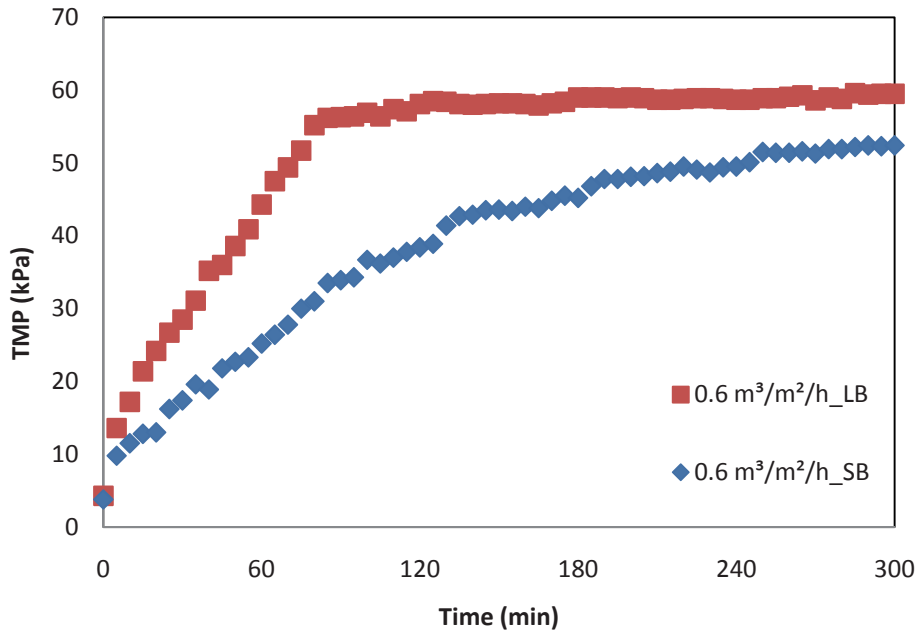

Figure 7.13 Variation of TMP profiles at different air bubble sizes (J = 40 L/m^2/h)

The effect of bubble size in particle deposition (Figure 7.14) was not significant on particle deposition at a higher filtration flux of 40 L/m^2/h. It seems that at higher permeate flux, changing the bubble size at very low air flow (0.6 m^3/m^2/h) was not sufficient to detach the cake layer from the membrane surface, because higher flux produces a high drag force that rapidly draws particles towards the membrane surface, causing very high TMP development and deposition.

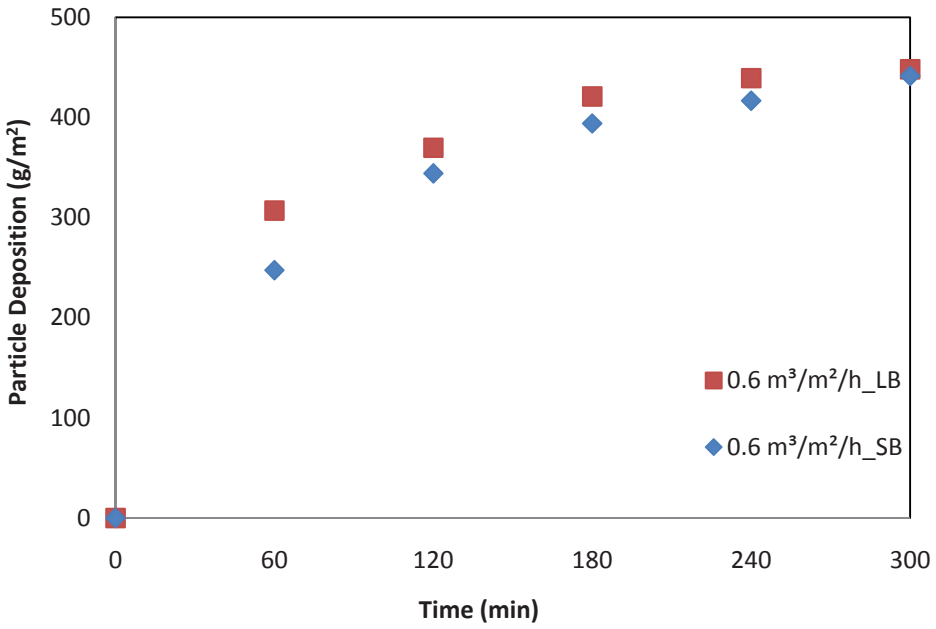

Figure 7.14 Particle deposition at different air bubble sizes (J = 40 L/m^2/h)

Different air flow rates (1.2, 2.4, 3.0 m^3/m^2/h) were applied with small air bubbles only to study the effect of increased air flow with small bubbles. Figure 7.15 demonstrates the TMP with time for different air flow rates. TMP development at 0.6 m^3/m^2/h (54.6 kPa) is far higher than it is at 1.2 m^3/m^2/h (23.2 kPa) after 6 hours of filtration time. An increase in air flow (from 0.6 to 1.2 m^3/m^2/h) resulted in a 12% and 19% reduction of TMP and particle deposition respectively (Figures 7.15 and 7.16). TMP dropped by 33% and 56% when air flow was increased from 0.6 to 0.96 and 1.2 m^3/m^2/h respectively. Increased air flow always reduced TMP development. This result indicates

that small bubbles were more active in scouring especially after a certain period of filtration (i.e. after sufficient deposits were formed on the membrane surface).

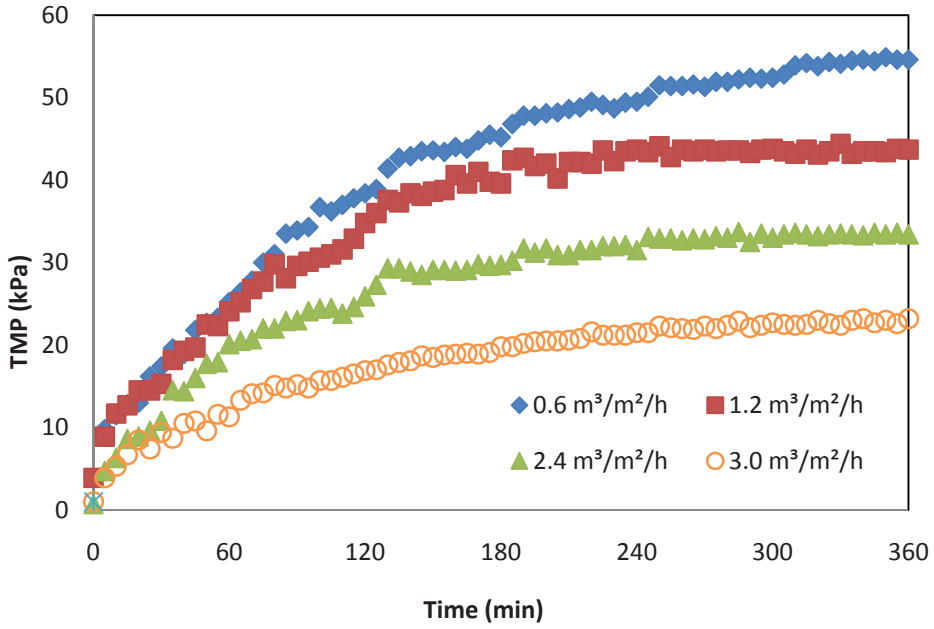

Figure 7.15 TMP profiles at different air flow rates with small air bubble sizes (J = 40 L/m^2/h)

Figure 7.16 describes the variation on particle deposition at different air flow rates. Fouling reductions were 19%, 51% and 54% when the air flow was increased to 1.2, 2.4 and 3.0 m^3/m^2/h from the base flow of 0.6 m^3/m^2/h.

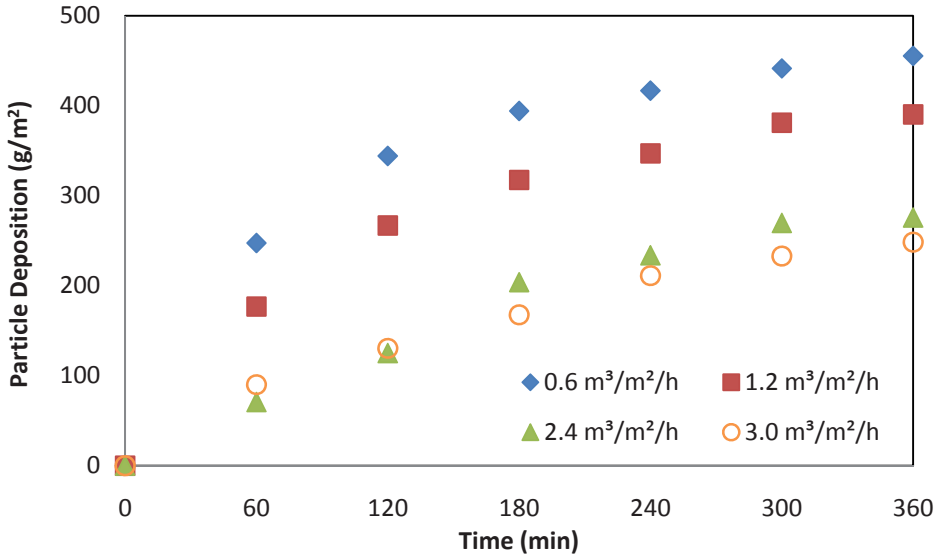

Figure 7.16 Variation of particle deposition at different air flow with small air bubble sizes

The total membrane resistance for 40 L/m^2/h is analysed by plotting the relative resistance between the total resistance and clean membrane resistance (Figure 7.17). The clean membrane resistance was the same for all operating conditions. An increased air flow reduced the total membrane resistance significantly, especially when small air bubbles were employed.

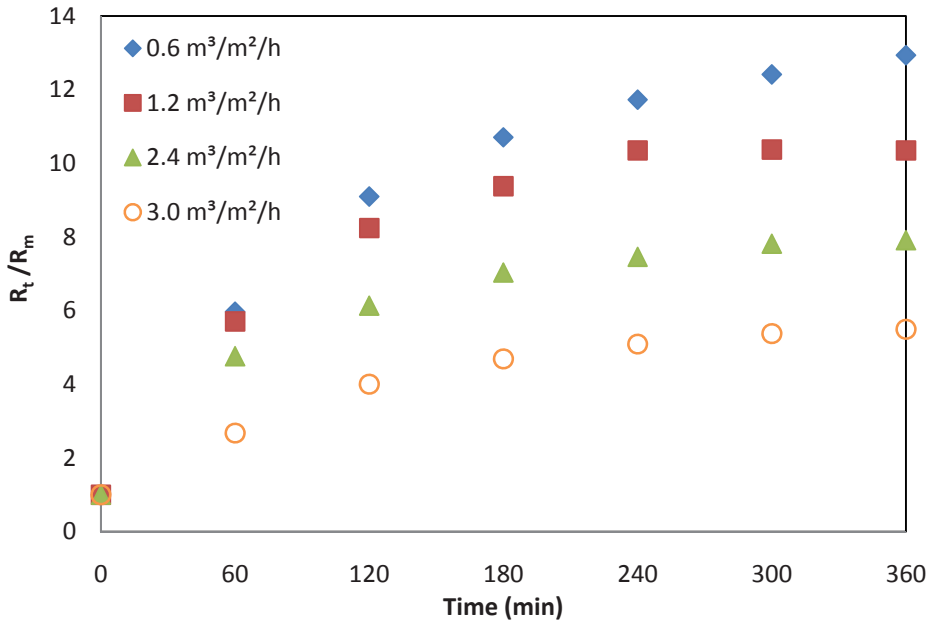

Figure 7.17 Total membrane resistance at different air flow rates

7.3.5 A Permeate Flux of 50 L/m²/h

Experiments were carried out at a very high flux of 50 L/m^2/h. Air flow rates of 0.6 and 1.2 m^3/m^2/h were used with small bubbles only. Only small bubbles were applied to study their effect on TMP and deposition reduction, because large bubbles were found to be less effective in TMP reduction. TMP development at different rates of air flow is presented in Figure 7.18. With small air bubbles, doubling air flow (from 0.6 to 1.2 m^3/m^2/h) reduced TMP and particle deposition by 22% and 19% respectively. Similar to the previous result with 40 L/m^2/h, a very sharp rise in both TMP and particle

deposition (Figure 7.19) were observed within the first hour of filtration. This rapid jump was followed by a steady state where there was no further increase in TMP.

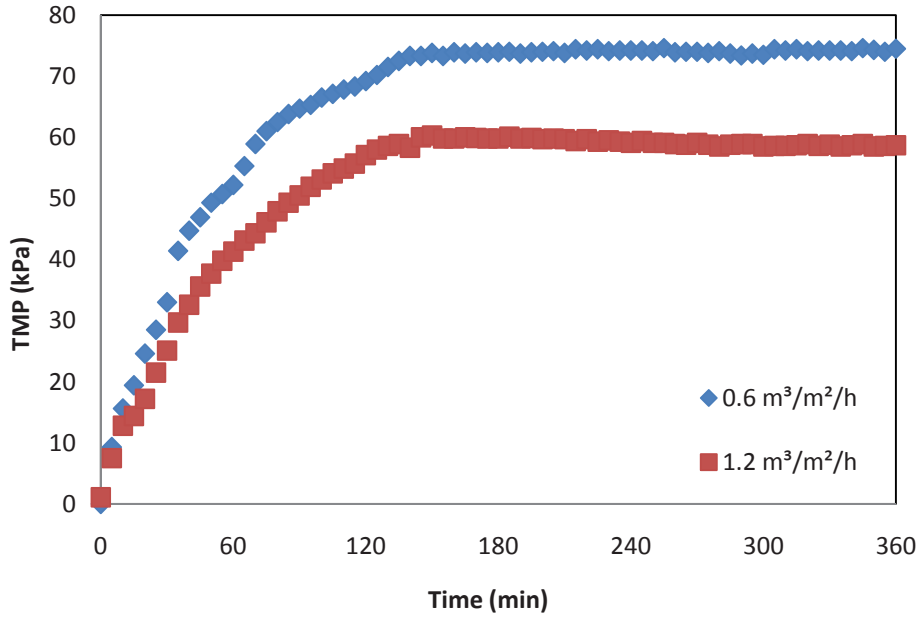

Figure 7.18 Variation of TMP profiles with small air bubbles

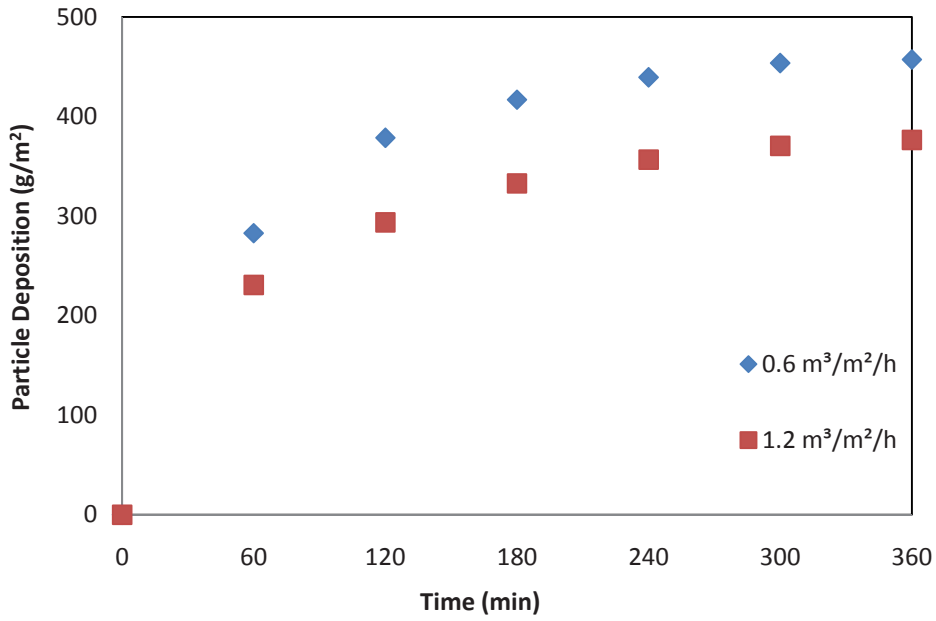

Figure 7.19 Variation of particle deposition with small air bubbles

The total membrane resistance in terms of the ratio of total resistance to clean membrane resistance with small bubbles is presented in Figure 7.20. The total

membrane resistance data followed the same trend as other permeate flux rates (20, 30 and 40 L/m^2/h).

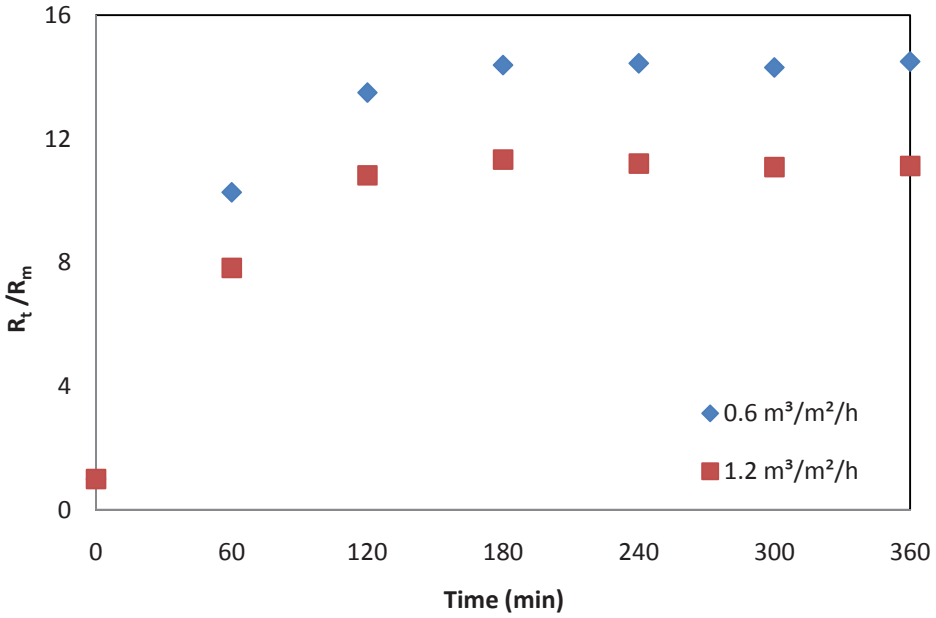

Figure 7.20 Total membrane resistance at small air bubble sizes (J = 50 L/m^2/h)

Tables 7.1 and 7.2 summarise the TMP and fouling reduction under various operating conditions (air flow and bubble size). It is concluded that an increased air flow reduced both TMP and deposition in both experiments (with large and small bubble). Similar results have been reported by other researchers (Cabassud, Laborie & Lainé 1997; Cui, Chang & Fane 2003; Mercier, Fonade & Lafforgue-Delorme 1997). Changing the bubble size (small) by using a different aeration device also resulted in a reduction in TMP rise and deposition.

Table 7.1 TMP reduction under various air flow and air bubble sizes

Flux ($L/m^2/h$)	TMP Reduction (%)				
	Air flow with large bubble ($m^3/m^2/h$)	Air flow with small bubble ($m^3/m^2/h$)	Air flow with large to small bubble ($m^3/m^2/h$)		
	0.6 to 1.2	0.6 to 1.2	0.6 to 0.6	1.2 to 1.2	0.6 to1.2
15	25			62	
20	21	48	50	68	75
30	10	40	35	57	62
40		15	26		34
50		22			

Table 7.2 Particle deposition reduction under various air flow and air bubble sizes

Flux ($L/m^2/h$)	Fouling reduction (%)				
	Air flow with large bubble ($m^3/m^2/h$)	Air flow with small bubble ($m^3/m^2/h$)	Air bubble changed from large to small ($m^3/m^2/h$)		
	0.6 to 1.2	0.6 to 1.2	0.6 to 0.6	1.2 to 1.2	0.6 to 1.2
15	30			61	
20	19	35	39	49	59
30	5	31	10	35	38
40		19			13
50		19			

7.4 Transmembrane Pressure Reduction Factor (TPRF)

To assess insights into the effectiveness of bubble size on TMP development in detail, the TMP reduction factor was computed for different permeate flux rates (Figure 7.21). This figure shows a higher TPRF for low permeate flux at 1.2 $m^3/m^2/h$ of air flow. The TMP reduction factor was calculated as follows:

$$\text{TPRF} = \frac{\text{TMP developed with large bubble}}{\text{TMP developed with small bubble}} \tag{7.7}$$

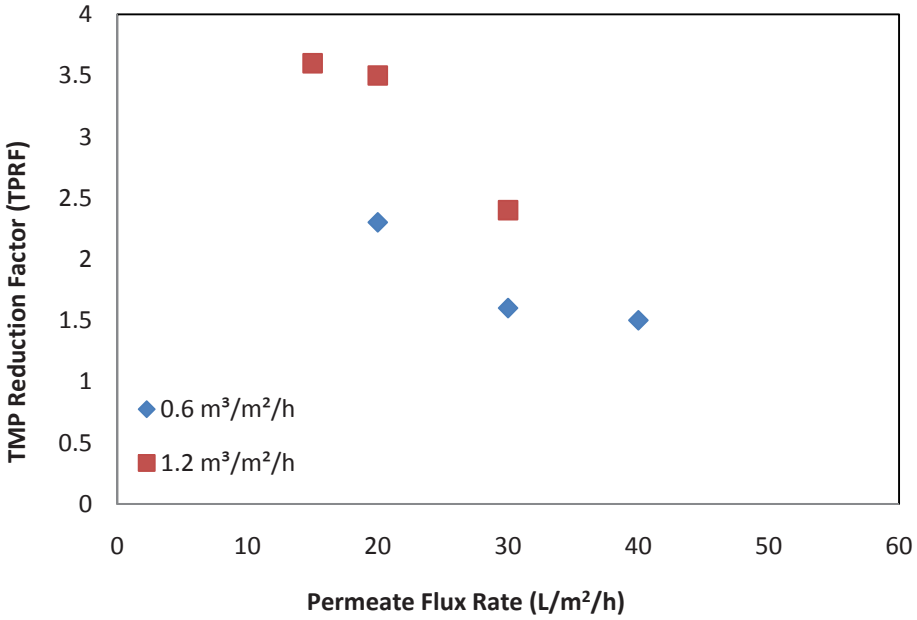

Figure 7.21 TMP reduction factors for different permeate flux rates

7.5 Discussion

Since the mean particle size of kaolin clay is much larger than the pore size of the membrane, the internal fouling due to pore blocking is negligible; hence, membrane fouling is due to particle deposition occurring on the membrane surfaces. This causes TMP development and higher total membrane resistance. An application of air bubbles through the gas-liquid two phase flow has been demonstrated to be an efficient method to reduce membrane fouling. In all experiments (with both large and small bubbles), increased air flow reduced both TMP rise and particle deposition. Cui et al. (2003) has described the reason behind this phenomenon. They identified the fouling mechanism control by bubbles as (i) bubble-induced secondary flow, (ii) physical displacement of the deposited cake layer, (iii) pressure pulsing caused by passing bubbles and (iv) increase in superficial cross-flow velocity. They also reported that large bubbles, or slugs, are more beneficial due to their larger wake regions which produce stronger

secondary flows and are more effective in promoting local mixing, but they did not discuss the detailed effect of air bubble size and frequency on membrane fouling. In addition to air flow (aeration), air bubble characteristics (size, frequency, type etc.) have decisive effects on the membrane fouling control mechanism.

In this study, the experimental results show that small bubbles are more effective than large bubbles for membrane fouling control. Similar results were reported by Sofia et al. (2004). They analysed the cross-flow velocity induced by coarse and fine bubbles in a submerged membrane bioreactor. They concluded that the fine bubbles (small bubbles) appeared to initiate higher cross-flow velocities, and under the same aeration intensity, uniformly distributed fine bubbles provided better fouling control to prolong the membrane operation. Fane et al. (2005) also observed that at the same air flow rate, the smaller bubbles noticeably improved fouling control in submerged hollow fibre systems. Zhang et al. (2009) also suggested that the fine bubbles to be used for aeration. In the case of smaller bubbles, the number of bubbles is greater and they have a higher surface area than larger bubbles, so they produce higher shear stress.

In submerged membrane system, bubble size, frequency and distribution directly affect the hydrodynamics and hence the antifouling behaviour. As the configuration of the flat sheet membrane module is noticeably different from other membrane configurations, such as the tubular and hollow fibre membrane modules, the effect of air flow depends highly on air bubble motion. The bubble size is the main parameter that governs its motion (Malysa, Krasowska & Krzan 2005). The effects of confined bubbles and slugs as observed in a tubular module, and those of less confined bubbles and slugs found in a submerged flat sheet membrane are different (Zhang, Cui & Field 2009). In the tubular system, a slug bubble will cover the entire membrane area, whereas in a flat sheet

system, only a portion of the membrane surface will be in contact with the large air bubble. The flat sheet membrane used in this study consists of eight flat sheets, separated by a gap of 12 mm. An application of small bubble can easily move through these gaps and cover a larger membrane surface, removing the cake layer. As the aerator device used to produce small bubble is circular in shape, bubble production was concentrated at the centre part of the device and the membrane module was placed just above it. The tendency of bubbles to colloid and coalesce was also observed when air flow rate was increased. This eventually led to the formation of slugs, or Taylor bubbles, which occupy almost the entire surface of the membrane. It is well known that slug flow is the most efficient regime for the significant enhancement of flux because it delivers the most effective impact on shear stress to scour and disturb the membrane surface (Cabassud, Laborie & Lainé 1997; Li, Cui & Pepper 1997). Zhang et al. (2009) also found that slug bubbles show better antifouling performance in flat sheet MBR at high flux operation. Therefore, it is concluded that in this study, slug formation in small bubble air flow (especially at higher rates of air flow) is responsible for low membrane fouling (TMP development, particle deposition, total membrane resistance). With the increase in air flow, the circular aerator (with small air pore) produced more bubbles, with very high bubble density. Thus the deposited cake layers were scoured and transported back to the tank. In the case of large bubbles, free bubbles were generated through the square aerator plate.

7.6 Conclusions

The performance of a submerged flat sheet membrane system is highly affected by the geometry of the air diffuser device that generates different sizes of air bubbles. An enhanced reduction in TMP and particle deposition was observed with a circular air diffuser plate that produces small bubbles, compared to the square air diffuser plate that

produces larger air bubbles for all employed permeate flux and air flow rates. Fouling was reduced by 19% at a permeate flux of 20 L/m^2/h when air flow was doubled (from 0.6 to 1.2 m^3/m^2/h) with large bubbles, i.e. the square aerator plate, while with small bubbles (circular aerator), a 35% fouling reduction was achieved for the same operating condition, doubling air flow from 0.6 to 1.2 m^3/m^2/h. Similarly changing the aerator plate at different air flow rates significantly improved fouling reduction. When the aerator was changed from square to circular, the particle deposition was observed to be less by 39% and 49% for 0.6 and 1.2 m^3/m^2/h air flow rates respectively.

It can be concluded that a change in the design of the aerator plate and air bubble size can play an important role in controlling membrane fouling. Based on the analysis of TMP and particle deposition reduction, the most effective operating condition was suggested at a permeate flux rate of 20 L/m^2/h and air flow rate 1.2 m^3/m^2/h with a circular aerator (for kaolin clay suspension and tank configuration). It should be noted that the situation would be different in the pilot scale unit compared to lab scale experiments. The size of the bubbles is the same in the lab scale experiments as it would be at full scale, but the size of the modules should be different and air bubbles should be produced ascending in a channel of 12 mm width (flat sheet membrane). For this reason, the conclusion concerning the greater efficiency of small bubbles with a circular aerator should be confirmed in a pilot scale experiment. However, such extensive efficiency of small bubbles has been reported previously by a number of researchers (Fane et al. 2005; Sofia, Ng & Ong 2004).

Chapter 8

Assessment of fouling behaviour during microfiltration coupled with flocculation in submerged flat sheet system

Abstract

Microfiltration coupled with flocculation has the potential to remove colloidal and dissolved matter and hence mitigate membrane fouling. This study investigates the effects of flocculation on the performance of a submerged membrane microfiltration of kaolin suspension. The addition of flocculant (ferric chloride: $FeCl_3$) demonstrated better control of colloidal membrane fouling. The experimental results showed that TMP development at optimal flocculant concentration (75 mg/L) was significantly less than it was with unflocculated feed. In the case of 30 $L/m^2/h$, TMP was reduced by 85% at this optimum concentration of flocculant and air flow of 1.0 $m^3/h/m^2$. The increase in particle size by the combined flocculation and microfiltration process reduced the rise of TMP. A regression analysis conducted between cake resistance and particle deposition showed low specific cake resistance with an increased concentration of flocculant. The results indicate that flocculation modified the cake properties (cake structure, porosity, compactness) which reduced membrane fouling.

8.1 Introduction

Membrane fouling is considered to be an impediment to the widespread adoption of microfiltration in the water treatment industry. Although the detailed mechanisms of fouling are not well understood at present, practical experience and research works indicate that the problem is associated with the presence of dissolved organic materials and small colloidal particles in wastewater. Matsumoto et al. (1988) speculated that

significant fouling was due to colloids in cross-flow microfiltration units. The membrane fouling process is widely recognised as being responsible for flux decline impeding the performance of the whole filtration system.

To mitigate membrane fouling and enhance the permeate flux (system performance), a number of different approaches have been pursued. These include (a) chemical, (b) hydrodynamic, and (c) physical (Belfort et al. 1994) approaches. Chemical methods involve the modification of the membrane surface chemistry to increase the repulsion between the membrane and the particulate available in the feed suspension. This increased repulsion causes less deposition and results in less membrane fouling. Hydrodynamic methods consist of the application of secondary flow to produce turbulence in the membrane module and/or the reactor tank, such that deposited particles on the membrane surface are transported back to the tank. While chemical and hydrodynamic approaches focus on changes to the membrane properties and the operating conditions of the filtration system respectively, physical methods involve the pretreatment of the feed solution. Pretreatment of biologically treated sewage effluent prior to its application to the membrane processes will reduce cell deposition and subsequent bio-growth due to dissolved organic matter (Redondo & Lomax 2001). Pretreatment also reduces the need for frequent chemical cleaning, which is a major factor impacting membrane life. Pretreatment offers considerable potential for improving the efficiency of membrane processes, and different types of pretreatment methods are described in the literature. Each method has advantages and disadvantages. For instance, physico-chemical treatment produces a considerable amount of sludge but takes a shorter time, while biological processes take longer but have a lower operational cost. This study focuses on a physico-chemical treatment methods, of which a popular method is coagulation and flocculation.

In the coagulation-flocculation process, external agents (chemical) are added to the feed suspension to facilitate the agglomeration of fine particles and colloids into larger particles so that they can be easily separated from the liquid, Coagulation and flocculation constitute essential processes in the most water and advanced wastewater treatment plants. The objective is to enhance the separation of particulates in downstream processes such as sedimentation and filtration. Colloidal particles and other finely divided matter are brought together and agglomerate to form larger particles that can subsequently be removed more easily. The traditional use of coagulation has been primarily to decrease the turbidity of potable water. In-line coagulation refers to the dosing of coagulant into feed water with rapid mixing, allowing flocs to form but not to settle, and finally feeding the resulting water with flocs for microfiltration or ultrafiltration. In-line coagulation, therefore, involves the use of flocculants without the removal of coagulated solids prior to the filtration process. The coagulation process deals with the destabilization of colloidal particles, usually of sub-micron size, that are often encountered in water and wastewater treatment (Johnson & Amirtharajah 1983). During this process, colloids keep changing chemically and overcome the forces maintaining the stable suspension, promoting aggregation and the formation of larger particles called floc. Removal is accomplished through a series of destabilization and precipitation processes; (1) compression of the diffusion layer, (2) adsorption to produce charge neutralization, (3) enmeshment in precipitate, and (4) adsorption to permit inter-particle bridging (Duan & Gregory 2003; Johnson & Amirtharajah 1983).

In the operation of membrane separation systems, membrane fouling is dependent on many parameters such as membrane characteristics, source or feed water characteristics, and the operating conditions of the system. Among them, organic materials contained in wastewater effluent, designated as effluent organic matter (EfOM) such as refractory

natural organic matter (NOM), synthetic organic compounds (SOC) and DBP, and soluble microbial product (SMP), are considered important foulants that play a crucial role in membrane fouling (Jarusutthirak, Amy & Croué 2002). Moreover, many researchers have found that hydrophobic portion such as proteins, polysaccharides, and humic acids are mostly responsible for membrane fouling. Therefore, coagulation can be used to reduce the fouling of membranes because it preferentially removes the hydrophobic organic matter present in water (Liang & Singer 2003).

Similarly, Haberkamp et al. (2007) observed that the most severe fouling from colloidal and dissolved organic substances occurs during membrane ultrafiltration in tertiary treatment. A number of researchers have focused on the identification of the constituents of colloidal matter and dissolved organic matter that most severely contribute to membrane fouling. Lee et al. (2007) observed colloids in the size range of 0.2-1.2 μm as being the most significant particle size range to cause fouling during the microfiltration of secondary effluent. Previous researchers (Huisman, Tragardh & Tragardh 1999; Tanaka et al. 1994; Wickramasinghe 1999) have reported that the presence of smaller particles results in flux decline for poly-dispersed feeds during microfiltration. Foley et al. (1992) studied the particle size distribution of yeast cells in the retentate during microfiltration and found that the smaller cells in suspension preferentially deposited on the membrane surface.

Previous studies have shown that the use of flocculants/coagulants in a feed suspension prior to microfiltration can enhance system performance, leading to an improved permeate flux (Kim, Akeprathumchai & Wickramasinghe 2001a; Peuchot & Ben Aim 1992; Wickramasinghe, Wu & Han 2002). Fan et al. (2007) suggested that this effect is due to the aggregation of colloidal and dissolved matter into particles that are too large

to cause pore narrowing and pore plugging. Moreover, Cho et al. (2006) also indicated that the coagulation-microfiltration system has the potential to remove natural organic matter and reduce membrane fouling. They observed higher flux during microfiltration with longer flocculation times, due to the formation of loose and porous flocs and the reduction of small colloidal particles.

The study investigates the fouling behaviour of kaolin clay acting as colloidal particles during flat sheet membrane microfiltration coupled with direct and in-line flocculation. The flocculant used in this study was ferric chloride ($FeCl_3$). The impact of the addition of flocculant was evaluated by examining the development in TMP and particle deposition at particular time of microfiltration. The study also considered the effects of air flow during in-line coagulation-microfiltration.

8.2 Materials and Method

8.2.1 Materials

(a) Flocculant: Primary flocculants are lime, aluminium sulfate (alum), ferrous sulfate, ferric sulfate and ferric chloride. In this research, ferric chloride ($FeCl_3$) was used as the flocculant. A laboratory reagent, ferric chloride anhydrous, was used. Table 8.1 presents the specification of ferric chloride used in this study.

(b) Feed material: Small colloidal particles have been identified as the principal cause of membrane fouling; therefore, clay particles (often present in surface water) were selected as a model contaminant. The feed solution was prepared from commercially available kaolin clay (Sigma) which was dissolved in tap water to a concentration of 10 g/L. The detailed characteristics of kaolin clay were described in Chapter 3 (refer to section 3.2.2).

Table 8.1 Specification of ferric chloride

Properties		Impurities (maximum level)	
Appearance	Black-brown power	Arsenic	0.001%
Chemical Formula	$FeCl_3$	Copper	0.1%
Molecular Weight	162.21	Manganese	0.3%
ASSAY	98.7%	Lead	0.02%
Melting point	~300 ˚C	Zinc	0.1%
Boiling point	~316 ˚C		
Density	2.898		

8.2.2 Method

Submerged membrane microfiltration coupled with batch and in-line flocculation was separately conducted to investigate the fouling behaviour of kaolin particles in an aerated reactor tank. Prior to these experiments, jar tests were carried out to determine the optimum dose of the flocculant. Six different jars with kaolin clay suspension of 1 L at a concentration of 10 g/L were used with different concentrations of coagulant ($FeCl_3$). The standard test involved 1 minute rapid mixing at 100 rpm (revolutions per minute) and 20 minutes slow mixing at 25 rpm, followed by quiescent settling. After 30 minutes of settling, the turbidity, suspended solids and pH were measured. Based on the turbidity, suspended solids and pH value, the optimum dose of $FeCl_3$ was determined as 150 mg/L.

8.2.2.1 Batch Flocculation-Microfiltration Test

Batch flocculation experiments were conducted using flat sheet membrane in a submerged microfiltration system. A flat sheet membrane with pore size 0.14 μm and effective area 0.2 m^2 was submerged into the reactor tank of full 12 L capacity. Ferric

chloride (1% of $FeCl_3$ Anhydrous) was used as a flocculant. Before the start of the experiment, different doses of $FeCl_3$ were directly added to the process tank filled with feed suspension which was prepared from kaolin at 10 g/L concentration. Sufficient time (15-20 minutes) was allowed for flocculation. A gentle mixing stage was achieved with the application of a nominal air flow rate (1.0 $m^3/m^2/h$). During flocculation, the particle size increased from submicroscopic micro-floc to visible flocs. The schematic diagram of the experimental set-up of the batch flocculation-microfiltration test is shown in Figure 8.1.

Batch filtration of flocculated suspension was performed under different permeate flux rates (30, 60 and 90 $L/m^2/h$). Flocculant was added to the suspension only once, prior to commencing the experiment. The permeate flux was extracted through a peristaltic pump and returned to the reactor tank to maintain a constant concentration. TMP was continuously monitored online and stored in a data logger which was later downloaded to a computer. Samples from the suspension tank were collected at hourly intervals.

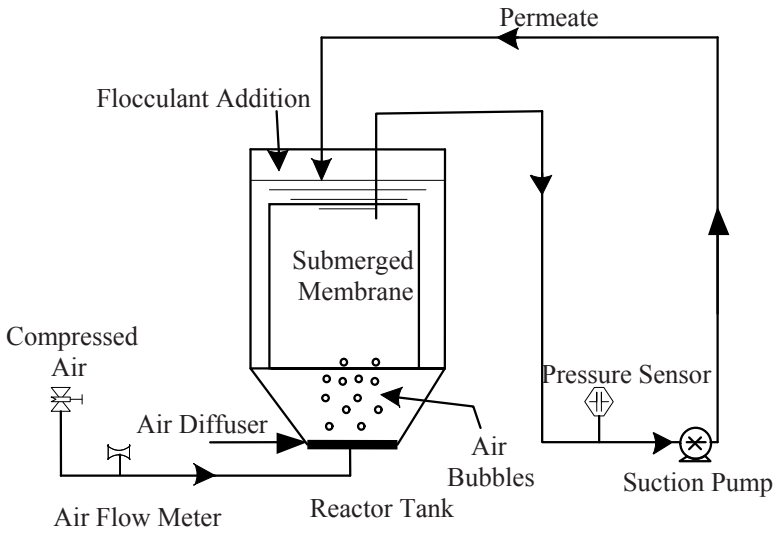

Figure 8.1 Schematic diagram of experimental set-up of batch flocculation-microfiltration test

8.2.2.2 In-Line Flocculation - Microfiltration Test

In-line flocculation coupled with microfiltration were carried out for different permeate flux rates of 15, 30 and 50 L/m^2/h with the optimum dose (150 mg/L) of $FeCl_3$. The experiments were operated in constant-flux mode. The membrane used in this experiment was the same as that used in the previous experiment (batch flocculation-microfiltration). Ferric chloride ($FeCl_3$) was used as flocculant. A feed suspension was prepared by mixing kaolin clay (Sigma) in tap water to a concentration of 10 g/L. A stock solution of flocculant was made by adding the calculated quantity of flocculant in distilled water.

The kaolin suspension (10 g/L) was poured into the reactor tank and the predetermined quantity of flocculant was added to the tank to achieve the required concentration. Air bubbles (2-4 mm in size) were continuously supplied from the bottom of the tank to prevent the floc from settling. Sufficient time (15-20 minutes) was allowed for mixing and floc formation. Kaolin feed and stock solution of the flocculant were continuously fed into the reactor after performing rapid mixing of feed and flocculant. Peristaltic pumps were used to control the feed and stock solution rates. Trans-membrane pressure (TMP) was continuously monitored online by a pressure transducer and stored in a data logger. The experimental set-up is shown in Figure 8.2. Samples from the reactor tank were collected at regular intervals (hourly) to determine the particle deposition. Permeate was withdrawn from the membrane module through a pump and discharged into a drain.

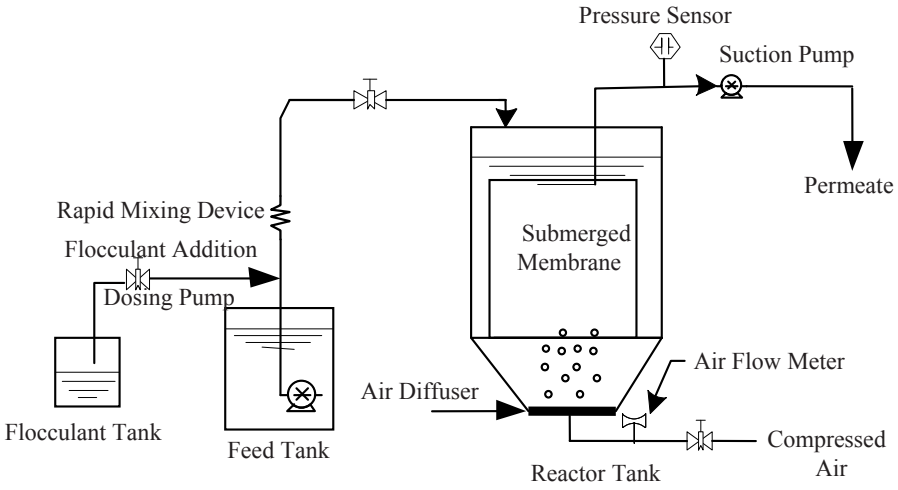

Figure 8.2 Schematic diagram of experimental set-up of in-line flocculation-microfiltration test

The optimum dose for $FeCl_3$ was found from the jar test to be 150 mg/L. With this optimum dose, in-line flocculation-microfiltration experiments were performed for different permeate flux rates (15, 30 and 50 L/m^2/h). Air flow was supplied at a rate of 1.2 $m^3/m^2/h$ for the permeate fluxes of 15 and 30 L/m^2/h, whereas a lower air flow rate of 0.6 $m^3/m^2/h$ was applied for a flux of 50 L/m^2/h. No TMP development was observed in any of the three throughout the test period, therefore in-line flocculation microfiltration tests (described earlier) were carried out at different doses of flocculants ($FeCl_3$; 20, 50, 60, 75, 100 mg/L) to directly determine the optimum dose from the in-line flocculation membrane system. These experiments were performed for a flux rate of 30 L/m^2/h and air flow rate of 1.5 $m^3/m^2/h$.

The short runs of in-line flocculation microfiltration established a new value of optimum dose i.e. 75 mg/L for $FeCl_3$. With this new optimum dose, similar experiments were conducted for a long period under various air flow rates (0.5, 1.0 and 1.5 $m^3/m^2/h$) at a flux of 30 L/m^2/h.

8.2.2.3 Determination of Particle Deposition

Two methods were used to determine particle deposition on the membrane surface. First, turbidity values were measured during the filtration test (at hourly intervals) and particle depositions were indirectly calculated from the balance of material. Second, the weight of clay particles available in a tank at specific times was directly determined by the oven dry method (gravimetric method). In this method, a predetermined volume (30 ml) of sample collected every hour was placed inside the oven to obtain the dry weight of the clay. These values were used to calculate particle deposition on the membrane surface. Figure 8.3 compares the particle deposition obtained by the above mentioned methods for a permeate flux of 60 L/m^2/h at a flocculant dose of 75 mg/L. Similarly, Figure 8.4 presents the particle deposition on the membrane surface for 90 L/m^2/h for a flocculant dose of 60 mg/L and air flow 1.0 m^3/m^2/h. There was good agreement between the values from both methods.

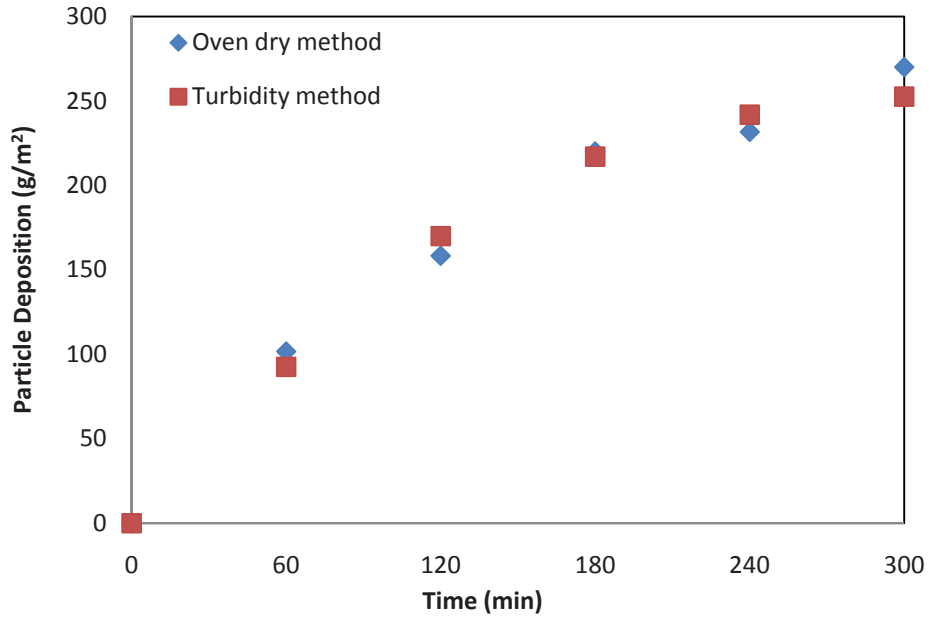

Figure 8.3 Particle depositions from two methods at 60 L/m^2/h and 1.0 m^3/m^2/h air flow rate ($FeCl_3$ = 75 mg/L)

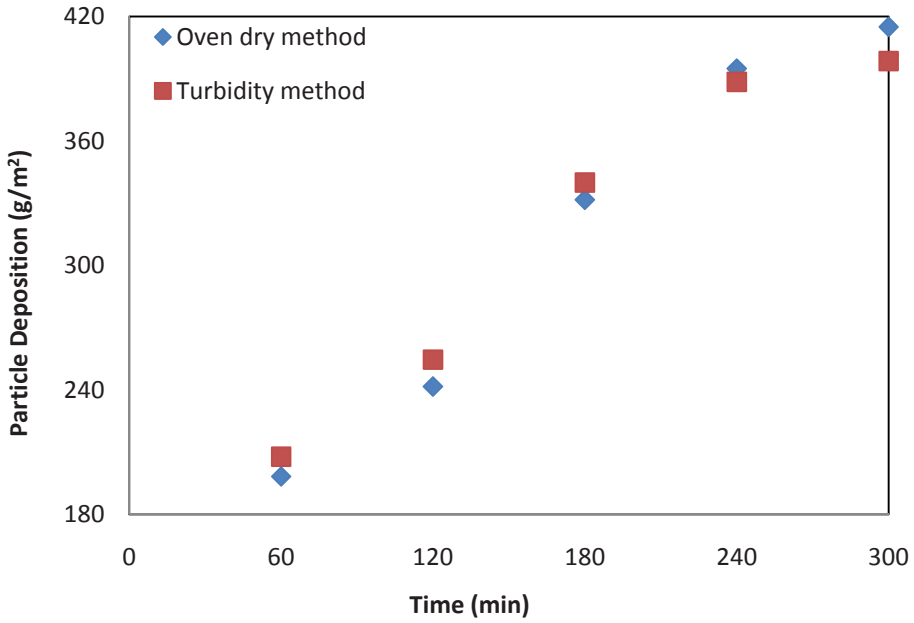

Figure 8.4 Particle depositions from two methods at 90 L/m^2/h and 1.0 m^3/m^2/h air flow rate ($FeCl_3$ = 60 mg/L)

8.3 Results and Discussion

To assess the impact of flocculant addition on membrane fouling, two parameters were considered: TMP and particle deposition. The optimum doses of flocculants were established based on the analysis of TMP development during operation. The pressure development and particle deposition during batch flocculation experiments were analysed to evaluate the effect of different doses of ferric chloride on fouling for different permeate flux rates. Membrane fouling for flocculated solution under different rates of air flow was also investigated through an in-line flocculation microfiltration test.

8.3.1 Batch Flocculation-Microfiltration Test

Different permeate flux rates (30, 60 and 90 L/m^2/h) were employed to investigate the impact of flocculant on membrane fouling during batch flocculation coupled with microfiltration. This section separately describes the influence of different doses of

flocculant on TMP and particle deposition during the batch flocculation-microfiltration test for different flux rates.

8.3.1.1 A Permeate Flux of 30 L/m²/h

Figure 8.5 shows the TMP profiles at 30 L/m^2/h with different doses of $FeCl_3$. The TMP development was significantly reduced in the presence of $FeCl_3$. A 50 mg/L dose of $FeCl_3$ reduced TMP development by 30% compared to rise in TMP without flocculant but at a higher dose of 75 mg/L, TMP growth was almost nil (87% reduction compared to unflocculated feed) for a flux of 30 L/m^2/h and air flow rate 1.0 m^3/m^2/h.

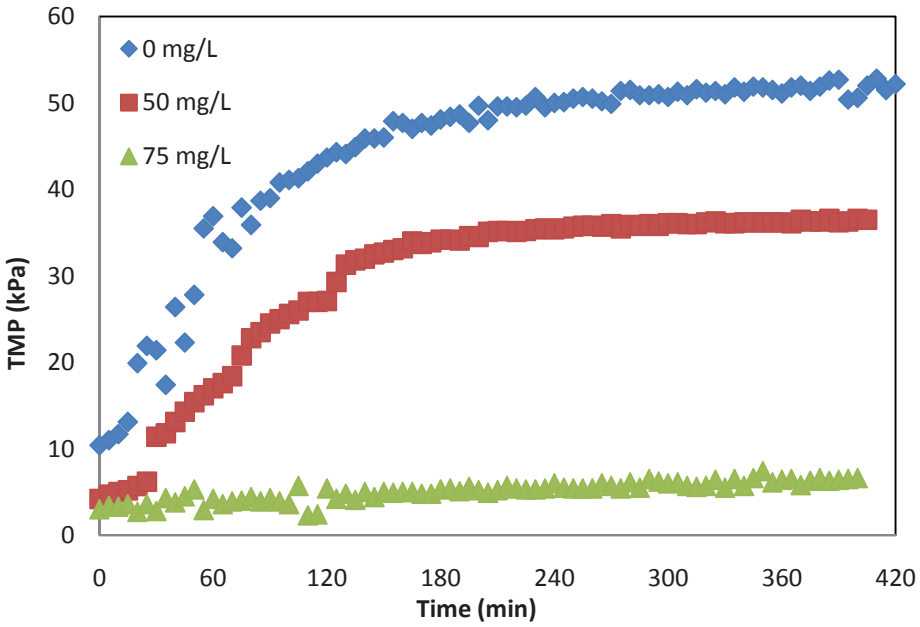

Figure 8.5 Impact of flocculant ($FeCl_3$) on TMP development at air flow rate of 1.0 m^3/m^2/h (J = 30 L/ m^2/h)

At this permeate flux, a sharp difference in TMP increase was noticeable during the initial period of filtration (up to 120 minutes). This was probably related to the deposition of fine particles available in the non-flocculated suspension and to a lesser extent to the suspension flocculated at a dosage that did not correspond to the optimum (50 mg/L). Mietton-Peuchot and Ben Aim (1992) also reported that fouling in cross-

flow filtration is principally caused by fine particles. Flocculation increases the particle size and improves the permeate flux. In the absence of flocculant ($FeCl_3$), or at a low dose, filtration forces attract small particles to form a compact cake which directly raises TMP values. The addition of a flocculant increases the size of particles by forming large flocs which may not clog membrane pores. After this sharp rise, TMP increased slowly for another hour, after which a steady state was observed for both conditions (low dose and without flocculant). Figure 8.6 shows the TMP development after saturation (after 180 minutes). In all the conditions studied, the rate of change of TMP (dP/dt) was almost the same.

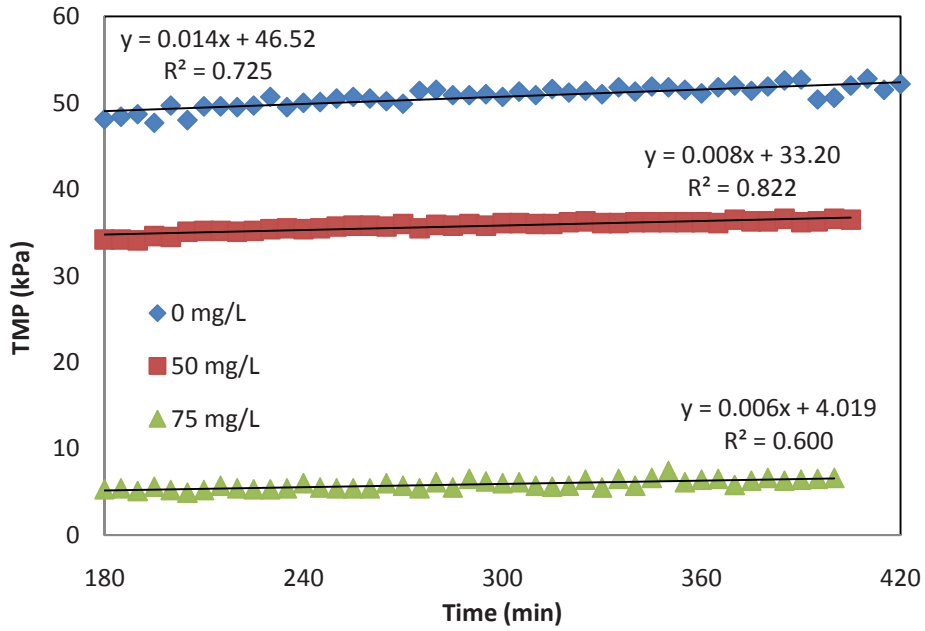

Figure 8.6 TMP variations after 180 minutes of filtration

Figure 8.7 presents the particle deposition at different flocculent doses of $FeCl_3$ at 30 $L/m^2/h$. In the event of a rise in TMP (Figure 8.6), increasing the flocculent dose significantly reduced the TMP, but similar results were not observed for particle deposition. Only small reductions in particle deposition were observed. From Figure 8.7, it can be seen that the addition of 50 and 75 mg/L of $FeCl_3$ had almost the same

deposition pattern, which was slightly less than the particle deposition without $FeCl_3$. A possible reason for this could be the formation of a very porous cake layer which could lead to a higher deposition but not a higher rise in TMP. The larger flocs create more porous cake on the membrane surface that may act as a dynamic membrane, resulting in fouling reduction (Wiesner, Tarabara & Cortalezzi 2005).

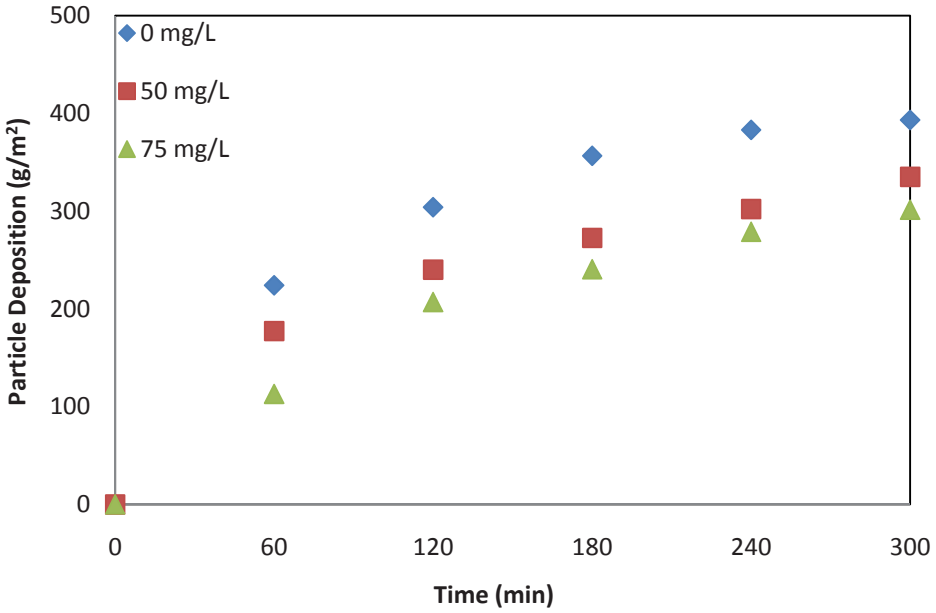

Figure 8.7 Impact of flocculant ($FeCl_3$) on particle deposition at a flux of 30 L/m^2/h and air flow rate of 1.0 m^3/m^2/h

The particle deposition profiles followed the trend in TMP development, as shown in Figure 8.5. The initial sharp rise in particle deposition is due to the abrupt increase in TMP and is caused by the deposition of finer particles on the membrane surface. Figure 8.8 shows the particle deposition trends after saturation state (after 180 minutes). This figure presents the slopes of particle deposited vs. time but only in the final period of filtration when this variation may be considered as linear (for instance, from time 180 to 420 minutes).

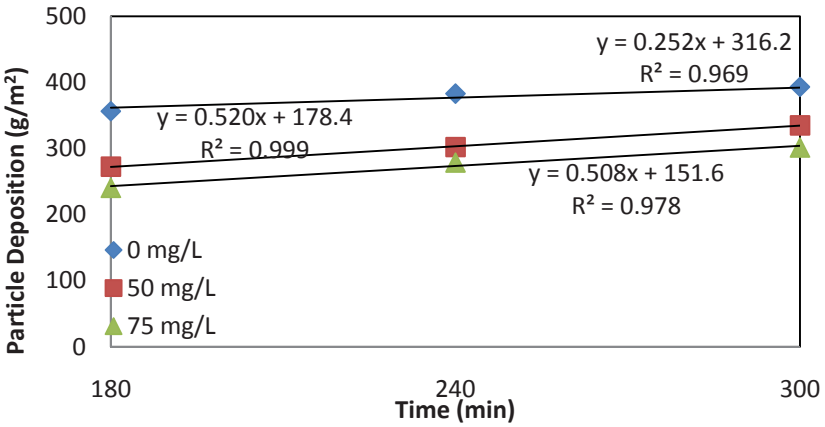

Figure 8.8 Particle deposition variation after 180 minutes of filtration

A calculation was also made to see whether the quantity of ferric hydroxide in the tank was of the same order of the quantity of kaolin clay suspension used. When Fe (III) salts are dissolved in water, the metal ion hydrates, coordinating six water molecules and forms an aquometal ion, $Fe(H_2O)_6^{3+}$. The aquometal ion can then hydrolyse and form monomeric and polymeric ferric species (Morel & Hering 1993). In general, the hydrolysis reactions of Fe(III) in aqueous solution can be written as:

$$xFe^{3+} + yH_2O = Fe_x(OH)_y^{(3x-y)+} + yH^+ \quad (8.1)$$

Based on this chemical reaction, the mass of ferric hydroxide was calculated. At a dose of 75 mg/L $FeCl_3$, the mass of ferric hydroxide formed was 0.493g and thus the amount is negligible compared to the mass of kaolin particles available in the tank (100 g).

During filtration, the hydraulic resistance of the membrane increases with the rate of particle deposition. The resistance due to deposited particles (R_c) is calculated using Darcy's equation:

$$R_c = R_t - R_m = \frac{\Delta P}{\mu J} - R_m \quad (8.2)$$

The resistance due to pore blocking was considered to be negligible because the kaolin particles were much larger than the pore size of the membrane. It is therefore possible to determine cake resistance by deducting the clean membrane resistance (R_m) from the total resistance (R_t). The clean membrane resistance was 3.8 x 10^{11} m^{-1}. Table 8.2 presents the average value of the specific resistance at the end of the experiment (after the same given time of filtration) for the 3 different dosages of coagulant (0, 50, 75 mg/L). The effect of the flocculant dose and filtration time on specific resistance can be accessed from this table.

Table 8.2 Average value of the specific resistance (α_{av}) x 10^{12} (m/kg)

	Concentration of $FeCl_3$ (mg/L)		
Operating Time (h)	0	50	75
After 1st hour	18.06	9.35	1.09
After 5th hour	15.67	11.9	1.16

Figure 8.9 shows the relationship between cake resistance and particle deposition. This relationship was regressed to calculate the value of specific filtration resistance (α_{av}) in the equation $R_c = \alpha_{av} w_c$, where w_c stands for particle deposition. The regression analysis clearly demonstrated a reduction in specific resistance with the addition of flocculent (Figure 8.9). A higher dose of flocculent resulted in higher reductions in specific resistance. The value of specific resistance was reduced by a factor of 10 for flocculated suspension with a dose of 75 mg/L.

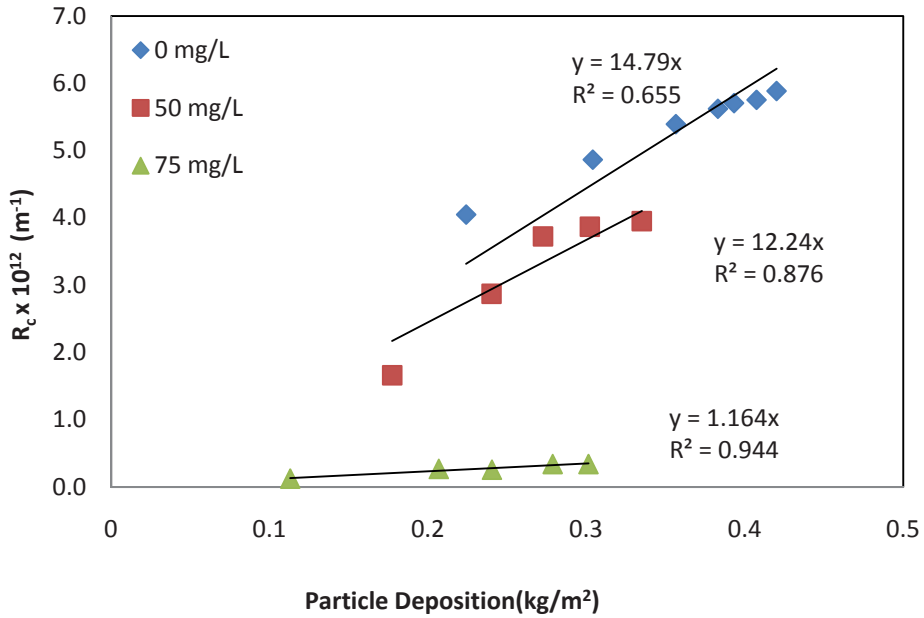

Figure 8.9 Relationship of cake resistance and particle deposition at different doses of $FeCl_3$

8.3.1.2 A Permeate Flux of 60 L/m²/h

In the case of a permeate flux of 60 L/m^2/h, three flocculants doses (20, 40 and 75 mg/L) were applied. The highest TMP growth was observed without $FeCl_3$ and a very small TMP rise was observed at the high dose of 75 mg/L (Figure 8.10). An addition of 40 mg/L $FeCl_3$ reduced the TMP by 37% compared to an unflocculated feed. There was an 86% reduction in TMP with the flocculent dose of 75 mg/L compared to the unflocculated feed.

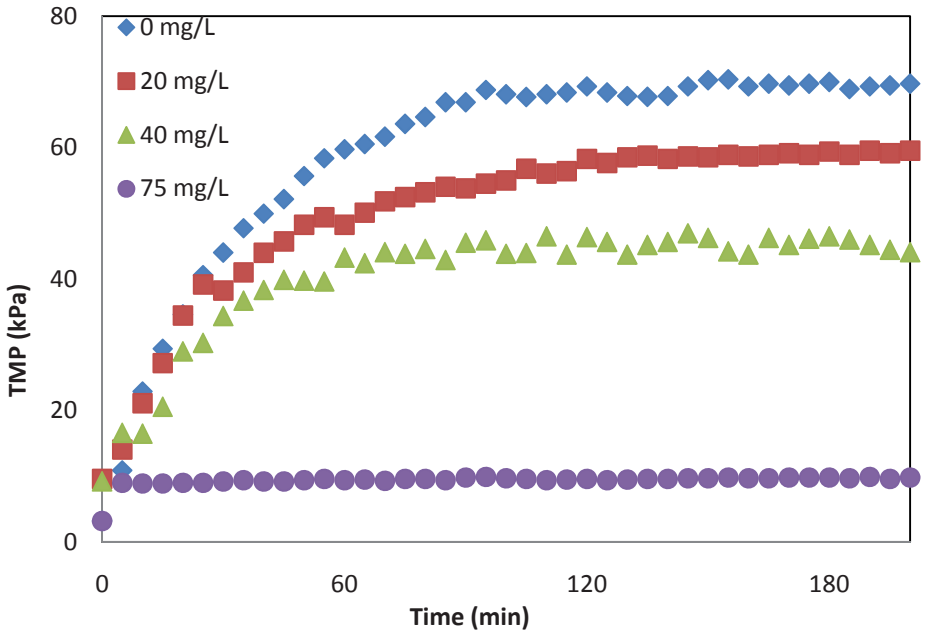

Figure 8.10 Impact of flocculant ($FeCl_3$) on TMP development at a flux of 60 L/m^2/h and air flow rate of 1.0 m^3/m^2/h

Figure 8.11 shows the particle deposition at different doses of $FeCl_3$. The addition of flocculant caused a reduction in deposition. There was no significant reduction at small doses of $FeCl_3$ (20 and 40 mg/L) but at a dose of 75 mg/L, 50% fouling reduction was achieved compared to an unflocculated feed. The TMP development at this dose (75 mg/L) was very minimal (Figure 8.10) but the particle deposition was significantly higher than the rise in TMP. The probable reason for this disproportional relation of TMP rise and particle deposition may be the formation of a very loose or porous cake layer. Another possible reason could be the insufficient drag force available to attach larger particles onto the membrane surface, because the addition of larger doses of the flocculent caused the formation of larger flocs of kaolin particles; however, filtration forces were not analysed in this study. A significant quantity of kaolin particles were observed on the membrane surface during membrane cleaning at the end of the filtration test with the flocculant dose of 75 mg/L.

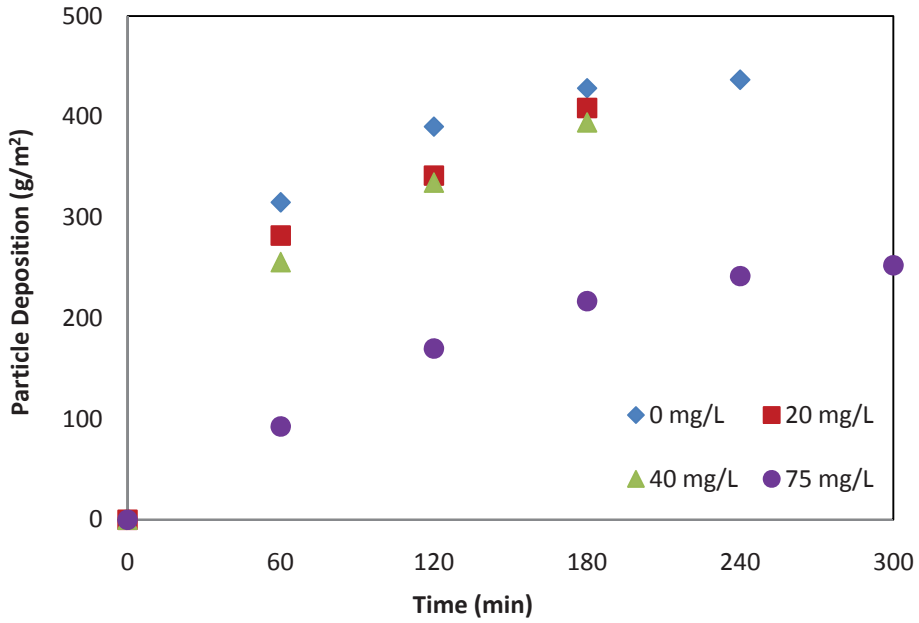

Figure 8.11 Impact of flocculant ($FeCl_3$) on particle deposition at a flux of 60 L/m^2/h and air flow rate of 1.0 m^3/m^2/h

The relationship was established between the cake resistance (R_c) and particle deposition (w_c) (Figure 8.12). This relationship was regressed to determine the specific resistance (α_{av}) for different doses of flocculant ($FeCl_3$). The specific resistance was derived from Figure 8.12 by comparing regression equations with the general relationship of $R_c = \alpha_{av} w_c$. An addition of flocculant substantially reduced the value of specific filtration resistance. A larger dose of flocculant reduced the specific resistance. Figure 8.13 shows the dependence of specific resistance on the concentration of flocculant and indicates that the specific resistance was highest with a low concentration of flocculant or with no flocculant. This is because the formation of large flocs at high concentrations of flocculant caused a reduction in both TMP and particle deposition.

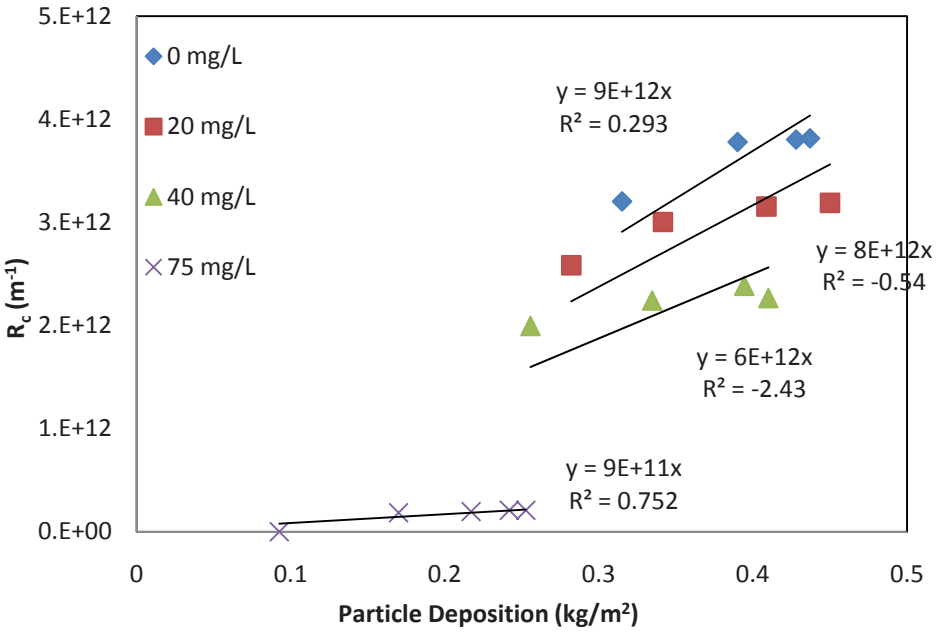

Figure 8.12 Relationship of cake resistance and particle deposition at different concentrations of flocculant (J = 60 L/m^2/h)

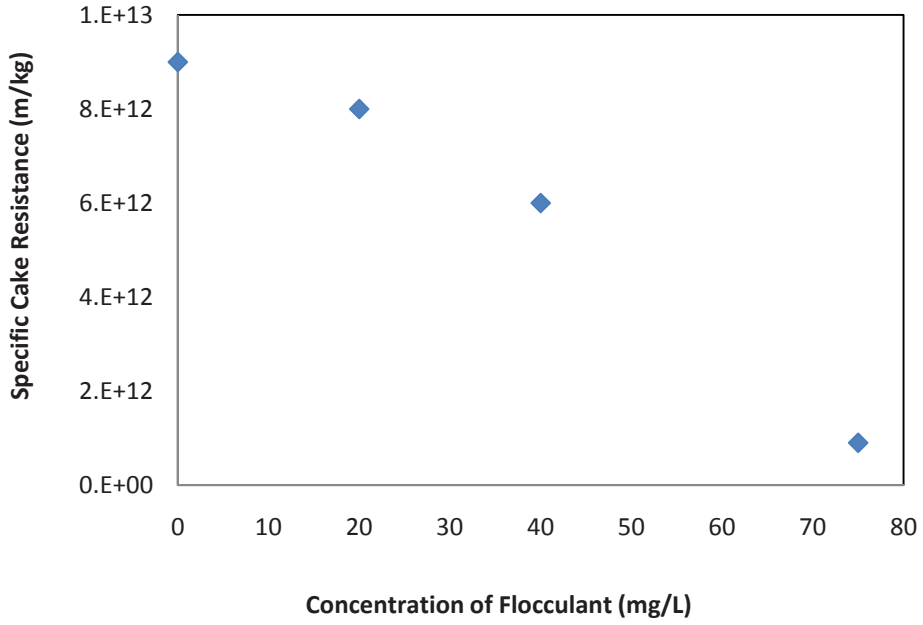

Figure 8.13 Decrease in specific cake resistance (α_{av}) with an increase of flocculant concentration (J= 60 L/m^2/h)

8.3.1.3 A Permeate Flux of 90 L/m^2/h

Four different doses (20, 40, 50 and 60 mg/L) were used to investigate the effect of flocculant ($FeCl_3$) on the TMP and particle deposition for a high permeate flux of 90 L/m^2/h. Figure 8.14 shows the TMP profiles for different concentrations of flocculant

over a period of three hours. These TMP profiles, without flocculant and with low doses of flocculant, are different from those obtained with a permeate flux of 60 L/m^2/h (Figure 8.10) and 30 L/m^2/h (Figure 8.5). Contrary to the three stages of TMP development with time (sharp rise, slow rise and steady state) as seen with other permeate flux, only two stages (sharp rise and steady stage) were observed at this high flow rate. When no flocculant or low doses of flocculant were used, the TMP jumped rapidly within an hour and reached saturation conditions. The increase in TMP with time is due to particle deposition on the membrane. An increased dose of flocculant limited the rise of TMP. Over a period of three hours, the TMP rise with a flocculant dose of 60 mg/L was observed to be 89% less than without flocculant.

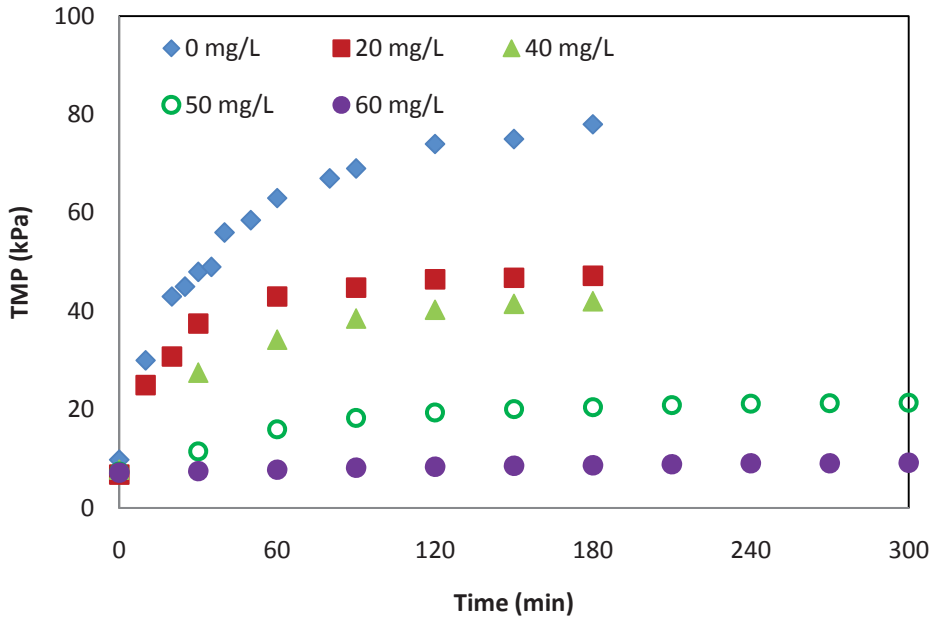

Figure 8.14 TMP development for different concentrations of flocculant (J = 90 L/m^2/h and air flow rate = 1.0 m^3/m^2/h)

Similarly, Figure 8.15 presents the particle deposition at different concentrations of flocculant. An increased dose of flocculant concentration reduced the deposition with time, but the reduction in TMP was observed to be greater than the reduction in particle deposition. It appears that the increments in TMP and particle deposition are not always

correlated; therefore, TMP does not always represent the state of particle deposition. Cake properties (cake structure, compactness, particle size distribution) significantly affect the relationship between TMP and particle deposition.

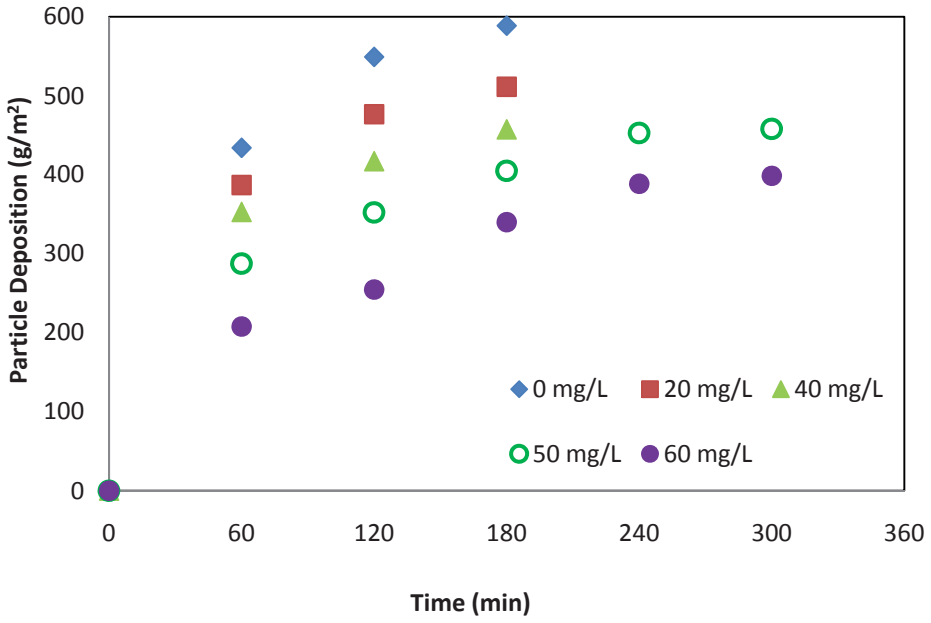

Figure 8.15 Particle deposition for different concentrations of flocculant (J = 90 L/m^2/h and air flow rate = 1.0 m^3/m^2/h)

Specific cake resistance (α_{av}) was determined by regressing the relationship between cake resistance (R_c) and particle deposition (w_c) at different concentrations of flocculant, as shown in Figure 8.16. A higher dose of $FeCl_3$ caused a significant reduction in specific resistance. The most likely reason for this reduction is the change in particle size of the kaolin particles/ flocs. Higher doses of the flocculant increased the mean size of kaolin particles/floc in the feed tank (Figure 8.17). According to the Carman-Kozeny equation, the filterability of flocs increases with floc size, therefore flocs formed with a high dose of flocculant have low specific resistance, resulting in higher filterability due to the increased floc size.

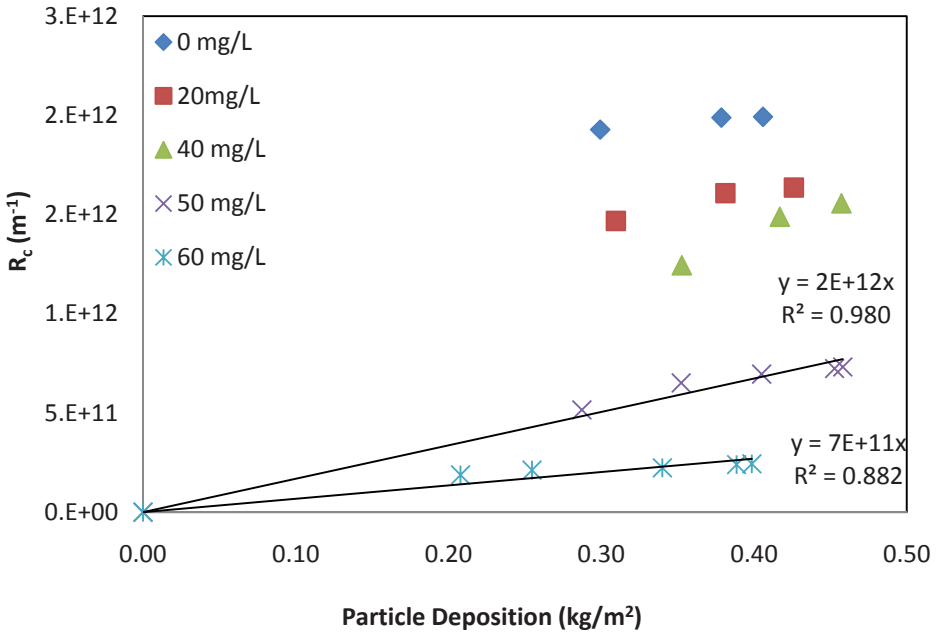

Figure 8.16 Relationship of cake resistance and particle deposition at different concentrations of flocculant (J = 90 L/m²/h)

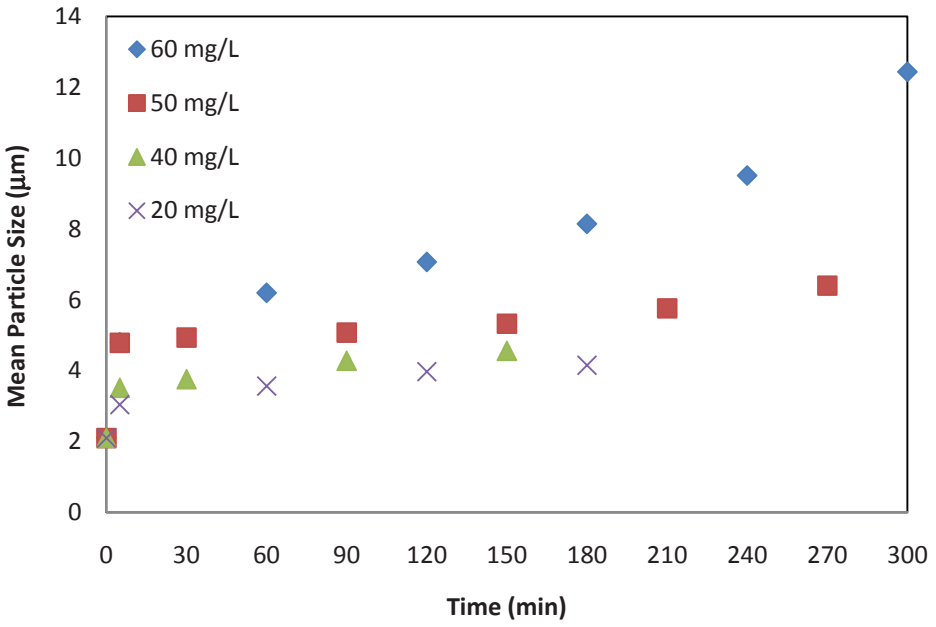

Figure 8.17 Effect of flocculant on mean particle size of kaolin particles

8.3.1.4 Effect of Air Flow Rate on Batch Flocculation-Microfiltration Test

Experiments combining membrane microfiltration with batch flocculation were carried out at a flux rate of 30 L/m^2/h with a flocculant ($FeCl_3$) dose of 75 mg/L under three different air flow rates (0.5, 1.0 and 1.5 m^3/m^2/h). It can be seen that TMP profiles were

affected by an increment in air flow rate (Figure 8.18). Increasing air flow may have complex effects, such as scouring the deposited layer (increasing back transport of particles from the cake formed on the filter surface), floc breakage due to excessive shearing force (re-flocculation), and variations in the mixing behaviour. At lower air flow, these effects are likely to be less significant.

Doubling the air flow rate from 0.5 $m^3/m^2/h$ to 1.0 $m^3/m^2/h$ did not significantly reduce the TMP rise, although some reduction in TMP was observed (Figure 8.18). This was due to the insufficient shear force generated by air bubbles which were unable to scour the deposited layer. The most probable reason for the slight reduction in TMP was the good mixing of flocs within the tank. At low air flow, large flocs were observed to settle, resulting in a less turbid suspension in the reactor tank or filtration unit and a lower TMP.

A slight reduction in TMP development was observed when the air flow rate was tripled (from 0.5 to 1.5 $m^3/m^2/h$) with a permeate flux rate of 30 $L/m^2/h$ (Figure 8.18). It was observed that this air flow scoured the deposited layer that caused a reduction in the TMP rise. Larger particles formed due to flocculation were attached on the membrane surface and required a large shearing force to detach.

Figure 8.19 shows the amount of fouling at the same flocculant dose (75 mg/L) at different air flow rates. Increased air flow caused a reduction in particle deposition. In the case of 1.0 $m^3/m^2/h$, the deposition pattern was observed to be in contrast to the TMP profile (Figure 8.18).

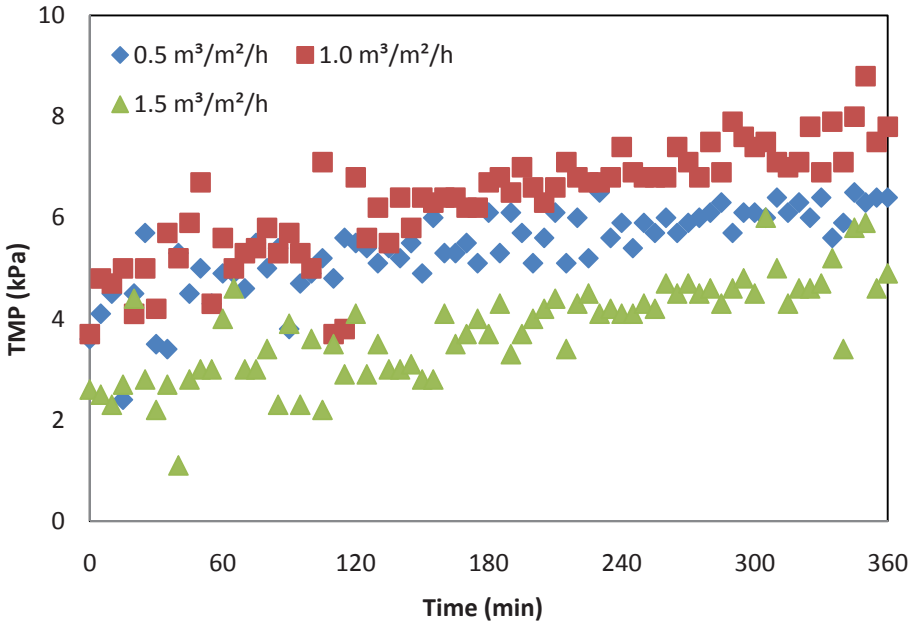

Figure 8.18 TMP development profiles for 30 LMH with 75 mg/L of $FeCl_3$ under various air flow rates

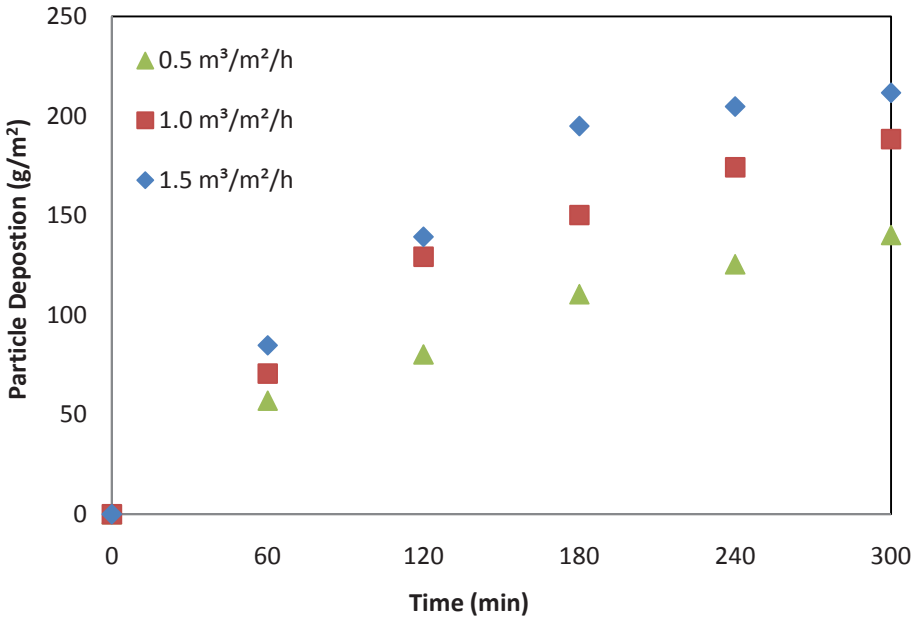

Figure 8.19 Particle depositions for 30 L/m^2/h with 75 mg/L $FeCl_3$ under various air flow rates

8.3.2 Effect of Air Flow Rate on In-Line Flocculation-Microfiltration Test

Laboratory scale filtration experiments showed that the optimum dose of $FeCl_3$ obtained from the jar test was high, and the optimum dose was therefore determined through an in-line flocculation-microfiltration test. Figure 8.20 presents the TMP profiles for

different doses of $FeCl_3$ during this test. An increased dose of flocculant reduced TMP development. Based on the TMP development, 75 mg/L was considered to be an optimum dose; beyond this dose (at 100 and 150 mg/L) there was a very slight rise in TMP, whereas at a smaller dose (60 mg/L) there was a significant rise in TMP. Quantitatively, TMP reductions for different doses of 20, 50, 60, 75, 100 mg/L were found to be 36%, 52%, 67%, 90% and 93.5% respectively compared to TMP development using an unflocculated solution. Therefore 75 mg/L was adopted as the optimum dose for $FeCl_3$.

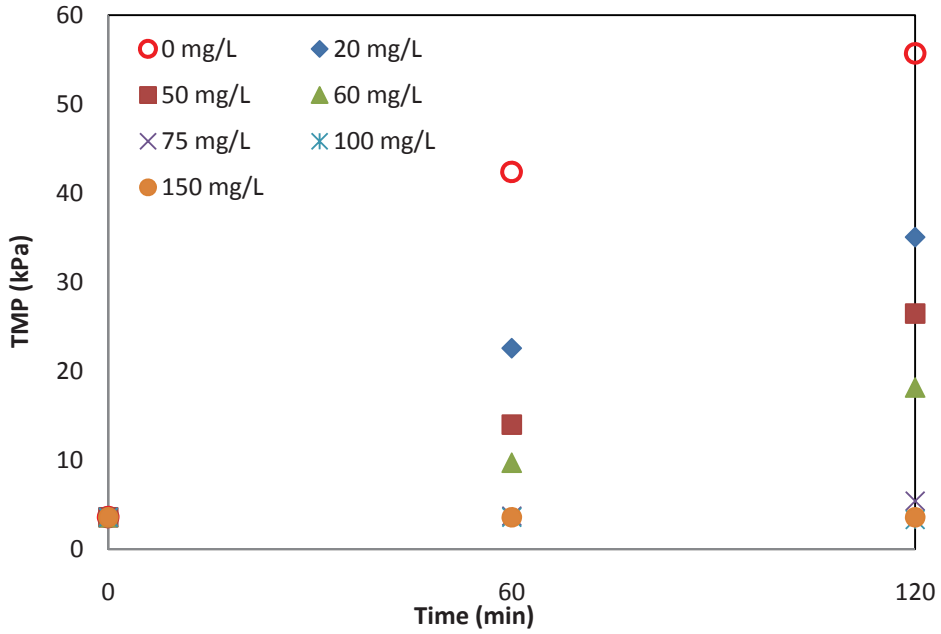

Figure 8.20 Determination of optimum dose of $FeCl_3$

The influence of air bubbles on the aggregation phenomenon was also investigated during the in-line flocculation-microfiltration test with the optimum dose of $FeCl_3$ (75 mg/L) at a flux rate of 30 $L/m^2/h$. Three air flow rates (0.5, 1.0 and 1.5 $m^3/m^2/h$) were tested. Figure 8.21 shows the effect of air flow on TMP development of the flocculated feed. In contrast to the previous results, the TMP profiles indicated a higher TMP with the increased air flow rate. In general, higher air flow rates should reduce TMP due to

the scouring effect on the deposited cake layer, but in the case of flocculated feed, the reverse occurred. Most probably, this is because (i) the high air flow broke down the large floc into smaller flocs that were easily attracted towards the membrane surface and deposited there, (ii) good mixing of the particles in suspension that occurred at a high air flow rate did not allow floc particles to settle at the bottom of the tank, and (iii) bubbles were not strong enough to scour large floc particles that were deposited on the membrane. However, low air flow rates facilitated the deposition of large particles which provided a suspension with a lower turbidity in the reactor tank, resulting in low TMP development. Large flocs also settled easily during filtration, a phenomenon which was clearly observed during the experiment.

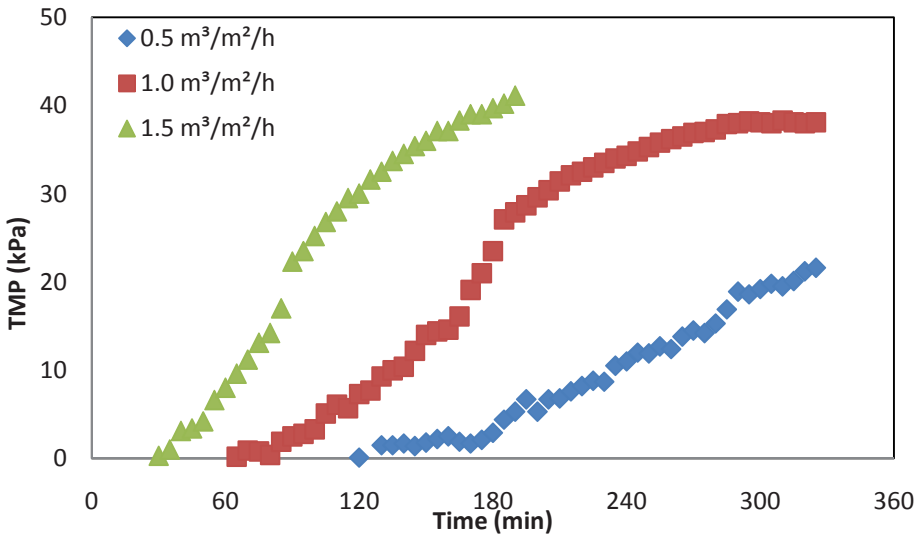

Figure 8.21 Effect of air flow rates on in-line flocculation-microfiltration test at 30 L/m^2/h

The TMP values in batch flocculation were comparatively lower than in in-line flocculation experiments. In batch flocculation, a constant concentration was maintained through recycling permeate to the reactor tank, whereas in case of in-line flocculation, a mixture of feed and stock solution was continuously added to the reactor tank, which increased the concentration of the suspension. The latter situation obviously resulted in higher TMP development.

8.4 Conclusions

The effect of different process conditions for flocculation was examined in terms of membrane performance. The addition of flocculant ($FeCl_3$) produced better control of colloidal membrane fouling, and TMP development at optimal flocculant concentration (75 mg/L) was far less than with an unflocculated feed. With a permeate rate of 30 $L/m^2/h$, TMP was reduced by 85% at the optimum concentration of flocculant compared a condition with no flocculation (at an air flow of 1.0 $m^3/m^2/h$). The increase of particle size by flocculation limited the rise in TMP in the microfiltration; moreover, a regression analysis between cake resistance and particle deposition indicated a relationship between low specific cake resistance and an increased concentration of flocculant. The same results were observed for all permeate flux rates (30, 60, 90 $L/m^2/h$) examined. This result allows us to conclude that flocculation aggregated the small particles to form larger particles which modified the cake properties (cake structure, porosity, compactness, etc.).

The effect of air flow on the flocculated suspension was studied during the microfiltration process coupled with an in-line flocculation test. Contrary to previous results, higher air flow rate increased the TMP development and particle deposition. This was probably because of (i) breakage of flocs into smaller ones that were easily attracted towards to and deposited on the membrane surface, (ii) reduction of settling due to well mixing of particles in suspension with high air flow rate and (iii) lack of scouring of large floc particle. However a low air flow rate facilitated large particle deposition that resulted in a suspension of low turbidity in the reactor tank which resulted in low TMP development. Large flocs were easily settled during filtration. Thus selection of appropriate air flow/scour is essential in the case of in-line flocculation-microfiltration system.

Chapter 9

Benefit of adsorbent addition in submerged membrane microfiltration in wastewater treatment

Abstract

It is known that the dissolved organic materials in water and wastewater are mostly responsible for membrane fouling, which causes flux decline resulting in a reduction in membrane performance that demands more frequent replacement of the membrane. The removal of organic materials before they enter the membrane surface is very effective in minimising membrane fouling. In this study therefore, three different adsorbents (PAC, GAC and Purolite) were investigated for their effectiveness in removing organic matter during the microfiltration of synthetic wastewater. Of these three adsorbents, PAC was observed to be the most effective, with higher removal efficiency for DOC (78% at 0.5 g/L), even at the low dose applied. A higher dose of PAC showed almost 100% reduction of hydrophobic compounds. Moreover, a simple mathematical model was developed to quantify the adsorption of organic matter on the PAC and Purolite including the effect of the adsorbent dose. From the model value, it is evident that an increase in adsorbent dose results in lower adsorption of organic matter on the membrane surface, which also reduces the concentration of organic matter in the tank. It can thus be concluded that the addition of adsorbents (PAC, GAC, Purolite) in the submerged membrane reactor during microfiltration is a very effective technique for removing organic matter which directly mitigates the membrane fouling.

9.1 Introduction

The low pressure-driven membrane processes such as microfiltration (MF) and ultrafiltration (UF) are becoming very popular in wastewater treatment. Microfiltration

easily removes some specific pollutants of wastewater which are not normally removed by conventional processes. MF is commonly used to remove microorganisms and colloidal particles; however, it cannot remove colour and dissolved organic matter.

It is known that the dissolved organic materials in water and wastewater are mostly responsible for membrane fouling, which causes flux decline resulting in a reduction in membrane performance that demands more frequent replacement of the membrane. Membrane fouling, an inevitable phenomenon in the membrane process, makes the system less efficient and reduces the economic viability of the membrane system. The physical, chemical and biological parameters of wastewater to be treated such as concentration, temperature, pH, ionic strength, dissolved organic materials and so on highly influence membrane fouling. The deposition and accumulation of foulants such as particles and organics on the membrane surface not only cause permeate flux decline with time but also the deterioration of the permeate quality. The initial decrease in the permeate flux during microfiltration is mainly due to rapid, irreversible adsorption of dissolved organic matter on the membrane surface (Ben Aim, Liu & Vigneswaran 1993). To recognize the phenomenon of the flux decline in membrane filtration, it is necessary to know the types of organics and/or the range of molecular weight distribution (MWD) of the organic matter removed from the wastewater (Tandanier, Berry & Knocke 2000). Some researchers have suggested that the hydrophobic (HP) fraction (humic substance) of organic matter is the major foulant that controls the rate and extent of fouling (Yuan & Zydney 2000). Other studies have reported that hydrophilic (HL) (non-humic) organic matter might be the most significant foulant. For example, Gray and Bolto (2003) reported that neutral and basic HL, and basic HP components of organic matter, lead to continuous flux decline. Fan et al. (2001) reported that the organics causing membrane fouling are found the following order: HL neutrals > HP acids >

transphilic (TP) acids. Jarusutthirak et al. (2002) found that the colloidal fraction consisting of large size HL compounds contributed the most to fouling when wastewater was used as the feed. The fractions alone cannot represent the fouling, and it is also important to investigate the molecular weight (MW) as different substances are present in each fraction; for example, the adsorption tendency of the polysaccharides (large MW) on the membranes is approximately three times that of humics (Jarusutthirak, Amy & Croué 2002).

The removal of the organic materials before they enter the membrane surface will be very effective in minimising membrane fouling. The membrane hybrid system, such as the membrane-adsorption filtration system, is considered to be an alternative technique for removing organic matter efficiently (Lebeau et al. 1998). Since the MF and UF do not have the capacity to completely remove organic foulants that include colour, natural organic matter (especially low molecular humic substances) and synthetic organic chemicals, a conventional treatment process like adsorption is coupled with the membrane process to enhance membrane performance in removing the dissolved organic matter. Membrane hybrid systems are emerging as the most promising solution for controlling fouling because they are simple and easy to implement. The physico-chemical treatments such as adsorption and ion-exchange to be incorporated in the submerged membrane system depend on the characteristics of the feed water and the quality of the output requirement. Many researchers have studied the short- and long term adsorption effect of PAC with the membrane processes (Guo et al. 2005; Smith et al. 2005; Vigneswaran et al. 2007). In these studies, the main aim of adding powdered activated carbon (PAC) to the system was to reduce the direct organic loading to the membrane surface. Based on the long term operation of a membrane hybrid system, Vigneswaran et al. (2007) recommended a minimal use of PAC as 10-15 g/m^3 of water

treated. They found that the energy requirement of the submerged membrane system was very low (as low as 0.2 kwh/m^3). Guo et al. (2005), and Campos et al. (2000a, 2000b) studied the effect of PAC on organic removal in the adsorption-membrane hybrid system.

Similarly, granular activated carbon (GAC) is also used as an adsorbent in microfiltration-adsorption system for treating organic-laden wastewater because GAC has a strong affinity for binding organic substances, even at low concentrations. Many researchers found that the lower molecular weight fractions of the organic materials are more adsorbable by GAC in a multi-component system (Lee, Snoeyink & Crittenden 1981; Yuasa et al. 1997). In the competitive adsorption circumstance that usually exists in a multi-component system, hydrophobic substances are more adsorbable onto the GAC surface than hydrophilic substances. Chaudhary et al. (2003) investigated a low strength synthetic wastewater for biodegradation and adsorption onto granular activated carbon with and without the presence of background inorganic compounds. They observed the slow biodegradation of organic compounds in the wastewater and concluded that the state of adsorption equilibrium depends on the initial adsorbate (organic) concentration.

Adsorption removes large and small molecular weight hydrophobic organic compounds; however, the biologically treated sewage effluent also contains a significant portion of hydrophilic organic compounds. These compounds can successfully be removed by a pretreatment of ion exchange. Ion Exchange resins such as Magnetic Ion Exchange resin (MIEX®) and Purolite can effectively remove dissolved organic matter from biologically treated sewage effluent (secondary effluent) and produce high quality water. When a MIEX® contactor was used as the pretreatment for a submerged

membrane hybrid system, higher effluent quality and longer operation time could be achieved (Zhang et al. 2007) . Croue et al. (1999) reported that strong anion exchange resins removed dissolved organic carbon (DOC) better than weak anion exchange resins and the increase in ionic strength enhanced the removal of natural organic matter. The Purolite resins have been used in several water treatment plants to remove toxic ions such as ammonia, nitrate, cyanide, lead, and cerium (Abo Farha et al. 2009; Fernando, Tran & Zwolak 2005; Samatya et al. 2006). Very little information is available on the use of Purolite in the removal of organic matter from wastewater.

The above studies did not investigate in detail the nature of organic matter removed by adsorption and ion exchange when they were separately combined with a submerged membrane reactor. Thus in this investigation, the effect of coupling ion-exchange resin (Purolite) and activated carbons (GAC and PAC) in a submerged membrane reactor was studied with regard to the removal of different classes of organic matter. An attempt was also made to model the degree of fouling (in terms of transmembrane pressure development) and organic removal efficiency in the membrane hybrid system using a simple, semi-empirical model.

9.2 Materials and Method

9.2.1 Materials

(a) Synthetic wastewater: The synthetic wastewater used in this research consisted of persistent organic compounds such as humic acid, tannic acid, polysaccharide, lignin and different salts. This wastewater represents biologically treated sewage effluent (BTSE). The chemical constituents of synthetic wastewater used in this study are given in Table 9.1; this type of composition of synthetic wastewater was first recommended by Seo et al. (1996).

Table 9.1 Constituents of the synthetic wastewater

Compounds	Concentration (mg/L)	Compounds	Concentration (mg/L)
Beef extract	1.8	Acacia gum powder	4.7
Peptone	2.7	Arabic acid	5.0
Humic acid	4.2	$(NH_4)_2SO_4$	7.1
Tannic acid	4.2	K_2HPO_4	7.0
Sodium lignin sulfonate	2.4	NH_4HCO_3	18.8
Sodium lauryle sulphate	0.94	$MgSO_4.3H_2O$	0.71

(b) Purolite A500PS: This is a macroporous (polyvinylbenzyl-trimethylammonium) exchanger which has been used as an adsorbent to remove organic matter such as tannins, fulvic and humic acids, from industrial and domestic wastewater. It either replaces or is used with traditional carbon adsorbents in special applications. The resin is normally used in the chloride salt form. The properties of Purolite are presented in Table 9.2.

(c) Activated Carbon: Activated carbons in both powdered (PAC) and granular (GAC) forms were separately used as the adsorbent in this study. The activated carbon adsorbs molecules (organic matter) onto its surface as a result of the forces exerted on the molecules by the carbon surfaces. The absorbate diffuses through the larger pores ("transport pores") of the activated carbon particle into the smallest pore diameter regions ("adsorption pores") where they are used in pseudo-precipitated or pseudo-condensed form. Activated carbon exhibits the strongest physical adsorption forces of any known material due to its large internal surface area (typically of the order of 1000

square metres per gram). The characteristics of the PAC and GAC are given in Tables 9.3 (a) and (b) respectively.

Table 9.2 Typical chemical & physical characteristics of Purolite A500PS

Parameters	A500PS	Parameters	A500PS
Polymer Matrix Structure	Macroporous Styrene-Divinylbenzene	Moisture Retention, Cl^- form	63-70%
Physical Form and Appearance	Opaque-Near-White Spheres	Reversible Swelling Cl^- ® OH	15%
Functional Groups	$R\text{-}(CH_3)_3N^+$	Specific Gravity, Moist Cl^- Form	1.06
Ionic Form (as shipped)	Cl^-	Total Exchange Capacity, Cl^- Form (wet, volumetric)	0.8 meq/ml min
Screen Size Range (British Standard Screen)	14-52 mesh, wet	pH Range (Stability), Cl^- Form	0-14
Particle Size Range (microns)	+1200 <5 %, -300 <1%	(Operating), Cl^- Form	5-10

Table 9.3 (a) Characteristics of powdered activated carbon (PAC)

Properties	Value
Nominal Size	55-65% minimum finer than 45μm
Internal surface area	1000-1100 m^2/g
Iodine No.	1000 mg/g min.
Bulk density	300-400 kg/m^3
Moisture content	4% maximum
Ash content	13% maximum
Water soluble ash content	0.5% maximum

Table 9.3 (b) Characteristics of granular activated carbon (GAC)

Properties	Value
BET surface area	1112 m^2/g
Iodine No.	800 mg/g min.
Bulk density	748 kg/m^3
Moisture content	5% maximum
Ash content	5% maximum
Nominal size range	300-600 μm

9.2.2 Method

Hollow fibre micro-filter membranes were submerged in the reactor containing synthetic wastewater. The hollow fibre membrane module with an area of 0.2 m^2 made of hydrophilic modified poly acrylic nitrile (PAN) (inner and outer diameter of fibre was 1.1 and 2.1 mm respectively) was used in this study (Mann Hummel Ultra Flo Pte Ltd, Singapore). The average pore size of the membrane was 0.10 μm. The reactor tank of 5 L capacity was filled to 4 L and the membrane module was placed in the centre of tank: just above the aerator plate. Air bubbles were continuously injected at a fixed rate (1.8 m^3/m^2 membrane area/h) from the bottom of the tank. Figure 9.1 shows the schematic diagram of the submerged membrane reactor (SMR) system used to investigate synthetic wastewater.

The filtration system was operated at constant flux mode. Different fixed permeate flux rates (20 and 30 $L/m^2/h$) were used, and a peristaltic pump was used to maintain a constant permeate flux, was adjusted carefully to the predetermined value by the regulator. Transmembrane pressure (TMP) was measured by a pressure transducer

installed between the suction pump and the membrane. The filtration pressure was continuously monitored online and transferred to a personal computer. A continuous filtration process was maintained by supplying feed water through the pump at a predetermined rate. The effluent samples were collected at regular interval for analysis purposes, and no backwash was applied during the experiment.

The submerged membrane microfiltration was operated both with and without adsorbents (Purolite A500PS, PAC, GAC) in suspension. The predetermined quantities of different adsorbents were added to the tank prior to the commencement of the experiment to adsorb the dissolved organic matter. The Purolite dose ranged between 0.1–1.0 g/L of the volume of the reactor, whereas the PAC and GAC doses varied between 0.01–0.5 g/L and 1-3 g/L respectively of the volume of the reactor. It should be noted that these adsorbents were added to the tank only once, i.e. at the beginning of the filtration test.

Air flow at a fixed rate of 1.8 $m^3/h/m^2$ membrane effective area was applied, i) to produce shear stress on the membrane surface, and ii) to suspend the PAC, GAC and Purolite in the reactor. Apart from the adsorption of organic matter, the PAC, GAC or Purolite placed in suspension scoured the pollutants on the membrane surface through shear action. In the long-running experiments, the air bubbles also helped to provide oxygen to the microbial mass for biological activity. Since the membrane fouling in this study was mainly due to the deposition of organic matter, chemical cleaning was performed after each experiment. The membrane module was submerged into the 5% NaOH solution and placed in a shaker for 3 hours. The membrane was then submerged into the 0.5% NaOCl solution. Before commencement of the next test, the hydraulic resistance of the membrane was checked by filtering the tap water and comparing its

resistance with a virgin membrane.

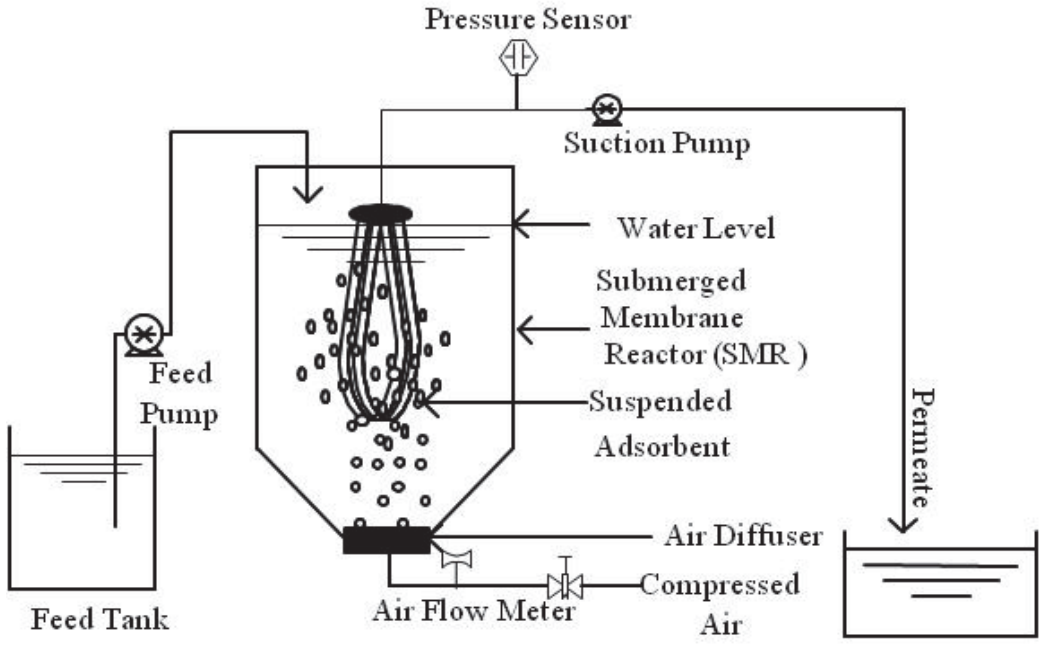

Figure 9.1 Schematic diagram of SMR with adsorbent in suspension

A size exclusion liquid chromatograph with carbon detector (LC-OCD) was used to investigate the hydrophilic and hydrophobic fractions of the filtrate. This provided quantitative information on the organic matter as well as qualitative results regarding the molecular size distribution of the organics present in the wastewater. Quantification was made through carbon mass determination, similar to total organic carbon (TOC) analysis. It was performed with a special organic carbon detector. The qualitative analysis is based on size exclusion chromatography (SEC).

In addition to LC-OCD, 3-dimensional fluorescence spectra (Excitation Emission Matrices or EEMs) were also used to analyse the filtrate of each experiment to study the organic type by using a spectrofluorometer (Varian Cary Eclipse Fluorescence Spectrophotometer, USA) with a wavelength range of 200 nm to 500 nm for excitation and 280 nm to 500 nm for emission by increasing the wavelength by 5 nm in each. All slit widths were set to 5 nm. The EEM value of the blank (synthetic substrate) was

subtracted from the value of samples with a TOC of 5 mg/L) for blank correction.

9.3 Mathematical Modelling of Submerged Membrane Reactor with Suspended Adsorption (Adsorbent)

In this study, a simple mathematical model was used which incorporates (i) the adsorption of organic material by PAC and Purolite in suspension in a submerged membrane reactor, and (ii) membrane resistance in terms of TMP development.

The homogeneous surface diffusion model (HSDM) represented in equations (9.1) to (9.4) was used to calculate the mass balance of dissolved organic matter inside a spherical porous particle. This model consists of a three step adsorption process (Najm, 1996): (1) adsorbate diffuses through a stagnant liquid film layer around the carbon element; (2) the adsorbate is adsorbed from the liquid stage on the external surface on the carbon element; (3) the adsorbate diffuses along the internal surface of the carbon particles until it reaches its adsorption site.

$$\frac{dq}{dt} = D_s \left(\frac{\partial^2 q}{\partial r^2} + \frac{2}{r} \frac{\partial q}{\partial r} \right) \tag{9.1}$$

This equation can be solved using the following initial and boundary conditions:

$$t = 0 \; ; \;\; q = 0 \tag{9.2}$$

$$r = 0 \; ; \; \frac{\partial q}{\partial r} = 0 \tag{9.3}$$

$$r = r_p \; ; \; \frac{\partial q}{\partial r} = \frac{k_f}{\rho_p D_s} (C - C_s) \tag{9.4}$$

where q is the rate of change of surface concentration with time (t) at any radial distance (r) from the center of the PAC (or Purolite) particle during adsorption, mg/g. The surface diffusion (D_s) coefficient represents the rate of diffusion of the target compound along the surface of the adsorbent particle, m^2/s; k_f is the external mass transfer

coefficient, m/s; ρ_p is the apparent particle density of PAC (or Purolite), kg/m^3; C is the bulk phase concentration, mg/L; C_s is the concentration on the external surface of PAC (or Purolite) particles, mg/L.

Using the Freundlich isotherm parameters k_F and n (equation 9.5) and the above equations k_f and D_s values were calculated. The Freundlich isotherm parameters for Purolite and PAC are presented in Table 9.4**.**

$$M = k_F C_e^{1/n} \tag{9.5}$$

where k_F and n are the Freundlich isotherm parameters (adsorption and exponential constants respectively) and M is the adsorbed mass.

Table 9.4: Freundlich adsorption isotherms parameters

	PAC		Purolite	
Freundlich	k_F	1/n	k_F	1/n
	1.19	2.54	1.6	1.14

The mass balance in bulk solution in the membrane tank was calculated using the following equation (9.6):

$$\frac{dC_b}{dt} = \frac{Q}{V}(C_0 - C_b) - \frac{M}{V}\frac{dq}{dt} - \frac{A_M}{V_M} - MCCC_b \tag{9.6}$$

where C_b is the organic concentration in the bulk phase in the reactor (mg/L); Q, the flow rate (m^3/s); V, the volume of the bulk solution in the reactor (m^3); C_o, the organic concentration in the feeding tank (mg/L); M, the weight of PAC (Purolite) used (g); A_M, the surface area of the membrane (m^2); V_M, the volume of the membrane (m^3); MCC, membrane correlation coefficient. The details and assumptions of equation (9.6) are

given elsewhere (Guo et al. 2005). The term [(M/V)(dq/dt)] represents the adsorption of the organics onto PAC (or Purolite) in suspension, and the other term [(A_M/V_M)MCC.C_b] describes the adsorption onto the PAC (or Purolite) layer deposited on the membrane surface and A_M/V_M is the packing density of the membrane. Moreover, the membrane filtration flux can be expressed by Darcy's law as:

$$J = \frac{\Delta P}{\mu(R_m + \alpha_{av} w_c(t))} \tag{9.7}$$

where J is permeate flux ($m^3/m^2/s$), ΔP is the TMP (kPa), R_m is membrane resistance (m^{-1}), α_{av} is flow resistance per unit mass of solid or specific cake layer resistance (m/kg) and $w_c(t)$ is the amount of solids and organics deposited on the membrane surface as a function of time.

The amount of organic matter $w_c(t)$ retained on the membrane (kg/m^2.s or mg/m^2.s) as function of time was calculated from the equation below:

$$w_c(t) = Q \frac{C_{Tank}(t) - C_{eff}(t)}{A_m} \tag{9.8}$$

where Q is the flow rate which is the flux (J) multiplied by membrane area (A_m), C_{Tank}(t) is the organic (TOC) concentration in the membrane tank at time (t) after adsorption, which can be calculated form adsorption equation. C_{eff} (t) is the organic concentration in permeate. The value of C_{eff} (t) was taken from experimental data and was found to be constant during the experimental period.

9.4 Results and Discussion

9.4.1 Characterisation of Organic Matter with and without Addition of Adsorbents

In this study, the wastewater samples with and without adsorption (Purolite and PAC)

were analysed using LC-OCD. The different conditions tested were with the addition of Purolite (doses between 0.5-1.0 g/L) and PAC (doses between 0.01-0.50 g/L) operated at a filtration flux of 20 L/m^2/h. The results on the different fractions of organic material are summarized in Table 9.5. From this table it can be seen that adsorption with Purolite and PAC removed the majority of the organic matter from the wastewater. The raw wastewater contained 28.5% of hydrophobic and 71.5% of hydrophilic compounds. Within the hydrophilic compounds, there were 7.5% of bio-polymers, 32.8% of humic acids, 13.3% of building block and 17.9% of low molecular weight neutrals. The removal efficiency of the dissolved organic carbon (DOC) increased with the addition of the adsorbent in the membrane tank. The removal efficiency of DOC with the ion exchange resin (Purolite) with doses of 0.1, 0.5 and 1.0 g/L (of volume of liquid in the reactor) were 67%, 69% and 73% respectively. Similarly, the removal efficiency of DOC with GAC with dose 1.0 and 3.0 g/L (of volume of liquid in the reactor) were 77% and 87% respectively. On the other hand, the removal efficiency of DOC with a PAC dose of 0.05, 0.1 and 0.5 g/L (of volume of reactor) were 78%, 89% and 93% respectively. The Purolite showed 73%-88% reduction of hydrophobic compounds (from 1.488 to 0.168-0.392 mg/L) and 58%-67% of hydrophilic compounds (from 3.731 to 1.196-1.535 mg/L). However a higher dose of PAC showed almost 100% reduction of hydrophobic compounds.

In addition to LC-OCD, organic characterization was also made by using fluorescence spectroscopy (excitation emission matrix, EEM). EEM was used in our earlier studies for both wastewater and membrane foulant analysis. The spectra showed a wide range of organics (Aryal et al. 2009). Every excitation emission spectrum would be useful when studying the chemical properties of organics of various origins. Based on the nature of organics and their origin, the spectra are generally divided into five groups (i)

aromatic proteins (Ex:Em 200-250: 280-330) and (ii) amino acid substances (Ex:Em 200-250: 330-380) (iii) peptides and proteins (microbial byproducts) (Ex:Em 250-340: 280-380) (iv) fulvic acids type substances (Ex:Em 200-250: 380-500) and (v) humic acids type substances (Ex:Em 250-500: 380-500) (Chen et al. 2003).

Table 9.5: Characterization of organic matter with and without adsorbent addition in submerged membrane reactor (Flux 20 L/m^2/h)

Operating conditions	DOC Dissolved	HOC Hydrophobic	CDOC Hydrophilic	Bio-polymer	Humic	Building Block	LMW Neutrals
	mg/L	mg/L	mg/L	mg/L	mg/L	mg/L	mg/L
Wastewater	5.219	1.488	3.731	0.389	1.712	0.696	0.934
	100%	28.50%	71.50%	7.50%	32.80%	13.30%	17.90%
0.1 g/L Purolite+MF	1.702	0.168	1.535	0.162	0.176	0.318	0.878
	100%	9.80%	90.20%	9.50%	10.40%	18.70%	51.60%
0.5 g/L Purolite+MF	1.612	0.392	1.22	0.114	0.326	0.135	0.645
	100%	24.30%	75.70%	7.10%	20.20%	8.40%	40.00%
1 g/L Purolite+MF	1.409	0.213	1.196	0.07	0.162	0.263	0.701
	100%	15.10%	84.90%	4.90%	11.50%	18.70%	49.70%
0.05 g/L PAC+MF	1.109	0.152	0.957	0.182	0.225	0.271	0.279
	100%	13.70%	86.30%	16.40%	20.30%	24.40%	25.20%
0.10 g/L PAC+MF	0.555	0.036	0.52	0.068	0.231	0.107	0.14
	100%	6.40%	93.60%	12.20%	41.70%	19.20%	20.50%
0.50 g/L PAC+MF	0.348	n.q	0.348	n.q	0.085	0.173	0.09
	100%	--	100%	--	24.50%	50.20%	26.30%
1.0 g/L GAC+MF	1.38	0.446	0.934	nq	0.456	0.151	0.325
	100%	32.31%	67.96%	--	32.71%	10.83%	23.31%
3.0 g/L GAC+MF	0.76	0.483	0.276	0.05	nq	0.02	0.206
	100%	63.0%	36.30%	6.52%	--	2.61%	26.77%

From the experimental results, it was found that the wastewater sample contained only a very small amount of aromatic protein-type substances which resulted in very weak intensity in this region (Ex:Em 200-250: 280-330) but had a strong peak in the fulvic and humic acid-type regions (Ex:Em 200-250: 380-500 and Ex:Em 250-500: 380-500) (Figure 9.2a). This indicates that the wastewater was mainly composed of humic and fulvic acid substances and a very small amount of bio-polymers. These results were also in accordance with the result obtained from LC-OCD (Table 9.5). Pretreatment with Purolite showed the intensity of the peak to be in the order of 0.1<0.5<1.0 g/L (Figure 9.2b). On the other hand, PAC at a dose of 0.5 g/L gave the best result in terms of organic removal, resulting in negligible intensity in the humic and fulvic acid regions (Figure 9.2c).

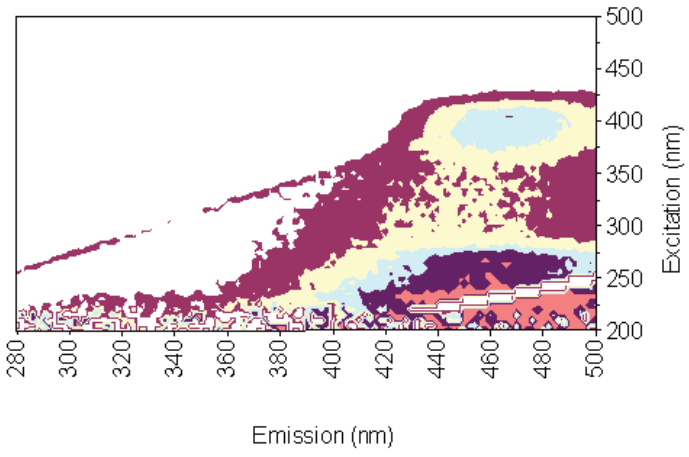

Figure 9. 2(a) EEM of synthetic wastewater

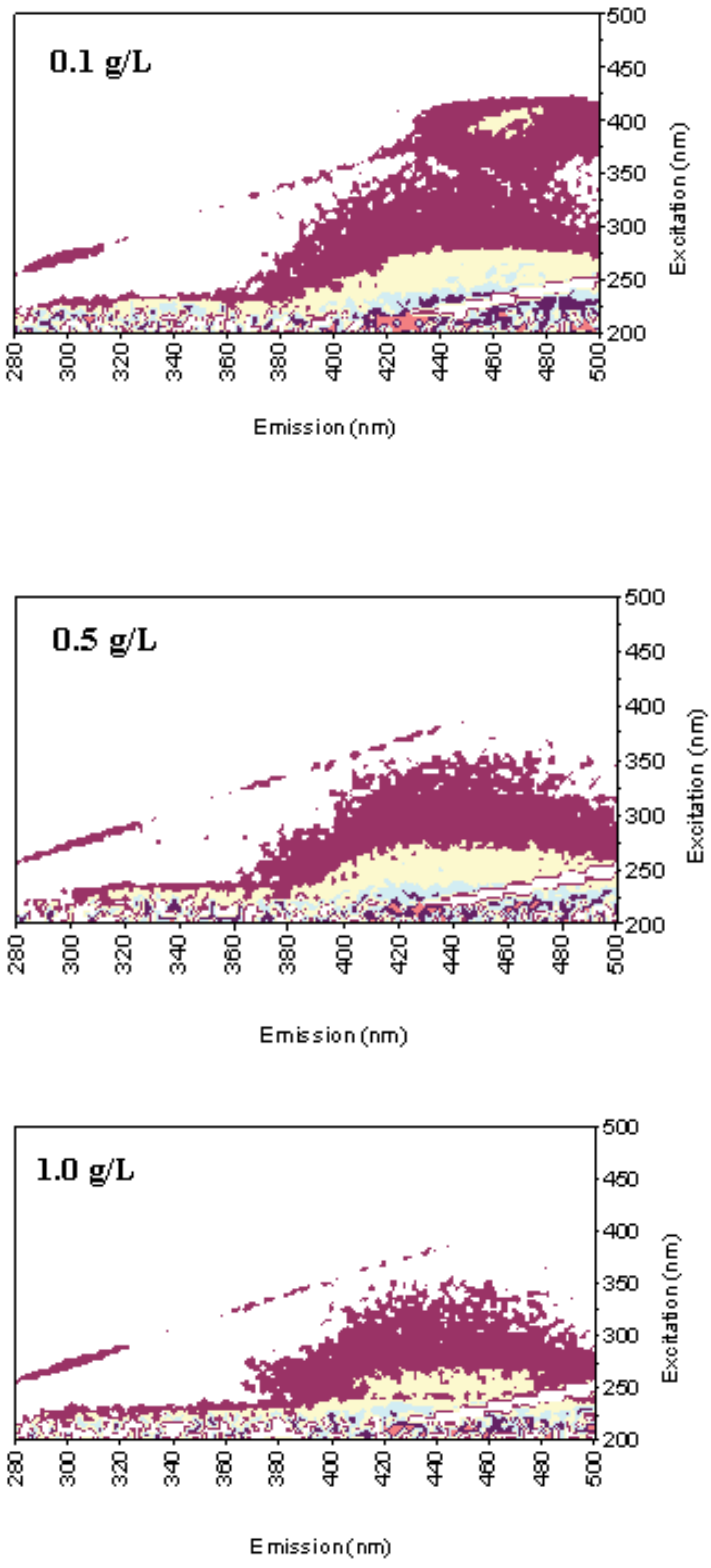

Figure 9.2 (b) EEM of wastewater after pretreatment with the ion exchange (Purolite) in different doses (0.1-1.0 g/L)

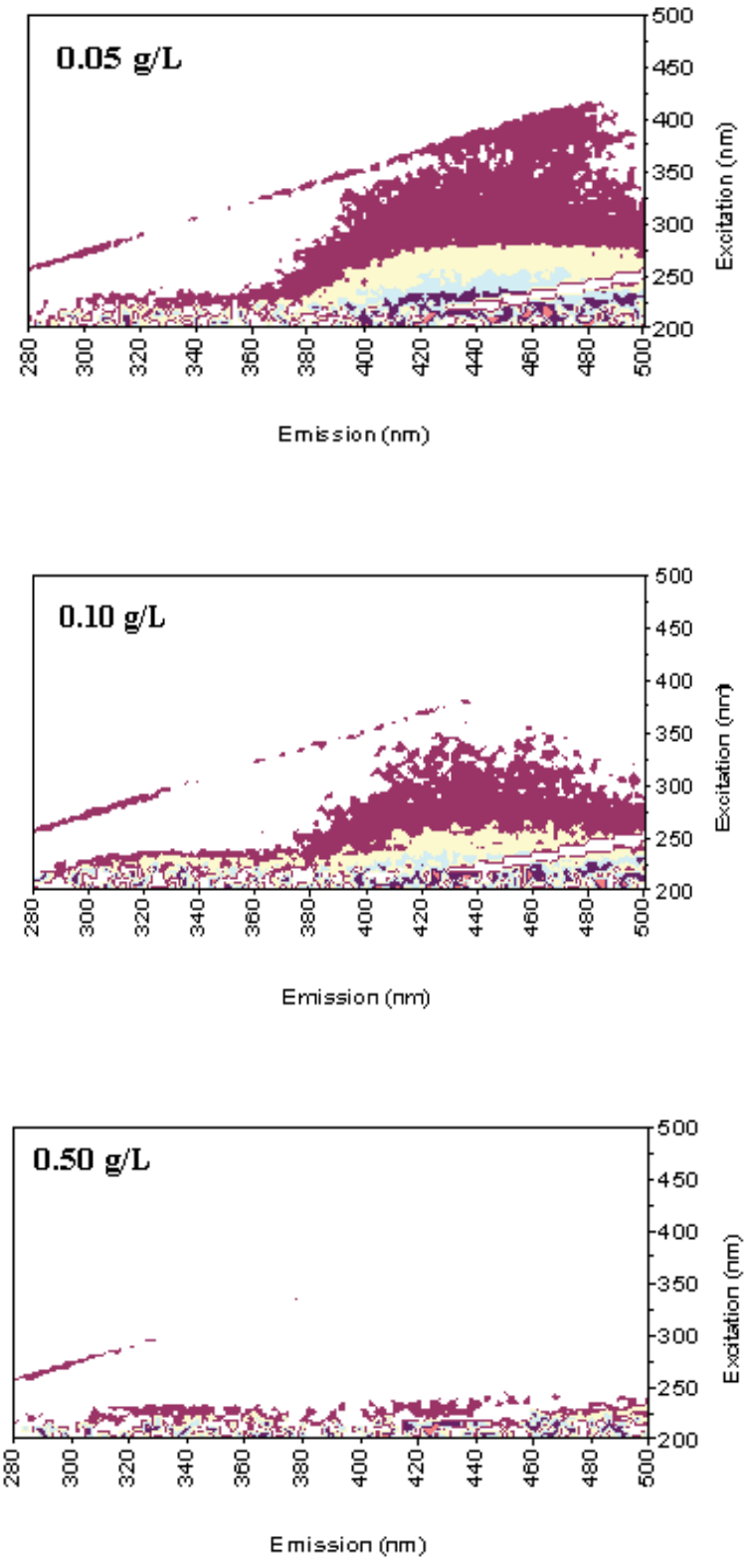

Figure 9.2 (c) EEM of wastewater after pretreatment with the PAC in different doses (0.05-0.5 g/L)

9.4.2 Mathematical Modelling on the Effect of the Addition of Adsorbents (PAC and Purolite)

A simple mathematical modelling was developed to quantify the effect of the addition of adsorbent in suspension in the submerged membrane reactor. The system parameters are presented in Table 9.6. The variation of organic concentration (measured in terms of DOC) is given in Figure 9.3. In this model, it was assumed that the concentration of organic matter remained constant in the reactor without the addition of PAC and the use of a membrane. This implies that the normalized organic concentration (C/C_o) is 1. When PAC is placed in the tank, it will adsorb part of the organic matter, and the amount will vary with the contact time.

Table 9.6: System parameters – reactor, membrane and adsorbent (PAC and Purolite)

Reactor		Membrane		Adsorbent		
Parameters	Values	Parameters	Value	Parameters	PAC	Purolite
Inlet concentration	5.2 mg/L	Flow rate ($m^2/m^3/h$)	50	Radius (m)	1.97E-07	1.25E-04
Volume	4.00E-03 m^3			Particle Density (kg/m^3)	340	992

9.4.2.1 Effect of Adsorbent Doses on Organic Removal

Figure 9.3 (a, b) shows the effect of adsorbent dose on the adsorption of organic matter. A higher dose of PAC and Purolite showed a higher level of adsorption of organic matter, as expected. The higher adsorption of organic matter at a higher dose is due to the larger available surface area of the adsorbents for adsorbing the organics. The saturation time was also found to be slightly longer for the higher adsorbent dose; however, no distinct difference between the decay curves was observed in the case of Purolite, where the adsorption became steady after an operating time of 20 min. In the

case of PAC, adsorption was stable after a period of 30 min.

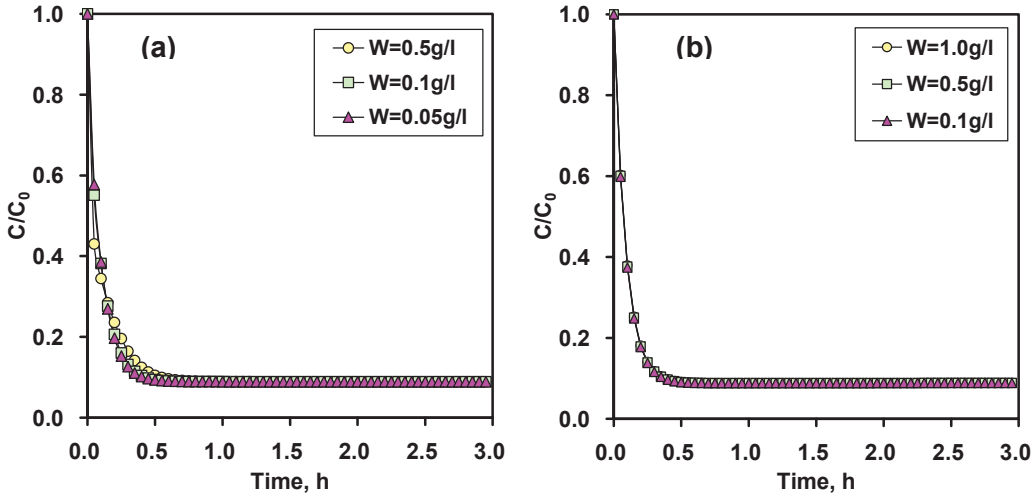

Figure 9.3 Effect of adsorbent dose on the adsorption of organic matter by (a) PAC and (b) Purolite A500PS (Flux 20 L/m^2/h, W=concentration of adsorbent)

9.4.2.2 Effect of Adsorbent Dose on the Adsorption of Organic Matter

In this study, the effect of the adsorbent dose on the quantity of organics retained on the membrane [$w_c(t)$] was studied. Model data for the effect of different adsorbent doses is presented in Figure 9.4 (a, b). Here, the quantity of organic material present in the tank at various times was calculated from the difference between the influent organic concentration and the amount of adsorbed by adsorbent at different times (equation 9.8). The quantity adsorbed was calculated from the adsorption isotherm and kinetic equation (Equations 9.1 and 9.4). The amount retained on the membrane is the difference of the organic concentration in the tank and the membrane effluent. The membrane effluent concentration and influent concentrations were measured experimentally. From the model value, it is evident that the increase in adsorbent concentration results in lower adsorption of solids onto the membrane, which also reduces the concentration of organic matter in the tank. The reduction of concentration in the tank is because of the higher adsorption of organics by the higher dose of adsorbent (higher available surface area). Thus, a higher dose of adsorbents resulted in lower effluent organic

concentration. The model data also showed that most of the cases the saturation occurred within 30 min.

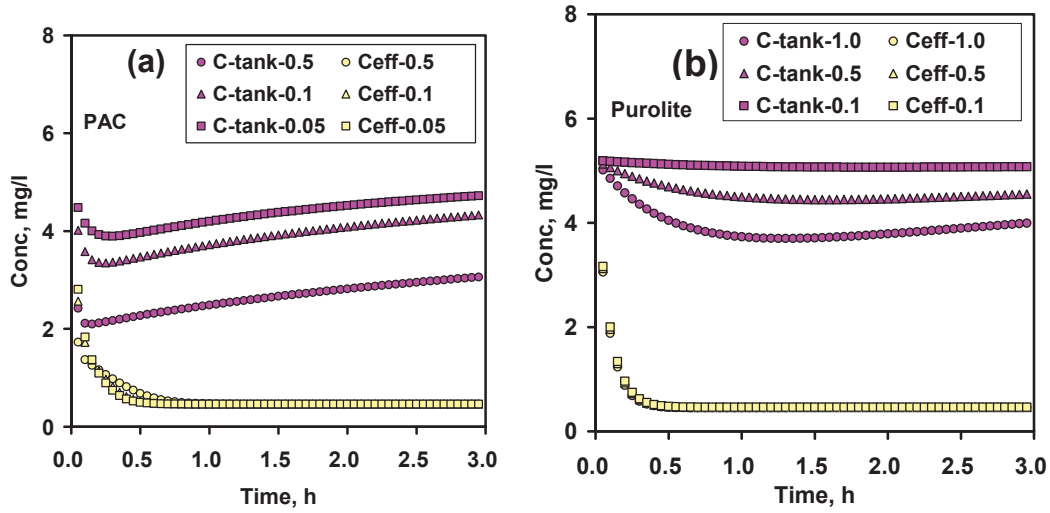

Figure 9.4 Effect of adsorbent dose on the adsorption of organic matter onto membrane (Flux 20 L/m^2/h)

9.4.2.3 Effect of Adsorbent Dose on Membrane Cake Resistance (R_c)

The effect of the concentration of the adsorbent dose on the TMP and cake resistance is presented in Figure 9.5 (a, b) and Table 9.7. It can be concluded from Table 9.7 that cake resistance reduced by using a higher concentration of adsorbent. A higher dose of adsorbent caused higher adsorption of organic matter due to the larger surface area which, resulting in lower adsorption of solids on the membrane surface. These phenomena led to the reduction of cake resistance.

Table 9.7: Effect of adsorbent dose on membrane cake resistance (R_c) [Flux: 30 L/m^2/h, clean membrane resistance (R_m): 2.1x 10^{12} m^{-1}]

PAC Dose (g/L)	R_c (m^{-1})	Purolite Dose (g/L)	R_c (m^{-1})
0.01	1.10E+15	0.1	1.10E+15
0.1	1.09E+15	0.5	8.50E+14
0.5	7.00E+14	1.0	5.50E+14

Figure 9.5 compares the TMP data from the experiment and the model. Even for short experiments lasting only two hours, the TMP rise increased with the evolution of time but the addition of an increased dose of adsorbents (both PAC and Purolite) significantly reduced TMP development. The presence of adsorbents reduced the organic matter in the suspension through adsorption, which resulted in low membrane fouling. A higher dose of adsorbents resulted in the adsorption of a larger quantity of organic matter, leading to lower TMP development. The model and experimental data of TMP were well matched (Figure 9.5).

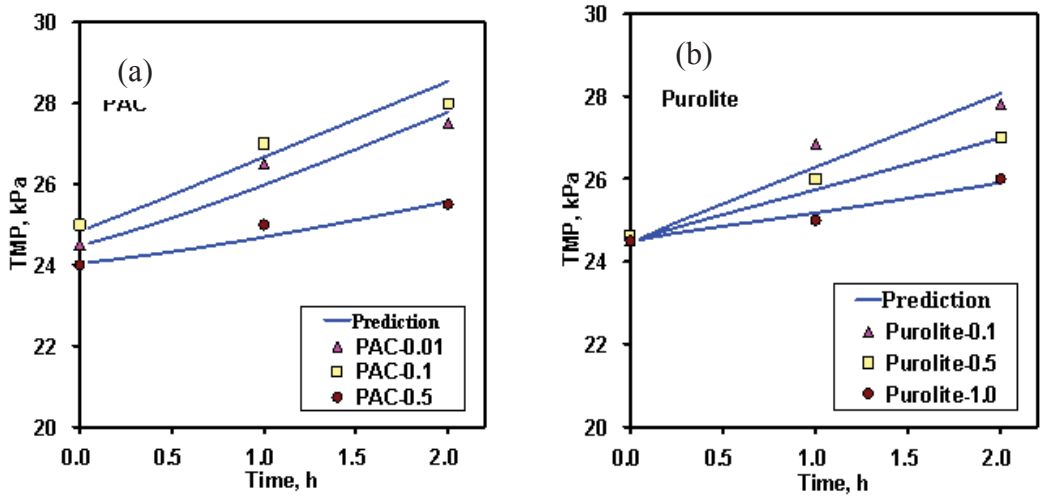

Figure 9.5 Effect of adsorbent dose on TMP development (Flux 30 L/m^2/h)

9.5 Conclusions

The effect of adsorbents (PAC, GAC and Purolite) on the removal of organic matter during the microfiltration of synthetic wastewater was studied using a hollow fibre membrane module. The submerged membrane adsorption system was very effective in removing dissolved organic matter from the synthetic wastewater. Of these three adsorbents, PAC was noted to be the most effective, with a higher removal efficiency for DOC (78% at 0.5 g/L) even with the application of a low dose in terms of the volume of liquid in the reactor. However, a higher dose of PAC showed almost 100%

reduction of hydrophobic compounds.

According to an excitation emission matrix analysis (EEM), it was found that the wastewater sample contained a very small amount of aromatic protein-type substances which resulted in very weak intensity in this region (Ex:Em 200-250: 280-330) but that there was a strong peak in the fulvic and humic acid-type region (Ex:Em 200-250: 380-500 and Ex:Em 250-500: 380-500). LC-OCD results also indicated that the wastewater was mainly composed of humic and fulvic acid-type substances and a very small quantity of bio-polymers. Pretreatment with Purolite showed that the peak intensity was in the order of 0.1<0.5<1.0 g/L. On the other hand, PAC at a dose of 0.5 g/L gave the best result in terms of organic removal, resulting in negligible intensity in both the humic and fulvic acid regions.

A simple mathematical model was developed to quantify the adsorption of organic matter on the PAC and Purolite including the effect of the adsorbent dose. From the model value, it is evident that an increase in adsorbent dose resulted in lower adsorption of solids on the membrane surface, which also reduced the concentration of organic matter in the tank. The reduction of the concentration in the tank is because of the higher adsorption of organic material by the higher adsorbent dose (higher available surface area). Thus, a higher dose of adsorbents resulted in lower effluent organic concentration. Low TMP and cake resistance were observed with a higher concentration of adsorbent, and it can thus be concluded that the addition of adsorbents (PAC, GAC, Purolite) in the submerged membrane reactor during microfiltration is a very effective technique in minimizing membrane fouling.

Chapter 10

Conclusions and recommendations

In the last two decades, membrane separation technology has emerged as a reliable alternative to conventional water treatment methods. Membrane systems have become state-of-the-art in water and wastewater treatment due to their unique advantages, such as excellent effluent quality, small footprint, and good disinfection capability. However membrane fouling, an intrinsic problem of membrane separation systems, is a major drawback and process limiter which inevitably decreases filtration performance. Extensive efforts have been made in recent years to understand the nature of fouling and a variety of realistic fouling control strategies have been developed. One of the most promising anti-fouling strategies is the application of air flow beneath the membrane modules (air scouring), but the main drawback of air flow systems is their high operating energy requirement. The optimisation of air flow in membrane filtration systems is therefore still the subject of practical and research interest, both in terms of reducing the the membrane fouling, thereby increasing the life of the membrane, and in reducing the energy cost. The optimisation of air flow leads directly to reduce operating costs. A more detailed investigation into the impact of air flow rates on membrane fouling is needed so that the operation and design system can be modified to reduce the cost of air flow (which is one of the major operational costs of membrane processes) and yet still minimise fouling. This thesis has focused on the problem of fouling by colloidal particles in an aerated submerged membrane microfiltration (similar to membrane bioreactors), and has sought different approaches to optimise the air flow rate and to reduce membrane fouling. A kaolin clay suspension of 10 g/L was used

which is similar to mixed liquor suspended solids (MLSS) in submerged membrane bioreactors treating domestic wastewater. However, in wastewater applications the floc/particle size in MLSS is higher.

10.1 Conclusions

Based on the experimental findings in this study, the following conclusions can be drawn:

10.1.1 Application of Air Flow for Mitigation of Particle Deposition in Submerged Membrane Microfiltration

This study demonstrates the effect of air flow on microfiltration performance, expressed as a reduction in TMP and particle deposition on the membrane surface. An increased air flow appears to augment the scouring effect on particles that accumulate on the membrane surface. A smaller amount of particle deposition on membrane surface was observed at high air flow rates for all permeate flux rates. At a low air flow rate, a large quantity of particles was deposited on the membrane causing a high TMP. At a lower permeate flux, an increase in air flow rate caused an effective reduction in particle deposition and TMP, whereas at higher flux rate, the reduction in these two parameters was minimal.

A sharp rise in TMP that occurred during the initial period of operation indicated that the use of air flow as a fouling mitigation strategy should be concentrated within this period to optimise the design process. The study showed that air flow and flux rates are the two major governing factors of particle deposition on the membrane surface. A single parameter consideration may not be effective for the design of an efficient membrane filtration system.

The linear relationship between the TMP and particle deposition has been established for different air flow rates and permeate flow rates. Air flow was more effective for low permeate flux under the experimental conditions studied. A flux of 15 L/m^2/h flux was observed to be a transitional flux beyond which a rise in the permeate flux showed a sharp jump in TMP and particle deposition. Experimental results showed a better reduction for both TMP and particle deposition with increasing air flow rates. In particular, an air flow rate of 1.2 $m^3/m^2_{membrane\ area}$/h was found to be the most effective for this permeate flux. Hence it can be concluded that a permeate flux of 15 L/m^2/h operated at an air flow rate of 1.2 $m^3/m^2_{membrane\ area}$/h is the most efficient operating condition compared to other conditions.

10.1.2 Modelling of Particle Deposition in Submerged Membrane Microfiltration

The effect of operating conditions such as permeate flux, air flow rates in terms of reduction in TMP, volume of water filtered, membrane resistance, and particle deposition were studied in detail. Internal membrane fouling was observed to be negligible due to the larger size of feed particle compared to membrane pore size, thus the major resistance contributing to the total membrane resistance was the measured resistance due to the cake layer. An almost 60% reduction in particle deposition was observed when the air flow rate was tripled from 0.6 to 1.8 $m^3/m^2_{membrane\ area}$/h at a flux rate of 15 L/m^2/h. A higher permeate flux increased particle deposition as well as TMP, but an increase in air flow rate reduced both TMP and particle deposition.

The relationships between the cake resistance and particle deposition were established for different permeate flux rates in equations 4.18-4.20 of Chapter 4 as; $R_C = 9.1 \times 10^{12}\delta$; $R^2 = 0.91$ (for 10 L/m^2/h), $R_C = 15.7 \times 10^{12}\delta$; $R^2 = 0.98$ (for 15 L/m^2/h) and $R_C =$

20.3 x $10^{12}\delta$; R^2 = 0.98 (for 20 L/m^2/h). Here R_C and δ are cake resistance (m^{-1}) and particle deposition (kg/m^2) respectively. These equations (4.18-4.20) suggest the gradient is proportional to the flux. Thus a general formula could be R_C = 1.01 x 10^{12}Jδ Therefore, it can be concluded that the cake resistance is proportional to the multiplication of flux and cake deposition.

10.1.3 Combined Effect of Air and Mechanical Scouring on Fouling Reduction in Submerged Membrane Microfiltration

This study investigated the effects of air flow and mechanical scouring on membrane fouling when a support medium (GAC) was added in the suspension to provide mechanical scouring. Low membrane fouling was observed for high air flow rates for all permeate flux rates. Further reductions in particle deposition were observed in the presence of a support medium used for mechanical scouring. A substantial reduction in particle deposition (78%) was obtained for a permeate flux of 15 L/m^2/h when the air flow rate was tripled in the presence of a support medium from a base case that used an air flow of 0.6 $m^3/m^2_{\text{membrane area}}$/h without a support medium. The results for the flux of 15 L/m^2/h showed that in the absence of the granular medium, TMP development was decreased by 60% when air flow was tripled (from 600 to 1800 L/h/m^2). There was a further drop in TMP to 85% with the addition of a granular medium (for the same air flow rate). The doubling of the air flow rate (from 600 to 1200 L/h/m^2) without the granular medium led to a 32% reduction in TMP development at 10 L/m^2/h. The same result was obtained at a lower air flow rate of 600 L/h/m^2 with the granular medium. This result shows that the same reduction in TMP can be obtained by adding a granular medium instead of doubling the air flow rate. Therefore, it was concluded that an application of air flow with a support medium to provide mechanical scouring has additional benefit for membrane fouling control compared to the application of air flow

only. The addition of a support medium with air flow could be a good alternative to the application of very high rates of air flow in submerged membrane microfiltration systems. The optimisation of the combined effect of support medium and air flow will help in the design of less energy-intensive operations.

10.1.4 Experimental Investigation on the Effects of Viscosity and Air Bubbles on Membrane Fouling in Submerged Membrane Microfiltration

In a membrane bioreactor, similar to conventional activated sludge processes, biomass viscosity is closely related to the concentration of mixed liquor suspended solids (MLSS) and has been referred as a foulant parameter. In wastewater applications, a high concentration of MLSS in the reactor results in high viscosity. In this study, the influence of viscosity was investigated by adding predetermined quantities of glycerol during submerged membrane microfiltration of a kaolin clay suspension in the presence of air sparging. It has been demonstrated that the viscosity of the suspension plays a significant role in membrane fouling control. An increase in viscosity caused a large rise in TMP and particle deposition leading to high membrane cake resistance. The application of air flow (air scour) helped to reduce the TMP and particle deposition on the membrane surface. Conversely, an increase in feed viscosity aggravated membrane fouling. Due to the increased viscosity, the increment in cake resistance was far greater than the reduction in resistance caused by the increased air flow. Moreover, the cake resistance demonstrated strong dependency on the permeate flux even in a viscous suspension.

The relationship between cake resistance and particle deposition at various air flow rates was an approximately linear correlation to the viscosity. The specific cake resistance

reduced with the application of higher rates of air flow but increased with higher viscosities of the suspension.

10.1.5 Influence of Aerator Geometry (Bubble Size) on Particle Deposition Control during Submerged Membrane Microfiltration

The performance of a submerged flat sheet membrane system is highly affected by the geometry of the air diffuser device that generates different sizes of air bubble at the same air flow rate. A greater reduction in TMP and particle deposition was observed with a circular air diffuser plate that produced small bubbles compared to a square air diffuser plate that produced larger air bubbles for all permeate flux and applied air flow rates. Hence it can be concluded that air bubble size (or a change in the design of the aerator plate) can play an important role in controlling membrane fouling.

At a flux of 20 $L/m^2/h$ with large bubbles, when air flow was doubled (from 0.6 to 1.2 $m^3/m^2/h$), TMP was reduced by 21%, whereas the reduction was more than twice (almost 48%) in the case of small bubbles at the same rate of air flow. Based on the analysis of TMP and the reduction in particle deposition, the most effective operating condition was at a permeate flux rate of 20 $L/m^2/h$, an air flow rate of 1.2 $m^3/m^2/h$ and small bubbles (circular aerator) for the kaolin clay suspension and tank configuration used. Although the aerator geometry used in this study may not be the most effective in a pilot scale filtration plant, the results indicate that the selection of aerator geometry has to be seriously considered when designing a membrane filtration system.

10.1.6 Assessment of Fouling Behaviour during Microfiltration Coupled with Flocculation in a Submerged Flat Sheet System

The effects of different operating conditions for direct and in-line flocculation and membrane performance were examined in this study. The addition of flocculant ($FeCl_3$)

showed better control of colloidal membrane fouling. The development of TMP at an optimal flocculant concentration (75 mg/L of $FeCl_3$) was far less than TMP with unflocculated feed. In the case of a permeate flux of 30 L/m^2/h, TMP was reduced by 85% at the optimum concentration of flocculant and air flow rate of 1.2 $m^3/m^2_{membrane\ area}$/h. The increase in particle size (floc formation) due to flocculation in a microfiltration process limited the rise in TMP. A regression analysis between cake resistance and particle deposition showed lower specific cake resistance with an increased concentration of flocculant. The flocculation aggregated small particles to form larger ones which directly affected the cake properties (cake structure, porosity, compactness, etc.) and reduced fouling.

10.1.7 Benefits of Adsorbent Addition with Submerged Membrane Microfiltration in Wastewater Treatment

The effect of adsorbents (PAC, GAC and Purolite) on the removal of organic matter during the microfiltration of synthetic wastewater was studied with a hollow fibre membrane module. Here PAC, GAC and Purolite act both as adsorbents and mechanical scouring media. The submerged membrane adsorption system was found to be very effective in removing dissolved organic matter from the synthetic wastewater. Of the three adsorbents used, PAC was found to be the most effective, with higher DOC removal efficiency (78% at 0.05 g/L of volume of liquid in the reactor) even at the low doses applied relative to the volume of reactor used. A higher dose of PAC showed an almost a 100% reduction of hydrophobic compounds. On the other hand, PAC at a dose of 0.5 g/L gave the best result in terms of organic removal and resulted in the high removal of humic and fulvic acid types of organics.

A simple mathematical model was developed to quantify the adsorption of organic

matter on the PAC and Purolite, including the effect of the adsorbent dose. From the model values, it is evident that an increase in adsorbent concentration results in lower adsorption of solids onto the membrane surface, which also reduces the concentration of organics in the tank. The reduction in the concentration of organics in the tank is because of the higher adsorption of organics onto the larger doses of adsorbent (higher available surface area). Thus, larger doses of adsorbents (in a sustainable range) resulted in lower effluent organic concentrations, and as a result, low TMP and cake resistance were observed with higher concentrations of adsorbent. Hence it can be concluded that the addition of adsorbents (PAC, GAC, Purolite) in a submerged membrane reactor during microfiltration is a very effective technique for minimizing membrane fouling.

10.2 Recommendations for Future Work

From the outcomes of the present study, the following recommendations for future research work are proposed.

10.2.1 Application of Variable Air Flow Rate Analysing Energy Consumption

The experimental results of submerged membrane microfiltration indicate that a higher air flow rate increases filtration performance. However, higher air flow rates also increase the energy demand and the operating costs of the filtration system. The outcomes of this study have highlighted the existence of a sharp rise in TMP during the initial period of filtering kaolin clay suspension which has been attributed to severe fouling of the membrane surface. To address this critical period of filtration, the application of variable air flow could be a topic for future research. A higher air flow at the beginning of filtration and a gradual stepping down of the flow rate instead of a constant, continuous air flow rate would reduce energy consumption but at the same time would enhance filtration performance. Further research investigating energy

consumption with varying air flow rates and their effect on the filtration performance would be beneficial.

10.2.2 Optimisation of Combined Effect of Support Medium and Air Flow Rate

An aerated submerged membrane microfiltration in the presence of an external support material (such as GAC) evidently provides additional benefit. To minimise the air flow rate, the addition of an external scouring material could be a good alternative and further work could therefore be carried out on optimising the combined effect of the support medium and air flow rate. This would suggest the optimum dose of support medium, air flow rate and permeate flux. The size and durability of the support medium and the damage caused to the membrane should also be investigated.

References

Abo Farha, S.A., Abdel-Aal, A.Y., Ashourb, I.A. & Garamon, S.E. 2009, 'Removal of some heavy metal cations by synthetic resin purolite C100', *Journal of Hazardous Materials*, vol. 169, pp. 190-194.

Adamis, Z. & Timar, M. 1980, 'Investigations of the effect of quartz, aluminum silicates and colliery dusts on peritoneal macrophages in vitro', in R. C. Brown, I. P. Gormley, M. Chamberlain & R. Davies (eds), *The in Vitro Effects of Mineral Dusts*, Academic Press, New York/London., pp. 13-18.

Al Akoum, O., Ding, L.H. & Jaffrin, M.Y. 2002a, 'Microfiltration and ultrafiltration of UHT skim milk with a vibrating membrane module', *Separation and Purification Technology*, vol. 28, no. 3, pp. 219-234.

Al Akoum, O., Jaffrin, M.Y., Ding, L., Paullier, P. & Vanhoutte, C. 2002b, 'An hydrodynamic investigation of microfiltration and ultrafiltration in a vibrating membrane module', *Journal of Membrane Science*, vol. 197, no. 1–2, pp. 37-52.

Al akoum, O., Mercier-Bonin, M., Ding, L., Fonade, C., Aptel, P. & Jaffrin, M. 2002c, 'Comparison of three different systems used for flux enhancement: Application to crossflow filtration of yeast suspensions', *Desalination*, vol. 147, no. 1–3, pp. 31-36.

Aoustin, E., Schaefer, A.I., Fane, A.G. & Waite, T.D. 2001, 'Ultrafiltration of natural organic matter', *Separation and Purification Technology*, vol. 22, pp. 63-78.

Aryal, R., Lebegue, J., Vigneswaran, S., Kandasamy, J. & Grasmick, A. 2009, 'Identification and characterisation of biofilm formed on membrane bio-reactor', *Separation and Purification Technology*, vol. 67, no. 1, pp. 86-94.

Aryal, R.K., Vigneswaran, S. & Kandasamy, J. 2010, 'Influence of buoyant media on particle layer dynamics in microfiltration membranes', *Water Science and Technology*, pp. 1733-1738.

Atkinson, S. 2006, 'Research studies predict strong growth for MBR markets', *Membrane Technology*, pp. 8-10.

Bae, T.-H. & Tak, T.-M. 2005, 'Interpretation of fouling characteristics of ultrafiltration membranes during the filtration of membrane bioreactor mixed liquor', *Journal of Membrane Science*, vol. 264, no. 1, pp. 151-160.

Bai, R. & Leow, H.F. 2001, 'Microfiltration of polydispersed suspension by a membrane screen/hollow-fiber composite module', *Desalination*, vol. 140, no. 3, pp. 277-287.

Bai, R. & Leow, H.F. 2002, 'Microfiltration of activated sludge wastewater: The effect of system operation parameters', *Separation and Purification Technology*, vol. 29, no. 2, pp. 189-198.

Basu, O.D. & Huck, P.M. 2005, 'Impact of support media in an integrated biofilter-submerged membrane system', *Water Research*, vol. 39, no. 17, pp. 4220-4228.

Belfort, G., Davis, R.H. & Zydney, A.L. 1994, 'The behavior of suspensions and macromolecular solutions in crossflow microfiltration', *Journal of Membrane Science*, vol. 96, no. 1-2, pp. 1-58.

Bellara, S.R., Cui, Z.F. & Pepper, D.S. 1997, 'Fractionation of BSA and lysozyme using gas sparged ultrafiltration in hollow fibre membrane modules', *Biotechnology Progress*, vol. 13, no. 6, pp. 869-872.

Bellhouse, B.J. & Sobey, I.J. 1994, 'Enhanced filtration using flat membranes and standing vortex waves', *Bioseparation*, vol. 4, pp. 127-138.

Ben Aim, R., Liu, M.G. & Vigneswaran, S. 1993, 'Recent development of membrane processes for water and waste water treatment', *Water Science and Technology*, vol. 27, no. 10, pp. 141-149.

Bertram, C.D., Raymond, C.J. & Pedley, T.J. 1991, 'Application of nonlinear dynamics concepts to the analysis of self-excited oscillations of a collapsible tube conveying a fluid', *Journal of Fluids and Structures*, vol. 5, no. 4, pp. 391-426.

Bouhabila, E.H., Ben Aim, R. & Buisson, H. 1998, 'Microfiltration of activated sludge using submerged membrane with air bubbling (application to wastewater treatment)', *Desalination*, vol. 118, no. 1, pp. 315-322.

Bouhabila, E.H., Ben Aïm, R. & Buisson, H. 2001, 'Fouling characterisation in membrane bioreactors', *Separation and Purification Technology*, vol. 22-23, pp. 123-132.

Brookes, A., Jefferson, B., Le-Clech, P. & Judd, S. 2003, 'Fouling of membrane bioreactors during treatment of produced water', *Proceedings of the IMSTEC*, Sydney, Australia.

Cabassud, C., Laborie, S., Durand-Bourlier, L. & Laine, J.M. 2001, 'Air sparging in ultrafiltration hollow fibers: relationship between flux enhancement, cake characteristics and hydrodynamic parameters', *Journal of Membrane Science*, vol. 181, no. 1, pp. 57-69.

Cabassud, C., Laborie, S. & Laina, J.M. 1997, 'How slug flow can improve ultrafiltration flux in organic hollow fibres', *Journal of Membrane Science*, vol. 128, no. 1, pp. 93-101.

Cabassud, C., Laborie, S. & Lainé, J.M. 1997, 'How slug flow can improve ultrafiltration flux in organic hollow fibres', *Journal of Membrane Science*, vol. 128, no. 1, pp. 93-101.

Campos, C., Mariñas, B., Snoeyink, V., Baudin, I. & Lainé, J. 2000a, 'PAC-membrane filtration process. I: Model development', *Journal of Environmental Engineering*, vol. 126, no. 2, pp. 97-103.

Campos, C., Mariñas, B., Snoeyink, V., Baudin, I. & Lainé, J. 2000b, 'PAC-membrane filtration process.II: Model application', *Journal of Environmental Engineering*, vol. 126, no. 2, pp. 104-111.

Chang, I.S. & Judd, S.J. 2002, 'Air sparging of a submerged MBR for municipal wastewater treatment', *Process Biochemistry*, vol. 37, no. 8, pp. 915-920.

Chang, I.S. & Lee, C.H. 1998, 'Membrane filtration characteristics in membrane-coupled activated sludge system: The effect of physiological states of activated sludge on membrane fouling', *Desalination*, vol. 120, no. 3, pp. 221-233.

Chang, I.S., Lee, C.H. & AHN, K.H. 1999, 'Membrane filtration characteristics in membrane-coupled activated sludge system: The effect of floc structure on membrane fouling', *Separation Science and Technology*, vol. 34, no. 9, pp. 1743-1758.

Chang, S. & Fane, A.G. 2001, 'The effect of fibre diameter on filtration and flux distribution: Relevance to submerged hollow fibre modules', *Journal of Membrane Science*, vol. 184, no. 2, pp. 221-231.

Chaudhary, D.S., Vigneswaran, S., Ngo, H.H. & Moon, H. 2003, 'Comparison of association theory and Freundlich isotherm for describing granular activated carbon adsorption of secondary sewage effluent', *Journal of Environmental Engineering and Science*, vol. 2, pp. 111-118.

Chen, W., Westerhoff, P., Leenheer, J.A. & Booksh, K. 2003, 'Fluorescence excitation−emission matrix regional integration to quantify spectra for dissolved

organic matter', *Environmental Science and Technology*, vol. 37, no. 24, pp. 5701-5710.
Cheryan, M. 1998, *Ultrafiltration and microfiltration handbook*, Technomic Publishing Lancaster PA.
Chinu, K., Johir, A.H., Vigneswaran, S., Shon, H.K. & Kandasamy, J. 2010, 'Assessment of pretreatment to microfiltration for desalination in terms of fouling index and molecular weight distribution', *Desalination*, vol. 250, no. 2, pp. 644-647.
Cho, M.H., Lee, C.H. & Lee, S. 2006, 'Effect of flocculation conditions on membrane permeability in coagulation-microfiltration', *Desalination*, vol. 191, no. 1, pp. 386-396.
Choi, H., Zhang, K., Dionysiou, D.D., Oerther, D.B. & Sorial, G.A. 2005, 'Influence of cross-flow velocity on membrane performance during filtration of biological suspension', *Journal of Membrane Science*, vol. 248, no. 12, pp. 189-199.
Choi, J.G., Bae, T.H., Kim, J.H., Tak, T.M. & Randall, A.A. 2002, 'The behavior of membrane fouling initiation on the crossflow membrane bioreactor system', *Journal of Membrane Science*, vol. 203, no. 12, pp. 103-113.
Choo, K.H. & Lee, C.H. 1996, 'Effect of anaerobic digestion broth composition on membrane permeability', *Water Science and Technology*, vol. 34, no. 9, pp. 173-179.
Choo, K.H. & Stensel, H.D. 2000, 'Sequencing batch membrane reactor treatment: Nitrogen removal and membrane fouling evaluation', *Water Environment Research*, vol. 72, no. 4, pp. 490-498.
Chua, H.C., Arnot, T.C. & Howell, J.A. 2002, 'Controlling fouling in membrane bioreactors operated with a variable throughput', *Desalination*, vol. 149, no. 13, pp. 225-229.
Churchouse, S. & Wildgoose, D. 1998, 'Membrane bioreactor progress from the laboratory scale to full-scale use', *Membrane Technology*, vol. 111, p. 4.
Citulski, J., Farahbakhsh, K., Kent, F. & Zhou, H. 2008, 'The impact of in-line coagulant addition on fouling potential of secondary effluent at a pilot-scale immersed ultrafiltration plant', *Journal of Membrane Science*, vol. 325, no. 1, pp. 311-318.
Clift, R., Grace, J.R. & Weber, M.E. 1978, *Bubbles, drops, and particles*, New York Academic Press, New York.
Cote, P. & Thompson, D. 1999, 'Wastewater treatment using membranes: The North American experience', *Proceedings Membrane Technology in Environmental Management* Tokyo, p. 46.
Croué, J.P., Violleau, D., Bodaire, C. & Legube, B. 1999, 'Removal of hydrophobic and hydrophilic constituents by anion exchange resin', *Water Science and Technology*, vol. 40, no. 9, pp. 207-214.
Cui, Z.F., Bellara, S.R. & Homewood, P. 1997, 'Airlift crossflow membrane filtration -- a feasibility study with dextran ultrafiltration', *Journal of Membrane Science*, vol. 128, no. 1, pp. 83-91.
Cui, Z.F., Chang, S. & Fane, A.G. 2003, 'The use of gas bubbling to enhance membrane processes', *Journal of Membrane Science*, vol. 221, no. 1-2, pp. 1-35.
Cui, Z.F. & Wright, K.I.T. 1994, 'Gas-liquid two-phase cross-flow ultrafiltration of BSA and dextran solutions', *Journal of Membrane Science*, vol. 90, no. 1-2, pp. 183-189.
Culkin, B. & Armando, A.D. 1992, 'New separation system extends the use of membranes', *Filtration and Separation*, vol. 29, pp. 376-378.

De Swart, J.W.A., van Vliet, R.E. & Krishna, R. 1996, 'Size, structure and dynamics of large bubbles in a two-dimensional slurry bubble column', *Chemical Engineering Science*, vol. 51, no. 20, pp. 4619-4629.

Defrance, L. & Jaffrin, M.Y. 1999, 'Comparison between filtrations at fixed transmembrane pressure and fixed permeate flux: Application to a membrane bioreactor used for wastewater treatment', *Journal of Membrane Science*, vol. 152, no. 2, pp. 203-210.

Defrance, L., Jaffrin, M.Y., Gupta, B., Paullier, P. & Geaugey, V. 2000, 'Contribution of various constituents of activated sludge to membrane bioreactor fouling', *Bioresource Technology*, vol. 73, no. 2, pp. 105-112.

Drews, A. 2010a, 'Membrane fouling in membrane bioreactors: Characterisation, contradictions, cause and cures', *Journal of Membrane Science*, vol. 363, no. 1-2, pp. 1-28.

Duan, J. & Gregory, J. 2003, 'Coagulation by hydrolysing metal salts', *Advances in Colloid and Interface Science*, vol. 100–102, pp. 475-502.

Ducom, G., Puech, F.P. & Cabassud, C. 2002, 'Air sparging with flat sheet nanofiltration: A link between wall shear stresses and flux enhancement', *Desalination*, vol. 145, no. 1-3, pp. 97-102.

EUROBRA 2008, *Membrane bioreactor technology (MBR) with an EU perspective for advanced municipal wastewater treatment strategies for the 21st century*, viewed 20 March 2010, <http://www.ist-world.org/ProjectDetails.aspx?ProjectId=7158900d67c2499d8aae26dbee30ee36.>.

Faibish, R.S. & Cohen, Y. 2001, 'Fouling and rejection behavior of ceramic and polymer-modified ceramic membranes for ultrafiltration of oil-in-water emulsions and microemulsions', *Colloids and Surfaces A: Physicochemical and Engineering Aspects*, vol. 191, no. 1-2, pp. 27-40.

Fan, F., Zhou, H. & Husain, H. 2007, 'Use of chemicalcoagulants to control fouling potential for wastewater membrane bioreactor processes', *Water Environment Research*, vol. 79, no. 9, pp. 952-957.

Fan, L.S. & Tsuchiya, K. 1990, *Bubble wake dynamics in liquid and liquid solid suspensions*, Butterworth-Heinemann Stoneham MA, pp. 17-69.

Fane, A.G., Chang, S. & Chardon, E. 2002, 'Submerged hollow fibre membrane module: Design options and operational considerations', *Desalination*, vol. 146, no. 1-3, pp. 231-236.

Fane, A.G. & Fell, C.J.D. 1987, 'A review of fouling and fouling control in ultrafiltration', *Desalination*, vol. 62, pp. 117-136.

Fane, A.G., Fell, C.J.D., Hodgson, P.H., Leslie, G. & Marshall, K.C. 1991, 'Microfiltration of biomass and biofluids: Effects of membrane morphology and operating conditions', *Filtration and Separation*, vol. 28, no. 5, pp. 332-331.

Fane, A.G., Fell, C.J.D. & Nor, M.T. 1981, 'Ultrafiltration/activated sludge system: Development of a predictive model', *Polymer Science and Technology*, vol. 13, pp. 631-658.

Fane, A.G., Yeo, A., Law, A., Parameshwaran, K., Wicaksana, F. & Chen, V. 2005, 'Low pressure membrane processes: Doing more with less energy', *Desalination*, vol. 185, no. 1-3, pp. 159-165.

Fernando, K., Tran, T. & Zwolak, G. 2005, 'The use of ion exchange resins for the treatment of cyanidation tailings. Part 2-pilot plant testing', *Minerals Engineering*, vol. 18, no. 1, pp. 109-117.

Finnigan, S.M. & Howell, J.A. 1990, 'The effect of pulsed flow on ultrafiltration fluxes in a baffled tubular membrane system', *Desalination*, vol. 79, no. 2–3, pp. 181-202.

Foley, G., MacLoughlin, P.F. & Malone, D.M. 1992, 'Preferencial deposition of smaller cells during crossflow microfiltraion of yeast suspensions', *Biotechnology Techniques*, vol. 6, no. 2, pp. 115-120.

Fradin, B. & Field, R.W. 1999, 'Crossflow microfiltration of magnesium hydroxide suspensions: Determination of critical fluxes, measurement and modelling of fouling', *Separation and Purification Technology*, vol. 16, no. 1, pp. 25-45.

Gander, M., Jefferson, B. & Judd, S. 2000, 'Aerobic MBRs for domestic wastewater treatment: A review with cost considerations', *Separation and Purification Technology*, vol. 18, no. 2, pp. 119-130.

Germain, E., Stephenson, T. & Pearce, P. 2005a, 'Biomass characteristics and membrane aeration: Toward a better understanding of membrane fouling in submerged membrane bioreactors (MBRs)', *Biotechnology and Bioengineering*, vol. 90, no. 3, pp. 316-322.

Germain, E., Stephenson, T. & Pearce, P. 2005b, 'Biomasscharacteristics and membrane aeration: toward a better understanding of membrane fouling in submergedmembrane bioreactors (MBRs)', *Biotechnology and Bioengineering*, vol. 90, no. 3, pp. 316-322.

Ghosh, R. 2006, 'Enhancement of membrane permeability by gas-sparging in submerged hollow fibre ultrafiltration of macromolecular solutions: Role of module design', *Journal of Membrane Science*, vol. 274, no. 1-2, pp. 73-82.

Gray, S.R. & Bolto, B.A. 2003, 'Predicting NOM fouling rates of low pressure membranes', *Proceedings of the International Membrane Science and Technology (IMSTEC)*, Sydney, Australia.

Grim, R. 1968, *Clay mineralogy.*, McGraw-Hill, New York.

Guibert, D., Aim, R.B., Rabie, H. & Cote, P. 2002, 'Aeration performance of immersed hollow-fiber membranes in a bentonite suspension', *Desalination*, vol. 148, no. 1-3, pp. 395-400.

Guibert, D., Aim, R.B., Rabie, H. & Côté, P. 2002, 'Aeration performance of immersed hollow-fiber membranes in a bentonite suspension', *Desalination*, vol. 148, no. 1-3, pp. 395-400.

Guo, W.S., Shim, W.G., Vigneswaran, S. & Ngo, H.H. 2005, 'Effect of operating parameters in a submerged membrane adsorption hybrid system: Experiments and mathematical modeling', *Journal of Membrane Science*, vol. 247, no. 1-2, pp. 65-74.

Guo, W.S., Vigneswaran, S., Ngo, H.H., Van Nguyen, T.B. & Ben Aim, R. 2006, 'Influence of bioreaction on a long-term operation of a submerged membrane adsorption hybrid system', *Desalination*, vol. 191, no. 1-3, pp. 92-99.

Haberkamp, J., Ruhl, A.S., Ernst, M. & Jekel, M. 2007, 'Impact of coagulation and adsorption on DOC fractions of secondary effluent and resulting fouling behaviour in ultrafiltration', *Water Research*, vol. 41, no. 17, pp. 3794-3802.

Hasar, H., Kinaci, C., Unlu, A., Togrul, H. & Ipek, U. 2004, 'Rheological properties of activated sludge in a sMBR', *Biochemical Engineering Journal*, vol. 20, no. 1, pp. 1-6.

Hong, S.P., Bae, T.H., Tak, T.M., Hong, S. & Randall, A. 2002, 'Fouling control in activated sludge submerged hollow fiber membrane bioreactors', *Desalination*, vol. 143, no. 3, pp. 219-228.

Howell, J.A., Chua, H.C. & Arnot, T.C. 2004, 'In situ manipulation of critical flux in a submerged membrane bioreactor using variable aeration rates, and effects of membrane history', *Journal of Membrane Science*, vol. 242, no. 1-2, pp. 13-19.

Huisman, I.H., Tragardh, G. & Tragardh, C. 1999, 'Particle transport in crossflow microfiltration – II. Effects of particle–particle interactions', *Chemical Engineering Science*, vol. 54, no. 2, pp. 281-289.

Hwang, K.J. & Lin, K.P. 2002, 'Cross-flow microfiltration of dual-sized submicron particles.', *Separation Science and Technology*, vol. 37, no. 1-2, pp. 2231-2249.

Hwang, K.J. & Sz, P.Y. 2010, 'Membrane fouling mechanism and concentration effect in cross-flow microfiltration of BSA/dextran mixtures', *Chemical Engineering Journal*, vol. 166, no. 2, pp. 669-677.

Imasaka, T., Kanekuni, N., So, H. & Yoshino, S. 1989, 'Cross-flow filtration of methane fermentation broth by ceramic membranes', *Journal of Fermentation and Bioengineering*, vol. 68, no. 3, pp. 200-206.

Itonaga, T., Kimura, K. & Watanabe, Y. 2004, 'Influence of suspension viscosity and colloidal particles on permeability of membrane used in membrane bioreactor (MBR)', *Water Science and Technology*, vol. 50, no. 12, pp. 301-309.

Ivanovic, I. & Leiknes, T. 2008a, 'Impact of aeration rates on particle colloidal fraction in the biofilm membrane bioreactor (BF-MBR)', *Desalination*, vol. 231, no. 1-3, pp. 182-190.

Ivanovic, I., Leiknes, T. & Odegaard, H. 2008, 'Fouling control by reduction of submicron particles in a BF-MBR with an integrated flocculation zone in the membrane reactor ', *Separation Science and Technology*, vol. 43, no. 7, pp. 1871-1883.

Jarusutthirak, C., Amy, G. & Croué, J.-P. 2002, 'Fouling characteristics of wastewater effluent organic matter (EfOM) isolates on NF and UF membranes', *Desalination*, vol. 145, no. 1–3, pp. 247-255.

Ji, L. & Zhou, J. 2006, 'Influence of aeration on microbial polymers and membrane fouling in submerged membrane bioreactors', *Journal of Membrane Science*, vol. 276, no. 1-2, pp. 168-177.

Johir, M.A.H., Aryal, R., Vigneswaran, S., Kandasamy, J. & Grasmick, A. 2011, 'Influence of supporting media in suspension on membrane fouling reduction in submerged membrane bioreactor (SMBR)', *Journal of Membrane Science*, vol. 374, no. 1–2, pp. 121-128.

Johnson, P.N. & Amirtharajah, A. 1983, 'Ferric chloride and alum as single and dual coagulants', *Journal (American Water Works Association)*, vol. 75, no. 5, pp. 232-239.

Jucker, C. & Clark, M.M. 1994, 'Adsorption of aquatic humic substances on hydrophobic ultrafiltration membranes', *Journal of Membrane Science*, vol. 97, pp. 37-52.

Judd, S. 2006, *The MBR book: Principles and applications of membrane bioreactors in water and wastewater treatment*, Elsevier Oxford UK.

Judd, S.J. & Till, S.W. 2000, 'Bacterial rejection in crossflow microfiltration of sewage', *Desalination*, vol. 127, no. 3, pp. 251-260.

Kim, J.S., Akeprathumchai, S. & Wickramasinghe, S.R. 2001a, 'Flocculation to enhance microfiltration', *Journal of Membrane Science*, vol. 182, no. 1-2, pp. 161-172.

Kim, J.S., Lee, C.H. & Chang, I.S. 2001b, 'Effect of pump shear on the performance of a crossflow membrane bioreactor', *Water Research*, vol. 35, no. 9, pp. 2137-2144.

Kim, J.S., Lee, C.H. & Chun, H.D. 1998, 'Comparison of ultrafiltration characteristics between activated sludge and BAC sludge', *Water Research*, vol. 32, no. 11, pp. 3443-3451.

Krantz, W.B., Bilodeau, R.R., Voorhees, M.E. & Elgas, R.J. 1997, 'Use of axial membrane vibrations to enhance mass transfer in a hollow tube oxygenator', *Journal of Membrane Science*, vol. 124, no. 2, pp. 283-299.

Krause, S., Tournier, R., Cornel, P. & Siembida, B. 2008a, 'Granulate-driven fouling control in a submerged membrane module for MBR application', *6th World Water Congress*, Vienna, Austria.

Krause, S., Zimmermann, B., Meyer-Blumenroth, U., Lamparter, W., Siembida, B. & Cornel, P. 2008b, 'Enhanced MBR process without chemical cleaning', paper presented to the *Design and operation of membrane plants for water, wastewater and industrial water*, Amsterdam, The Netherlands, October 1-2, 2008.

Krstić, D.M., Tekić, M.N., Carić, M.Đ. & Milanović, S.D. 2002, 'The effect of turbulence promoter on cross-flow microfiltration of skim milk', *Journal of Membrane Science*, vol. 208, no. 1–2, pp. 303-314.

Kumar, S., Kusakabe, K., Raghunathan, K. & Fan, L.S. 1992, 'Mechanism of heat transfer in bubbly liquid and liquid-solid systems: Single bubble injection', *AIChE Journal*, vol. 38, no. 5, pp. 733-741.

Laborie, S., Cabassud, C., Durand-Bourlier, L. & Laine, J.M. 1997, 'Flux enhancement by a continuous tangential gas flow in ultrafiltration hollow fibres for drinking water production: Effects of slug flow on cake structure', *Filtration and Separation*, vol. 34, no. 8, pp. 887-891.

Laborie, S., Cabassud, C., Durand-Bourlier, L. & Lainé, J.M. 1998, 'Fouling control by air sparging inside hollow fibre membranes: Effects on energy consumption', *Desalination*, vol. 118, no. 1-3, pp. 189-196.

Le-Clech, P., Chen, V. & Fane, T.A.G. 2006, 'Fouling in membrane bioreactors used in wastewater treatment', *Journal of Membrane Science*, vol. 284, no. 1-2, pp. 17-53.

Le-Clech, P., Jefferson, B. & Judd, S.J. 2003, 'Impact of aeration, solids concentration and membrane characteristics on the hydraulic performance of a membrane bioreactor', *Journal of Membrane Science*, vol. 218, no. 1-2, pp. 117-129.

Lebeau, T., Lelièvre, C., Buisson, H., Cléret, D., Van de Venter, L.W. & Côté, P. 1998, 'Immersed membrane filtration for the production of drinking water: Combination with PAC for NOM and SOCs removal', *Desalination*, vol. 117, no. 1–3, pp. 219-231.

Lebegue, J., Heran, M. & Grasmick, A. 2009, 'Membrane air flow rates and HF sludging phenomenon in SMBR', *Desalination*, vol. 236, no. 1-3, pp. 135-142.

Lebegue, J., Heran, M. and Grasmick, A. 2007, 'Membrane air flow rates and HF sludging phenomenon in SMBR', paper presented to the *Sixth International Membrane Science and Technology conference*, Sydney, Australia, November 5-9, 2007.

Lee, C., Chang, W. & Ju, Y. 1993, 'Air slugs entrapped cross-flow filtration of bacteria suspension', *Biotechnology and Bioengineering*, vol. 41, pp. 525-530.

Lee, J.C., Kim, J.S., Kang, I.J., Cho, M.H., Park, P.K. & Lee, C.H. 2001, 'Potential and limitations of alum or zeolite addition to improve the performance of a submerged membrane bioreactor,' *Water Science and Technology*, vol. 43, pp. 59-66.

Lee, M.C., Snoeyink, V.L. & Crittenden, J.C. 1981, 'Activated carbon adsorption of humic substances', *Journal of the American Water Works Association*, vol. 73, pp. 440-446.

Lee, W.N., Chang, I.S., Hwang, B.K., Park, P.K., Lee, C.H. & Huang, X. 2007, 'Changes in biofilm architecture with addition of membrane fouling reducer in a membrane bioreactor', *Process Biochemistry*, vol. 42, no. 4, pp. 655-661.

Leiknes, T., Lazarova, M. & Odegaard, H. 2004, 'Development of a hybrid ozonation biofilm-membrane filtration process for the production of drinking water.', *Proceedings of Water Environment-Membrane Technology (WEMT) Conference*, Seoul, Korea, pp. 79-86.

Li, H., Fane, A.G., Coster, H.G.L. & Vigneswaran, S. 1998, 'Direct observation of particle deposition on the membrane surface during crossflow microfiltration', *Journal of Membrane Science*, vol. 149, no. 1, pp. 83-97.

Li, Q.Y., Cui, Z.F. & Pepper, D.S. 1997, 'Effect of bubble size and frequency on the permeate flux of gas sparged ultrafiltration with tubular membranes', *Chemical Engineering Journal*, vol. 67, no. 1, pp. 71-75.

Liang, L. & Singer, P.C. 2003, 'Factors influencing the formation and relative distribution of haloacetic acids and trihalomethanes in drinking water', *Environmental Science and Technology*, vol. 37, no. 13, pp. 2920-2928.

Limited, M. 1990, *Cleaning of hollow fibre filters*, Patent PCT/AU87/00214.

Lipson, S.M. & Stotzky, G. 1983, 'Adsorption of reovirus to clay minerals: Effects of cation-exchange capacity, cation saturation, and surface area', *Applied Environmental Microbiology*, vol. 46, no. 3, pp. 673-682.

Liu, R., Huang, X., Wang, C., Chen, L. & Qian, Y. 2000, 'Study on hydraulic characteristics in a submerged membrane bioreactor process', *Process Biochemistry*, vol. 36, no. 3, pp. 249-254.

Low, S.C., Han, H.J. & Jin, W.X. 2004, 'Characteristics of a vibration membrane in water recovery from fine carbon-loaded wastewater', *Desalination*, vol. 160, no. 1, pp. 83-89.

Lu, W.M. & Hwang, K.J. 1995, 'Cake formation in 2-D cross-flow filtration', *AICheE Journal*, vol. 41, no. 6, pp. 1443-1455.

Lu, W.M. & Ju, S.C. 1989, 'Selective particle deposition in cross-flow filtration', *Separation Science and Technology*, vol. 24, no. 7-8, pp. 517-540.

Lu, Y., Ding, Z., Liu, L., Wang, Z. & Ma, R. 2008, 'The influence of bubble characteristics on the performance of submerged hollow fiber membrane module used in microfiltration', *Separation and Purification Technology*, vol. 61, no. 1, pp. 89-95.

Madec, A., Buisson, H., Ben Aim, R. 2000, 'Aeration to enhance membrane critical flux', *Proceedings of World Filtration Congress 8, UK.*, vol. 1, pp. 199-202.

Malysa, K., Krasowska, M. & Krzan, M. 2005, 'Influence of surface active substances on bubble motion and collision with various interfaces', *Advances in Colloid and Interface Science*, vol. 114-115, pp. 205-225.

Matsumoto, Y., Nakao, S. & Kimura, S. 1988, 'Cross-flow filtration of solutions of polymers using ceramic microfiltration', *International Chemical Engineering*, vol. 28, pp. 677-683.

Mavrov, V., Nikolov, N.D., Islam, M.A. & Nikolova, J.D. 1992, 'An investigation on the configuration of inserts in tubular ultrafiltration module to control concentration polarization', *Journal of Membrane Science*, vol. 75, no. 1–2, pp. 197-201.

Meng, F., Shi, B., Yang, F. & Zhang, H. 2007, 'New insights into membrane fouling in submerged membrane bioreactor based on rheology and hydrodynamics concepts', *Journal of Membrane Science*, vol. 302, no. 1-2, pp. 87-94.

Meng, F., Yang, F., Shi, B. & Zhang, H. 2008, 'A comprehensive study on membrane fouling in submerged membrane bioreactors operated under different aeration intensities', *Separation and Purification Technology*, vol. 59, no. 1, pp. 91-100.

Meng, F., Zhang, H., Yang, F., Li, Y., Xiao, J. & Zhang, X. 2006, 'Effect of filamentous bacteria on membrane fouling in submerged membrane bioreactor', *Journal of Membrane Science*, vol. 272, no. 1-2, pp. 161-168.

Mercier-Bonin, M., Lagane, C. & Fonade, C. 2000, 'Influence of a gas/liquid two-phase flow on the ultrafiltration and microfiltration performances: Case of a ceramic flat sheet membrane', *Journal of Membrane Science*, vol. 180, no. 1, pp. 93-102.

Mercier, M., Fonade, C. & Lafforgue-Delorme, C. 1995, 'Influence of the flow regime on the efficiency of a gas-liquid two-phase medium filtration', *Biotechnology Techniques*, vol. 9, p. 853.

Mercier, M., Fonade, C. & Lafforgue-Delorme, C. 1997, 'How slug flow can enhance the ultrafiltration flux in mineral tubular membranes', *Journal of Membrane Science*, vol. 128, no. 1, pp. 103-113.

Mercier, M., Maranges, C. & Fonade, C. 1998, 'Yeast suspension filtration, flux enhancement using an upward gas/liquid slug flow application to continuous alcohholic fermentation with cell recycle', *Biotechnology and Bioengineering*, vol. 58, pp. 47-57.

Mesdaghinia, A., Rafiee, M.T., Vaezi, F., Mahvi, A., Torabian, A. & Ghasri, A. 2005, 'Control of disinfection by products formation potential by enhanced coagulation', *International Journal of Environmental Science and Technology*, vol. 2, no. 4, pp. 335-342.

Mikulasek, P., Pospisil, P., Dolecekk, P. & Cakl, J. 2002, 'Gas-liquid two-phase flow in microfiltration mineral tubular membranes: Relationship between flux enhancement and hydrodynamic parameters', *Desalination*, vol. 146, no. 1-3, pp. 103-109.

Millward, H.R., Bellhouse, B.J. & Sobey, I.J. 1996, 'The vortex wave membrane bioreactor: Hydrodynamics and mass transfer', *The Chemical Engineering Journal and the Biochemical Engineering Journal*, vol. 62, no. 3, pp. 175-181.

Miyahara, T., Tsuchiya, K. & Fan, L.S. 1988, 'Wake properties of a single gas bubble in a three-dimensional liquid-solid fluidised bed,' *International Journal of Multiphase Flow*, vol. 41, p. 749.

Morel, F.M.M. & Hering, J.G. 1993, *Principles and applications of aquatic chemistry*, John Wiley & Sons, New York.

Mulder, M. 1996, *Basic principles of membrane science and technology*, 2nd edn, Kluwer Academic, Dordredit

Ndinisa, N.V., Fane, A.G. & Wiley, D.E. 2006, 'Fouling control in a submerged flat sheet membrane system: Part I- Bubbling and hydrodynamic effects', *Separation Science and Technology*, vol. 41, no. 7, pp. 1383-1409.

Ndinisa, N.V., Fane, A.G., Wiley, D.E. & Fletcher, D.F. 2006b, 'Fouling Control in a submerged flat sheet membrane system: Part II-Two-phase flow characterization and CFD simulations', *Separation Science and Technology*, vol. 41, no. 6, pp. 1411-1445.

Ng, C.A., Sun, D. & Fane, A.G. 2006, 'Operation of membrane bioreactor with powdered activated carbon addition', *Separation Science and Technology*, vol. 41, pp. 1447-1466.

PallSep 2004, 'http://www.pall.com'.
Parameshwaran, K., Fane, A.G., Cho, B.D. & Kim, K.J. 2001, 'Analysis of microfiltration performance with constant flux processing of secondary effluent', *Water Research*, vol. 35, no. 18, pp. 4349-4358.
Park, D., Lee, D.S. & Park, J.M. 2005, 'Continuous biological ferrous iron oxidation in a submerged membrane bioreactor', *Water Science and Technology*, vol. 51, no. 59-68.
Park, H.S., Choo, K.H. & Lee, C.H. 1999, 'Flux enhancement with powdered activated carbon addition in the membrane anaerobic bioreactor', *Separation Science and Technology*, vol. 34, pp. 2781-2792.
Peuchot, M.M. & Ben Aim, R. 1992, 'Improvement of crossflow microfiltration performances with flocculation', *Journal of Membrane Science*, vol. 68, no. 3, pp. 241-248.
Pirbazari, M., Ravindran, V., Badriyha, B.N. & Kim, S.-H. 1996, 'Hybrid membrane filtration process for leachate treatment', *Water Research*, vol. 30, no. 11, pp. 2691-2706.
Pospísil, P., Wakeman, R.J., Hodgson, I.O.A. & Mikulásek, P. 2004, 'Shear stress-based modelling of steady state permeate flux in microfiltration enhanced by two-phase flows', *Chemical Engineering Journal*, vol. 97, no. 2-3, pp. 257-263.
Postlethwaite, J., Lamping, S.R., Leach, G.C., Hurwitz, M.F. & Lye, G.J. 2004, 'Flux and transmission characteristics of a vibrating microfiltration system operated at high biomass loading', *Journal of Membrane Science*, vol. 228, no. 1, pp. 89-101.
Pradhan, M., Aryal, R., Vigneswaran, S. & Kandasamy, J. 2011, 'Application of air flow for mitigation of particle deposition in submerged membrane microfiltration', *Desalination and Water Treatment* vol. 32, pp. 201-207.
Pradhan, M., Vigneswaran, S., Kandasamy, J. & Aim, R.B. 2012, 'Combined effect of air and mechanical scouring of membranes for fouling reduction in submerged membrane reactor', *Desalination*, vol. 288, pp. 58-65.
Redondo, J.A. & Lomax, I. 2001, 'Y2K generation FILMTEC RO membranes combined with new pretreatment techniques to treat raw water with high fouling potential: Summary of experience', *Desalination*, vol. 136, no. 1–3, pp. 287-306.
Riesmeier, B., Kroner, K.H. & Kula, M.R. 1987, 'Studies on secondary layer formation and its characterization during cross-flow filtration of microbial cells', *Journal of Membrane Science*, vol. 34, no. 3, pp. 245-266.
Rosenberger, S., Krüger, U., Witzig, R., Manz, W., Szewzyk, U. & Kraume, M. 2002, 'Performance of a bioreactor with submerged membranes for aerobic treatment of municipal waste water', *Water Research*, vol. 36, no. 2, pp. 413-420.
Rosenberger, S., Laabs, C., Lesjean, B., Gnirss, R., Amy, G., Jekel, M. & Schrotter, J.C. 2006, 'Impact of colloidal and soluble organic material on membrane performance in membrane bioreactors for municipal wastewater treatment', *Water Research*, vol. 40, no. 4, pp. 710-720.
Samatya, S., Kabay, N., Yuksel, U., Arda, M. & Yuksel, M. 2006, 'Removal of nitrate fromaqueous solution by nitrate selective ion exchange resins', *Reactive and Functional Polymer*, vol. 66, pp. 1206-1214.
Schafer, A.I., Fane, A.G. & Waite, T.D. 2000, 'Fouling effects on rejection in the membrane filtration of natural waters', *Desalination*, vol. 131, no. 1â€“3, pp. 215-224.

Schafer, R., Merten, C. & Eigenberger, G. 2002, 'Bubble size distributions in a bubble column reactor under industrial conditions', *Experimental Thermal and Fluid Science*, vol. 26, no. 6-7, pp. 595-604.

Schiffenbauer, M. & Stotzky, G. 1982, 'Adsorption of coliphages T1 and T7 to clay minerals', *Applied Enviromental Microbiology*, vol. 43, no. 3, pp. 590-596.

Scott, J.A., Neilson, D.J., Liu, W. & Boon, P.N. 1998, 'A dual function membrane bioreactor system for enhanced aerobic remediation of high-strength industrial waste', *Water Science and Technology*, vol. 38, no. 4–5, pp. 413-420.

Seo, G.T., Suzuki, Y. & Ohgaki, S. 1996, 'Biological powdered activated carbon (BPAC) microfiltration for wastewater reclamation and reuse', *Desalination*, vol. 106, no. 1–3, pp. 39-45.

Shannon, M.A., Bohn, P.W., Elimelech, M., Georgiadis, J.G., Marieas, B.J. & Mayes, A.M. 2008, 'Science and technology for water purification in the coming decades', *Nature*, vol. 452, pp. 301-310.

Sheely, M.L. 1932, 'Glycerol viscosity tables', *Industrial and Engineering Chemistry*, vol. 24, no. 9, pp. 1060-1064.

Sherwood, J.D. 1988, 'The force on a sphere pulled away from a permeable half-space ', *Physicochemical Hydrodynamics*, vol. 10, pp. 3-12.

Shimizu, Y., Uryu, K., Okuno, Y.-I. & Watanabe, A. 1996, 'Cross-flow microfiltration of activated sludge using submerged membrane with air bubbling', *Journal of Fermentation and Bioengineering*, vol. 81, no. 1, pp. 55-60.

Siembida, B., Cornel, P., Krause, S. & Zimmermann, B. 2010, 'Effect of mechanical cleaning with granular material on the permeability of submerged membranes in the MBR process', *Water Research*, vol. 44, no. 14, pp. 4037-4046.

Smith, C.W., Gregorio, D. & Talcott, R.M. 1969, 'The use of ultrafiltration membranes for activated sludge separation', *The 24th Purdue Industrial Waste Conference*, p. 1300.

Smith, P.J., Vigneswaran, S., Ngo, H.H., Ben-Aim, R. & Nguyen, H. 2005, 'Design of a generic control system for optimising back flush durations in a submerged membrane hybrid reactor', *Journal of Membrane Science*, vol. 255, no. 1–2, pp. 99-106.

Sofia, A., Ng, W.J. & Ong, S.L. 2004, 'Engineering design approaches for minimum fouling in submerged MBR', *Desalination*, vol. 160, no. 1, pp. 67-74.

Stephenson, T., Judd, S., Jefferson, B. & Brindle, K. 2000, *Membrane bioreactors for wastewater treatment*, IWA Publishing, London.

Sur, H.W. & Cui, Z.F. 2001, 'Experimental study on the enhancement of yeast microfiltration with gas sparging', *Journal of Chemical Technology and Biotechnology*, vol. 76, p. 477.

Sur, H.W. & Cui, Z.F. 2005, 'Enhancement of microfiltration of yeast suspensions using gas sparging - Effect of feed conditions', *Separation and Purification Technology*, vol. 41, no. 3, pp. 313-319.

Sur, H.W., Li, Q.Y. & Cui, Z.F. 1998, 'Gas sparging to enhance crossflow ultrafiltration in turbulent flow', *The 1998 IChemE Research Events, Paper-159 (CD-ROM), IChemE, UK*.

Taitel, Y., Bonea, D. & Dulker, A.E. 1980, 'Modeling flow pattern transitions for steady upward gas-liquid flow in vertical tubes', *AIChE Journal*, vol. 26, p. 345.

Tanaka, T., Kamimura, R., Fujiwara, R. & Nakanishi, K. 1994, 'Crossflow filtration of yeast broth cultivated in molasses', *Biotechnology and Bioengineering*, vol. 43, pp. 1094-1101.

Tandanier, C.J., Berry, D.F. & Knocke, W.R. 2000, 'Dissolved organic matter apparent molecular distribution and number-average apparent molecular weight by batch ultrafiltration.', *Environmental Science and Technology*, vol. 34, no. 11, pp. 2348-2353.

Tao, G., Kekre, K., Wei, Z., Lee, T., Viswanath, B., Seah, H., 2005, 'Membrane bioreactors for water reclamation', *Water Science and Technology*, vol. 51 no. 6-7, pp. 431-440.

Tardieu, E., Grasmick, A., Geaugey, V. & Manem, J. 1998, 'Hydrodynamic control of bioparticle deposition in a MBR applied to wastewater treatment', *Journal of Membrane Science*, vol. 147, no. 1, pp. 1-12.

Ueda, T., Hata, K. & Kikuoka, Y. 1996, 'Treatment of domestic sewage from rural settlements by a membrane bioreactor', *Water Science and Technology*, vol. 34, no. 9, pp. 189-196.

Ueda, T., Hata, K., Kikuoka, Y. & Seino, O. 1997, 'Effects of aeration on suction pressure in a submerged membrane bioreactor', *Water Research*, vol. 31, no. 3, pp. 489-494.

Vigneswaran, S., Guo, W.S., Smith, P. & Ngo, H.H. 2007, 'Submerged membrane adsorption hybrid system (SMAHS): Process control and optimization of operating parameters', *Desalination*, vol. 202, no. 1–3, pp. 392-399.

Visvanathan, C., Yang, B.S., Muttamara, S. & Maythanukhraw, S. 1997, 'Application of air backflushing technique in membrane bioreactor', *Water Science and Technology*, vol. 36, no. 12, pp. 259-266.

Wang, P., Tan, K.L., Kang, E.T. & Neoh, K.G. 2002, 'Plasma-induced immobilization of poly(ethylene glycol) onto poly(vinylidene fluoride) microporous membrane', *Journal of Membrane Science*, vol. 195, no. 1, pp. 103-114.

Weber, J.B., Perry, P.W. & Upchurch, R.P. 1965, 'The influence of temperature and time on the adsorption of paraquat, diquat, 2,4-D and prometone by clays, charcoal, and an anion-exchange resin', *Proceeding of the Soil Science Society of America*, pp. 678-688.

Wicaksana, F., Fane, A.G. & Chen, V. 2006a, 'Fibre movement induced by bubbling using submerged hollow fibre membranes', *Journal of Membrane Science*, vol. 271, no. 1-2, pp. 186-195.

Wicaksana, F., Fane, A.G. & Chen, V. 2006b, 'Fibre movement induced by bubbling using submerged hollow fibre membranes', *Journal of Membrane Science*, vol. 271, pp. 186-195.

Wickramasinghe, S.R. 1999, 'Washing cryopreserved blood products using hollow fibres', *Food and Bioproducts Processing*, vol. 77, pp. 287-292.

Wickramasinghe, S.R., Wu, Y. & Han, B. 2002, 'Enhanced microfiltration of yeast by flocculation', *Desalination*, vol. 147, no. 1-3, pp. 25-30.

Wiesner, M.R., Tarabara, V. & Cortalezzi, M. 2005, 'Processes of particle depostion in membrane operation and fabrication', *Water Science and Technology*, vol. 51, no. 6-7, pp. 345-348.

Wisniewski, C. & Grasmick, A. 1998, 'Floc size distribution in a membrane bioreactor and consequences for membrane fouling', *Colloids and Surfaces A: Physicochemical and Engineering Aspects*, vol. 138, no. 2-3, pp. 403-411.

Wisniewski, C., Grasmick, A. & Leon Cruz, A. 2000, 'Critical particle size in membrane bioreactors: Case of a denitrifying bacterial suspension', *Journal of Membrane Science*, vol. 178, no. 1-2, pp. 141-150.

Worrel, L.S., Morehouse, J.A., Shimko, L.A., Lloyd, D.R., Lawler, D.F. & Freeman, B.D. 2007, 'Enhancement of track-etched membrane performance via stretching', *Separation and Purification Technology*, vol. 53, no. 1, pp. 71-80.

Wu, J., Chen, F., Huang, X., Geng, W. & Wen, X. 2006, 'Using inorganic coagulants to control membrane fouling in a submerged membrane bioreactor', *Desalination*, vol. 197, no. 1-3, pp. 124-136.

Yamamoto, K., Hiasa, M., Mahmood, T. & Matsuo, T. 1989, 'Direct solid-liquid separation using hollow fiber membrane in an activated sludge aeration tank', *Water Science and Technology*, vol. 21, no. 4-5, p. 43.

Yamato, N., Kimura, K., Miyoshi, T. & Watanabe, Y. 2006, 'Difference in membrane fouling in membrane bioreactors (MBRs) caused by membrane polymer materials', *Journal of Membrane Science*, vol. 280, no. 1-2, pp. 911-919.

Yeo, A.P.S., Law, A.W.K. & Fane, A.G. 2006, 'Factors affecting the performance of a submerged hollow fiber bundle', *Journal of Membrane Science*, vol. 280, no. 1-2, pp. 969-982.

Yeom, I.T., Lee, K.R., Choi, Y.G., Kim, H.S. & Lee, Y. 2004, 'Evalution of a membrane bioreactor system coupled with sludge pretreatment for aerobic sludge digestion', *Proceedings of the Water Environment-Membrane Technology Conference*, Seoul, Korea.

Yoon, S.-H., Kim, H.-S. & Yeom, I.-T. 2004, 'Optimization model of submerged hollow fiber membrane modules', *Journal of Membrane Science*, vol. 234, no. 1-2, pp. 147-156.

Yoon, S.H., Kim, H.S., Park, J.K., Kim, H. & Sung, J.Y. 1999, 'Influence of important operational parameters on performance of a membrane biological reactor', *Proceedings of Membrane Technology in Environmental Management Conference*, Tokyo, pp. 278-285.

Yu, H.-Y., Hu, M.-X., Xu, Z.-K., Wang, J.-L. & Wang, S.-Y. 2005a, 'Surface modification of polypropylene microporous membranes to improve their antifouling property in MBR: NH3 plasma treatment', *Separation and Purification Technology*, vol. 45, no. 1, pp. 8-15.

Yu, H.-Y., Xie, Y.-J., Hu, M.-X., Wang, J.-L., Wang, S.-Y. & Xu, Z.-K. 2005b, 'Surface modification of polypropylene microporous membrane to improve its antifouling property in MBR: CO2 plasma treatment', *Journal of Membrane Science*, vol. 254, no. 1-2, pp. 219-227.

Yuan, W. & Zydney, A.L. 2000, 'Humic acid fouling during ultrafiltration', *Environmental Science and Technology*, vol. 34, p. 5043.

Yuasa, A., Li, F., Matsui, Y. & Ebie, K. 1997, 'Characteristics of competitive adsorption of aquatic humic substances onto activated carbon', *Water Science and Technology*, vol. 36, no. 12, pp. 231-238.

Zhang, J., Chua, H.C., Zhou, J. & Fane, A.G. 2006, 'Factors affecting the membrane performance in submerged membrane bioreactors', *Journal of Membrane Science*, vol. 284, no. 1-2, pp. 54-66.

Zhang, K., Cui, Z. & Field, R.W. 2009, 'Effect of bubble size and frequency on mass transfer in flat sheet MBR', *Journal of Membrane Science*, vol. 332, no. 1-2, pp. 30-37.

Zhang, K., Wei, P., Yao, M., Field, R.W. & Cui, Z. 2011, 'Effect of the bubbling regimes on the performance and energy cost of flat sheet MBRs', *Desalination*, vol. 283, pp. 221-226.

Zhang, R., Vigneswaran, S., Ngo, H. & Nguyen, H. 2007, 'A submerged membrane hybrid system coupled with magnetic ion exchange (MIEX®) and flocculation in wastewater treatment', *Desalination*, vol. 216, no. 1–3, pp. 325-333.

Zhang, R., Vigneswaran, S., Ngo, H. & Nguyen, H. 2008, 'Fluidized bed magnetic ion exchange (MIEX®) as pre-treatment process for a submerged membrane reactor in wastewater treatment and reuse', *Desalination*, vol. 227, no. 1–3, pp. 85-93.

Zhu, X. & Elimelech, M. 1995, 'Fouling of Reverse Osmosis Membranes by Aluminum Oxide Colloids', *Journal of Environmental Engineering*, vol. 121, no. 12, pp. 884-892.

Appendix

List of Publications

1. Pradhan, M., Aryal, R., Vigneswaran, S. & Kandasamy, J. 2011, 'Application of air flow for mitigation of particle deposition in submerged membrane microfiltration', *Desalination and Water Treatment* vol. 32, pp. 201-207
2. Pradhan, M., Vigneswaran, S., Kandasamy, J. & Aim, R.B. 2012, 'Combined effect of air and mechanical scouring of membranes for fouling reduction in submerged membrane reactor', *Desalination*, vol. 288, pp. 58-65.
3. Pradhan, M., Vigneswaran, S. 2012, 'Particle deposition reduction in air-sparged submerged membrane microfiltration', *IWA regional conference on wastewater and reuse*, Heraklion Greece, March 28-30, 2012.
4. Pradhan, M., Johir, M.A.H. 2011,' Effect of operating conditions for fouling control in submerged membrane microfiltration', *MBR Asia 2011*, Kuala Lumpur, Malaysia , April 25-26, 2011.